UNIVERSIDADE ESTADUAL DE CAMPINAS
Faculdade de Engenharia Química

RAFAEL MACEDO DIAS

DISSOLUÇÃO DE LIGNINA EM LÍQUIDOS IÔNICOS PRÓTICOS

LIGNIN DISSOLUTION IN PROTIC IONIC LIQUIDS (*)

Campinas
2020

RAFAEL MACEDO DIAS

DISSOLUÇÃO DE LIGNINA EM LÍQUIDOS IÔNICOS PRÓTICOS

LIGNIN DISSOLUTION IN PROTIC IONIC LIQUIDS (*)

Tese apresentada à Faculdade de Engenharia Química da Universidade Estadual de Campinas como parte dos requisitos exigidos para a obtenção do título de Doutor em Engenharia Química.

Thesis presented to the School of Chemical Engineering of the University of Campinas as partial fulfillment of the requirements for the degree of Doctor in Chemical Engineering.

Orientadora: Mariana Conceição da Costa

ESTE TRABALHO CORRESPONDE À VERSÃO FINAL DA TESE DE DOUTORADO DEFENDIDA PELO ALUNO RAFAEL MACEDO DIAS, E ORIENTADA PELA PROFA DRA MARIANA CONCEIÇÃO DA COSTA

Campinas – SP
2020

Ficha catalográfica
Universidade Estadual de Campinas
Biblioteca da Área de Engenharia e Arquitetura
Luciana Pietrosanto Milla - CRB 8/8129

Dias, Rafael Macedo, 1989-
D543d Dissolução de Lignina em líquidos iônicos próticos / Rafael Macedo Dias. – Campinas, SP : [s.n.], 2020.

Orientador: Mariana Conceição da Costa.
Tese (doutorado) – Universidade Estadual de Campinas, Faculdade de Engenharia Química.

1. Líquidos iônicos. 2. Lignina. 3. Solubilidade. 4. Solventes. I. Costa, Mariana Conceição da, 1977-. II. Universidade Estadual de Campinas. Faculdade de Engenharia Química. III. Título.

Informações para Biblioteca Digital

Título em outro idioma: Lignin dissolution in protic ionic liquids
Palavras-chave em inglês:
Ionic liquids
Lignin
Solubility
Solvents
Área de concentração: Engenharia Química
Titulação: Doutor em Engenharia Química
Banca examinadora:
Mariana Conceição da Costa [Orientador]
Verônica Maria de Araújo Calado
André Luis Ferraz
Marcus Bruno Soares Forte
Roberta Ceriani
Data de defesa: 06-03-2020
Programa de Pós-Graduação: Engenharia Química

Identificação e informações acadêmicas do(a) aluno(a)
- ORCID do autor: https://orcid.org/0000-0002-0810-2381
- Currículo Lattes do autor: http://lattes.cnpq.br/4907808183266433

BANCA EXAMINADORA

Profa. Dra. Mariana Conceição da Costa (orientadora)

Profa. Dra. Verônica Mariana de Araújo Calado (UFRJ)

Prof. Dr. André Luis Ferraz (USP)

Prof. Dr. Marcus Bruno Soares Forte (UNICAMP)

Profa. Dra. Roberta Ceriani (UNICAMP)

A ata de defesa assinada pelos membros da Comissão Examinadora, consta no SIGA/Sistema de Fluxo de Dissertação/Tese e na Secretaria do Programa da Unidade.

Este exemplar corresponde à redação final da Tese de Doutorado defendida pelo aluno **Rafael Macedo Dias**, aprovada pela Comissão Julgadora em 6 de março de 2020.

AGRADECIMENTOS

A Deus, por ter me dado a coragem e força necessárias para continuar meus estudos e aperfeiçoamento, pela saúde para que não me deixasse abater frente aos desafios, e pela capacidade de ver o lado positivo de todos os obstáculos vencidos.

A minha orientadora Profa. Dra. Mariana Conceição da Costa, por ter aceitado a minha orientação, por estar sempre presente e disposta a discutir o nosso trabalho, pelos valorosos ensinamentos ao longo dessa jornada, e pela amizade e confiança desenvolvidas em nossa relação. Meu muito obrigado! O período do Doutorado será para sempre lembrado em minhas memórias pela nossa boa relação.

Ao Prof. Dr. João Coutinho, por ter me dado a oportunidade de fazer parte de sua equipe de pesquisa, e pelos valiosos ensinamentos no período em que estive em Portugal sob sua orientação.

Ao Dr. André Miguel da Costa Lopes e ao grupo PATh, pela paciência, pelos ensinamentos, pela amizade firmada, e por toda a ajuda que me foi dada durante a minha estadia em Portugal.

Aos meus pais, irmãos, sobrinhos, cunhados pelo amor incondicional, por me acolherem nos meus momentos de desânimo, pelo apoio emocional, e por cuidarem de mim sempre, sem vocês nada seria possível.

Aos meus amigos, especialmente do Grupo LEF, que estiveram sempre presentes durante a minha jornada, apoiando, compartilhando momentos, mensagens, e celebrando cada vitória juntos.

Ao apoio técnico e financeiro do Programa de Pós-Graduação em Engenharia Química da UNICAMP, ao Conselho Nacional de Desenvolvimento Científico e Tecnológico - CNPq (169743/2018-7; 140723/2016-1), à Fundação de Amparo à Pesquisa do Estado de São Paulo - FAPESP (2014/21252-0; 2016/08566-1), ao Fundo de Apoio ao Ensino, à Pesquisa e à Extensão -

FAEPEX, e ao Banco Santander S.A. Além disso, o presente trabalho foi realizado com apoio da Coordenação de Aperfeiçoamento de Pessoal de Nível Superior - Brasil (CAPES) - Código de Financiamento 001.

A todos que participaram direta ou indiretamente deste trabalho, e que contribuíram para a minha formação pessoal e profissional. Obrigado!

RESUMO

O crescente interesse em biocombustíveis e produtos renováveis de alto valor agregado tem atraído a atenção de pesquisadores para as biorrefinarias. Neste tipo de refinaria a biomassa necessita ser separada em seus principais constituintes, ou seja, celulose, hemicelulose, e lignina, e a partir disso, suas frações podem ser potencialmente aplicadas e convertidas em biomateriais, biocombustíveis e produtos renováveis de grande interesse financeiro e comercial. Esses constituintes estão fortemente interligados em um arranjo cristalino de difícil ruptura. Para ocorrer a quebra dessa estrutura, tem sido proposta a utilização de líquidos iônicos próticos como meio deslignificante para separação desses três componentes. Sendo assim, o presente estudo avaliou a capacidade de uma série de líquidos iônicos próticos produzidos a partir de alcanolaminas e ácidos orgânicos, e suas soluções aquosas, de dissolver os componentes da biomassa através da determinação da solubilidade à temperatura constante. Foi demonstrado o papel majoritário do ânion, e secundário do cátion que formam os líquidos iônicos próticos, assim como o efeito antissolvente da água, e o efeito da temperatura, e do tempo no favorecimento do processo de dissolução. Além disso, foi demonstrado que as frações da lignina com menor massa molar permanecem dissolvidas nos líquidos iônicos, enquanto as de maior massa molar são facilmente recuperadas com a adição de água à solução. Assim sendo, os líquidos iônicos próticos se mostraram meios promissores para dissolução da lignina, sem causar grandes alterações em sua estrutura, se mostrando, então, solventes interessantes para aplicações industriais em que se deseja apenas dissolver a lignina.

Palavras-chave: Líquidos Iônicos Próticos. Lignina Kraft. Solubilidade. Solventes verdes.

ABSTRACT

A crescent interest in biofuels and high-value added and renewable products have been attracting the attention of researches to the biorefinery. In this kind of refinery, the biomass needs to be separated in rich fractions of its compounds (cellulose, hemicellulose, and lignin), and, afterwards, its fractions may be potentially converted into biomaterials, biofuels and renewable products of great economical and financial interest. The lignocellulosic biomass is mainly formed by cellulose, hemicellulose, and lignin, which are tightly bounded in a crystalline array hardly broken. To induce this disruption, recently, the use of Protic Ionic Liquids have been proposed as solvent media to delignification and separation processes of these three components. So, in this study was evaluated the ability of a novel of alkanolammonium-based Protic Ionic Liquids formed by organic acids, and their aqueous solutions to dissolve lignin through determination of lignin solubility at constant temperature. It was demonstrated the key role of anion, and the secondary role of cation, besides the anti-solvent effect of water, and the favored behavior induced by the increasing in temperature and time in solubility values. Also, it was demonstrated that lignin fractions formed by lower molecular weight remained dissolved in Protic Ionic Liquids, while the higher molecular weight were easily recovered by addiction of water in the solution. Therefore, the Protic Ionic Liquids have shown potential to be applied as solvent media to dissolution of Kraft lignin without changing significantly the structure of lignin, being considered as interesting solvents to industrial applications in which the only effect would be the dissolution of lignin.

Keywords: Protic Ionic Liquids. Kraft lignin. Solubility. Green solvents.

Sumário

PARTE 1

INTRODUÇÃO GERAL, OBJETIVOS E ESTRUTURA DA TESE, REVISÃO BIBLIOGRÁFICA E MATERIAL E MÉTODOS

CAPÍTULO 1 – INTRODUÇÃO

1. Introdução

As preocupações acerca do impacto ambiental gerado pelo alto consumo de energia, associadas à diminuição das reservas de combustíveis fósseis, além do crescimento das demandas por novos materiais têm incentivado pesquisadores a procurar novas fontes de energia e produtos renováveis, como a utilização de matéria lignocelulósica, na tentativa de se atingir uma sociedade mais sustentável. Neste cenário, surgem as biorrefinarias que têm como princípio o fracionamento da matéria lignocelulósica, proveniente de florestas, agricultura e resíduos agroindustriais, e sua posterior conversão em combustíveis, químicos finos e materiais, visando substituir, ao menos em parte, o papel da petroquímica na sociedade moderna (Gillet et al., 2017).

Nas biorrefinarias, a biomassa lignocelulósica tem um papel primordial, uma vez que esta é uma matéria-prima renovável e de grande disponibilidade. A matéria lignocelulósica é formada por 3 componentes principais: celulose é o componente principal (38-50%), sendo aplicada atualmente na indústria de papel e têxtil para a produção de produtos manufaturados, além de poder ser transformada em biocombustível e também convertida, bioquimicamente, em produtos de alto valor agregado (GANDLA; MARTÍN; JÖNSSON, 2018;Grishkewich et al., 2017); hemicelulose é o segundo componente presente em maior quantidade (23-32%), e pode ser aplicada nos ramos medicinal, na síntese de polímeros, na indústria química (furfural), e, tal qual a celulose, na produção de biocombustíveis (etanol) (Chandel et al., 2018;Luo et al., 2019). Por fim, a lignina (15-25%) pode ser convertida para aplicação na síntese e produção de hidrogéis, bioplásticos, resinas, produtos químicos, além de biocombustíveis, entretanto, recebe pouco investimento e atenção em sua conversão, quando comparado com a celulose, por exemplo (Wang et al., 2013;ISIKGOR; BECER, 2015). Sabe-se que a lignina está organizada em uma complexa matriz resistente e recalcitrante, e que fornece resistência contra patógenos, rigidez à parede celular e força de compressão aos tecidos e fibras da biomassa (RUBIN,2008).

Como um dos objetivos de uma biorrefinaria, o fracionamento da biomassa lignocelulósica em frações ricas em cada um dos componentes é uma etapa de suma importância, visto que se deseja a posterior conversão destas frações em bio-produtos, e que seu sucesso depende da pureza deste fracionamento. Devido à sua rígida estrutura e a necessidade da separação dos componentes da biomassa, uma etapa de pré-tratamento se faz necessária, visando a quebra desta estrutura e tornando suas frações disponíveis para uma futura conversão (Gillet et al., 2017).

Diversos tipos de pré-tratamento têm sido propostos ao longo dos anos, como: ultrassom (BUSSEMAKER; ZHANG, 2013), explosão a vapor, organosolv (Zhu et al., 2009), e microondas (Brahim et al., 2016). Entretanto, estes métodos têm apresentado baixa eficiência na remoção de lignina, altos custos, além de alguns não serem considerados ambientalmente amigáveis, dificultando a sua implementação em larga escala (Alvira et al., 2010). Diante deste cenário, surgem os Líquidos Iônicos Próticos (LIPs), uma classe de Líquidos Iônicos (LIs) notadamente mais barata e de fácil síntese, como solventes promissores para o processo de deslignificação e dissolução da lignina, que poderiam facilitar o adequado desenvolvimento de processos de conversão desta macromolécula (Achinivu et al., 2014;Rashid et al., 2016).

Os LIPs são considerados sais orgânicos com ponto de fusão abaixo de 100 °C, formados por uma combinação de ânions e cátions. Além disso, são facilmente sintetizados a partir de uma reação de neutralização entre uma base e um ácido orgânico, e, ao final da reação, as espécies neutras se encontram em equilíbrio com as espécies com carga (GREAVES; DRUMMOND, 2015). A combinação de diferentes cátions e ânions resulta em uma infinidade de LIPs (solventes projetáveis), cujas propriedades (densidade, viscosidade, condutividade) também podem ser projetadas, de forma a se obter um LIP interessante para uma tarefa específica. Ainda com relação às propriedades, os LIPs podem apresentar propriedades notáveis: baixa pressão de vapor, alta condutividade, estabilidade térmica e química, o que os torna aptos a uma quantidade imensurável de aplicações, entretanto, necessitam ser recuperados e reciclados para redução de custos (Greaves et al., 2006).

Recentemente, os LIPs têm sido aplicados no pré-tratamento da biomassa lignocelulósica e na dissolução da lignina, se mostrando uma alternativa aos métodos já existentes, além de terem se mostrado solventes adequados para a dissolução da lignina, apresentando um alto potencial de aplicabilidade na problemática exposta (Merino et al., 2018;Reis et al., 2017). Ademais, sabe-se que alguns LIs são capazes de alterar a estrutura química da lignina, o que poderia acarretar em aplicações mais nobres desta macromolécula, visto que este componente é o que apresenta menor suscetibilidade a tratamentos químicos e biológicos, além de ser, quase em sua totalidade, queimado como combustível de baixo valor (CHATEL; ROGERS, 2014). Sendo assim, estudar a solubilidade de lignina em LIPs pode abrir novas perspectivas da aplicação da lignina em um processo industrial e no contexto de uma biorrefinaria, tanto como meio reacional, como meio solvente para transporte da lignina.

Em vista disto, o presente trabalho teve como objetivo avaliar o equilíbrio de fases (sólido-líquido) envolvendo lignina e soluções aquosas de LIPs, para futuras aplicações industriais destes solventes, assim como a possibilidade de utilizá-los na valorização e/ou partição da lignina. Para isso, foi avaliada a solubilidade de lignina em soluções aquosas de LIPs em diferentes temperaturas, além da possibilidade de reciclo de alguns LIPs, assim como a caracterização da lignina antes e depois de dissolvida nos LIPs através de técnicas como *Gel Permeation Chromatography* (GPC), *Fourrier-Transform Infrared Spectroscopy* (FT-IR), e *2D Heteronuclear Single Quantum Coherence Nuclear Magnetic Ressonance* (2D HSQC NMR).

CAPÍTULO 2 – OBJETIVOS E ESTRUTURA DA TESE

2. Objetivos

Este trabalho teve como objetivo avaliar se os LIPs produzidos a partir de alcanolaminas e suas soluções aquosas são capazes de dissolver e solubilizar os principais componentes da biomassa lignocelulósica, notadamente a lignina, visando encontrar solventes adequados para o desenvolvimento dos processos e operações necessárias em uma biorrefinaria. Além disso, para escrutinar a capacidade dos LIPs em realizar essa tarefa, os seguintes objetivos específicos também foram desenvolvidos:

- Avaliar se ocorre a dissolução de celulose, xilose e lignina alkali em LIPs formados por monoetanolamina e os ânions formato, acetato e propionato, utilizando a técnica de microscopia óptica de luz polarizada com diferentes taxas de aquecimento. Além de avaliar se a capacidade de dissolução destes componentes está relacionada à variação da cadeia alquílica da parte aniônica, e a ionicidade destes LIPs;
- Determinar a solubilidade de lignina Kraft em soluções aquosas de LIPs formados por alcanolaminas e ácidos orgânicos (málico, malônico, succínico, glicólico, e lático) a baixas temperaturas, além de avaliar a influência do tempo e do modo de agitação neste fenômeno;
- Determinar a solubilidade de lignina Kraft em soluções aquosas de LIPs formados por alcanolaminas e ácidos orgânicos (fórmico, acético, propiônico, hexanóico e octanóico) a baixas temperaturas;
- Verificar se ocorrem possíveis modificações estruturais (e/ou o fracionamento) na lignina Kraft dissolvida nos LIPs e precipitada, através de técnicas como *Gel Permeation Chromatography* (GPC), *Fourrier-Transform Infrared Spectroscopy* (FT-IR), e *2D Heteronuclear Single Quantum Coherence Nuclear Magnetic Ressonance* (2D HSQC NMR);

- Avaliar se é possível reciclar os LIPs em sucessivas etapas de dissolução e precipitação de lignina Kraft por etapas consecutivas de destilação.

Estrutura da Tese

Esta Tese está dividida em três partes e subdividida em dez capítulos que abordam os seguintes tópicos:

PARTE 1

Capítulo 1 – Introdução;

Capítulo 2 – Objetivos e estrutura da Tese;

Capítulo 3 – Introdução sobre a biomassa lignocelulósica e seus constituintes, e uma revisão da literatura sobre LIPs e suas aplicações no pré-tratamento da biomassa e a solubilidade de lignina nestes solventes. Este capítulo apresenta o estado da arte sobre o assunto.

Capítulo 4 – Material e métodos

PARTE 2

Capítulo 5 – **Dissolution of lignocellulosic biopolymers in ethanolamine-based protic ionic liquids**, artigo publicado na revista *Polymer Bulletin*, que teve como objetivo avaliar a capacidade de dissolução dos principais componentes da biomassa lignocelulósica (celulose, xilose e lignina Álkali) em 3 LIPs: HEAF, HEAA, e HEAP utilizando a técnica de microscopia óptica de luz polarizada (MOP) e diferentes taxas de aquecimento (1; 0,5, e 0,1 °C/min). A ionicidade destes LIPs foi determinada usando o *Walden Plot*, e tal propriedade foi associada à capacidade de dissolução de xilose e lignina álkali nestes solventes;

Capítulo 6 – **An investigation of Kraft lignin solubility in protic ionic liquids and their aqueous solutions**, artigo submetido à revista *Industrial Crops and Products*, que teve por objetivo determinar a solubilidade da lignina Kraft em soluções aquosas contendo sete LIPs: HEAM, HEAMn, HEASu, HEAG, HEAL, BHEAL, e THEAL, a baixas temperaturas (40 a 80 °C). Além disso, a influência do tempo foi avaliada através de ensaios de dissolução da lignina em LIPs em tempos pré-determinados, e curvas de

cinética de dissolução foram construídas. Um comparativo de métodos de agitação mecânica também foi realizado visando atingir a saturação mais rapidamente. A capacidade de reciclo do THEAL e do HEAM no processo de dissolução da lignina foi avaliada por 3 ciclos consecutivos.

Capítulo 7 – **Uncovering the potentialities of protic ionic liquids and their aqueous solutions as non-derivatizing solvents of Kraft lignin**, artigo publicado na revista *Industrial Crops and Products*, que teve por objetivo determinar a solubilidade de lignina Kraft em soluções aquosas contendo sete LIPs: HEAF, HEAA, HEAP, HEAH, HEAO, BHEAP, e THEAP, a 50 °C. Neste trabalho foi avaliada a influência da cadeia alquílica do ânion na capacidade de dissolução da lignina, além de estabelecer uma relação entre o tamanho do cátion (aumento da sua cadeia aquílica e de grupamentos hidroxila extra) com a solubilidade da lignina. Ainda neste trabalho, possíveis mudanças estruturais da lignina após a sua dissolução e precipitação em LIPs foi avaliada através de técnicas como *Gel Permeation Chromatography* (GPC), *Fourrier-Transform Infrared Spectroscopy* (FT-IR), e *2D Heteronuclear Single Quantum Coherence Nuclear Magnetic Ressonance* (2D HSQC NMR).

Capítulo 8 – **Discussão Geral** apresenta uma discussão dos principais resultados obtidos nos trabalhos realizados;

PARTE 3

Capítulo 9 – **Conclusões gerais e Desafios futuros** apresenta as principais conclusões observadas e sugestões para trabalhos futuros relacionados ao tema desenvolvido nesta Tese.

Capítulo 10 – **Referências**

3. REVISÃO DA LITERATURA

3.1. Biorrefinaria

A crescente demanda por energia, bem como o uso de produtos derivados de combustíveis fósseis e derivados de petróleo, entre outros fatores tem provocado o aquecimento global. Associado a isso, há uma preocupação acerca do tempo que resta até que as reservas de petróleo sejam capazes de suprir a demanda global antes de se esgotarem (Kudakasseril et al., 2013).

Neste cenário, a humanidade tem buscado formas de obter energia através de fontes alternativas e mais sustentáveis, como por exemplo, a eólica, solar e também a biomassa. Devido a sua grande abundância, sua natureza renovável, e por ser favorável na redução de emissão de gases de efeito estufa (fotossíntese), a biomassa tem atraído grande atenção nos últimos anos (Brahim et al., 2016; Travaini et al., 2013), e a biorrefinaria tem se mostrado uma opção promissora (Figura 1).

Figura 1 - A Biorrefinaria

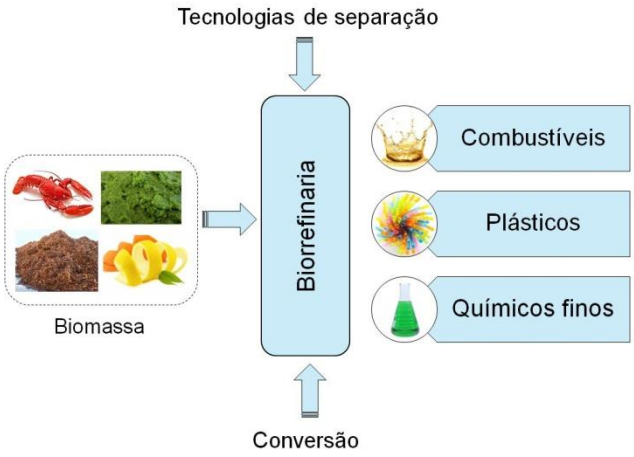

(Acervo Pessoal)

Uma biorrefinaria se apoia no uso da biomassa como matéria-prima para a produção de uma ampla faixa de biocombustíveis, bioquímicos e biomateriais, sendo uma solução mais sustentável. Neste conceito, a biomassa poderia ser potencialmente convertida com base em uma abordagem similar as refinarias petroquímicas (MORAIS;

COSTA LOPES; BOGEL-ŁUKASIK, 2015); uma série de processamentos seriam aplicados na transformação da biomassa, tais quais: liquefação, fracionamento, hidrólise, pirólise, gaseificação, catálise, e fermentação, produzindo ao final, combustíveis, químicos e energia (FATIH DEMIRBAS, 2009).

Entre as principais metas de uma biorrefinaria está o fracionamento da biomassa lignocelulósica em frações ricas de seus principais componentes: celulose, hemicelulose e lignina. Estes compostos depois de separados serão aplicados para produção de biomateriais de alto valor agregado. No âmbito da Agenda 2030 para o Desenvolvimento Sustentável, onde foram decididos os novos caminhos a serem adotados visando a melhoria da vida e do bem-estar das pessoas, o fim da pobreza, o aumento da prosperidade e a proteção do meio-ambiente pela ONU (2015), uma biorrefinaria atende os objetivos de "*Assegurar o acesso confiável, sustentável, moderno e a preço acessível à energia para todos*", "*promover o crescimento econômico sustentado, inclusivo e sustentável, emprego pleno e produtivo e trabalho descente para todos*", "*Construir infraestruturas resilientes, promover a industrialização inclusiva e sustentável e fomentar a inovação*", e "*Assegurar padrões de produção e de consumo sustentáveis*".

3.2. A Biomassa Lignocelulósica

A biomassa lignocelulósica é uma matéria-prima abundante e renovável que pode ser aplicada na biorrefinaria. Esse material pode ser encontrado em florestas, resíduos da agricultura e cultivos agrícolas, e resíduos industriais (indústria papel, principalmente), sendo sua produção mundial estimada em 15-17 Mt/ano (CHU; MAJUMDAR, 2012; XU; DUAN; WANG, 2015). A biomassa lignocelulósica é formada por três constituintes principais: celulose (38-50%), hemicelulose (23-32%), e lignina (15-25%), além de cinzas e extrativos. Tais compostos estão altamente organizados e ligados, formando uma rede rígida e complexa (Figura 2) (Zavrel et al., 2009).

Figura 2 - A biomassa lignocelulósica: parede celular vegetal

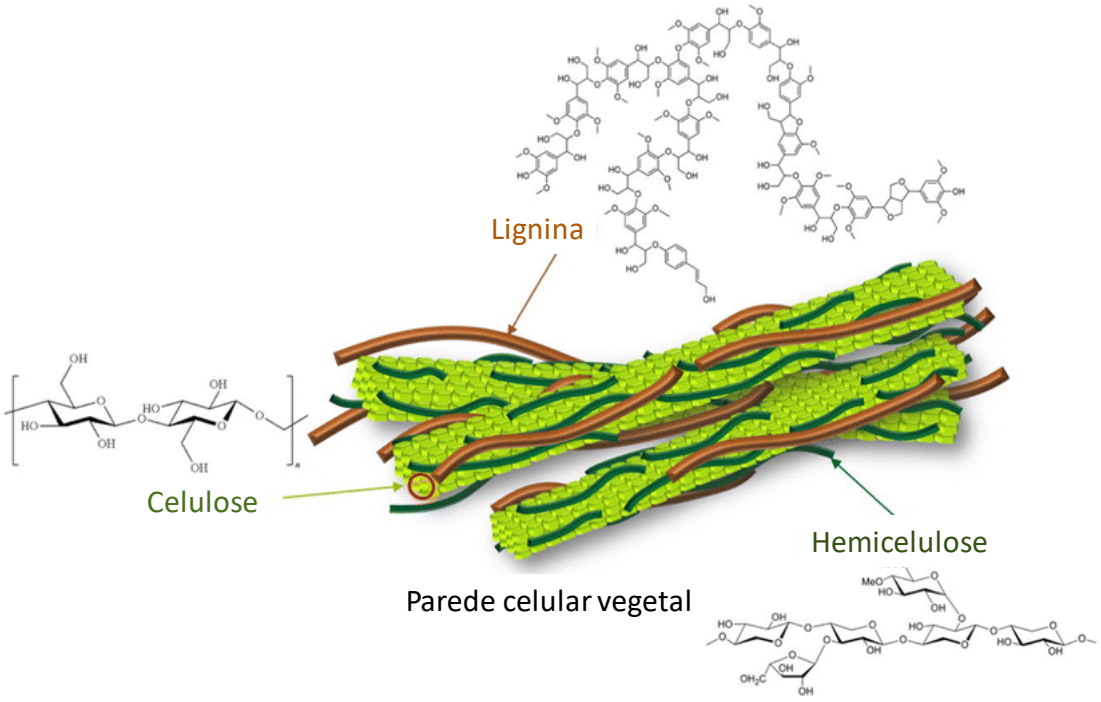

(adaptado de Jensen et al., 2017)

Os principais carboidratos encontrados na estrutura da biomassa são celulose e hemicelulose, que estão ligados entre si através de ligações de hidrogênio, e interações de van der Waals, criando uma rede altamente resistente (Langan et al., 2014). Por fim, a lignina reveste a parede celular da célula, fornecendo proteção contra patógenos, rigidez, e força de compressão aos tecidos e fibras vegetais (RUBIN, 2008).

Mais detalhes sobre a estrutura e as principais aplicações de celulose, hemicelulose, e lignina estão fornecidos nas seções 3.2.1, 3.2.2, e 3.2.3, respectivamente.

3.2.1. Celulose

A celulose (Figura 3) é um homopolímero linear formado de repetidas unidades de D-glicose, unidas através de ligações de β-D (1, 4) glicosídicas, sendo o principal constituinte dos materiais lignocelulósicos (BLEDZKI; GASSAN, 1996). As

unidades de glicose se repetem desde algumas centenas até mais de 10.000 unidades (ZHAO; ZHANG; LIU, 2012), cuja massa molar é estimada em 100.000 g/mol (SAXENA; ADHIKARI; GOYAL, 2009), sendo um homopolissacarídeo linear.

Figura 3 - Ligações de hidrogênio intra e intermolecular na celulose

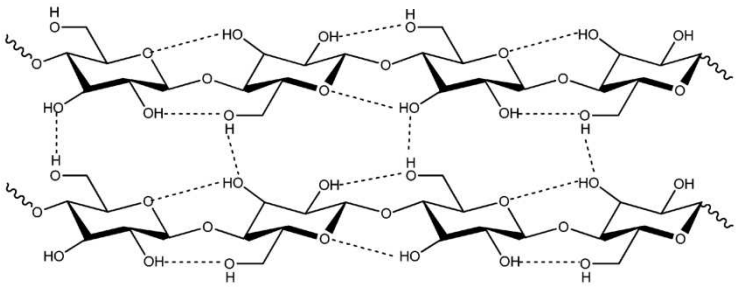

(WANG; GURAU; ROGERS, 2012)

As cadeias de celulose interagem entre si através de ligações de hidrogênio (ligações cruzadas entre grupos hidroxilas), resultando em uma estrutura de matriz cristalina, que estão arranjadas em micro e macro fibrilas fortalecendo a estrutura celular (BLEDZKI; GASSAN, 1996). Esta estrutura faz com que a celulose seja insolúvel em água e resistente a despolimerização (Mosier et al., 2005).

Atualmente, a celulose é amplamente empregada na indústria têxtil e de papel, sendo utilizada na produção de uma variedade de manufaturados (metil celulose). Além disso, a celulose pode ser quimicamente transformada em biocombustível através da sacarificação enzimática (GANDLA; MARTÍN; JÖNSSON, 2018), e bioquimicamente em produtos de alto-valor agregado (Klemm et al., 1998).

3.2.2. Hemicelulose

A hemicelulose (Figura 4) é um heteropolímero formado por cadeias ramificadas curtas, médias e longas, e que apresenta uma estrutura amorfa. Os principais monômeros são hexoses (β-D-glicose, α-D-galactose, e β-D-manose) e pentoses (β-D-xilose e α-L-arabinose) e ácidos urónicos (α-D-glucurônico, α-D-

galacturônico e α-D-4-O-metilgalacturônico) (LIMAYEM, 2012; SAXENA, 2009; RAVINDRAN, 2016).

Figura 4 - Estrutura representativa da hemicelulose

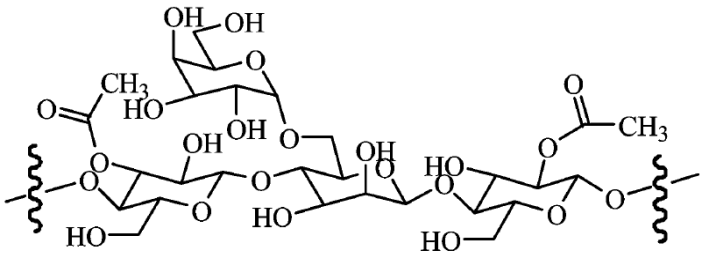

(Sun et al., 2009)

A hemicelulose, juntamente com a celulose, forma a fração de polissacarídeos da biomassa. Apesar de ambos serem açúcares, existem importantes diferenças de comportamento reacional entre as hemiceluloses e as celuloses, devido, principalmente, a estrutura física. As hemiceluloses são totalmente amorfas e, portanto, menos resistentes ao ataque de agentes químicos. Embora não haja evidências de que a celulose e as hemiceluloses estejam ligadas quimicamente, as ligações de hidrogênio e a interpenetração física existente entre elas tornam a sua separação quantitativa impossível. A presença de hemicelulose junto à celulose resulta em importantes propriedades para as fibras, contribuindo para o intumescimento, a mobilidade interna e o aumento da flexibilidade das fibras (BIANCHI, 1995).

Assim como a celulose, a hemicelulose pode ser aplicada em uma série de áreas, tais como: produção de biocombustíveis (etanol) (WYMAN, 1996), indústria química (furfural, xilitol, e ácido levulínico) (Luo et al., 2019), e síntese de polímeros (Chandel et al., 2018).

3.2.3. Lignina

A lignina (Figura 5) é uma macromolécula ramificada, aromática e mononuclear presente nas paredes celulares de certas plantas, particularmente

biomassa lenhosa, e é frequentemente adjacente as fibras celulósicas formando o complexo lignocelulósico (DRUMMOND; DRUMMOND, 1996).

É composta de 3 componentes fenólicos altamente ramificados: álcool p-cumarílico (H), coniferílico (G) e sinapílico (S) ligados através de ligações C-O e C-C. Devido as diversas ligações presentes na estrutura da lignina, os átomos de carbono presentes na cadeia alifática são rotulados como α, β e γ, enquanto que os presentes nas cadeias aromáticas são nomeados de 1 até 6. Ademais, as principais ligações encontradas entre essas unidades são β-O-4, β-β e β-5, além de ligações em menor quantidade, como α-O-4 e β-1 (RALPH, 2010).

Nas plantas, a lignina age como um agente ligante entre as células, formando uma estrutura resistente ao impacto, compressão e dobra. Ela também está envolvida no transporte interno de água, nutrientes e metabólitos (BRISTOW; KOLSETH, 1986).

Figura 5 - Estrutura representativa da lignina*

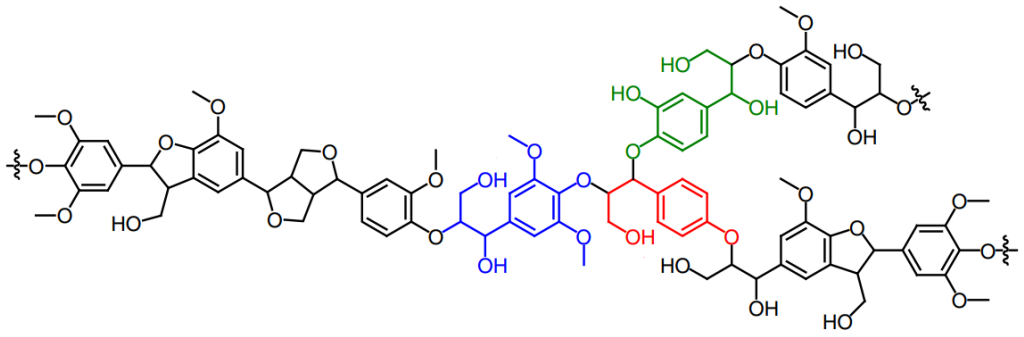

*vermelho: grupos p-cumarílico (H); azul: sinapílico (S); verde: coniferílico (G)
(Adaptado de Shao et al., 2017)

A lignina é incorporada durante o crescimento vegetal, formada por unidades de fenilpropano, resultando em uma macromolécula amorfa e tridimensional. Possui estrutura muito complexa e não determinada completamente, sendo não homogênea, e contendo estruturas globulares (BIDLACK; MALONE, 1992).

A estrutura singular e as propriedades físico-químicas da lignina permitem a produção de uma ampla gama de compostos aromáticos (Wang et al., 2013), além de biodispersantes, emulsificantes, fibras de carbono, e materiais termoplásticos, e faz com que a lignina seja uma alternativa interessante para os produtos derivados da petroquímica (ISIKGOR; BECER, 2015). Apesar disso, a valorização da lignina tem recebido pouca atenção, se comparado com a celulose. É estimado que a indústria de polpa e papel é capaz de produzir 50 milhões de toneladas de lignina, que é extraída da biomassa, e que apenas 2% desta lignina está disponível para comercialização, como agentes dispersantes e ligantes, e o restante é queimado como combustível de baixo valor calórico (Zakzeski et al., 2010). Sendo assim, mais atenção é necessária na valorização da lignina, como fonte de produtos aromáticos.

Finalmente, a lignina encapsula o complexo celulose-hemicelulose, e forma uma barreira física que impede a quebra da biomassa (Taha et al., 2016). Portanto, uma etapa de pré-tratamento (Seção 3.4) é necessária para quebrar o complexo lignina-celulose-hemicelulose, e tornar a matéria acessível para as diversas conversões e aplicações de cada fração da biomassa em uma biorrefinaria.

3.4. O pré-tratamento da biomassa

O principal desafio na valorização da biomassa é transpor a sua alta recalcitrância e separar as frações macromoleculares para posterior conversão. Para ultrapassar este desafio, uma etapa de pré-tratamento (Figura 6) se faz necessária para quebrar este complexo e alterar a estrutura macroscópica, microscópica e submicroscópica da biomassa, tornando-a acessível e passível de ser fracionada. As alterações da biomassa ocorrem durante o pré-tratamento basicamente removendo a lignina, diminuindo a cristalinidade da celulose, e aumentando a porosidade e a área superficial da biomassa (Wyman et al., 2005).

Figura 6 - Quebra da estrutura lignocelulósica após o pré-tratamento.

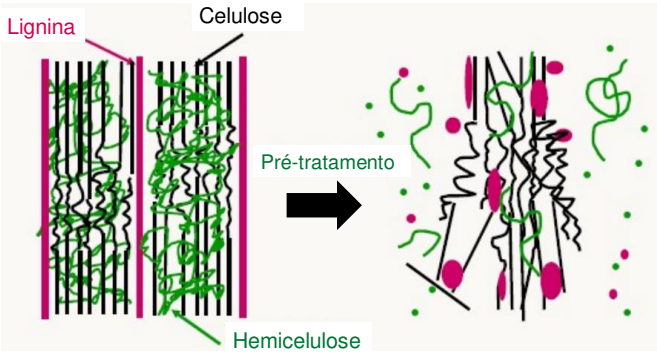

(Adaptado de Mosier et al., 2005)

Após o pré-tratamento, os componentes da biomassa se encontram separados, e estão disponíveis para os demais tratamentos necessários para as suas respectivas valorização/conversão.

Até hoje, muitos métodos de pré-tratamento foram investigados para biomassa de diferentes fontes: explosão a vapor (Pielhop et al., 2016), organosolv (Qing et al., 2017), microondas, térmico e ultrassônico (PASSOS; CARRETERO; FERRER, 2015), alkali (KIM; LEE; KIM, 2016) dentre outros. O modo de ação e as condições de reação variam significativamente para cada um deles (Mosier et al., 2005). Cada pré-tratamento tem suas vantagens e desvantagens no que diz respeito às suas condições técnico-econômicas e de processo, entretanto, no geral, tais métodos necessitam de reagentes perigosos para a saúde humana e que oferecem riscos ao meio ambiente, têm baixa eficiência, bem como alto consumo de energia (Alvira et al., 2010).

Em vista disto, alternativas mais eficientes e sustentáveis para realizar o pré-tratamento têm sido propostas. Neste contexto, os Líquidos Iônicos (LIs) sugiram como uma alternativa promissora aos métodos tradicionais (Brandt et al., 2010; Mora-pale et al., 2011), além de serem capazes de alterar quimicamente a estrutura da lignina, tornando-a mais interessante do ponto de vista econômico e aplicável (Dutta et al., 2017; George et al., 2011).

3.4. O que são Líquidos Iônicos?

Líquidos Iônicos (LIs) são geralmente definidos como líquidos eletrólitos, ou sais compostos inteiramente por íons (soluções iônicas) e que são fluidos a temperaturas abaixo de 100 °C, apresentando estruturas cristalinas iônico-covalentes (VEKARIYA, 2017; WASSERCHEID; WELTON, 2008). Os LIs representam uma classe de materiais líquidos com perfil de propriedades que os tornam únicos, originadas de suas complexas interações Coulômbicas, ligações de hidrogênio, interações de van der Waals entre os íons que os constituem (WASSERSCHEID; SCHRÖER, 2014). Os LIs são formados a partir da combinação de cátions e ânions, na sua grande maioria orgânicos, em que os grupos funcionais são incorporados covalentemente como parte da estrutura do íon (DAVIS, 2004). A natureza modular dos LIs implica que modificações estruturais podem ser feitas no cátion ou no ânion, e que tais alterações implicam em uma grande diversidade de possibilidades de produção de LIs. Tais modificações tornam possível a alteração das propriedades físico-químicas dos LIs, tais como densidade, viscosidade, e poder de solvatação, podendo ser ajustadas de acordo com o interesse de aplicação (VEKARIYA, 2017). Notadamente, os LIs possuem características peculiares, tais como: não-inflamabilidade, pressão de vapor negligenciável, alta estabilidade química e térmica, entre outros (WELTON, 2018). Tais propriedades conferem a eles o status de ambientalmente amigáveis, o que tem incentivado as pesquisas recentes em suas aplicações. É estimado ser possível produzir cerca de um bilhão de LIs (Mora-pale et al., 2011), o que, aliado às suas propriedades físico-químicas, os tornam aptos a serem aplicados em diversas áreas, tais como: síntese e catálise, biotecnologia, farmácia e medicina, eletroquímica, extração e separação dentre outros (EGOROVA; GORDEEV; ANANIKOV, 2017; Sawant et al., 2011).

Os LIs são considerados na literatura como uma nova classe de solventes, sendo tradicionalmente divididos em duas classes de LIs: Líquidos Iônicos Apróticos (LIAs) e Líquidos Iônicos Próticos (LIPs). Em geral, os LIAs apresentam uma carga positiva permanente no cátion, que é duradoura e cujos íons não estão em equilíbrio químico com as espécies neutras. No caso dos LIPs, os cátions, ânions e suas

espécies precursoras estão em equilíbrio químico, estima-se que menos de 1% dos ácidos e bases precursores estão presentes na solução final (Mirjafari et al., 2013). Há um grande interesse no estudo dos LIAs, entretanto, o interesse pelos LIPs tem crescido rapidamente (GREAVES; DRUMMOND, 2008) devido a sua fácil síntese; Os LIPs são produzidos a partir de uma reação de neutralização ácido-base (Figura 7), o que os torna consideravelmente mais baratos que os LIAs, além disso formam fortes ligações de hidrogênio, e a disponibilidade de prótons H^+, os tornam candidatos promissores para aplicação em materiais condutivos (Mirjafari et al., 2013).

Figura 7 - Reação de produção de LIPs

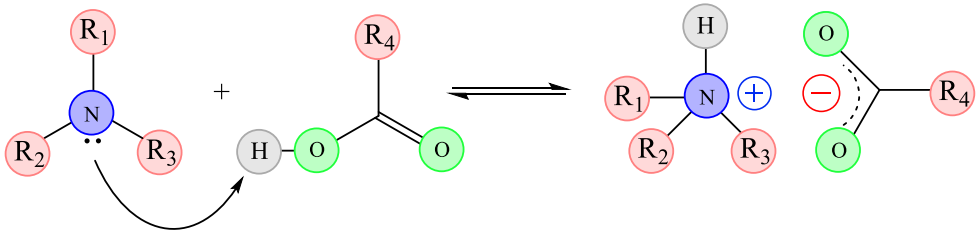

(Acervo Pessoal)

Devido às vantagens apresentadas anteriormente, notadamente o custo e facilidade de sua produção, este estudo foi conduzido utilizando LIPs e os principais componentes naturalmente presentes na biomassa lignocelulósica.

3.5. Os Líquidos Iônicos Próticos e a Biomassa

Na literatura são reportados alguns estudos demonstrando a inabilidade dos LIPs em dissolver celulose (Pinkert et al., 2009; PINKERT; MARSH; PANG, 2010), e a possibilidade de sua aplicação no pré-tratamento da biomassa lignocelulósica (An et al., 2015; ASAKAWA et al., 2015; Brandt-Talbot et al., 2017; Miranda et al., 2019; Chambon et al., 2018; George et al., 2015; Merino et al., 2017; Pin et al., 2019; Rashid et al., 2018; Reis et al., 2017; Rocha et al., 2017; SEMERCI; GÜLLER, 2018), e na dissolução de lignina Kraft (Merino et al., 2018; Rashid et al., 2016).

Tais aspectos os tornam particularmente interessantes em determinadas aplicações, nas quais se deseja dissolver apenas um dos componentes presentes na biomassa, como no caso da produção do etanol de 2ª geração (etanol 2G). Nesse tipo de aplicação, há interesse em remover a lignina da biomassa lignocelulósica, e separar os demais componentes (açúcares), que devem seguir para uma etapa de hidrólise, a fim de produzir o etanol 2G.

3.5.1. O pré-tratamento com Líquidos Iônicos Próticos

Ao longo dos anos, os LIPs têm se mostrado candidatos promissores no pré-tratamento da biomassa lignocelulósica. Diferentes tipos de fontes de biomassa foram testadas e, no geral, resultados encorajadores foram encontrados, como detalhado a seguir.

Em 2014, Achinivu et al. (2014) demonstrou a capacidade de extrair mais de 70% da lignina presente em palha de milho utilizando acetato de pirrolidínio, sem significante impacto na porção de celulose. Brandt-Talbot et al. (2017) utilizaram hidrogenosulfato de trietilamônio no pré-tratamento de gramínea (*Miscanthus x giganteus*) a 120 °C, atingindo mais de 85% de deslignificação, e reciclo do LIP por múltiplas vezes sem perda significativa de eficiência, com recuperação maior que 99% utilizando um rotaevaporador. Hidrogenosulfato de trietilamônio também foi utilizado na forma de soluções aquosas por Chambon et al. (2018) para realizar o pré-tratamento de bagaço de cana-de-açúcar, alcançando mais de 90% de remoção de lignina. Além disso, Reis et al. (2017) e Rocha et al. (2017) utilizaram soluções aquosas de acetato de 2-hidroxietilamônio para efetuar a deslignificação de bagaço de abacaxi e bagaço de cana-de-açúcar, respectivamente, e os autores observaram que a etapa enzimática teve aumento significativo no rendimento. Merino et al. (2017) investigaram alguns LIPs baseados em imidazólio como precursor para o pré-tratamento de gramínea Taiwan (*Pennisetum Purpureum Schum*) a 120 °C durante 1 hora de agitação. De acordo com os autores, o pré-tratamento com LIPs foi efetivo e capaz de hidrolisar parcialmente a celulose e a hemicelulose. Rashid et al. (2018) avaliaram a cinética de extração de

lignina da biomassa da palmeira (dendezeiro) usando formato de pirrolidínio, e concluíram que este LIP pode realizar o pré-tratamento eficientemente (> 90% de remoção de lignina, em massa). Ademais, SEMERCI e GÜLER (2018) usaram quatro LIPs para pré-tratar talos de algodão adicionando metanosulfônicos/sulfúrico como precursor dos LIPs. Os autores demonstraram que o hidrogenosulfato de 1-metilimidazólio na presença de 20% em massa de água reduziu o conteúdo de lignina em 35%, e que tal remoção aumentou a acessibilidade enzimática na biomassa em quase 5 vezes. Recentemente, Pin et al. (2019) avaliaram onze LIPs para o pré-tratamento de bagaço de cana-de-açúcar, utilizando ácido acético e sulfúrico como precursores. De acordo com os autores, o acetato de N-metil-2-hidroxietilamônio apresentou melhor desempenho quando analisada a etapa de hidrólise enzimática posterior, alcançando 72% de conversão de glicose após o pré-tratamento de bagaço de cana-de-açúcar a 160 °C por 3 horas, o que foi considerado competitivo frente a outros tipos de pré-tratamento. Mais recentemente, Miranda et al. (2019) investigaram doze LIPs formados a partir de ácidos orgânicos e aminas como precursores para realizar a deslignificação de biomassa de abacaxi, e concluíram que propionato de 2-hidroxidietilamônio foi o melhor dentre eles, com eficácia maior que 80% para deslignificar a biomassa, sendo considerado efetivo para a remoção da lignina. A Tabela 1 apresenta um resumo de alguns dos resultados encontrados na literatura.

Tabela 1 – LIPs, biomassa e resultados obtidos encontrados na literatura

Amostra	**LIP**	**Condições**	**Resultados**	**Referência**
Palha de arroz	LIPs de Colina	90 °C, 12h	79,6% de extração de lignina	(An et al., 2015)
Bagaço de cana-de-açúcar	acetato de colina	130 °C, 3h	39,2% de extração de lignina	(Asakawa et al., 2015)
Gramínea (*Miscanthus x giganteus*)	hidrogenoSulfato de trietilamônio	120 °C, 8h	85% de extração de lignina	(Brandt-Talbot et al., 2017)
Coroa de abacaxi	propionato de 2-hidroxietilmetilamônio	100 °C, 1h	82,3% de extração de lignina	(Miranda et al., 2019)
Bagaço de cana-de-açúcar	hidrogenoSulfato de trietilamônio	120 °C, 4h	> 90% de extração de lignina	(Chambon et al., 2018)
Gramínea (*Panicum virgatum*)	hidrogenosulfatos de alcanolaminas	120 °C, 1,5h	78% de extração de lignina	(George et al., 2015)
Bagaço de cana-de-açúcar	LIPs de alcanolaminas e misturas	90 °C, 3h	98% de digestibilidade de celulose	(Ferrari et al., 2019)
Bagaço de cana-de-açúcar	alcanolaminas e ácido sulfúrico/acético	160 °C, 1-3h	72% de rendimento de glicose depois do pré-tratamento	(Pin et al., 2019)
Partes da Planta de óleo de palma	formato de pirrolidínio	78-97 °C, 172-238 minutos	Mais de 90% de remoção de lignina	(Rashid et al., 2018)
Bagaço de abacaxi	acetato de 2-hidroxietilamônio	130 °C, 24h	95,8% de remoção de lignina	(Reis et al., 2017)
Bagaço de cana-de-açúcar	acetato de 2-hidroxietilamônio	150 °C, 3,5h	>80% de rendimento de glicose depois do pré-tratamento	(Rocha et al., 2017)
Talos de algodão	hidrogenosulfato de 1-metilimidazólio	120 °C, 4h	Redução de 35% do conteúdo de lignina	(SEMERCI; GÜLER, 2018)

(Acervo Pessoal)

Como apresentado, trabalhos recentes confirmam que os LIPs podem ser usados na etapa de pré-tratamento da biomassa lignocelulósica com grande eficácia na remoção de lignina. Tal aplicação é um avanço científico relativamente recente, e com poucos trabalhos reportados na literatura. Baseado na literatura, ainda não é completamente entendido de que forma os LIPs interagem com a biomassa e removem a lignina, dessa forma, uma maneira de se entender esse processo é através de um estudo de solubilidade da lignina, visando compreender os mecanismos de interação lignina-LIP e quais os fatores que favorecem a remoção de lignina mais eficientemente.

3.5.2. A solubilidade da lignina em Líquidos Iônicos Próticos

Embora alguns estudos do pré-tratamento de biomassa lignocelulósica tenham sido reportados na literatura, a solubilidade da lignina em LIPs tem sido pouco discutida (Merino et al., 2018; Rashid et al., 2016).

Rashid et al. (2016) investigaram a dissolução da lignina Kraft em LIPs e suas soluções aquosas. Os autores testaram três LIPs: formato de piridínio, acetato de piridínio, e propionato de piridínio em diferentes temperaturas e quantidade de água. De acordo com os autores, a água influencia negativamente o processo de dissolução, enquanto a temperatura influencia positivamente. Dentre os LIPs testados, o formato apresentou a maior capacidade de dissolver a lignina (70% de solubilidade em massa) a 75 °C o que aconteceu em 1 hora. Ainda de acordo com os autores, o aumento da cadeia carbônica da parte aniônica do LIP reduz a capacidade de dissolução dos LIPs.

Merino et al. (2018) avaliaram a habilidade de solubilizar lignina de dezoito LIPs multiaromáticos produzidos a partir de imidazólio utilizando a técnica de irradição por microondas. Segundo os autores, o Metanosulfonado de 2,3,4,5-tetrafenil-1H-imidazólio foi o melhor LIP, sendo capaz de dissolver 42% da lignina aplicando a radiação microondas a 90 °C em poucos minutos.

De acordo com o exposto, na literatura há escassez de informações sobre os mecanismos de dissolução da lignina em LIPs, assim como dos papéis do cátion e

ânion e suas interações com a lignina. Por isso, há a necessidade de se aprofundar nos tipos de interação que são estabelecidos entre os LIPs e a lignina, assim como as possíveis alterações estruturais que os LIPs são capazes de induzir na lignina.

3.5.3. Os Líquidos Iônicos Próticos e as modificações estruturais na lignina

A utilização de LIs para o processamento da biomassa (pré-tratamento e despolimerização da lignina) tem sido consideravelmente estudada, uma vez que estes solventes são considerados potencialmente eficientes devido as suas propriedades (HALLETT; WELTON, 2011). Alguns autores reportaram a capacidade dos LIs em modificar e fracionar a estrutura da lignina (Dutta et al., 2017; George et al., 2011; NANAYAKKARA; PATTI; SAITO, 2014; Wen et al., 2014; XIE et al., 2007; Yan et al., 2015). Entretanto, apesar de relativos avanços, a aplicação dos LIPs na modificação e no fracionamento da lignina seguem pouco explorados (ACHINIVU, 2018; Rashid et al., 2016).

De acordo com Rashid et al. (2016), a lignina dissolvida em LIPs formados por ácidos orgânicos e pirrolidinio como precursores, após sua dissolução e precipitação, apresentou maior estabilidade térmica, menor polidispersividade e maior uniformidade, e no geral, nenhuma reação química foi observada durante o processo de dissolução e regeneração da lignina.

ACHINIVU (2018) avaliou a estrutura da lignina após a sua extração/dissolução em acetato de pirrolidínio, 1-metilimidazólio, e piridínio, através de técnicas como FT-IR, GPC e análise elementar (C, N, e H) e concluiu que, em geral, a lignina dissolvida em LIPs apresenta certo grau de despolimerização, resultando em uma lignina com menor peso molar. Além disso, de acordo com o autor, a estrutura da lignina se manteve sem grandes alterações químicas, mantendo sua pureza e seus principais grupos funcionais.

Pelo exposto, ainda não são bem conhecidas as possíveis alterações físico-químicas que os diferentes LIPs são capazes de provocar na estrutura da lignina, e de

que forma a lignina recuperada pode ser aplicada na produção de novos produtos. Em vista disto, este trabalho visa contribuir para esta ausência de conhecimento, investigando as possíveis alterações na estrutura da lignina após a sua dissolução em LIPs, além de avaliar a possibilidade de se aplicar LIPs na dissolução da lignina, e de que forma a estrutura do LIP influencia na solubilidade da lignina, visando desenvolver novos processos industriais no contexto de uma biorrefinaria.

CAPÍTULO 4 – MATERIAL E MÉTODOS

4. Material e Métodos

Neste capítulo são apresentados todos os reagentes utilizados, sua fonte e purezas, bem como as metodologias aplicadas para o desenvolvimento deste estudo.

4.1. Material

Todos os reagentes usados na síntese dos LIPs estão listados na Tabela 2, assim como a sua massa molar, fonte e pureza. Os principais componentes da biomassa (ou seus monômeros) estão apresentados na Tabela 3, assim como seus fornecedores, pureza, número CAS, e estado físico.

Todos os reagentes foram utilizados sem qualquer preparação ou purificação prévia.

Tabela 2 - Ácidos e bases utilizados neste estudo para a síntese de LIPs

Nome Químico	Massa Molar (g/mol)	Fonte	Pureza	Fórmula Química	CAS
Ácidos					
Ácido fórmico	46,03	Merck	≥98%	CH_2O_2	64-18-6
Ácido acético	60,05	Merck	>99%	$C_2H_4O_2$	64-19-7
Ácido propiônico	74,08	Acros Organics	≥99%	$C_3H_6O_2$	79-09-4
Ácido hexanóico	116,16	Sigma	≥98%	$C_6H_{12}O_2$	142-62-1
Ácido octanóico	144,21	Sigma	≥98%	$C_8H_{16}O_2$	124-07-2
Ácido glicólico	76,05	Dinâmica	70%	$C_2H_4O_3$	79-14-1
Ácido lático	90,08	Sigma-Aldrich	85%	$C_3H_6O_3$	50-21-5
Ácido málico	134,09	Dinâmica	99%	$C_4H_6O_5$	6915-15-7
Ácido malônico	104,06	Reagent Plus®	99%	$C_3H_4O_4$	141-82-2
Ácido succínico	118,09	Synth	99%	$C_4H_6O_4$	110-15-6
Bases					
Monoetanolamina	61,08	Sigma-Aldrich	≥98%	C_2H_7NO	141-43-5
Dietanolamina	105,14	Sigma-Aldrich	≥98%	$C_4H_{11}NO_2$	111-42-2
Trietanolamina	149,19	Sigma-Aldrich	≥98%	$C_6H_{15}NO_3$	102-71-6

(Acervo Pessoal)

Tabela 3 - Componentes modelo da biomassa utilizados nesta Tese

Composto	Fornecedor	Pureza	Estado Físico	CAS
α-celulose	Sigma-Aldrich	>99%	Pó	9004-34-6
D-(+)-xilose	Sigma-Aldrich	≥99%	Pó	58-86-6
Lignina Álcali	Sigma-Aldrich	>96%	Pó	8068-05-1
Lignina Kraft from *E. globulus*	Suzano Papel & Celulose	N.D	Pó	-

(Acervo Pessoal)

4.2. Síntese dos LIPs

Os LIPs foram sintetizados por uma reação neutralização ácido-base, na proporção molar de 1:1, utilizando a metodologia proposta ÁLVAREZ et al. (2010) e IGLESIAS et al. (2010). A base foi inserida em um balão de vidro de 3 bocas equipado com um condensador de refluxo, um termopar para monitorar a temperatura, e um funil de decantação com gotejador. A base foi mantida sob refrigeração através de um banho de gelo (aproximadamente 10 °C), e o ácido gotejado lentamente de gota-a-gota, visto que a reação, em geral, é altamente exotérmica e necessita de um resfriamento para evitar sobreaquecimento e a ocorrência de reações paralelas durante a síntese dos PILs. Durante todo o processo um agitador magnético (200 rpm) garantiu a mistura dos reagentes. Após o gotejamento de todo o ácido, a solução foi mantida sob agitação constante por 24 horas a temperatura ambiente, para garantir a formação dos LIPs. Nenhum sólido foi observado ao final do processo, e uma coloração final variando entre incolor e amarelo claro foi observada.

A solução final foi introduzida em um rotaevaporador (pressão absoluta 70 Pa), com aquecimento brando (50-60 °C) para a remoção de excesso de reagentes e de água absorvida durante o processo de síntese. O teor final de água foi medido através de um Karl Fischer Coulorimétrico (Metrohm 831 Karl Fischer), e a formação

dos LIPs foi comprovada através das técnicas de Infravermelho (FT-IR) e Ressonância Magnética Nuclear (RMN). Finalmente, as soluções aquosas de LIPs foram preparadas considerando o teor de umidade medido no Karl Fischer.

Os LIPs utilizados neste trabalho estão apresentados na Tabela 4, com suas respectivas massas molares (MM) e estrutura química dos ácidos e bases precursores.

Tabela 4 – LIPs utilizados neste trabalho: ácidos e bases precursores

Nome	Ácido	Base	MM* (g/mol)	Abreviatura
Formato de 2-Hidroxietilamônio	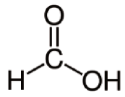 (Fórmico)	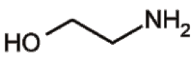 (Monoetanolamina)	107,11	HEAF
Acetato de 2-Hidroxietilamônio	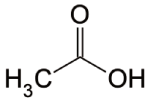 (Acético)	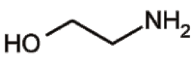 (Monoetanolamina)	121,13	HEAA
Propionato de 2-Hidroxietilamônio	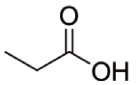 (Propiônico)	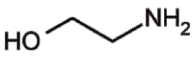 (Monoetanolamina)	135,16	HEAP
Hexanoato de 2-Hidroxietilamônio	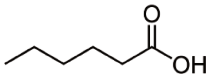 (Hexanóico)	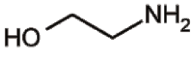 (Monoetanolamina)	177,24	HEAH
Octanoato de 2-Hidroxietilamônio	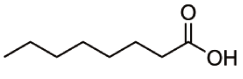 (Octanóico)	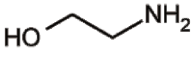 (Monoetanolamina)	205,29	HEAO
Glicolato de 2-Hidroxietilamônio	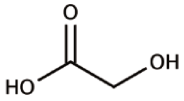 (Glicólico)	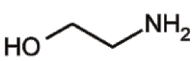 (Monoetanolamina)	137,13	HEAG

Nome	Ácido	Base	MM* (g/mol)	Abreviatura
Lactato de 2-Hidroxietilamônio	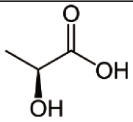 (Lático)	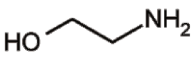 (Monoetanolamina)	151,16	HEAL
Malato de 2-Hidroxietilamônio	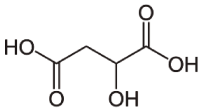 (Málico)	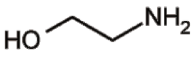 (Monoetanolamina)	256,25	HEAM
Malonato de 2-Hidroxietilamônio	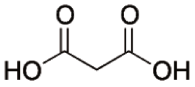 (Malônico)	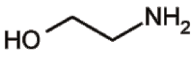 (Monoetanolamina)	226,22	HEAMn
Sucinato de 2-Hidroxietilamônio	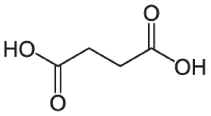 (Succínico)	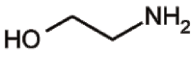 (Monoetanolamina)	240,25	HEASu
Propionato de 2-Hidroxidietilamônio	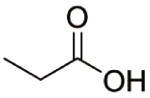 (Propiônico)	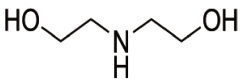 (Dietanolamina)	179,22	BHEAP
Lactato de 2-Hidroxidietilamônio	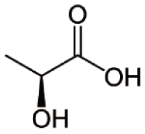 (Lático)	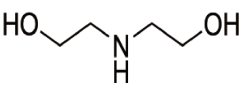 (Dietanolamina)	195,22	BHEAL

Nome	Ácido	Base	MM* (g/mol)	Abreviatura
Propionato de 2-Hidroxitrietilamônio	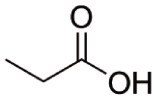 (Propiônico)	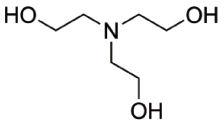 (Trietanolamina)	223,27	THEAP
Lactato de 2-Hidroxitrietilamônio	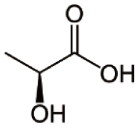 (Lático)	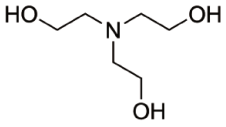 (Trietanolamina)	239,27	THEAL

* A MM (massa molar) é considerada a soma das massas molares dos precursores dos LIPs.

4.3. Caracterização dos LIPs

Após a síntese dos LIPs, eles foram caracterizados pelas técnicas de Infravermelho (*Fourrier-Transform Infrared Spectroscopy*: FT-IR), e Ressonância Magnética Nuclear de H e ^{13}C (*Proton and C*^{13} *- Nuclear Magnetic Ressonance Proton and carbon:* RMN-H, e RMN-^{13}C). Além disso, propriedades como densidade, viscosidade, condutividade também foram determinadas e, sempre que possível, relacionadas com os resultados obtidos nesta Tese.

4.3.1. *Fourrier-Transform Infrared Spectroscopy* (FT-IR)

As análises de espectroscopia na região de infravermelho foram realizadas utilizando um Espectrofotômetro PerkinElmer (Spectrum BX), equipado com uma célula cristal de diamante ATR (Reflectância Atenuada Total) com feixe único horizontal. Os

espectros foram obtidos utilizando 32 scans e resolução de 4 cm^{-1}, e o número de onda entre 4000 cm^{-1} e 600 cm^{-1}.

4.3.2. RMN-^{1}H e RMN-^{13}C

As análises de Ressonância Magnética Nuclear foram realizadas em um espectrômetro Bruker (AVANCE) com frequência de 300 MHz. Amostras de LIPs foram dissolvidas em DMSO deuterado (DMSO-d6), e utilizando Tetrametilsilano (TMS) como referência interna.

4.3.3. Densidade

As medidas de densidade dos PILs foram realizadas em um densímetro digital (Anton Paar, DMA 5000, Alemanha – precisão de 0.05 $kg.m^{3}$). As densidades foram medidas para faixas de temperatura entre 20 e 70 °C, com precisão de ±0.01 °C. As incertezas nas medidas de densidade foram estimadas como 0.07 $kg.m^{3}$.

4.3.4. Condutividade

Amostras de LIPs foram seladas e imersas em um banho termostático com controle de temperatura (PT-100 temperature sensor (±0.1 K)), e as condutividades das amostras foram medidas entre 30 e 70 °C (Analyser 650MA, Brazil). Antes de cada medida a célula de medida foi limpa com água deionizada e etanol. As incertezas das medidas de condutividade foram estimadas em 0.05 $mS.cm^{-1}$.

4.3.5. Viscosidade

As viscosidades dos LIPs em diferentes temperaturas (20 a 70 °C) foram medidas utilizando um microviscosímetro (Anton Paar, AMVn, Alemanha), aplicando o método de queda da esfera. O conteúdo de água presente nos LIPs foi medido antes de cada medida. Durante a operação do viscosímetro, a temperatura foi mantida constante com uma precisão de ±0.01 °C.

4.3.5. Termogravimetria (TGA)

A estabilidade térmica de alguns LIPs sintetizados foi investigada utilizando um equipamento Analisador Termogravimétrico (Shimadzu, TGA-50M, Japan), acoplado a uma microbalança (Mettler Toledo, MX5, Switzerland). Para isso, foi aplicada uma taxa de aquecimento constante de 10°C.min^{-1}.

4.4. Caracterização da lignina Kraft

4.4.1. *Fourrier-Transform Infrared Spectroscopy* (FT-IR)

As análises espectroscopia de lignina Kraft na região de infravermelho foram realizadas utilizando um Espectrofotômetro PerkinElmer (Spectrum BX), equipado com uma célula cristal de diamante ATR (Reflectância Atenuada Total) com feixe único horizontal. Os espectros foram obtidos utilizando 32 scans e resolução de 4 cm^{-1}, e o número de onda entre 4000 cm^{-1} e 600 cm^{-1}.

4.4.2. RMN 2D HSQC (*Heteronuclear Single Quantum Coherence*)

As análises de Ressonância Magnética Nuclear 2D HSQC foram realizadas em um espectrômetro Bruker (AVANCE) com frequência de 500 MHz. 50 mg de lignina Kraft foram dissolvidas em 500 µL de DMSO deuterado (DMSO-d6), e utilizando

Tetrametilsilano (TMS) como referência interna, e transferidas para os tubos de RMN. O espectrômetro é equipado com gradiente inverso 5 mm TXI $^{1}H/^{13}C/^{15}N$ *crioprobe*. As correlações entre os espectros ^{1}H-^{13}C foram medidas com o programa Bruker pulso padrão: “hsqcetgpshi” seguido de correlação 2D H-1/X através de dupla transferência pulso (*trim pulses*), e seleção do gradiente Echo/Antiecho-TPPI para melhoria da sensitividade da fase, com dissociação durante a aquisição. Os picos químicos foram referenciados com relação ao pico central do DMSO (δ_C 39.5 ppm, δ_H 2.49 ppm). Todos os experimentos foram mantidos a 25 °C com os seguintes parâmetros: largura espectral de 11 ppm em F2 (^{1}H) e 165 ppm em F1 (^{13}C) com 1024 pontos experimentais, 194 scan de resolução e delay de reciclo de 1,5 segundos.

Para as análises semi-quantitativas, a correção da linha base e de fase foram feitas em todo o espectro HSQC. A relativa abundância das principais unidades as subestruturas da lignina foram determinadas como percentual total da integração das cadeias de grupos metoxil dos sinais cruzados de ^{13}C-^{1}H no espectro de HSQC.

4.4.3. GPC (*Gel Permeation Cromatography*)

Tal análise foi feita utilizando um cromatógrafo PL-GPC 110 (Polymer Laboratories, UK), equipado com duas colunas PL gel MIXED- D 5 µm (300 x 7.5 mm) protegidas por uma pré-coluna PL aqua gel-OH Guard 5 µm. As colunas, o sistema injetor e detector (RI) foram mantidos a 70 °C durante as análises. Uma solução de LiCl em dimetilformamido (0.1 $mol \cdot L^{-1}$) foi preparada e usada como eluente. Amostras de lignina foram dissolvidas em solução eluente com concentração de cerca de 1% em massa (10 $mg \cdot mL^{-1}$). O volume de injeção das amostras foi de 100 µL, e o eluente foi bombeado a uma vazão de 0.9 mL min^{-1}. As colunas analíticas foram calibradas com compostos modelo da lignina (monômeros, dímeros e tetrâmeros), com massa molar conhecido na faixa de 1 a 4 kDa.

4.5. Experimentos de dissolução e solubilidade

4.5.1. Experimentos de dissolução de α-celulose, xilose e lignina álcali utilizando Microscopia Óptica de Luz Polarizada (MOP)

Ensaios preliminares foram realizados utilizando microscopia óptica de luz polarizada, para identificar o potencial dos LIPs de dissolver os componentes da biomassa. Tal técnica foi escolhida uma vez que se trata de um estudo pré-liminar, e tal técnica fornece resultados rápidos. Como primeiros passos, α-celulose, xilose e lignina álcali foram escolhidas como representantes dos principais componentes da biomassa, devido a sua pureza e sua disponibilidade comercial.

O procedimento experimental para observar a dissolução de biopolímeros encontrados na biomassa lignocelulósica foram semelhantes aos propostos por ANDANSON et al. (2014). Uma solução de aproximadamente 500 mg foi preparada, contendo o biopolímero e o LIP (<1% de água em massa). Esta solução foi agitada rapidamente e colocada em uma lâmina de vidro côncava. Esta lâmina foi introduzida em um estágio pré-aquecido a 30 °C (Linkam LTS420, Reino Unido), que se encontra acoplado a um microscópio óptico (Leica DM2700 M, China).

As amostras foram introduzidas no microscópio e foram expostas a 3 diferentes estágios: 1, 0,5, e 0,1 °C.min^{-1}. Em geral, o estágio sob a amostra foi aquecido até que todos os biopolímeros disaparecessem, ou até que fosse atingido 100 °C. Imagens (1392 x 1100 pixels) foram registradas em intervalos pré-determinados (a cada 60 segundos), com aumento de 50x.

4.5.2. Ensaios de solubilidade e dissolução de lignina Kraft utilizando placa de aquecimento

Excesso de lignina Kraft foi adicionada a 1,0 ± 0,05 g de cada solução aquosa de LIP ou água pura em frascos de vidro. Os frascos foram selados e colocados em um disco suporte de alumínio, que se encontrava sobre uma plataforma que permitisse a agitação e controle de aquecimento/temperatura Pt1000 (H03D Series from

LBX Instruments). Os ensaios de solubilidade foram realizados a temperatura constante e agitação de 200 rpm. Após atingir a saturação, as amostras foram filtradas utilizando filtros PTFE (0,45 μm de tamanho de poro), permitindo a sepação da lignina não dissolvida da fase líquida. Logo em seguida, a fase líquida foi diluída em dimetilsulfóxido (DMSO) e o montante de lignina dissolvida foi quantificado por espectroscopia UV (SHIMADZU UV-1700, Pharma-Spec spectrometer) no comprimento de onda de 280 nm. A determinação quantitativa foi feita com auxílio de curvas de calibração previamente construídas. Todos os experimentos foram realizados, pelo menos, em duplicata, e os resultados foram expressos como médias dos experimentos (com desvio menor que 5%).

Além disso, para avaliar a influência do tempo na dissolução da lignina Kraft, as amostras foram filtradas em diferentes intervalos de tempo (1, 2, 4, 8, 16, 24 e 48 horas), o conteúdo de lignina na fase líquida foi determinado como descrito anteriormente. Estes experimentos também foram realizados, pelo menos, em duplicata.

4.5.3. Ensaios de solubilidade de lignina Kraft utilizando banho ultrassônico

A dissolução de lignina Kraft em LIPs com relação ao tempo também foi avaliada utilizando um banho ultrassônico (Model 1400 A, Unique, Brazil) com potência de 135 W e frequência de 40 kHz, e os valores obtidos foram comparados com os resultados obtidos de acordo com o procedimento descrito em 4.5.2. Um banho termostático forneceu a recirculação da água, garantindo a constância da temperatura dentro do banho ultrassônico durante os ensaios, e a temperatura foi monitorada utilizando um termômetro (PT-100 temperature sensor (± 0,1 °C)). Os experimentos foram realizados com satisfatório controle de temperatura (± 0,5 °C). As amostras foram filtradas em diferentes intervalos de tempo, e diluídas com DMSO, como descrito na seção 4.5.2. A quantificação da lignina foi feita através das curvas de calibração

previamente construídas. Para efeitos comparativos, a temperatura do banho ultrassônico foi mantida no mesmo valor que os ensaios realizados na seção 4.5.2.

4.5.4. Precipitação da lignina e reciclo do LIP

Água deionizada foi adicionada a solução de lignina+LIP e agitada para a precipitação de lignina, uma vez que a água atua como anti-solvente na solução. Esta solução foi introduzida em um banho de gelo (aproximadamente 5 °C) para aumentar a eficiência da precipitação. A lignina recuperada foi separada por filtração a vácuo e lavada com água deionizada para garantir que todo o LIP foi removido. A lignina precipitada foi seca sob vácuo a 30 °C por 24 horas. A solução aquosa de LIP foi coletada para testar a capacidade de se reciclar os LIPs. Esta solução foi submetida a uma destilação simples a pressão ambiente para remoção da maior fração de água possível. Logo em seguida, a solução resultante foi submetida a um processo de evaporação à vácuo (60 °C e 10 kPa) até que quase toda a água fosse removida. O teor final de água foi medido utilizando um Karl Fischer Coulorimétrico (Metrohm 831 Karl Fischer), e a solução aquosa de LIP foi reutilizada nos ensaios de solubilidade de lignina, como descrito na seção 4.5.2.

PARTE 2

RESULTADOS E DISCUSSÃO

Objetivos do Capítulo 5

No Capítulo 5 dá-se início a apresentação dos resultados obtidos durante o desenvolvimento desta Tese. Neste Capítulo foram exploradas as habilidades de 3 LIPs em dissolver os principais componentes da biomassa, notadamente celulose, hemicelulose e lignina. Para isso, a técnica de Microscopia Óptica foi utilizada aplicando diferentes taxas de aquecimento. Além disso, foi investigada de que forma as propriedades dos LIPs (condutividade, viscosidade e densidade) influenciam na capacidade desses LIPs em dissolver os componentes da biomassa lignocelulósica.

CAPÍTULO 5 – Dissolution of lignocellulosic biopolymers in ethanolamine-based protic ionic liquids

Polymer Bulletin
https://doi.org/10.1007/s00289-019-02929-2

ORIGINAL PAPER

Dissolution of lignocellulosic biopolymers in ethanolamine-based protic ionic liquids

Rafael M. Dias[1] · Filipe H. B. Sosa[1] · Mariana C. da Costa[1]

Received: 7 June 2019 / Revised: 9 August 2019 / Accepted: 21 August 2019

Abstract

This work evaluates the potential use of 2-hydroxy ethylammonium-based protic ionic liquids (PILs) for dissolving the major lignocellulosic biopolymers such as cellulose, xylose and lignin. Three PILs, 2-hydroxy ethylammonium formate (2-HEAF), 2-hydroxy ethylammonium acetate (2-HEAA) and 2-hydroxy ethylammonium propionate 2-HEAPr, were synthesized and characterized (viscosity, density and conductivity). A small amount of biopolymer was added to the PILs; the biopolymers' dissolution curves were determined from 30 °C up to 100 °C on these solvents using a hot stage coupled to an optical microscope. The results show that while xylose and lignin could be dissolved by the PILs, cellulose could not, and also that 2-HEAF—which presented the higher ionicity—was the most appropriate PIL among those tested to dissolve these biopolymers (xylose and lignin). They also show that lignin dissolution is faster when an anion with a short alkyl carbon chain is used and that higher heating rates require a somewhat higher temperature to achieve full dissolution.

Electronic supplementary material The online version of this article (https://doi.org/10.1007/s00289-019-02929-2) contains supplementary material, which is available to authorized users.

✉ Mariana C. da Costa
mcosta@feq.unicamp.br

[1] Department of Process and Product Design (DDPP) - School of Chemical Engineering (FEQ), University of Campinas (UNICAMP), Campinas, São Paulo 13083-852, Brazil

Published online: 31 August 2019

Graphic abstract

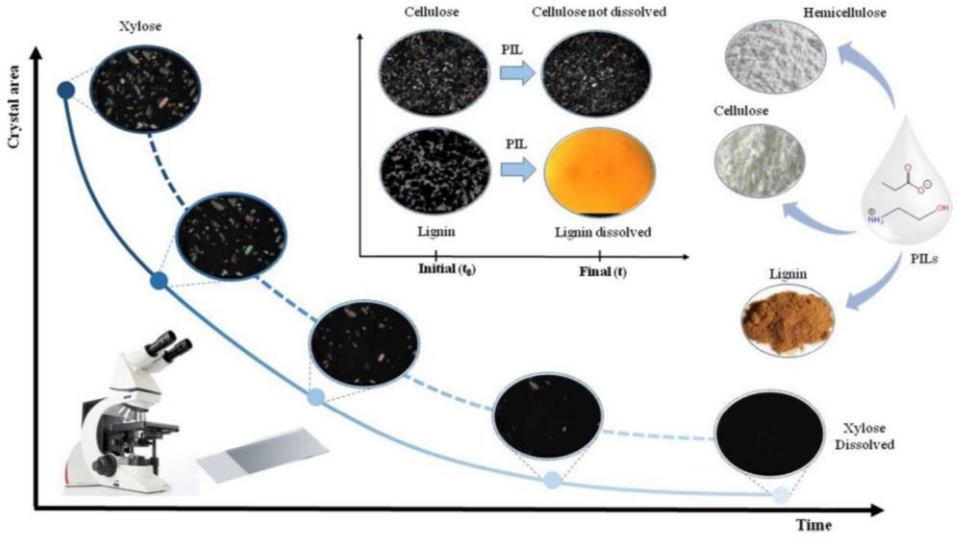

Keywords Protic ionic liquids · Biopolymers · Optical microscopy · Dissolution · Biomass pretreatment

Introduction

Biomass is a renewable source of raw materials, which presents great potential for use in the production of chemicals, materials and fuels while also helping in the reduction of greenhouse gas emissions. Biomass composition can change according to its source, but cellulose (35–50 wt%), lignin (5–30 wt%) and hemicellulose (20–35 wt%) are the major components present in lignocellulosic biomass [1, 2], in a complex structure formed by a combination of these compounds [3]. In this structure, cellulose is found in a crystalline form among hemicellulose and lignin. This structure makes the separation of these compounds and the enzymatic hydrolysis of cellulose a difficult task, since it has a rigid and highly crystalline structure [4]. A pretreatment step is necessary to break this physical barrier and make cellulose available to be hydrolyzed. A successful pretreatment can make cellulose more accessible, since the lignocellulosic complex is broken down and its crystalline structure is disrupted [5].

Pretreatment is just one of the operations (others being enzymatic hydrolysis, fermentation and distillation) in the process to produce bioethanol using lignocellulosic material as feedstock (2G ethanol). There are other bottlenecks that make this process difficult on a large scale, such as the biomass fractionation due to the natural biomass diversity and large energy consumption [6–8]. The pretreatment will affect the sequential steps of the process since it is responsible for removing

hemicellulose and lignin, reducing cellulose crystallinity and increasing the porosity of lignocellulosic material to facilitate enzymatic hydrolysis [9].

Due to the importance of biomass pretreatment, it has been studied extensively over the years [10–14] and different methods have been applied, such as mechanical size reduction [15, 16], ultrasound [17, 18], steam explosion [19, 20], alkaline hydrogen peroxide [21, 22], acid [23–27] and organosolv [28–31]. The most suitable technology to carry out pretreatment is not defined and depends on the biomass source and which biomass compound is to be modified [32].

In the last decade, a new class of solvents called ionic liquids (ILs) has been considered for use in biomass pretreatment due to their ability to dissolve cellulose and wood [33–38]. Besides, ILs are thermally and chemically stable, nonflammable and recyclable. Protic ionic liquids (PILs) are salts with a low melting point formed from an acid–base reaction, combining organic cations with organic or inorganic anions, chosen according to the PILs' desired properties [39, 40]. They are cheaper and easier to prepare than aprotic ionic liquids (AILs), although less stable [41, 42]. The possibility of combining ions to acquire a desired property is the reason that PILs are considered designer solvents [43]. The difference between AILs and PILs is the permanency of the positive charge on the cation after its synthesis in AILs and no equilibrium between neutral and ion species, while for PILs the charged and neutral species are in equilibrium [41, 42].

In literature research, there are several articles showing the potential of applying AILs to realize the pretreatment step [44–46]. Sun et al. [44] have demonstrated that 1-ethyl-3-methylimidazolium acetate ($[C_2mim]OAc$) was capable of dissolving completely both softwood (southern yellow pine) and hardwood (red oak) through the heating of the sample. Brandt et al. [45] applied seven ILs which shared the 1-butyl-3-methylimidazolium as cation and proved that the anionic part of AILs has a profound impact on the ability the dissolution of biomass. Teh et al. [46] showed that AILs may potentially be used in the macadamia nut shell pretreatment. The authors have demonstrated that 1-ethyl-3-methylimidazolium acetate [Emin][OAc] can almost entirely dissolve the nuts after 72 h of pretreatment and can be successfully recovered after this step.

There are also some research articles that evaluate PILs for lignocellulose pretreatment [47–53], and those report their ability to dissolve lignin and their inability to dissolve cellulose, which makes them useful for the pretreatment. Some works have demonstrated that PILs produced from the reaction between acetic acid and amines can be effective for lignocellulosic pretreatment, displaying an extraction capacity of over 70% of lignin from lignocellulosic biomass [51, 52, 54]. Achinivu et al. [54] have applied pyrrolidinium acetate ([Pyrr][Ac]) to extract lignin from corn stover achieving more than 70 wt% of the lignin content from biomass. Triethylammonium hydrogen sulfate ($[TEA][HSO_4]$) containing 20 wt% of water content was successfully applied to delignification with a yield over than 85 wt% from *Miscanthus giganteus* at 393.15 K. The use of $[TEA][HSO_4]$ containing 20 wt% of water has showed a delignification yield over than 85 wt% from *Miscanthus giganteus* at 393.15 K [50], and similar results were obtained using the same PIL and sugarcane bagasse as feedstock. Another PIL, such as 1-butylimidazolium hydrogen sulfate ($[HBMIM][HSO_4]$), was less

effective in the delignification step removing 35 wt% of the initial lignin content from cotton stalks [55].

Regarding the dissolution of lignin in PILs, Merino et al. [56] have demonstrated that protic multiaromatic ionic liquids are able to dissolve kraft lignin achieving 38 wt% of lignin solubility using 3-(p-Tolyl)-4,5-diphenyl-1H-imidazolium methanesulfonate in a microwave-assisted irradiation process at 363.15 K in few minutes. Moreover, Rashid et al. [57] have showed that pyridinium formate was capable of dissolving more than 70 wt% of kraft lignin at 348.15 K within just 1 h. Visual methods have been applied to evaluate the ability of solvents to dissolve biopolymers. In recent years, some authors have also used these methods to study cellulose dissolution in different solvents, especially ionic liquids [2, 58–60]. It has been demonstrated that visual methods are fast and allow for the monitoring of the dissolution of lignin and cellulose in ILs, or solvent mixtures containing ILs, using optical microscopy (POM), with or without the use of polarized light [59, 61, 62]. Another advantage of this kind of method is that it demands considerable fewer amounts of solvents, which decreases the expenditure of the studies performed.

In this study, we evaluate the ability of PILs formed by the neutralization reaction of monoethanolamine and carboxylic acids (formic, acetic and propionic) in dissolving lignin, xylose and cellulose. To evaluate the dissolution process, an optical microscope equipped with a temperature controller was used and different heating rates were applied. A synthetic sample was prepared with commercial cellulose, lignin and xylose, with PILs at different conditions of heating rates and biopolymer mass fraction. The main objective of this study was to evaluate the ability of ethanolammonium-based PILs, the effect of the PIL anion structure and the processing conditions, on the dissolution of biopolymers.

Materials and methods

Chemicals

Monoethanolamine (≥98%), α-cellulose (>99%, powder), D-(+)-xylose (≥99%, powder) and lignin alkali (>96%, powder) were purchased from Sigma-Aldrich; formic (≥98%) and acetic acids (glacial) were purchased from Merck; and propionic acid (≥99%) was purchased from Acros Organics, and all were used as received.

PILs' synthesis

The PILs were prepared according to the methodology suggested by Àlvarez et al. [39] and Iglesias et al. [63]. The monoethanolamine (approximately 6.77–8.55 g) was placed inside a three-necked flask equipped with a reflux condenser, a dropping funnel and a PT-100 temperature sensor to read temperature. This set was immersed in a thermostatic bath at 10 °C to avoid temperature increase, while the reaction was happening. Since the reaction is highly exothermic, acid (formic, acetic or propionic) was added dropwise (approximately 6.44–8.23 g) to the flask and a magnetic stirring

bar was used to mix the base and the acid. After the dropwise process, stirring was maintained for a further 24 h at room temperature to complete synthesis. After synthesis, the PILs were submitted to a vacuum (70.0 Pa absolute pressure) with a vigorous agitation and heating (60.0 °C) to remove water and any excess reactant. This process was considered complete when the water content measured by Karl Fischer (Karl Fischer Titrino Plus 848—Metrohm, Switzerland) was equal to or less than 0.5 (wt%). The water content was measured at least in triplicate and presented a standard deviation of 0.015 wt%. The PILs were characterized, and their physical properties were measured and compared with research data. Three PILs were synthesized: 2-hydroxy ethylammonium formate (2-HEAF); 2-hydroxy ethylammonium acetate (2-HEAA); and 2-hydroxy ethylammonium propionate (2-HEAPr).

To do all the measurements realized in this study at least in triplicate was required, approximately, 15.0 g of each PIL synthesized.

Chemical and physical characterization of the PILs

A well-sealed sample was immersed into a thermostatic bath at controlled temperature (PT-100 temperature sensor (± 0.1 K)), and the conductivity of PILs was measured between 30.0 and 70.0 °C (Analyser 650MA, Brazil). Before each conductivity measurement, the cell was cleaned with deionized water and ethanol and dried appropriately. The uncertainty in the conductivity measured was estimated to be 0.05 mS cm^{-1}.

The viscosity and density were also measured in the same temperature range using an automated micro-viscosimeter (Anton Paar, AMVn, Germany) and a digital densimeter (Anton Paar, DMA 5000, Germany—accuracy of 0.05 kg m^3). During the viscosimeter and densimeter operation, the temperature was kept constant within ± 0.01 K. The uncertainty in the densities was estimated to be 0.07 kg m^3).

The thermal stability of synthesized PILs was investigated in a thermogravimetric analyzer (Shimadzu, TGA-50 M, Japan) coupled with a microanalytical scale (Mettler Toledo, MX5, Switzerland) at a fixed heating rate of 10 °C min^{-1}.

Solubility measurements with optical microscopy (POM)

The experimental procedure for observing the biopolymers dissolution was similar to that proposed by Andanson et al. (2014). A solution of 500 mg was prepared containing the PIL and the biopolymer. It was stirred and quickly placed on a concave glass slide. With the biopolymer sample on it, the glass slide was placed on the 30.0 °C-preheated hot stage (Linkam LTS420, UK), which was coupled to the optical microscope (Leica DM2700 M, China).

The sample in the POM was exposed to three different heating rates: 1.0, 0.5 and 0.1 °C min^{-1}. In a typical experiment, the hot stage was heated until all the biopolymers disappeared or until it reached 100 °C. An image (1392×1100 pixels) was recorded at predetermined intervals (every 60 s) with $50\times$ magnification.

Results and discussion

Chemical and physical characterization of the PILs

Conductivity, viscosity and density of the PILs here studied are presented in Fig. 1a–c, and the values are presented in Tables S1, S2 and S3 (Supplementary Material). These properties have been previously reported [64–72]. Discrepancies between our data and those reported in the literature concerning conductivity [64, 65], viscosity [65–67] and density [65–69] were observed. However, it is important to emphasize that substantial discrepancies were also observed in the data from different authors as demonstrated in Fig. 2 and Figs. S1 and S2 (Supplementary Material). These discrepancies can be attributed to different methods being used to determine these data, the limited number of data reported, the method used to synthesize/purify the PILs, the impurities and especially the water content in each sample of PIL. Many authors have reported these data containing different water fractions, so the drying step must be done carefully since this factor plays a major role in properties, especially conductivity and viscosity. Moreover, the research literature-reported data show different water contents, so for this reason it is not possible to discuss these deviations profoundly.

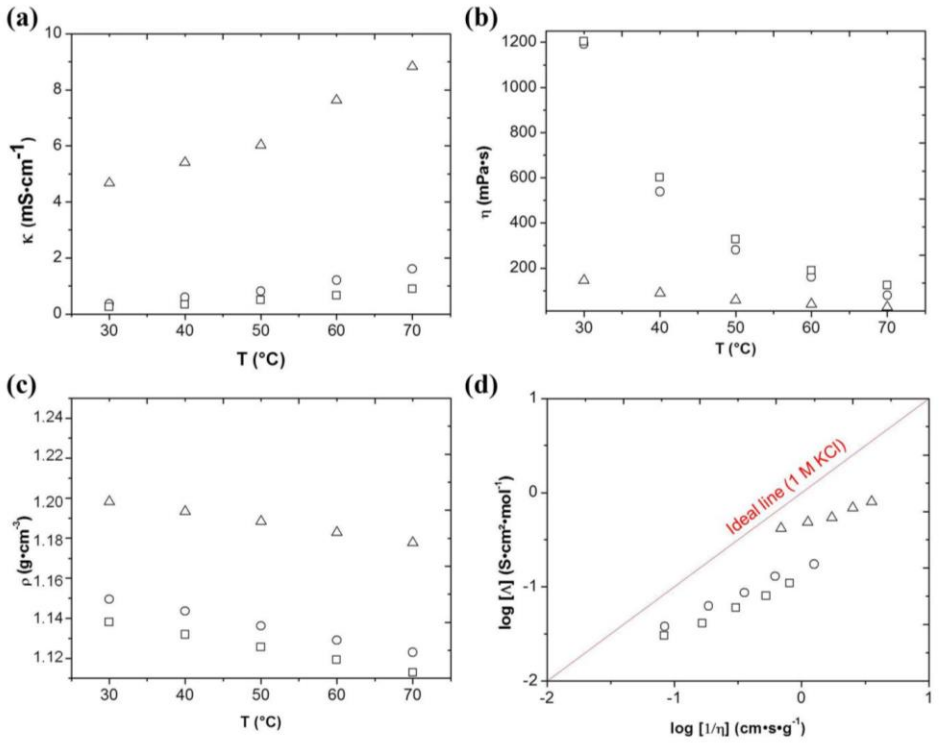

Fig. 1 **a** Conductivity, **b** viscosity, **c** density as a function of temperature, and **d** Walden plot of open triangle: 2-HEAF; open circle: 2-HEAA; and open square: 2-HEAPr

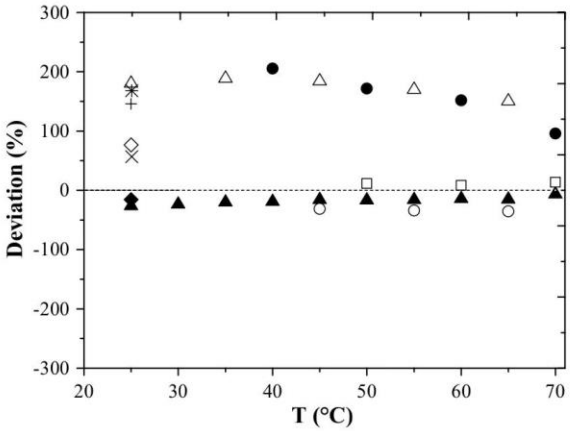

Fig. 2 Relative deviation between the experimental viscosity data of this work and those reported in the literature: filled black triangle: 2-HEAF [60]; open triangle: 2-HEAF [59]; cross: 2-HEAF [64]; open diamond: 2-HEAF [65]; filled black diamond: 2-HEAF [66]; plus: 2-HEAA [66]; open circle: 2-HEAA [59]; asterisk: 2-HEAA [64]; filled black circle: 2-HEAA [61]; open square: 2-HEAPr [61]

The ionicity of the three PILs used in this study was assessed using the Walden plot, providing a measure of effective ion fraction available to be involved in a conduction process [61, 73]. Figure 1d presents the Walden plot displaying 2-HEAF, 2-HEAA and 2-HEAPr. The Walden rule relates the molar conductivity (ionic mobility) to fluidity (inverse of viscosity), establishing that this product is constant for all the cases of electrolytic solution diluted with weakly coordinating ions in a solvent with nonspecific ion–solvent interactions [73, 74]. The ideal line was established using a diluted aqueous KCl solution (1 M) [73, 75]. The PILs which are found below the ideal line are classified as "poor" ionic liquids (low ionicity), while those that are close to the ideal line are considered "good" ionic liquids, and those above this line are considered "super" ionic liquids [73, 76]. Most of the PILs are classified as "poor" ionic liquids, as is the case of the three PILs used in this study. A tendency is observed in these three PILs with 2-HEAF presenting a higher ionicity (closer to the ideal line), followed by 2-HEAA and 2-HEAPr, respectively. The results agree with the difference in ΔpKa of the PILs: 2-HEAF (5.71), 2-HEAA (4.70) and 2-HEAPr (4.58) [77, 78], and the thermal stability measured for the PILs, as shown in Fig. 3.

The greater the ΔpKa is, the greater the reaction is driven to produce PIL, increasing the fraction of ions and consequently increasing the ionicity of the ionic liquid. Additionally, the TGA of the PILs studied (Fig. 3) shows a PIL mass loss at

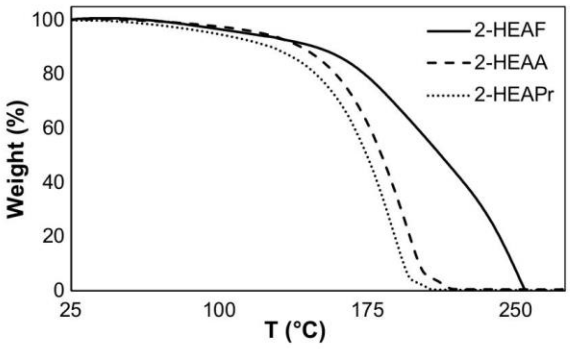

Fig. 3 Variable-temperature TGA heating traces (10 °C min^{-1}) of PILs (black solid line: 2-HEAF; black dash dotted line: 2-HEAA; black dotted line: 2-HEAPr)

temperatures ranging between 100 and 150 °C, which is considerably higher than the temperature range applied in the dissolution assays, so it is not expected considerable PIL mass loss during the experiments, and consequently no composition change of the sample. This behavior can be explained by the formation and subsequent loss of volatile reagents such as carboxylic acids and monoethanolamine, since the acid/base reaction is reversible. It is important to mention that a considerable loss of mass starts at a higher temperature in 2-HEAF than in 2-HEAA and is highest in 2-HEAPr. This is attributed to the proton transfer to the amine group that became more complete and provided a more stable N–H bond. In this context, 2-HEAF is more stable than 2-HEAA and 2-HEAPr, and this stability is associated with ionicity, in the following order: 2-HEAF > 2-HEAA > 2-HEAPr. The ionicity will be related to the dissolution results obtained in the next sections.

Cellulose dissolution

The cellulose dissolution (1 wt%) in 2-HEAF was monitored using the optical microscope coupled to a hot stage employing a heating rate equal to 1 °C min^{-1}. Some images captured during the dissolution process are presented in Fig. 4.

The dark areas in Fig. 4 are the 2-HEAF (liquid phase), and the multi-colored ones are the undissolved cellulose (solid). Figure 4a is captured at 30.0 °C, which is the experiments' initial temperature. Figure 4b is captured at an intermediate temperature (T = 69.7 °C), and Fig. 4c is captured at the end of the experiment, at a higher temperature (T = 100.0 °C).

It was observed that there is no change between the three images, which indicates that 2-HEAF did not dissolve cellulose (1 wt%) at the experimental condition studied. The same result (no cellulose dissolution) was observed in 2-HEAA and 2-HEAPr (Supplementary Material: Figures S3 and S4): All three PILs did not dissolve cellulose, although there was a very low mass fraction in the systems (1 wt%). According to Pinker et al. [58], who investigated the ability of alkanolamine ionic liquids to dissolve crystalline cellulose, 2-HEAF and 2-HEAA were unable to dissolve cellulose at 80.0 °C even after continuous stirring for 12 h, corroborating our results.

The process of cellulose dissolution occurs if a solvent can make stronger hydrogen bonds with cellulose polymers than the cellulose polymers themselves [79].

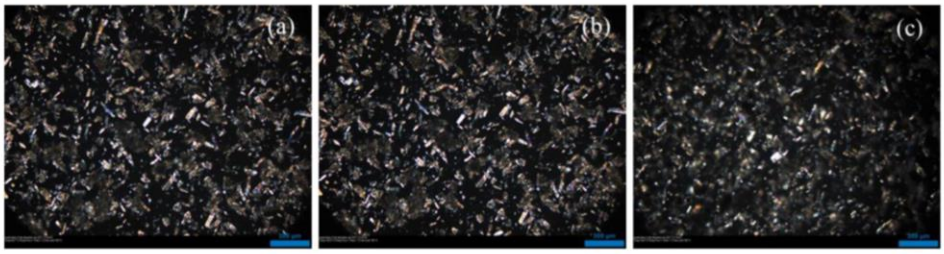

Fig. 4 Images captured by optical microscopy of cellulose (1 wt%) in 2-HEAF using heating rate of 1 °C min^{-1}. **a** T = 30.0 °C; **b** T = 69.7 °C; **c** T = 100.0 °C

Since cellulose dissolution was not observed (Fig. 4), we can conclude that the PILs used were unable to make strong hydrogen bonds with cellulose. Since no changes were observed when cellulose was in contact with the PILs tested at a heating rate of 1 °C min^{-1}, other heating rates were not evaluated.

Xylose dissolution

Recently, Rocha et al. [51] evaluated the potential of 2-HEAA in sugarcane bagasse pretreatment. The authors showed that 5% (w/w) of solids loaded, which were pretreated at 100 °C for 3.5 h, dissolved approximately 37% of hemicellulose. The authors also observed that higher temperatures induce a larger dissolution of hemicellulose in 2-HEAA. Despite xylose not being a hemicellulose (it is a monomer of hemicellulose), we applied the methodology previously used to study cellulose dissolution to evaluate the capacity of 2-HEAF, 2-HEAA and 2-HEAPr to dissolve xylose. The experimental results are presented in Fig. 5 for samples with xylose 15 wt% in each PIL, using a heating rate equal to 0.1 °C min^{-1}. Experiments were done using other xylose contents (5 and 10 wt%), and the images are presented in Supplementary Material (Fig. S5).

The dark areas observed in Fig. 5 are PILs (liquid phase), and the multi-colored ones are non-dissolved xylose (solid phase), which disappears with temperature increase. Full dissolution is achieved when no solids can be visually detected. One can observe that xylose was fully dissolved at 34.3 °C in 2-HEAF, at 41.7 °C in 2-HEAA and at 36.9 °C in 2-HEAPr. Complete dissolution in each case took 43 min, 2 h and 1 h of experiments, respectively. Based on the results displayed, 2-HEAF is the best PIL to dissolve xylose, since it is capable of fully dissolving it at lower temperatures (faster) when compared to 2-HEAA and 2-HEAPr.

The heating rate used was expected to have a direct correlation to the amount of solute dissolved as well as the final temperature and time to achieve full dissolution. To represent this relationship, the amount of solute dissolved was plotted as a function of time and temperature. These plots, called dissolution curves, are shown in Fig. 6 for xylose in 2-HEAF, 2-HEAA and 2-HEAPr at different heating rates. The amount of solute dissolved was quantified using Image Pro-Premier® (v. 9.2) software, which is capable of discerning between dark and multi-colored areas, making it possible to quantify the xylose. The initial area was assumed to be 100%, and the other ones were calculated as demonstrated in Eq. (1).

$$y(t) = \frac{\text{Area}(t)}{\text{Area}\left(t_0\right)} * 100\% \tag{1}$$

where $\text{Area}\left(t_0\right)$ is the area at initial time, and $\text{Area}(t)$ is the area at each selected time (t) every 5 min until the end of experiment.

The heating rates influence the dissolution and, consequently, the final temperature at which solid xylose is no longer observed. When a heating rate of 1 °C min^{-1} is used, the final temperature in which solid xylose is observed is higher than the final temperature observed when a heating rate of 0.5 or 0.1 °C min^{-1} is used.

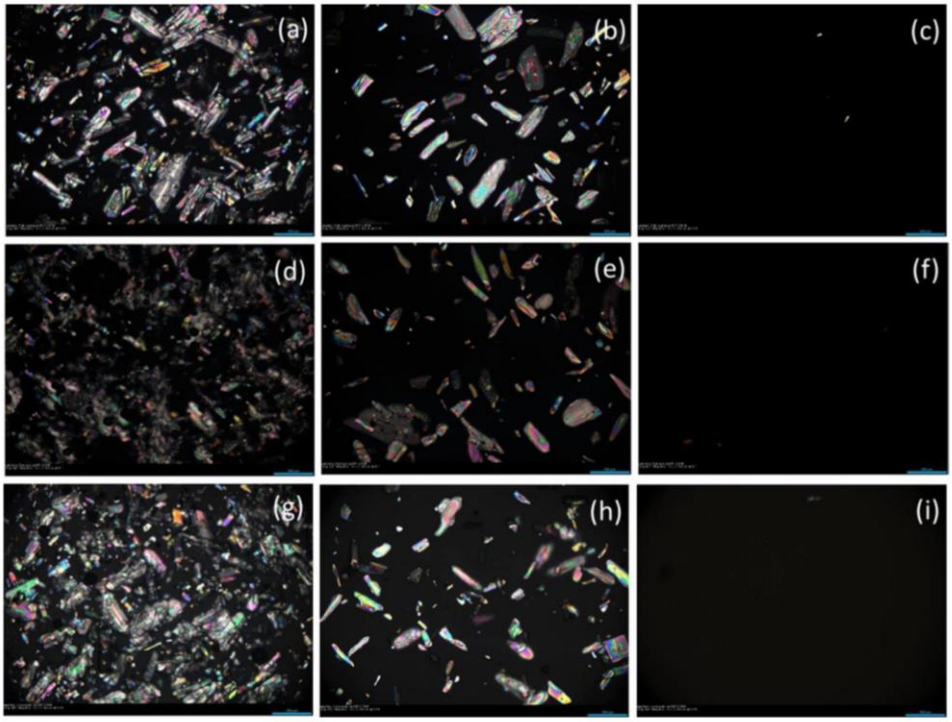

Biopolymer	PIL	Figure		
15 wt% of xylose 0.1 °C.min^{-1}	2-HEAF	(5-a) T = 30.0 °C	(5-b) T = 31.5 °C	(5-c) T = 34.3 °C
	2-HEAA	(5-d) T = 30.0 °C	(5-e) T = 34.0 °C	(5-f) T = 41.7 °C
	2-HEAPr	(5-g) T = 30.0 °C	(5-h) T = 31.5 °C	(5-f) T = 36.9 °C

Fig. 5 Images captured by optical microscopy of xylose in PILs

For example, for a composition equal to 15 wt% of xylose using a heating rate of 1 °C min^{-1}, the final temperature is equal to 63.7, 72.6 and 90 °C in each 2-HEAF, 2-HEAPr and 2-HEAA, respectively. However, lower heating rates will take longer to fully dissolve the xylose. The same behavior was observed by Andanson et al. (2014), and according to the authors, it can be attributed to the solvation process that is controlled by mass transport. Faster heating rates are expected to require less time to achieve full dissolution, since higher temperatures are achieved more quickly making the conclusion of the dissolution process faster.

Besides, it was observed that using a heating rate of 1.0 °C min^{-1}, 5 wt% of xylose is completely dissolved in 2-HEAA after 30 min, while mass fractions of 10% and 15% of full dissolution are observed after 40 and 60 min, respectively. An increase in the mass fraction of xylose implies that more time is required to achieve full dissolution, as well as an increase in temperature will be required to complete the process. Figure 7 summarizes the results of xylose dissolution in all conditions

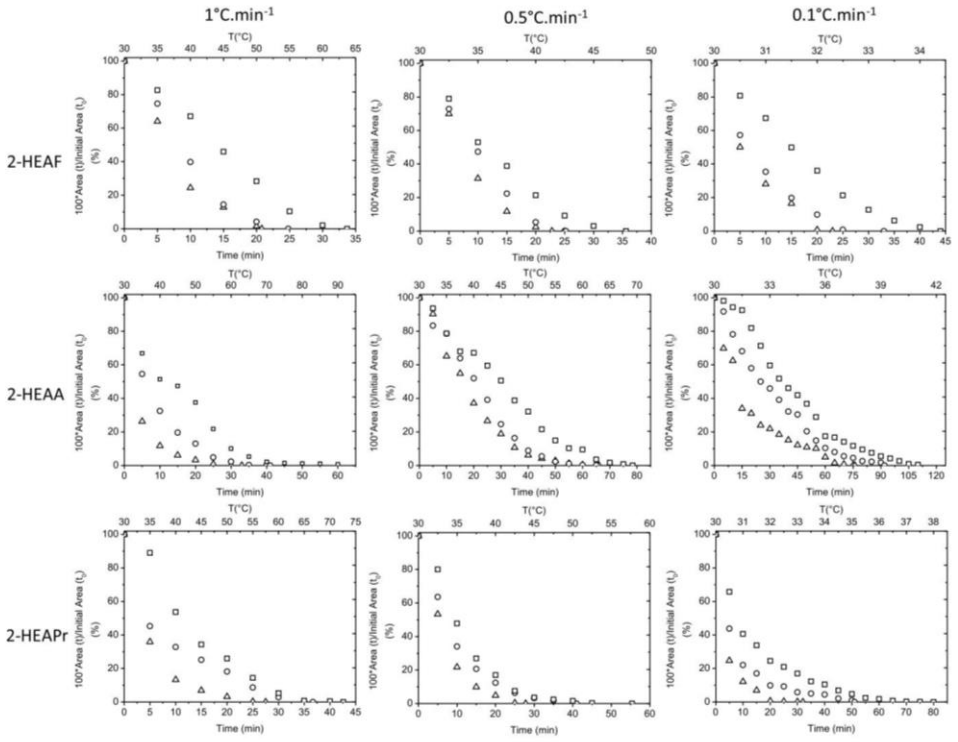

Fig. 6 Dissolution curves of xylose in 2-HEAF, 2-HEAA and 2-HEAPr: heating rates of 0.1, 0.5 and 1 °C min^{-1} (xylose: open triangle: 5 wt%; open circle: 10 wt%; and open square: 15 wt%)

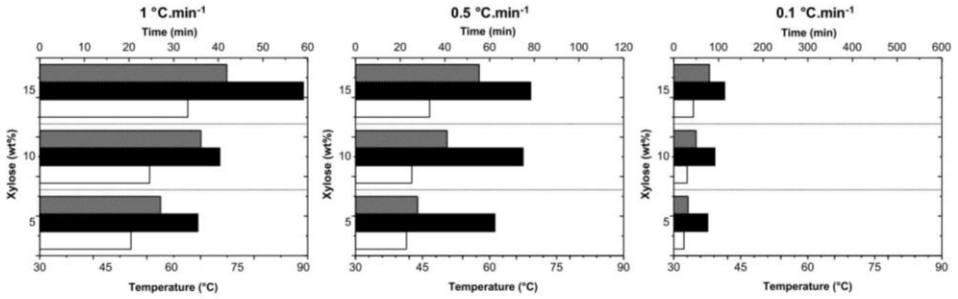

Fig. 7 Time and temperature (T) to achieve the full dissolution of xylose in 2-HEAF (open rectangle), 2-HEAA (filled black rectangle) and 2-HEAPr (filled stripes rectangle): heating rates of 0.1, 0.5 and 1 °C min^{-1}

studied. The final temperature to achieve full xylose dissolution for each PIL used was plotted. Detailed values are presented in Supplementary Material (Tables S7, S8 and S9).

The following behavior could be observed at the different heating rates applied: xylose dissolves faster in 2-HEAF > 2-HEAPr > 2-HEAA, respectively. Based on these results, it is not clear how the alkyl carbon chain length of the PILs anionic part influences the xylose dissolution. It was observed that 2-HEAF, which presents

a smaller anion chain length, dissolved the biopolymer faster than 2-HEAPr and 2-HEAA. However, 2-HEAPr dissolves xylose faster than 2-HEAA while presenting the larger anion chain length. Apparently, the carbon chain length of the anionic part of monoethanolammonium-based PILs has no direct correlation with their ability to dissolve xylose. Achinivu et al. [54] have reported that the solubility of xylan in PILs may be related to their ionicity, and it is favored by the increasing of this property; however, this relation was not observed in this study applying the POM technique.

Lignin dissolution

Lignin dissolution was performed in all PILs tested in this study using the optical microscope. Figure 8 shows the images captured during the lignin dissolution process in 2-HEAF, 2-HEAA and 2-HEAPr at a heating rate of 0.5 °C min^{-1}.

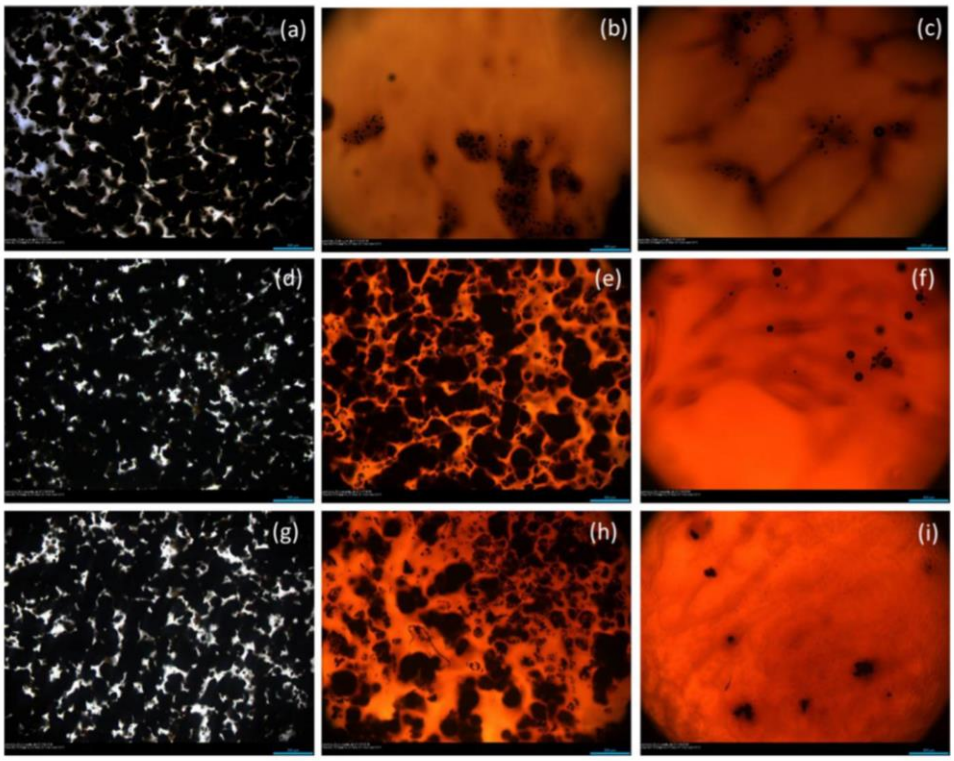

Biopolymer	PIL	Figure		
10 wt% of lignin 0.5 °C.min^{-1}	2-HEAF	(8-a) T = 30.0 °C	(8-b) T = 40.4 °C	(8-c) T = 49.8 °C
	2-HEAA	(8-d) T = 30.0 °C	(8-e) T = 54.8 °C	(8-f) T = 79.8 °C
	2-HEAPr	(8-g) T = 30.0 °C	(8-h) T = 64.2 °C	(8-i) T = 93.7 °C

Fig. 8 Images obtained by optical microscope of lignin in PILs

Figure 8a, d, g shows lignin and dark solid agglomerates at 30 °C. One can perceive that no lignin is dissolved in any of the PILs. The white areas are the PIL phase without dissolved lignin (liquid phase). As the dissolution process occurs, with the temperature increase, the PIL phase turns red (Fig. 8b, e, h) due to the dark agglomerate dissolution, and the lignin amount decreases significantly in the images. The remaining dark areas presented in Fig. 8c, f, i are gaseous bubbles initially trapped and released upon lignin dissolution [59, 61]. These dark points are attributed to gaseous bubbles and not to lignin due to their round shape with a bright point in the middle, noticeably different from dark agglomerates observed at lower temperatures.

The images presented in Fig. 8 demonstrate that lignin is fully dissolved by the PILs used in this study. It is dissolved faster in 2-HEAF than in 2-HEAA and slowest in 2-HEAPr. The time used for a full dissolution of a 10 wt% lignin mass fraction was 39, 99 and 127 min for 2-HEAF, 2-HEAA and 2-HEAPr, respectively. Images of lignin dissolution at other mass fractions can be seen in Supplementary Material (Fig. S6).

Figure 9 summarizes the temperature and time in which the lignin is completely dissolved in each PIL as function of the heating rate used. The temperature and time values to fully dissolve lignin in each of the PILs used are presented in Supplementary Material (Tables S7, S8 and S9).

The 2-HEAPr was able to dissolve 5% of lignin after 71 min ($T > 101$ °C), and 10% after 74 min ($T > 104$ °C), using a heating rate of 1 °C min^{-1}. Nevertheless, 2-HEAPr was not able to dissolve lignin in a concentration of 15 wt%, even when the temperature reached 130 °C after 100 min of experiment. When smaller heating rates were applied, the 2-HEAPr was able to dissolve lignin at lower temperatures, demonstrating that this parameter is an important factor to be considered. The same behavior observed of xylose was also observed of lignin, meaning that an increase in the solution's lignin mass fraction will require more time to reach its full dissolution. Moreover, the use of lower heating rates implies an increase in the time necessary to fully dissolve lignin, as observed by Andanson et al. [61] in cellulose dissolution.

When comparing the PILs and their ability to dissolve lignin, the experiments showed that lignin is dissolved faster in 2-HEAF and slowest in 2-HEAPr. Based on these observations, it may be hypothesized that lignin dissolution decreases with an increase in the precursor's alkyl chain length for monoethanolamine-based PILs, and

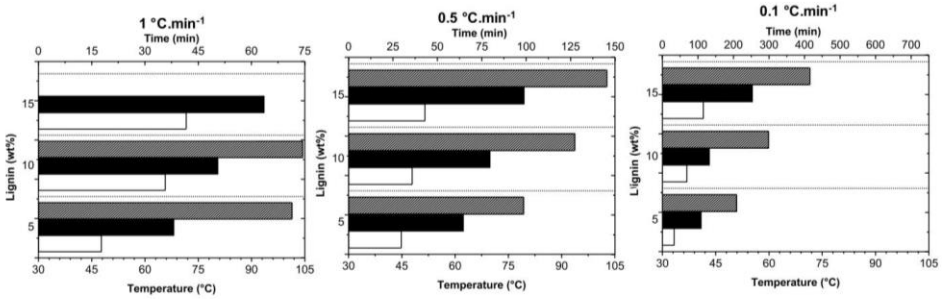

Fig. 9 Time and temperature (T) of lignin dissolution in 2-HEAF (open rectangle), 2-HEAA (filled black rectangle) and 2-HEAPr (filled stripes rectangle): heating rates of 0.1, 0.5 and 1 °C min^{-1}

this hypothesis is supported by Rashid et al. [57] who evaluated pyridium-based PIL and carboxylic acids (formic, acetic and propionic) as a proton donor to solubilize kraft lignin, concluding the same. Besides, as described in "Chemical and physical characterization of the PILs" section, the PILs' ionicity decreases in the following order: 2-HEAF > 2-HEAA > 2-HEAPr, so we conclude that the higher ionicity of 2-HEAF makes this PIL capable of dissolving lignin faster than the others tested, and 2-HEAPr is the slowest among those tested. This conclusion is supported by Rashid et al. [57], Hart et al. [80] and Glas et al. [81], that concluded that low hydrogen basicity of anionic part of ILs, and also shorter alkyl chain length favored the lignin dissolution.

A more direct comparison between the experimental data here presented and those reported in the literature for PILs [51, 52] is difficult since these authors used sugarcane bagasse and cashew apple bagasse, and in our work we have evaluated the components of lignocellulosic biomass in isolation. These authors have concluded that 2-HEAA was able to be used in the pretreatment step of the sugarcane bagasse, and in our study, we demonstrate that monoethanolammonium-based PILs can be used to dissolve the xylose and also lignin. However, the 2-HEAF dissolves xylose faster, so we expect that if it had been used in lignocellulosic biomass pretreatment it would present a better result too.

Lignin + xylose dissolution in 2-HEAF

The main components of lignocellulosic biomass are lignin, hemicellulose and cellulose. As presented before, cellulose is not dissolved by any of the PILs used in this study. However, we do not know how the presence of xylose can interfere in the lignin dissolution process. Thus, in order to verify how the presence of xylose interferes in the lignin dissolution process, some experiments were done at 1 °C min^{-1} with 2-HEAF, which presents the greatest dissolution capacity in samples composed of lignin and xylose in different proportions as presented in Table 1. Typical images of the experiments are presented in Fig. 10 (also in Fig. S7, in Supplementary Material), and Table 1 presents the time necessary to achieve full biopolymer dissolution.

In Fig. 10a, it is possible to observe solid lignin (dark color) and a bright well-defined shape that is xylose. Although xylose crystals seem to be hidden or even equal to lignin, it is possible to note the differences between them while the dissolution process is ongoing, as can be noted in Fig. 10b in regions indicated by the white circles. This experiment shows xylose full dissolution after approximately 22 min and lignin after approximately 28 min. A comparison of this result with the previous one obtained using the same amount of pure lignin (5 wt%) in 2-HEAF and

Table 1 Time needed to achieve the full dissolution of xylose and lignin

Xylose (wt%)	Lignin (wt%)	t_{xylose} (min)	t_{lignin} (min)
5	5	21.8	27.8
5	10	21.8	38.7
10	5	26.8	28.7

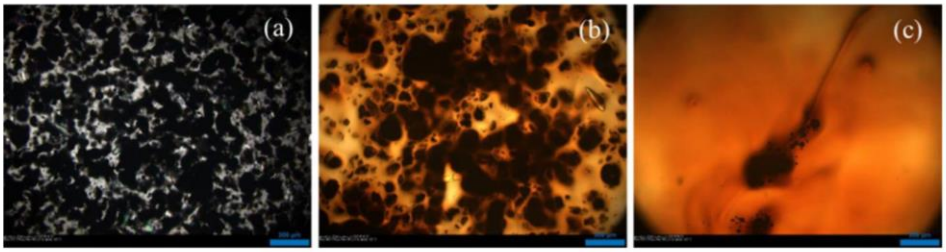

Fig. 10 Images obtained by optical microscope of lignin + xylose in 2-HEAF. 5 wt% of lignin and 5 wt% of xylose in 2-HEAF at heating rate of 1.0 °C min^{-1}: **a** $T = 30.0$ °C; **b** $T = 44.9$ °C; **c** $T = 57.8$ °C

pure xylose (5 wt%) in 2-HEAF shows that when both biopolymers are mixed, the time required for dissolution is higher (1 min higher than for pure xylose and 10 min higher than for pure lignin). In other words, both lignin and xylose influence each other's dissolution process, increasing the dissolution time by 4.8% and 57% if they are mixed.

Moreover, 2-HEAF can dissolve xylose more easily than lignin since it takes less time to dissolve lignin than the others. It is expected that biomass dissolution will take more time to be completed due to the complex rigid structure formed by cellulose, hemicellulose and lignin. Finally, the dissolution of xylose and lignin is easier in 2-HEAF, which is related to the higher ionicity of this PIL, when compared to 2-HEAA and 2-HEAPr. This result is corroborated by Achinivu et al. [54], Hart el al. [80] and Glas et al. [81]. It is known that the ionicity is related to the extent of the proton transfer, and the reaction is more driven to produce PIL, increasing the fraction of ions [73]. These ions interact with lignin and xylose and favor their dissolution.

Conclusions

Cellulose, xylose and lignin dissolution in 2-HEAF, 2-HEAA and 2-HEAPr (with 0.5 wt% water) using an optical microscope coupled with a hot stage was determined. Three different heating rates were applied to analyze its influence on the dissolution process. It was possible to conclude that the higher the heating rate is, the higher the final temperature to achieve full dissolution.

It was verified that these PILs do not dissolve cellulose, but they can dissolve xylose and lignin. Xylose is dissolved faster in 2-HEAF, in 2-HEAPr and in 2-HEAA (in that order), whereas lignin was dissolved faster in 2-HEAF, 2-HEAA and 2-HEAPr, in that order. When a mixture of lignin and xylose was dissolved, it was observed that the full dissolution time of both biopolymers increased by 4.8% and by 57%, indicating that lignin interferes with xylose dissolution and vice versa.

The best PIL tested was 2-HEAF because it dissolves the biopolymer faster than the others. Moreover, it presents lower viscosity and higher conductivity, being classified as more "ionic" than 2-HEAA and 2-HEAPr according to Walden plot. Based on the results obtained, 2-HEAF demonstrated its potential for the extraction of

lignin and xylose from biomass and its use is recommended for biomass pretreatment. Moreover, this study shows that the POM technique, which requires a small quantity of sample, can be used to study the cellulose, xylose or lignin dissolution in PILs. The experimental results demonstrate that the technique used in this study can be applied to rapidly scan potential solvents for cellulose, xylose or lignin.

Acknowledgements This study was financed in part by the Coordenação de Aperfeiçoamento de Pessoal de Nível Superior—Brasil (CAPES)—Finance Code 001. The authors also would like to thank the following national funding agencies FAPESP [2014/21252-0], CNPq [310272/2017-3, 140723/2016-1, 169743/2018-7] and FAEPEX/UNICAMP for financial support. The authors also thank Professor João Coutinho for his kindly suggestion and discussion.

Compliance with ethical standards

Conflict of interest The authors declare that they have no conflict of interest.

References

1. van Haveren J, Scott EL, Sanders J (2008) Bulk chemicals from biomass. Biofuels Bioprod Biorefining 2:41–57. https://doi.org/10.1002/bbb.43
2. Zavrel M, Bross D, Funke M, Buchs J, Spiess AC (2009) High-throughput screening for ionic liquids dissolving (ligno-)cellulose. Bioresour Technol 100:2580–2587. https://doi.org/10.1016/j.biortech.2008.11.052
3. Yang B, Wyman E (2008) Pretreatment: the key to unlocking low-cost cellulosic ethanol. Biofuels Bioprod Biorefining 2:26–40. https://doi.org/10.1002/bbb.49
4. Kim TH (2013) Pretreatment of lignocellulosic biomass. In: Bioprocessing technologies in biorefinery for sustainable production of fuels, chemicals, and polymers, pp 91–105
5. Mosier N, Wyman CE, Dale BD, Elander RT, Lee YY, Holtzapple M, Ladisch CM (2005) Features of promising technologies for pretreatment of lignocellulosic biomass. Bioresour Technol 96:673–686. https://doi.org/10.1016/j.biortech.2004.06.025
6. Taha M, Foda M, Shahsavari E, Aburto-medina A, Adetutu E, Ball A (2016) Commercial feasibility of lignocellulose biodegradation: possibilities and challenges. Curr Opin Biotechnol 38:190–197. https://doi.org/10.1016/j.copbio.2016.02.012
7. Tye YY, Lee KT, Wan Abdullah WN, Leh CP (2016) The world availability of non-wood lignocellulosic biomass for the production of cellulosic ethanol and potential pretreatments for the enhancement of enzymatic saccharification. Renew Sustain Energy Rev 60:155–172. https://doi.org/10.1016/j.rser.2016.01.072
8. Paulová L, Melzoch K, Rychtera M, Patáková P (2013) Production of 2nd generation of liquid biofuels. In: Fang Z (ed) Liquid, gaseous and solid biofuels: conversion techniques, 1st edn. INTECH Open Acess Publisher, Rijeka, pp 47–74
9. Kumar P, Barret DM, Delwiche MJ, Stroeve P (2009) Methods for pretreatment of lignocellulosic biomass for efficient hydrolysis and biofuel production. Ind Eng Chem Res 48:3713–3729. https://doi.org/10.1021/ie801542g
10. Yu Q, Zhuang X, Shuangliang LV, Zhang Y, Yuan Z, Qi W, Wang Q, Wang W, Tan X (2013) Liquid hot water pretreatment of sugarcane bagasse and its comparison with chemical pretreatment methods for the sugar recovery and structural changes. Bioresour Technol 129:592–598. https://doi.org/10.1016/j.biortech.2012.11.099
11. Travaini R, Otero MDM, Coca M, Da-Silva R, Bolado S (2013) Sugarcane bagasse ozonolysis pretreatment: effect on enzymatic digestibility and inhibitory compound formation. Bioresour Technol 133:332–339. https://doi.org/10.1016/j.biortech.2013.01.133
12. Moretti MMS, Bocchinni-Martins DA, Nunes CCC, Villena MA, Perrone OM, Silva R, Boscolo M, Gomes E (2014) Pretreatment of sugarcane bagasse with microwaves irradiation and

its effects on the structure and on enzymatic hydrolysis. Appl Energy 122:189–195. https://doi.org/10.1016/j.apenergy.2014.02.020
13. Bian J, Peng F, Peng X, Xiao X, Peng P, Xu F, Sun R (2014) Effect of [Emim]Ac pretreatment on the structure and enzymatic hydrolysis of sugarcane bagasse cellulose. Carbohydr Polym 100:211–217. https://doi.org/10.1016/j.carbpol.2013.02.059
14. Martins LHS, Rabelo SM, Costa AC (2015) Effects of the pretreatment method on high solids enzymatic hydrolysis and ethanol fermentation of the cellulosic fraction of sugarcane bagasse. Bioresour Technol 191:312–321. https://doi.org/10.1016/j.biortech.2015.05.024
15. Tassinari T, Macy C, Spano L (1980) Energy requirements and process design considerations in compression-milling pretreatment of cellulosic wastes for enzymatic hydrolysis. Biotechnol Bioeng 22:1689–1705. https://doi.org/10.1002/bit.260220811
16. Silva AS, Inoue H, Endo T, Yano S, Bom EPS (2010) Milling pretreatment of sugarcane bagasse and straw for enzymatic hydrolysis and ethanol fermentation. Bioresour Technol 101:7402–7409. https://doi.org/10.1016/j.biortech.2010.05.008
17. Bussemaker MJ, Zhang D (2013) Effect of ultrasound on lignocellulosic biomass as a pretreatment for biorefinery and biofuel applications. Ind Eng Chem Res 52:3563–3580. https://doi.org/10.1021/ie3022785
18. Imai M, Ikari K, Suzuki I (2004) High-performance hydrolysis of cellulose using mixed cellulase species and ultrasonication pretreatment. Biochem Eng J 17:79–83. https://doi.org/10.1016/S1369-703X(03)00141-4
19. Pielhop T, Amgarten J, Von Rohr PR, Studer MH (2016) Steam explosion pretreatment of softwood: the effect of the explosive decompression on enzymatic digestibility. Biotechnol Biofuels 9:1–13. https://doi.org/10.1186/s13068-016-0567-1
20. Grous WR, Converse AO, Grethlein HE (1986) Effect of steam explosion pretreatment on pore size and enzymatic hydrolysis of poplar. Enzyme Microb Technol 8:274–280. https://doi.org/10.1016/0141-0229(86)90021-9
21. Azzam AM (1989) Pretreatment of cane bagasse with alkaline hydrogen peroxide for enzymatic hydrolysis of cellulose and ethanol fermentation. J Environ Sci Heal Part B 24:421–433. https://doi.org/10.1080/03601238909372658
22. Rabelo SC, Andrade RR, Maciel Filho R, Costa AC (2014) Alkaline hydrogen peroxide pretreatment, enzymatic hydrolysis and fermentation of sugarcane bagasse to ethanol. Fuel 136:349–357. https://doi.org/10.1016/j.fuel.2014.07.033
23. Saha BC, Iten LB, Cotta MA, Wu YV (2005) Dilute acid pretreatment, enzymatic saccharification and fermentation of wheat straw to ethanol. Process Biochem 40:3693–3700. https://doi.org/10.1016/j.procbio.2005.04.006
24. Li C, Knierim B, Manisseri C, Arora R, Scheller HV, Auer M, Vogel KP, Simmons BA, Singh S (2010) Comparison of dilute acid and ionic liquid pretreatment of switchgrass: biomass recalcitrance, delignification and enzymatic saccharification. Bioresour Technol 101:4900–4906. https://doi.org/10.1016/j.biortech.2009.10.066
25. Shen Z, Jin C, Pei H, Shi J, Liu L, Sun J (2014) Pretreatment of corn stover with acidic electrolyzed water and $FeCl_3$ leads to enhanced enzymatic hydrolysis. Cellulose 21:3383–3394. https://doi.org/10.1007/s10570-014-0353-9
26. Demirel F, Germec M, Coban HB, Turhan I (2018) Optimization of dilute acid pretreatment of barley husk and oat husk and determination of their chemical composition. Cellulose 25:6377–6393. https://doi.org/10.1007/s10570-018-2022-x
27. Loow YL, Wu TY, Jahim JM, Mohammad AW, Teoh WH (2016) Typical conversion of lignocellulosic biomass into reducing sugars using dilute acid hydrolysis and alkaline pretreatment. Cellulose 23:1491–1520. https://doi.org/10.1007/s10570-016-0936-8
28. Zhao X, Cheng K, Liu D (2009) Organosolv pretreatment of lignocellulosic biomass for enzymatic hydrolysis. Appl Microbiol Biotechnol 82:815–827. https://doi.org/10.1007/s00253-009-1883-1
29. Zhang Z, Harrison MD, Rackemann DW, Doherty WOS, O'Hara IA (2016) Organosolv pretreatment of plant biomass for enhanced enzymatic saccharification. Green Chem 18:360–381. https://doi.org/10.1039/C5GC02034D
30. Mou H, Wu S (2017) Comparison of hydrothermal, hydrotropic and organosolv pretreatment for improving the enzymatic digestibility of bamboo. Cellulose 24:85–94. https://doi.org/10.1007/s10570-016-1117-5

31. Zhang H, Wu S (2015) Generation of lignin and enzymatically digestible cellulose from ethanol-based organosolv pretreatment of sugarcane bagasse. Cellulose 22:2409–2418. https://doi.org/10.1007/s10570-015-0678-z
32. Wyman CE, Dale BE, Elander RT, Holtzapple M, Ladisch MR, Lee YY (2005) Comparative sugar recovery data from laboratory scale application of leading pretreatment technologies to corn stover. Bioresour Technol 96:2026–2032. https://doi.org/10.1016/j.biortech.2005.01.018
33. Swatloski RP, Spear SK, Holbrey JD, Rogers RD (2002) Dissolution of cellulose with ionic liquids. J Am Chem Soc 124:4974–4975. https://doi.org/10.1021/ja025790m
34. Pu Y, Jiang N, Ragauskas AJ (2007) Ionic liquid as a green solvent for lignin. J Wood Chem Technol 27:23–33. https://doi.org/10.1080/02773810701282330
35. D'Andola G, Szarvas L, Massonne K, Stegmann V (2008) Ionic liquids for solubilizing polymers. Wo pat 43837
36. Fort DA, Remsing RC, Swatloski RP, Moyna P, Moyna G, Rogers RD (2007) Can ionic liquids dissolve wood? Processing and analysis of lignocellulosic materials with 1-*n*-butyl-3-methylimidazolium chloride. Green Chem 9:63–69. https://doi.org/10.1039/B607614A
37. Zhao H, Baker GA, Song Z, Olubajo O, Crittle T, Peters D (2008) Designing enzyme-compatible ionic liquids that can dissolve carbohydrates. Green Chem 10:696. https://doi.org/10.1039/b801489b
38. Saha KS, Dasgupta J, Chakraborty S, Antunes FAF, Sikder J, Curcio S, dos Santos JC, Arafat HA, da Silva SS (2017) Optimization of lignin recovery from sugarcane bagasse using ionic liquid aided pretreatment. Cellulose 24:3191–3207. https://doi.org/10.1007/s10570-017-1330-x
39. Álvarez VH, Dosil N, Gonzalez-Cabaleiro R, Mattedi S, Martin-Pastor M, Iglesias M (2010) Brønsted ionic liquids for sustainable processes: synthesis and physical properties. J Chem Eng Data 55:625–632. https://doi.org/10.1021/je900550v
40. Wassercheid P, Welton T (2008) Ionic liquids in synthesis. Wiley, New York
41. Mirjafari A, Pham LN, Mccabe JR, Mobarrez N, Salter EA, Wierzbicki A, West KN, Sykora RE, Davis JH Jr (2013) Building a bridge between aprotic and protic ionic liquids. RSC Adv 3:337–340. https://doi.org/10.1039/c2ra22752e
42. Greaves TL, Weerawardena A, Fong C, Krodkiewska I, Drummond CJ (2006) Protic ionic liquids: solvents with tunable phase behavior and physicochemical properties. J Phys Chem B 110:22479–22487. https://doi.org/10.1021/jp0634048
43. Huddleston JG, Willauer HD, Swatloski RP, Vissier AE, Rogers RD (1998) Room temperature ionic liquids as novel media for 'clean' liquid–liquid extraction. Chem Commun. https://doi.org/10.1039/A803999B
44. Sun N, Rahman M, Qin Y, Maxim ML, Rodríguez H, Rogers RD (2009) Complete dissolution and partial delignification of wood in the ionic liquid 1-ethyl-3-methylimidazolium acetate. Green Chem 11:646–655. https://doi.org/10.1039/b822702k
45. Brandt A, Hallett JP, Leak DJ, Murphy RJ, Welton T (2010) The effect of the ionic liquid anion in the pretreatment of pine wood chips. Green Chem 12:672–679. https://doi.org/10.1039/b918787a
46. Teh WX, Hossain MM, To TQ, Aldous L (2015) Pretreatment of macadamia nut shells with ionic liquids facilitates both mechanical cracking and enzymatic hydrolysis. ACS Sustain Chem Eng 3:992–999. https://doi.org/10.1021/acssuschemeng.5b00126
47. George A, Brandt A, Tran K, Zahari SMSNS, Klein-Marcuschamer D, Sun N, Sathitsuksanoh N, Shi J, Stavila V, Parthasarathi R, Singh S, Holmes BM, Welton T, Simmons BA, Hallett JP (2015) Design of low-cost ionic liquids for lignocellulosic biomass pretreatment. Green Chem 17:1728–1734. https://doi.org/10.1039/c4gc01208a
48. Asakawa A, Kohara M, Sasaki C, Asada C, Nakamura Y (2015) Comparison of choline acetate ionic liquid pretreatment with various pretreatments for enhancing the enzymatic saccharification of sugarcane bagasse. Ind Crops Prod 71:147–152. https://doi.org/10.1016/j.indcrop.2015.03.073
49. An YX, Zong MH, Wu H, Li N (2015) Pretreatment of lignocellulosic biomass with renewable cholinium ionic liquids: biomass fractionation, enzymatic digestion and ionic liquid reuse. Bioresour Technol 192:165–171. https://doi.org/10.1016/j.biortech.2015.05.064
50. Brandt-Talbot A, Gschwend FJV, Fennell PS, Lammens TM, Tan B, Weale J, Hallett JP (2017) An economically viable ionic liquid for the fractionation of lignocellulosic biomass. Green Chem 19:3078–3102. https://doi.org/10.1039/c7gc00705a
51. Rocha EGA, Pin TC, Rabelo SC, Costa AC (2017) Evaluation of the use of protic ionic liquids on biomass fractionation. Fuel 206:145–154. https://doi.org/10.1016/j.fuel.2017.06.014

52. Reis CLB, Silva LMA, Rodrigues THS, Félix AKN, Santiago-Aguiar RS, Km Canuto, Rocha MVP (2017) Pretreatment of cashew apple bagasse using protic ionic liquids: enhanced enzymatic hydrolysis. Bioresour Technol 224:694–701. https://doi.org/10.1016/j.biortech.2016.11.019
53. Brandt A, Gräsvik J, Hallett JP, Welton T (2013) Deconstruction of lignocellulosic biomass with ionic liquids. Green Chem 15:550–583. https://doi.org/10.1039/c2gc36364j
54. Achinivu EC, Howard RM, Li G, Gracz H, Henderson WA (2014) Lignin extraction from biomass with protic ionic liquids. Green Chem 16:1114–1119. https://doi.org/10.1039/c3gc42306a
55. Semerci I, Güler F (2018) Protic ionic liquids as effective agents for pretreatment of cotton stalks at high biomass loading. Ind Crops Prod 125:588–595. https://doi.org/10.1016/j.indcrop.2018.09.046
56. Merino O, Fundora-Galano G, Luque R, Martínez-Palou R (2018) Understanding microwave-assisted lignin solubilization in protic ionic liquids with multiaromatic imidazolium cations. ACS Sustain Chem Eng 6:4122–4129. https://doi.org/10.1021/acssuschemeng.7b04535
57. Rashid T, Kait CF, Regupathi I, Murugesan T (2016) Dissolution of kraft lignin using protic ionic liquids and characterization. Ind Crops Prod 84:284–293. https://doi.org/10.1016/j.indcrop.2016.02.017
58. Pinkert A, Marsh KN, Pang S (2010) Reflections on the solubility of cellulose. Ind Eng Chem Res 49:11121–11130. https://doi.org/10.1021/ie1006596
59. Fitzpatrick M, Champagne P, Cunningham MF, Falkenburger C (2012) Application of optical microscopy as a screening technique for cellulose and lignin solvent systems. Can J Chem Eng 90:1142–1152. https://doi.org/10.1002/cjce.20628
60. Deguchi S, Tsujii K, Horikoshi K (2008) Crystalline-to-amorphous transformation of cellulose in hot and compressed water and its implications for hydrothermal conversion. Green Chem 10:191–196. https://doi.org/10.1039/B713655B
61. Andanson J-H, Bordes E, Devémy J, Leroux F, Padua AAH, Gomes MFC (2014) Understanding the role of co-solvents in the dissolution of cellulose in ionic liquids. Green Chem 16:2528–2538. https://doi.org/10.1039/c3gc42244e
62. Abdulkhani A, Hojati Marvast E, Ashori A, Karimi AN (2013) Effects of dissolution of some lignocellulosic materials with ionic liquids as green solvents on mechanical and physical properties of composite films. Carbohydr Polym 95:57–63. https://doi.org/10.1016/j.carbpol.2013.02.040
63. Iglesias M, Gonzalez-Olmos R, Cota I, Medina F (2010) Brønsted ionic liquids: study of physicochemical properties and catalytic activity in aldol condensations. Chem Eng J 162:802–808. https://doi.org/10.1016/j.cej.2010.06.008
64. Cota I, Gonzalez-Olmos R, Iglesias M, Medina F (2007) New short aliphatic chain ionic liquids: synthesis, physical properties, and catalytic activity in aldol condensations. J Phys Chem B 111:12468–12477. https://doi.org/10.1021/jp073963u
65. Pinkert A, Ang KL, Marsh KN, Pang S (2011) Density, viscosity and electrical conductivity of protic alkanolammonium ionic liquids. Phys Chem Chem Phys 13:5136. https://doi.org/10.1039/c0cp02222e
66. Ghatee MH, Bahrami M, Khanjari N, Firouzabadi H, Ahmadi Y (2012) A functionalized high-surface-energy ammonium-based ionic liquid: experimental measurement of viscosity, density, and surface tension of (2-hydroxyethyl)ammonium formate. J Chem Eng Data 57:2095–2101. https://doi.org/10.1021/je201055w
67. Camargo D, Andrade RS, Ferreira GA, Mazzer H, Cardozo-Filho L, Iglesias M (2016) Investigation of the rheological properties of protic ionic liquids. J Phys Org Chem 29:604–612. https://doi.org/10.1002/poc.3553
68. Álvarez VH, Mattedi S, Martin-Pastor M, Aznar M, Iglesias M (2011) Thermophysical properties of binary mixtures of {ionic liquid 2-hydroxy ethylammonium acetate + (water, methanol, or ethanol)}. J Chem Thermodyn 43:997–1010. https://doi.org/10.1016/j.jct.2011.01.014
69. Kurnia KA, Wilfred CD, Murugesan T (2009) Thermophysical properties of hydroxyl ammonium ionic liquids. J Chem Thermodyn 41:517–521. https://doi.org/10.1016/j.jct.2008.11.003
70. Yuan XL, Zhang SJ, Lu XM (2007) Hydroxyl ammonium ionic liquids: synthesis, properties, and solubility of so2. J Chem Eng Data 52:596–599. https://doi.org/10.1021/je060479w
71. Bicak N (2005) A new ionic liquid: 2-hydroxy ethylammonium formate. J Mol Liq 116:15–18. https://doi.org/10.1016/j.molliq.2004.03.006
72. Greaves TL, Drummond CJ (2008) Protic ionic liquids: properties and applications. Chem Rev 108:206–237. https://doi.org/10.1021/cr068040u

73. Yoshizawa M, Xu W, Angell CA (2003) Ionic liquids by proton transfer: vapor pressure, conductivity, and the relevance of ΔpKa from aqueous solutions. J Am Chem Soc 125:15411–15419. https://doi.org/10.1021/ja035783d
74. Stoimenovski J, Izgorodina EI, MacFarlane DR (2010) Ionicity and proton transfer in protic ionic liquids. Phys Chem Chem Phys 12:10341–10347. https://doi.org/10.1039/c0cp00239a
75. Angell CA, Byrne N, Belieres JP (2007) Parallel developments in aprotic and protic ionic liquids: physical chemistry and applications. Acc Chem Res 40:1228–1236. https://doi.org/10.1021/ar7001842
76. Xu W (2003) Solvent-free electrolytes with aqueous solution-like conductivities. Science 302:422–425. https://doi.org/10.1126/science.1090287
77. Bacarella AL, Grunwald E, Marshall HP, Purlee EL (1955) The potentiometric measurement of acid dissociation constants and pH in the system methanol-water. pka values for carboxylic acids and anilinium ions. J Org Chem 20:747–762. https://doi.org/10.1021/jo01124a007
78. Hancock RD (1981) The chelate effect in complexes with ethanolamine. Inorg Chim Acta 49:145–148. https://doi.org/10.1016/S0020-1693(00)90474-2
79. Feng L, Chen ZL (2008) Research progress on dissolution and functional modification of cellulose in ionic liquids. J Mol Liq 142:1–5. https://doi.org/10.1016/j.molliq.2008.06.007
80. Hart WES, Harper JB, Aldous L (2015) The effect of changing the components of an ionic liquid upon the solubility of lignin. Green Chem 17:214–218. https://doi.org/10.1039/c4gc01888e
81. Glas D, Van Doorslaer C, Depuydt D et al (2015) Lignin solubility in non-imidazolium ionic liquids. J Chem Technol Biotechnol 90:1821–1826. https://doi.org/10.1002/jctb.4492

Supplementary Material

Dissolution of lignocellulosic biopolymers in ethanolamine-based protic ionic liquids

Rafael M. Dias, Filipe H. B. Sosa, Mariana C. da Costa.*

Department of Process and Product Design (DDPP) - School of Chemical Engineering (FEQ), University of Campinas (UNICAMP), 13083-852, Campinas, São Paulo, Brazil.

*Corresponding author: Mariana Conceição da Costa
Phone number: +551935213962
E-mail address: mcosta@feq.unicamp.br

List of Content

S1 – PROPERTIES OF PILS: CONDUCTIVITY, DENSITY AND VISCOSITY AS A FUNCTION OF TEMPERATURE

The conductivity, density and viscosity of PILs as a function of temperature are presented in Table S1, S2 and S3, respectively. . Equation (1), equation (2) and equation (3) were used to fit conductivity, density and viscosity experimental data, respectively, and the values were compared with previous research literature. The coefficients and R^2 are presented in Table S4, S5 and S6.

Table S1 Conductivity of PILs as a function of temperature

PIL	T (K)	Conductivity ($S.cm^{-1}$)	PIL	T (K)	Conductivity ($S.cm^{-1}$)	PIL	T (K)	Conductivity ($S.cm^{-1}$)
2-HEAF	293.15	0.00397	2-HEAA	293.15	0.000167	2-HEAPr	293.15	0.000176
	303.15	0.00467		303.15	0.000360		303.15	0.000255
	313.15	0.00540		313.15	0.000591		313.15	0.000343
	323.15	0.00602		323.15	0.000812		323.15	0.000500
	333.15	0.00762		333.15	0.001204		333.15	0.000662
	343.15	0.00882		343.15	0.001611		343.15	0.000898

Table S2 Density of PILs as a function of temperature

PIL	T (K)	Density ($g.cm^{-3}$)	PIL	T (K)	Density ($g.cm^{-3}$)	PIL	T (K)	Density ($g.cm^{-3}$)
2-HEAF	293.15	1.20306	2-HEAA	293.15	1.15536	2-HEAPr	293.15	1.14433
	303.15	1.19816		303.15	1.14945		303.15	1.13798
	313.15	1.19322		313.15	1.14360		313.15	1.13179
	323.15	1.18832		323.15	1.13622		323.15	1.12553
	333.15	1.18272		333.15	1.12901		333.15	1.11918
	343.15	1.17772		343.15	1.12301		343.15	1.11282

Table S3 Viscosity of PILs as a function of temperature

PIL	T (K)	Viscosity (mPa.s)	PIL	T (K)	Viscosity (mPa.s)	PIL	T (K)	Viscosity (mPa.s)
2-HEAF	303.15	145.1241 ± 0.0755	2-HEAA	303.15	1192.4726 ± 0.5865	2-HEAPr	303.15	1203.6021 ± 0.1541
	313.15	89.2978 ± 0.3138		313.15	537.9531 ± 0.5936		313.15	600.4013 ± 0.4368
	323.15	57.9564 ± 0.0148		323.15	281.3504 ± 0.0802		323.15	328.0829 ± 0.4518
	333.15	39.6467 ± 0.0088		333.15	161.1616 ± 0.1396		333.15	189.9581 ± 0.2181
	343.15	28.2766 ± 0.0294		343.15	79.8987 ± 0.1522		343.15	124.1003 ± 0.1643

$$ln\left(\frac{k}{k^0}\right) = \sum_{i=0}^{3} A_i (K/T)^i \quad (1)$$

In which $k^0 = 1$ S.cm^{-1}, k is conductivity, A_i the coefficient fitted, T is the temperature (K).

Table S4 Coefficients A_0, A_1, A_2 and A_3 of Equation 1 (Conductivity)

PIL	A_0 (S.cm^{-1})	A_1 (S.cm^{-1})	A_2 (S.cm^{-1})	A_3 (S.cm^{-1})	R^2
2-HEAF	2.0010	-2275.3	-47.000	6.9982	0.991
2-HEAA	5.2121	-3983.6	-38.565	-10022.8	0.994
2-HEAPr	2.5500	-3282.3	-59.830	-10021.0	0.999

$$\rho = \sum_{i=0}^{1} B_i (T/K)^i \quad (2)$$

In which ρ is the density (g.cm^{-3}), B_i the coefficient fitted, T is the temperature (K).

Table S5 Coefficients B_0 and B_1 of Equation 2 (Density)

PIL	B_0 (g.cm^{-3})	B_1 (g.cm^{-3})	R^2
2-HEAF	1.3528	-0.00051	1.000
2-HEAA	1.3497	-0.00066	0.998
2-HEAPr	1.3347	-0.00065	0.999

$$ln\left(\frac{\eta}{\eta^0}\right) = \sum_{i=0}^{3} C_i (K/T)^i \quad (3)$$

Where $\eta^0 = 1$ mPa.s, η is the viscosity, C_i the coefficient fitted, T is the temperature (K).

Table S6 Coefficients C_0, C_1, C_2 and C_3 of Equation 3 (Viscosity)

PIL	C_0 (mPa.s)	C_1 (mPa.s)	C_2 (mPa.s)	C_3 (mPa.s)	R^2
2-HEAF	-9.6261	4429.5	-651.13	270.02	1.000
2-HEAA	-15.972	6985.8	-621.06	275.33	0.999
2-HEAPr	-12.594	5949.2	-621.09	275.33	0.994

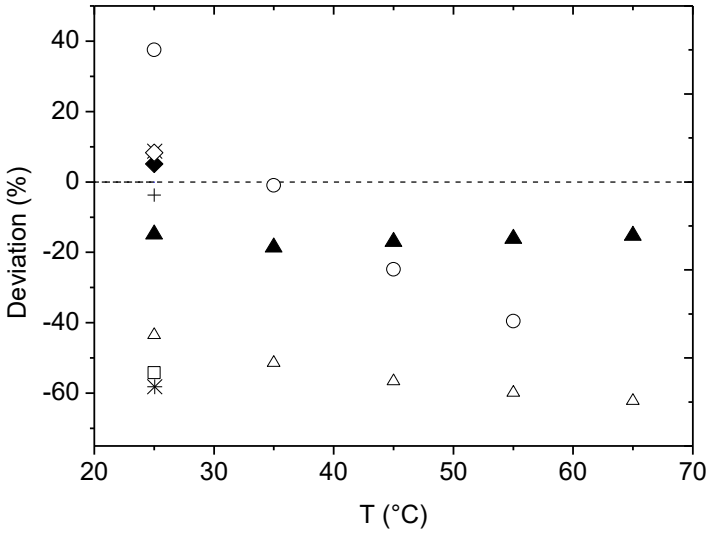

Fig. S1 Relative deviation between the experimental conductivity data of this article and those reported in other research literature. ▲2-HEAF (COTA et al., 2007); △ 2-HEAF (PINKERT et al., 2011); ◇ 2-HEAF (BICAK, 2005); × 2-HEAF (YUAN; ZHANG; LU, 2007); ◆ 2-HEAF (GREAVES; DRUMMOND, 2008a); + 2-HEAA (GREAVES; DRUMMOND, 2008a); ○ 2-HEAA (PINKERT et al., 2011); ✳ 2-HEAA (YUAN; ZHANG; LU, 2007); □ 2-HEAPr (CAMARGO et al., 2016)

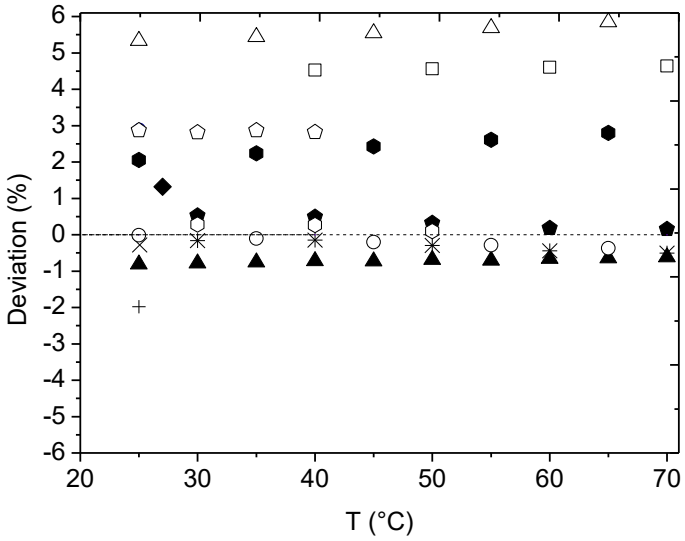

Fig. S2 Relative deviation between the experimental density data of this article and those reported in previous research literature. ▲2-HEAF (GHATEE et al., 2012)**; △ 2-HEAF** (PINKERT et al., 2011)**; ◆ 2-HEAF** (GREAVES; DRUMMOND, 2008a)**; ⬢ 2-HEAF** (COTA et al., 2007)**;** × **2-HEAF** (YUAN; ZHANG; LU, 2007)**; + 2-HEAA** (GREAVES; DRUMMOND, 2008a)**;** ○ **2-HEAA** (PINKERT et al., 2011)**; ⬟ 2-HEAA** (KURNIA; WILFRED; MURUGESAN, 2009)**;** ⬡ **2-HEAA** (ALVAREZ et al., 2011)**;** ✳ **2-HEAA** (PENTILLÄ; UUSI-

KYYNY; ALOPAEUS, 2014); ⬠ **2-HEAPr** (KURNIA; WILFRED; MURUGESAN, 2009); □ **2-HEAPr** (CAMARGO et al., 2016)

S2 - IMAGES CAPTURED USING AN OPTICAL MICROSCOPE

This section presents the images captured of cellulose, xylose and lignin dissolution in PILs.

Cellulose

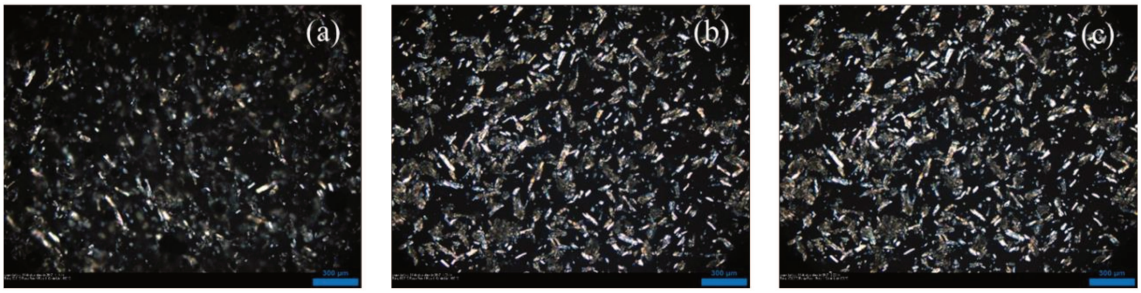

Fig. S3 Images captured using an optical microscope of 1 wt% cellulose in 2-HEAA. (a) T = 30.0 °C; (b) T = 69.7 °C; (c) T = 100.0 °C

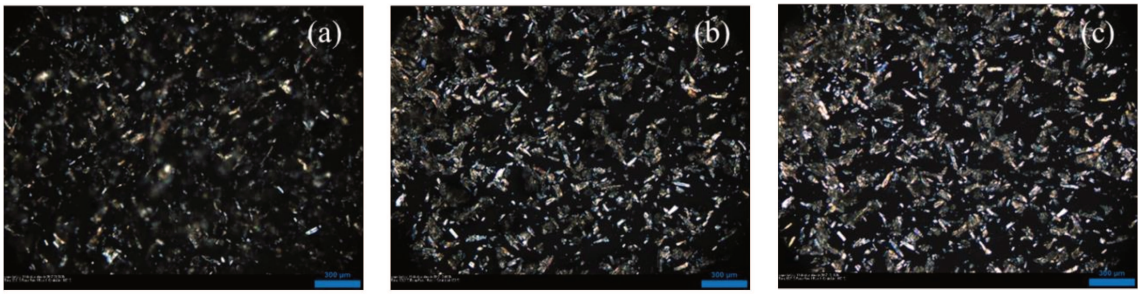

Fig. S4 Images captured using an optical microscope of 1 wt% cellulose in 2-HEAPr. (a) T = 30.0 °C; (b) T = 69.7 °C; (c) T = 100.0 °C

Xylose

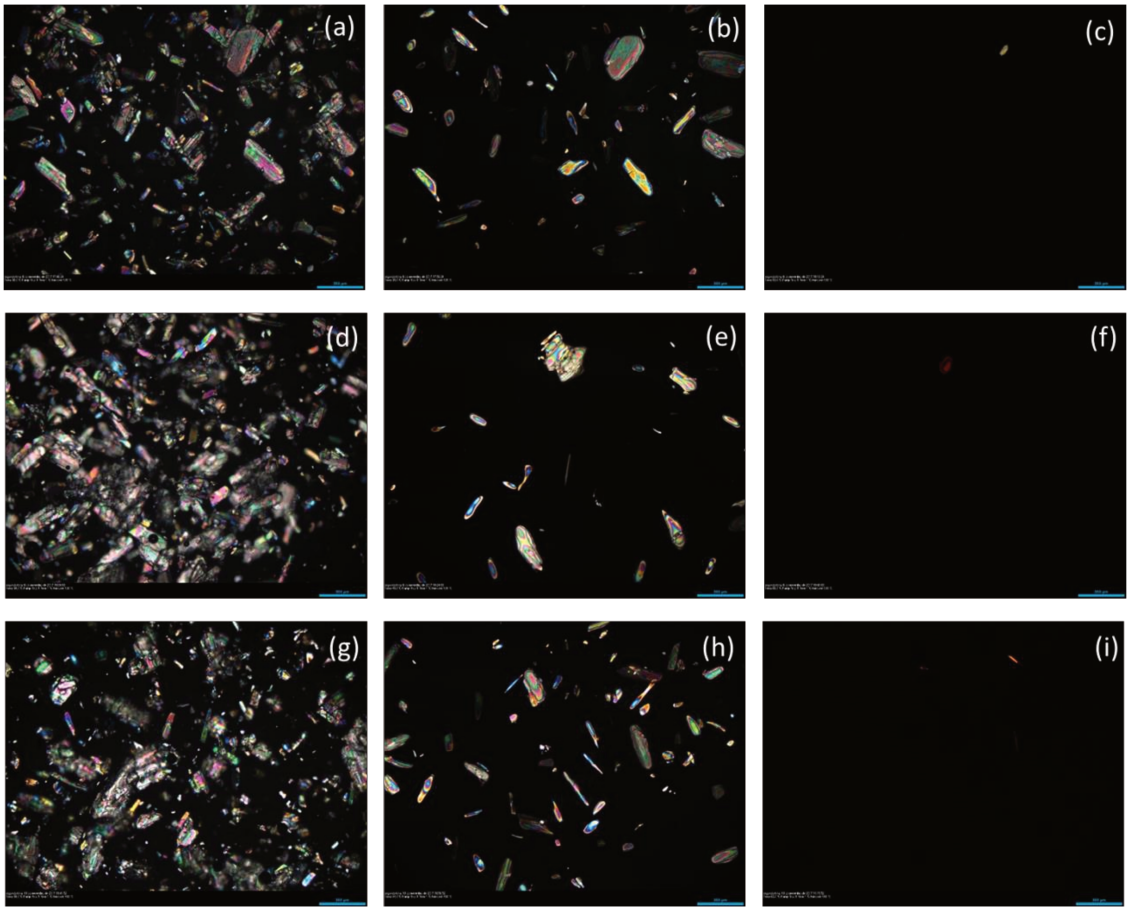

Biopolymer	PIL	Figure		
10 wt% of xylose 1 °C.min^{-1}	**2-HEAF**	(S5-a) T = 30.0 °C	(S5-b) T = 39.9 °C	(S5-c) T = 53.9 °C
	2-HEAA	(S5-d) T = 30.0 °C	(S5-e) T = 49.8 °C	(S5-f) T = 65.7 °C
	2-HEAPr	(S5-g) T = 30.0 °C	(S5-h) T = 44.9 °C	(S5-i) T = 63.7 °C

Fig. S5 Images captured using an optical microscope of xylose in 2-HEAF, 2-HEAA and 2-HEAPr

Lignin

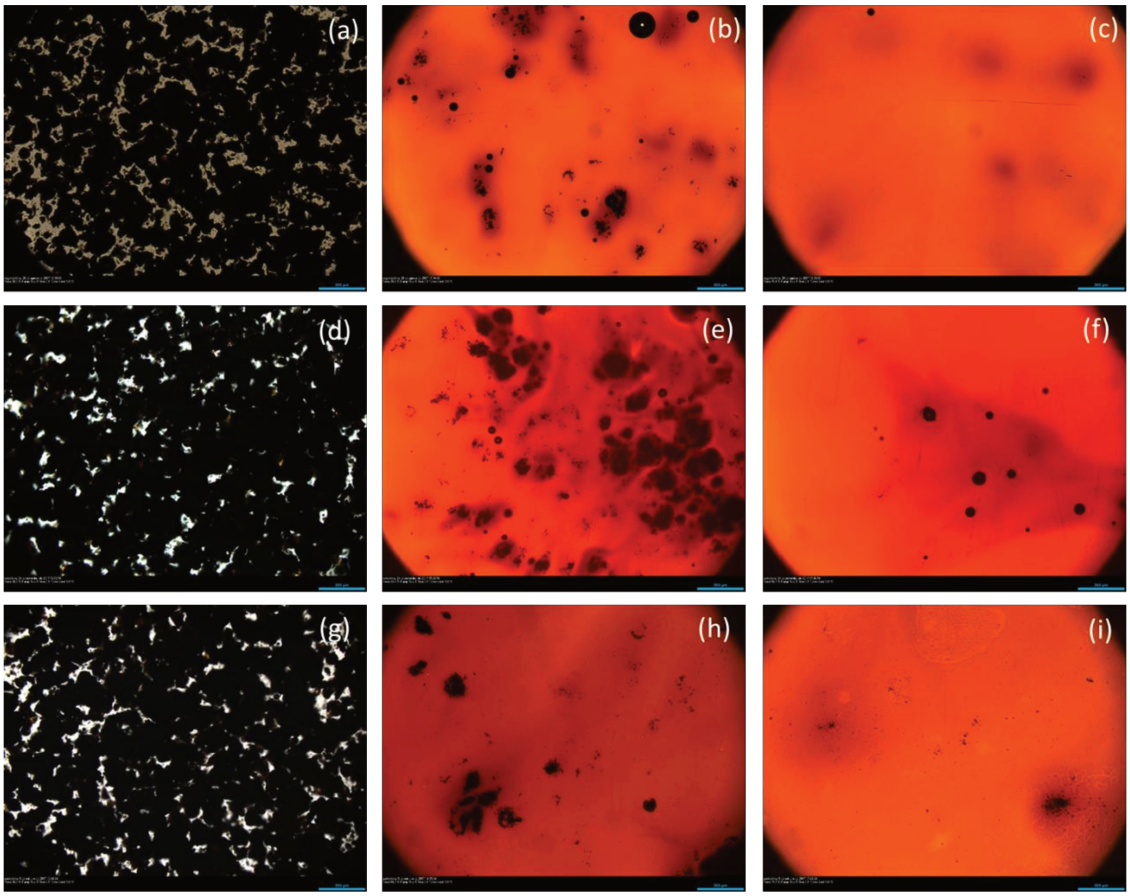

Biopolymer	PIL	Figure		
15 wt% of lignin 0.1 °C.min^{-1}	**2-HEAF**	(S6-a) T = 30.0 °C	(S6-b) T = 35.5 °C	(S6-c) T = 41.4 °C
	2-HEAA	(S6-d) T = 30.0 °C	(S6-e) T = 42.5 °C	(S6-f) T = 55.3 °C
	2-HEAPr	(S6-g) T = 30.0 °C	(S6-h) T = 50.7 °C	(S6-i) T = 71.5 °C

Fig. S6 Images captured using optical microscopy of lignin in PILs

Lignin+xylose dissolution in 2-HEAF

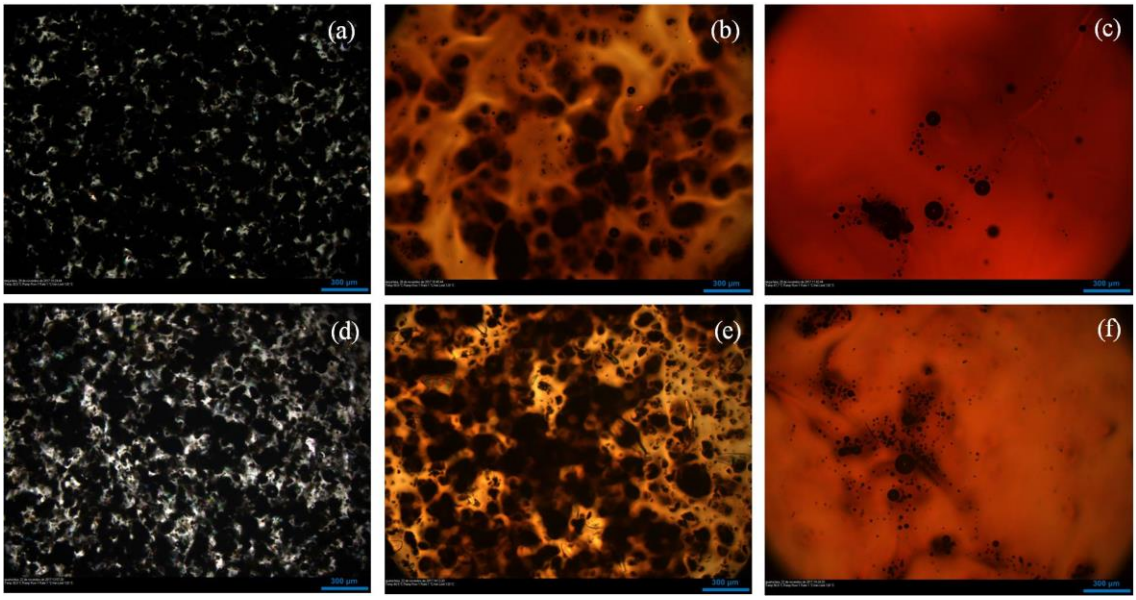

Biopolymer	PIL	Figure		
5 wt% of xylose + 10 wt% of lignin	**2-HEAF**	(S7-a) T = 30.0 °C	(S7-b) T = 50.8 °C	(S7-c) T = 67.7 °C
10 wt% of xylose + 5 wt% of lignin		(S7-d) T = 30.0 °C	(S7-e) T = 44.9 °C	(S7-f) T = 56.8 °C

Fig. S7 Images captured using optical microscopy of lignin in PILs

S3 – EXPERIMENTAL DATA

This section presents the temperature values which were observed in full dissolution of xylose or lignin in PILs.

Table S7 Temperature to achieve full dissolution of xylose or lignin in 2-HEAF at different heating rates

2-HEAF							
% xylose	**1°C.min^{-1}**	**0.5°C.min^{-1}**	**0.1°C.min^{-1}**	**% lignin**	**1°C.min^{-1}**	**0.5°C.min^{-1}**	**0.1°C.min^{-1}**
5%	50.8 °C	41.4 °C	32.3 °C	**5%**	47.7 °C	44.8 °C	33.3 °C
10%	54.8 °C	42.6 °C	33.3 °C	**10%**	65.7 °C	47.9 °C	36.9 °C
15%	63.7 °C	47.8 °C	34.4 °C	**15%**	71.6 °C	51.5 °C	41.5 °C

Table S8 Temperature to achieve full dissolution of xylose or lignin in 2-HEAA at different heating rates

2-HEAA							
% xylose	**1°C.min^{-1}**	**0.5°C.min^{-1}**	**0.1°C.min^{-1}**	**% lignin**	**1°C.min^{-1}**	**0.5°C.min^{-1}**	**0.1°C.min^{-1}**
5%	63.0 °C	63.0 °C	37.6 °C	**5%**	68.1 °C	62.3 °C	40.9 °C
10%	71.0 °C	67.5 °C	39.2 °C	**10%**	80.5 °C	69.8 °C	43.2 °C
15%	90.0 °C	69.2 °C	41.0 °C	**15%**	93.5 °C	79.4 °C	55.3 °C

Table S9 Temperature to achieve full dissolution of xylose or lignin in 2-HEAPr at different heating rates

2-HEAPr							
% xylose	**1°C.min^{-1}**	**0.5°C.min^{-1}**	**0.1°C.min^{-1}**	**% lignin**	**1°C.min^{-1}**	**0.5°C.min^{-1}**	**0.1°C.min^{-1}**
5%	57.5 °C	43.9 °C	33.2 °C	**5%**	101.4 °C	79.3 °C	50.9 °C
10%	66.7 °C	50.5 °C	35.1 °C	**10%**	104.4 °C	93.7 °C	59.9 °C
15%	72.6 °C	57.7 °C	38.0 °C	**15%**	x	102.7 °C	71.5 °C

REFERENCES

1. Cota I, Gonzalez-Olmos R, Iglesias M, Medina F (2007) New short aliphatic chain ionic liquids: Synthesis, physical properties, and catalytic activity in aldol condensations. J Phys Chem B 111:12468–12477. https://doi.org/10.1021/jp073963u
2. Pinkert A, Ang KL, Marsh KN, Pang S (2011) Density, viscosity and electrical conductivity of protic alkanolammonium ionic liquids. Phys Chem Chem Phys 13:5136-5143. https://doi.org/10.1039/c0cp02222e
3. Bicak N (2005) A new ionic liquid: 2-hydroxy ethylammonium formate. J Mol Liq 116:15–18. https://doi.org/10.1016/j.molliq.2004.03.006
4. Yuan XL, Zhang SJ, Lu XM (2007) Hydroxyl ammonium ionic liquids: Synthesis, properties, and solubility of SO_2. J Chem Eng Data 52:596–599. https://doi.org/10.1021/je060479w
5. Greaves TL, Drummond CJ (2008) Protic ionic liquids: Properties and applications. Chem Rev 108:206–237. https://doi.org/10.1021/cr068040u
6. Camargo D, Andrade RS, Ferreira GA, Mazzer H, Cardozo-Filho L, Iglesias M (2016) Investigation of the rheological properties of protic ionic liquids. J Phys Org Chem 29:604–612. https://doi.org/10.1002/poc.3553
7. Ghatee MH, Bahrami M, Khanjari N, Firouzabadi H, Ahmadi Y (2012) A Functionalized High-Surface-Energy Ammonium-Based Ionic Liquid: Experimental Measurement of Viscosity, Density, and Surface Tension of (2-Hydroxyethyl)ammonium Formate. J Chem Eng Data 57:2095–2101. https://doi.org/10.1021/je201055w
8. Kurnia KA, Wilfred CD, Murugesan T (2009) Thermophysical properties of hydroxyl ammonium ionic liquids. J Chem Thermodyn 41:517–521. https://doi.org/10.1016/j.jct.2008.11.003
9. Álvarez VH, Mattedi S, Martin-Pastor M, Aznar M, Iglesias M (2011) Thermophysical properties of binary mixtures of {ionic liquid 2-hydroxy ethylammonium acetate+(water, methanol, or ethanol)}. J Chem Thermodyn 43:997–1010. https://doi.org/10.1016/j.jct.2011.01.014
10. Pentillä A, Uusi-Kyyny P, Alopaeus V (2014) Distillable Protic Ionic Liquid 2-(Hydroxy)ethylammonium Acetate (2-HEAA): Density, Vapor Pressure, Vapor–Liquid Equilibrium, and Solid–Liquid Equilibrium. Ind Eng Chem Res 53:19322–19330. https://doi.org/10.1021/ie503823a

Springer Nature License Terms and Conditions

Considerações do Capítulo 5 e Objetivos Capítulo 6

Como demonstrado no Capítulo 5, os LIPs foram capazes de dissolver a xilose e a lignina, entretanto, não foi observada significativa dissolução de celulose, mesmo em baixas concentrações do polímero (1% em massa). Diferentes taxas de aquecimento foram aplicadas, e foi constatado que taxas de aquecimento menores resultavam em maior tempo para dissolver completamente os solutos analisados. Finalmente, a técnica de microscopia óptica se mostrou adequada para realizar um rápido *screening* da capacidade de LIPs em dissolver os principais constituintes da biomassa lignocelulósica.

Uma vez detectada a capacidade seletiva dos LIPs de dissolver os principais componentes da biomassa lignocelulósica (xilose e lignina), a lignina foi escolhida como objeto de estudo para continuar a pesquisa desenvolvida nessa Tese, uma vez que essa macromolécula é pouco aplicada na indústria (apenas 2% do produzido é comercializado), e por apresentar maior gama de aplicabilidade a depender do seu processamento. Assim, a solubilidade da lignina foi avaliada em diversos LIPs, visando obter alta quantidade de dissolução desse componente para auxiliar no desenvolvimento de processos futuros em uma biorrefinaria. Dentre os parâmetros analisados pode-se mencionar a estrutura do cátion e do ânion no LIP (número de carbonos na cadeia alquílica, presença de hidroxilas e grupos carboxílicos extra), a quantidade de água (naturalmente presente na biomassa lignocelulósica e nos LIPs por serem higroscópicos), a temperatura, e o modo de agitação. Esses parâmetros ajudaram a entender melhor a solubilidade da lignina e como essa solubilidade pode ser afetada por eles. Além disso, o reciclo dos LIPs foi avaliado com o objetivo de se planejar, futuramente, um processo industrial viável economicamente. As análises e resultados estão apresentados no Capítulo 6 dessa Tese.

CAPÍTULO 6 – An investigation of Kraft lignin solubility in protic ionic liquids and their aqueous solutions

6. An investigation of Kraft lignin solubility in protic ionic liquids and their aqueous solutions

(Submitted to Industrial Crops & Products)

Rafael M. Dias[1], Lívia C. G. Petrin[1], Filipe H. B, Sosa[1,2], André M. da Costa Lopes[2], João A. P. Coutinho[2], Mariana C. da Costa[1,].*

[1]Department of Process and Product Design (DDPP) - School of Chemical Engineering (FEQ), University of Campinas (UNICAMP), 13083-852, Campinas, São Paulo, Brazil.

[2]CICECO, Aveiro Institute of Materials, Department of Chemistry, University of Aveiro, 3810-193 Aveiro, Portugal.

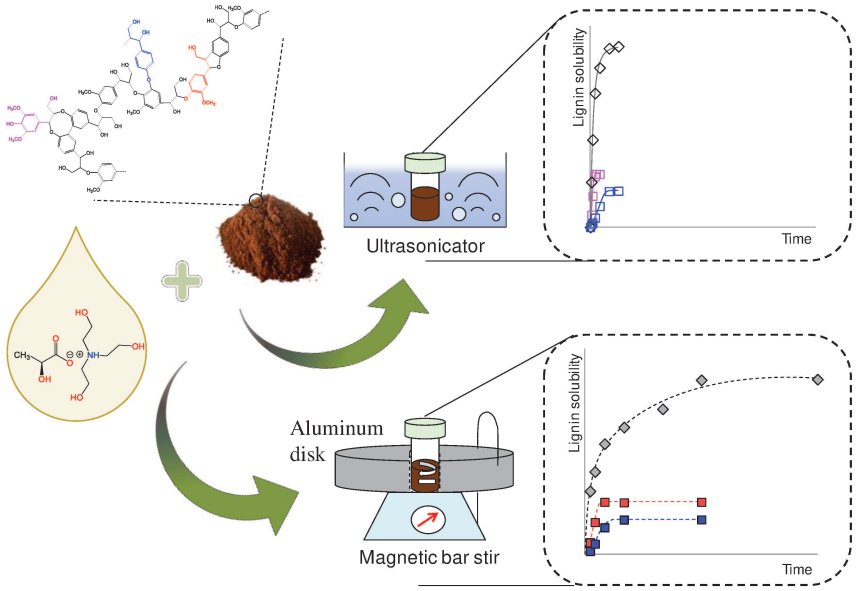

ABSTRACT

The interest in the conversion of lignin into value added products and energy has been growing over the years. However, an adequate solvent media for lignin dissolution is impeding the progress toward more sustainable and noble applications of lignin. In this study, the potential of alkanolammonium based Protic Ionic Liquids (PILs) and their aqueous solutions as solvent media of Kraft lignin was evaluated by changing the PIL's cation and anion, water content, temperature, time and also the type of heating. The results showed that the anionic part of PIL exhibited a key role in lignin dissolution, while the cationic part displayed a secondary action in this process. Moreover, the increase of water content reduced lignin solubility by impairing the interactions between PILs and lignin. Depending on the PIL cation/anion pair the influence of water on reducing lignin solubility is gradual or quick. The presence of extra hydroxyl and/or carboxylic groups in the anion structure also negatively affected the lignin solubility. On the other hand, the increase of the alkyl carbon chain present in cationic part of PILs favored the lignin dissolution. As expected, temperature increase leaded to higher lignin solubility values. Using a conventional heating method all tested PILs required 8 h to reach lignin saturation, excepting for lactate-based PILs that took at least 24 h. The efficiency of lignin dissolution was improved with an ultrasound heating water bath, which allowed a faster lignin dissolution performance by achieving saturation in only 4 hours. Finally, the recyclability of 2-hydroxyethyl malate and tris(2-hydroxyethyl)amine lactate was herein demonstrated for at least 3 cycles as proof of concept. The results disclosed in this work prove the capacity of applying this kind of solvents as media to dissolve lignin.

KEYWORDS: protic ionic liquids; Kraft lignin; solubility; time-dependence solubility; green solvents.

1. INTRODUCTION

Nowadays, the need for alternative energy sources has been growing due the environmental impact caused by fossil fuels, including the greenhouse effect and global warming. In addition, the dependency on non-renewable resources is a current societal issue that must be overcome. In this scenario, the use of biomass as raw material has been attracting the interest of scientific community as one of the most promising renewable sources of carbon and it can be a solution to replace the excessive use of crude-oil feedstocks. The conversion of biomass into energy, fuels, materials and high-value products through a series of integrated and sustainable processes in the frame of the biorefinery concept has been highly pursued.[1,2]

Among different types of biomass, lignocellulosic materials are the most abundant and available in the world and their processing has been tentatively performed.[3] Cellulose, hemicellulose and lignin are the major components of lignocellulose and are strongly linked into a recalcitrant matrix difficult to disrupt.[4,5] Cellulose and hemicellulose are polysaccharides attached through hydrogen bonds and Van der Waal's interactions, possessing a structural role in the plant biomass.[6,7] On the other hand, lignin consists of phenylpropanoid units linked by carbon-carbon and ether bonds forming a complex three-dimensional polymer, whose function is to provide resistance against pathogens, rigidity to the plant cell wall and compressive strength to the fibers and plant tissues.[8]

Due to its aromatic nature, lignin has a promising potential to be used as alternative to petrochemical-based products.[9] The singular structure and its physicochemical properties allow the production of several types of aromatic compounds.[10,11] Despite the fact lignin can be converted into fine chemicals, its valorization has received little attention compared to cellulose. The pulp and paper industry that largely produces cellulose from wood is capable of disposing 50 million tons of lignin as by-product. However, only 2 % of this fraction is commercialized as low-value product (e.g. dispersing or binding agents), while the other 98 % lignin is burned as a low value fuel.[10,12] Therefore, more efforts must be addressed to achieve a sustainable lignin valorization and to meet a biobased economy. In this regard, the

evaluation of an appropriate solvent for lignin would facilitate the development of efficient processes for its conversion. To promote lignin dissolution, a promising class of solvents has emerged: the Ionic Liquids (ILs).[13–18] These solvents have been considered as more sustainable and efficient alternative to traditional organic solvents, which are usually hazardous and present low selectivity for lignin dissolution.[19]

By definition, ILs are salts with melting point lower than 100 °C and are composed of cations and anions.[20,21] They present low vapor pressure, high conductivity, thermal and chemical stability, making them fascinating players in many fields such as synthesis and catalysis, biotechnology, pharmaceutics and medicine, electrochemistry, extraction and separation, among others. [22,23] Particularly, Protic Ionic Liquids (PILs) are a class of ILs that has been growing interest of scientific community lately. These ILs are easily synthesized by a proton transfer from an organic acid to an organic base, which is a considerably cheap synthesis when compared to that of traditional ILs. Due to this economical advantage, and also to their remarkable properties, such as high proton conductivity, chemical and thermal stability, PILs have been extensively studied. [24–29]

Recently, some PILs have been used in the lignin dissolution task. [30,31] The ability of 18 novel multiaromatic PILs for Kraft lignin dissolution was visually demonstrated by Merino et al. [17] using microwave-assisted irradiation at 363.15 K. The results showed that 42 wt% lignin can be dissolved in PILs with multiaromatic imidazolium cation at 363.15 K in few minutes. The lignin solubility was also determined in pyridinium based PILs aqueous solutions by Rashid et al. [31] The pyridinium formate ([Py][For]) was the best PIL, achieving 70 wt% lignin solubility at low temperature (348.15 K) within 1 hour. More recently, Dias et al. (2019) demonstrated the ability of seven alkanolammonium based PILs to dissolve Kraft lignin from *E. globulus*, obtaining more than 37 wt% at 323.15 K within 24 hours using 2-hydroxyethylammonium hexanoate ([HEAH]). [32]

A wide range of cation and anion combinations could be used to synthesize PILs, but only few of these possibilities were reported in literature for lignin dissolution. Therefore, new combinations of cations and anions were tested in this study and the

role of each ion in the solubility of lignin was investigated. PILs aqueous solutions composed of alkanolammonium cations with malate, malonate, succinate, glycolate and lactate anions were studied for their ability to dissolve Kraft lignin. The lignin solubility on those systems was correlated to their chemical structure as well as the acidity of precursors. Moreover, the time-dependence of lignin solubility in PILs was evaluated as another parameter to address their efficiency.

2. MATERIALS & METHODS

2.1 Chemicals

The acid and base precursors used to synthesize the examined PILs are depicted in Table 1. All the reagents were used as received. *Eucalyptus globulus* isolated lignin from Kraft process was supplied by the pulp and paper mill Suzano Papel & Celulose – Brazil.

Table 1 – Purities, chemical structures and suppliers of the pure bases and acids used in this study

Chemical Name	Chemical Structure	Purity (%)	pKa[a]	Supplier
	Bases			
2-hydroxyethylamine (HEA)		≥ 98	9.50	Sigma Aldrich
bis(2-hydroxyethyl)amine (BHEA)	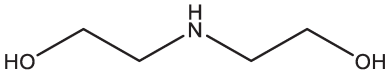	≥ 98	8.96	Sigma Aldrich
tris(2-hydroxyethyl)amine (THEA)	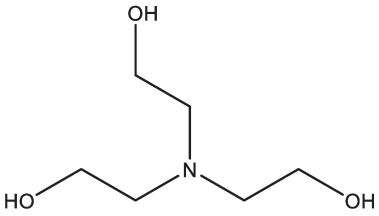	≥ 98	7.76	Sigma Aldrich
	Acids			
Glycolic acid (G)	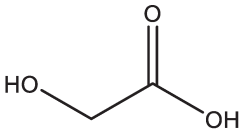	70	3.83	Dinâmica
Lactic acid (L)	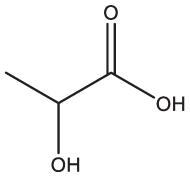	85	3.86	Sigma Aldrich
Malonic acid (Mn)	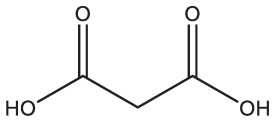	99	5.70	ReagentPlus®
Succinic acid (Su)	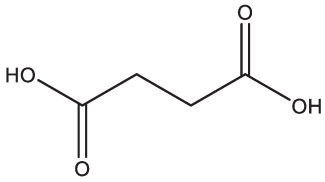	99	5.635	Synth
Malic acid (M)	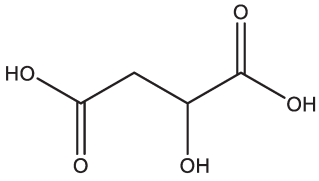	99	5.03	Dinâmica

[a] PubChem database. [33]

2.2 Synthesis of PILs and their characterization

The following PILs were synthesized: 2-hydroxyethylammonium malonate (HEAMn), 2-hydroxyethylammonium malate (HEAM), 2-hydroxyethylammonium succinate (HEASu), 2-hydroxyethylammonium glycolate (HEAG), 2-hydroxyethylammonium lactate (HEAL), bis(2-hydroxyethyl)ammonium lactate (BHEAL), and tris(2-hydroxyethyl)ammonium lactate (THEAL). An acid-base reaction was conducted to synthesize the PILs. The acids and bases were weighted in stoichiometric proportions. The base was placed in a bottom flask and stirred by a magnetic bar, while an aqueous solution of acid was prepared and added dropwise to the base. An ice bath was used to control the reaction temperature. The final solution was maintained over stirring for 24 hours. The IL solution was then placed in a rotary evaporator to remove any excess of water or reagents. The water content was determined using a Metrohm 831 Karl Fischer coulometer and these values were considered in the preparation of PIL aqueous solutions. The PILs were characterized through ^{1}H NMR, ^{13}C NMR and FT-IR (Electronic Supplementary Information – ESI).

For NMR analysis, IL samples were dissolved in deuterated DMSO (DMSO-d6) as solvent and tetramethylsilane (TMS) as an internal reference. All spectra were recorded by a Bruker AVANCE 300 NMR at 300 MHz (Figures S8-S21 in ESI).

For the FT-IR analysis, a PerkinElmer spectrometer (Spectrum BX) equipped with a single horizontal Golden Gate ATR cell (attenuated total reflectance) and diamond crystal was used. All spectra were acquired with 32 scans at 4 cm^{-1} of resolution and a wavenumber range between 4000 cm^{-1} and 600 cm^{-1} (Figures S1-S7 in ESI).

2.3 Kraft lignin solubility in PILs aqueous solutions

Excess of Kraft lignin was added to 2.0 ± 0.05 g of each PILs aqueous solutions (5, 15, 25, 40, 50, 60, 75, 80, 85, 87.5, 90, 92.5 and 95 wt% of PIL) or pure water in glass vials. The vials were sealed and placed on a specific aluminum disk support, which was transferred to a stirring plate with heat control Pt1000 (H03D Series from LBX

Instruments). The aluminum disk support was maintained at constant temperature (313.15, 323.15, 333.15 or 353.15 K) and the samples were kept under constant agitation (200 rpm - provided by magnetic bar stir) until saturation. The influence of time on the Kraft lignin solubility was also evaluated and the same methodology was performed at different periods of time (1, 2, 4, 8, 16, 24 and 48 hours). The solid phases were then separated from the liquid phases using PTFE filters (0.45 μm pore size). The filtered liquid samples were diluted using dimethylsulfoxide (DMSO) and the dissolved lignin was quantified by UV-spectroscopy (SHIMADZU UV-1700, Pharma-Spec spectrometer) at 280 nm wavelength. The lignin concentration was determined by appropriate calibration curves (Table S1 in ESI). All experiments were made at least in duplicate.

2.4 Kraft lignin solubility using ultrasonic water bath

The Kraft lignin dissolution in some neat PILs was also evaluated under an ultrasonic heating method (Model 1400 A, Unique, Brazil). The ultrasonic water bath was rated at 135 W with a resonating frequency of 40 kHz, while water was recirculated ensuring constant temperature during the assays. The temperature was monitored with a thermometer (PT-100 temperature sensor (± 0.1 K)) and the experiments were performed with satisfactory temperature control (± 0.5 K). The sample preparation and the determination of lignin solubility in PILs were performed as described in section 2.3.

2.5 neat PILs viscosity

The viscosities of neat PILs (5 wt%) at different temperatures (303.15 to 333.15 K) were measured using an automated micro viscosimeter (Anton Paar, AMVn, Germany), applying the falling ball method. The water content was determined (Metrohm 831 Karl Fischer coulometer) before each viscosity trial. During the viscosimeter operation the temperature was kept constant within ±0.01 K.

2.6 PIL recycling

Deionised water was added to the mixture of HEAM aqueous solution saturated with lignin to promote lignin precipitation. An ice bath (278.15 K) was used to decrease the temperature of the solution favouring the precipitation process. The precipitated lignin was separated by vacuum filtration, washed with water and the resulting PIL aqueous solution was subjected to rotary vacuum evaporation process (333.15 K and 10 kPa for 2.0 hours) until 5 wt% water content was achieved. The recovered HEAM aqueous solution was reused in lignin solubility assays as described in Section 2.3.

3. RESULTS AND DISCUSSION

3.1 The effect of anion structure on Kraft lignin solubility

The chemical nature of the anionic part of aprotic ionic liquids (AILs) has been shown to play a major role on the lignin solubility mechanism.[34–36] To stress out this effect on PILs, 2-hydroxyethylammonium-based PILs composed of mono and dicarboxylic anions with different carbon chain lengths (C2 to C4) in presence or absence of a hydroxyl group were tested for Kraft lignin solubility at 323.15 K. The obtained solubility values are depicted in Figure 1 and Table S2 (along with the corresponding standard deviations) in ESI.

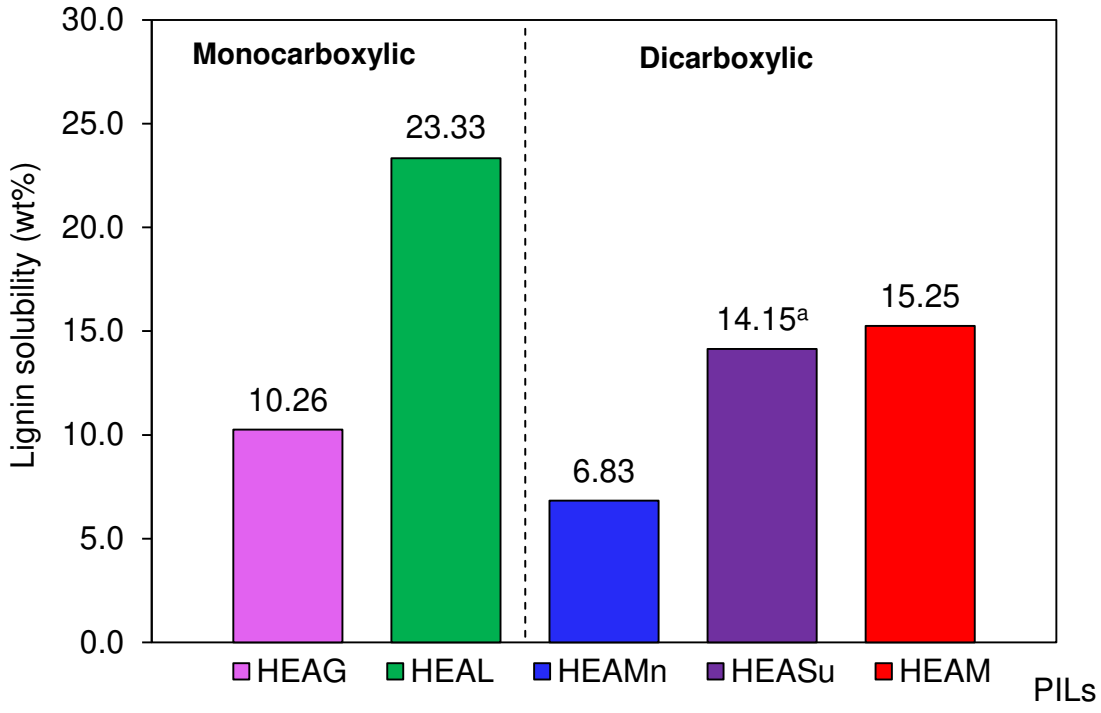

Figure 1 - Kraft lignin solubility in neat PILs (5 wt% of water) and HEASu aqueous solution (20 wt% of water) at 323.15 K. [a] The solubility in HEASu was determined in aqueous solution containing 20 wt% of water since it is solid for water contents lower than this value.

The results reported in Figure 1 shows that structure and chemical properties of the anion have high impact on Kraft lignin solubility in PILs. Amongst studied solvents, HEAL showed the best performance for lignin solubility reaching a value of 23.33 wt%, which was more than 2-fold the solubility value from HEAG (10.26 wt%). The Kraft lignin solubility obtained with HEAL is also comparable to that from neat 2-hydroxyethylammonium propionate (HEAP) at the same temperature (> 30 wt%) reported elsewhere. [32] Regarding to dicarboxylic-based PILs, HEAM achieved 15.25 wt% lignin solubility, while HEAMn presented the lowest solubility (6.83 wt%) among all. In case of HEASu, mixtures containing more than 80 wt% HEASu content were found as solid phase at 323.15 K, thus lignin solubility at these conditions were not determined. For this system, the best result was achieved at 80 wt% HEASu content, resulting in 14.15 wt% of lignin solubility.

Therefore, the performance of examined neat PILs (5 wt% water content) for Kraft lignin solubility can be ordered as follows: HEAL > HEAM > HEAG > HEAMn. From these results it can be inferred that increasing the carbon chain length of the anion from C2 to C3, particularly from glycolate to lactate, better lignin solubility is obtained. For dicarboxylic anions, the increase of carbon chain length of the anion from C3 (malonate) to C4 (succinate and malate) and the presence of a hydroxyl group (malate) seemed to favor lignin solubility.

Some authors have investigated the relation between the lignin solubility and the alkyl chain length effect of the anion. Hou et al. (2015) demonstrated that lignin solubility was favored by the increasing of the chain length of alkanoate anions using different cholinium-based ILs. [37] Soares et al. (2017) have reported that an increasing alkyl chain length resulted in an increasing of the lignin monomeric model compounds using deep eutectic solvent aqueous solutions. [38] Recently, Dias et al. (2020) also showed this phenomenon and revealed that the larger the alkyl chain length of carboxylate anions in monoethanolammonium-based PILs, the higher is the solubility of lignin in these solvents, which is related to a better affinity between lignin-PILs. [32] According to Xu et al. (2017) the alkyl chain in anion structure is able to interact with lignin. The authors supported this information observing the increasing in the electron cloud density in the alkyl chain anion part, which is an indication that interactions between this anionic part and lignin were established. [18] So, it is expected that an increasing in the alkyl chain would favor the lignin dissolution since allows more interactions between lignin and ILs. Concluding, the lignin solubility increases with the increasing of the alkyl chain length of the anion. Therefore, when the abilities of HEASu–HEAMn, and HEAL–HEAG to dissolve lignin are compared, the alkyl chain length may be the reason to succinate and lactate–based PIL exhibited higher solubility lignin values, as explained before.

In our previous study we determined the solubility of Kraft lignin in neat 2-hydroxyethylammonium acetate (HEAA; 22.12 wt%) and 2-hydroxyethylammonium propionate (HEAP; 30.86 wt%) at 323.15 K. [32] When comparing the lignin solubility in neat PILs (HEAA-HEAG, and HEAP-HEAL), it reveals that the presence of an extra hydroxyl group in anionic part of PILs decreases the ability of these solvents to dissolve

lignin. This extra hydroxyl group presents in HEAG and HEAL turns these PILs too polar and induces the formation of a network of hydrogen bonds between the PIL molecules or between PIL and water molecules, which reduces the interactions between lignin-PIL, resulting in a decreasing of the solubility. This behavior was previously reported using deep eutectic solvents to dissolve lignin monomeric model compounds and toluene by Soares et al. (2017) and Wang et al. (2016), respectively.

Regarding the water effect on lignin solubility (Figure 2 and Table S2 in ESI), the addition of water to PILs demonstrated different behaviors on their ability to dissolve lignin. The solubility curves of HEAM presented an abrupt decrease of lignin solubility with increased water content: this PIL dissolved 1.54 wt% of lignin when 15 wt% of water is presented in its solution. On the other hand, for HEASu, HEAMn, HEAL, and HEAG the anti-solvent role of water is less pronounced, but still important, and an increasing of water content reduced the solubility. As expected, a negligible value of lignin solubility on pure water (0.10 wt%) was reported at 323.15 K.

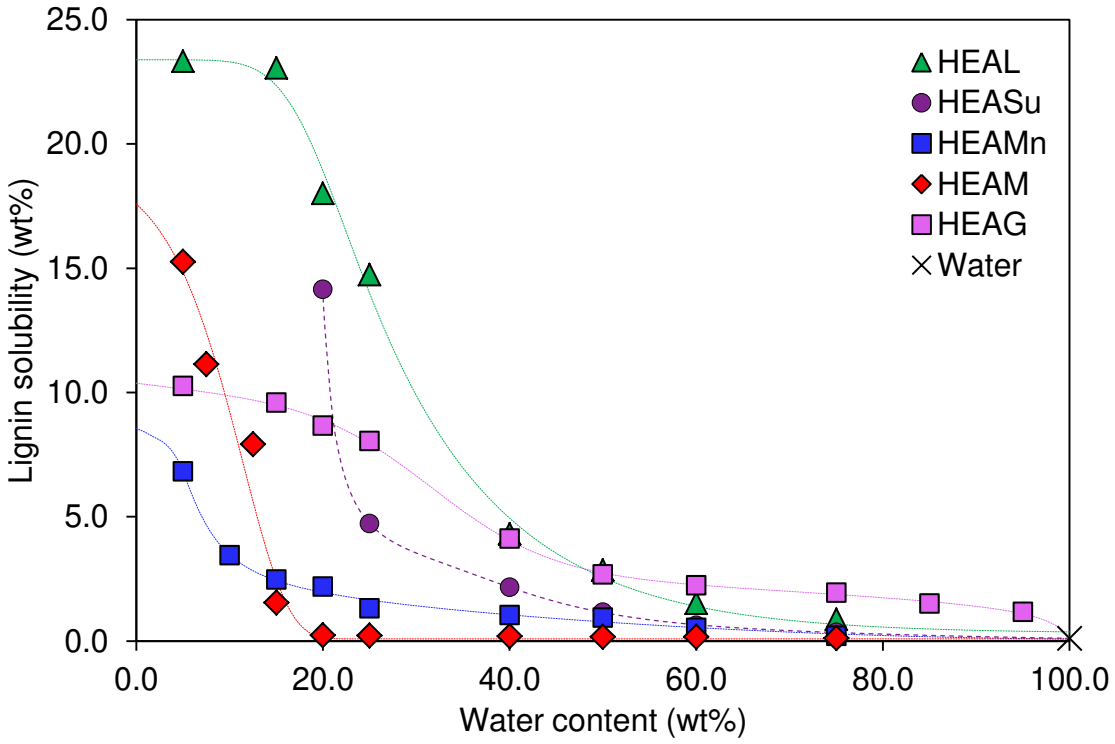

Figure 2 – Kraft lignin solubility in HEAL, HEASu, HEAMn, HEAM, and HEAG aqueous solutions and pure water at 323.15 K.

Indeed, some authors have also reported the negative effect of water on the Kraft lignin solubility in PILs, reducing their ability to dissolve lignin.[15,18,36] Xu et al.(2017) [18] reported that the cation and anion of the IL are solvated by water and this phenomenon impairs the interactions between IL and lignin. The obtained data shows that negative impact of water on lignin solubility seems to be more pronounced for dicarboxylic-based PILs than for monocarboxylic-based. It suggests that water strongly crowd the hydrogen bond accepting sites of malate, malonate, or succinate, and prevent these anions to make interactions with lignin. Ji et al. (2012) [39] investigated the interactions between water–IL–lignin applying theoretical calculations and concluded that the interaction energy and the active sites of IL and lignin decrease with the addition of water, making the bonds between them weaker or even destroyed. For instance, the lignin solubility decrease with increasing water content was steeper for HEAMn than for HEAL. Therefore, the interactions between water and the dicarboxylic–based PILs could be stronger than that of monocarboxylic-based.[40] In other words, an extra COO- group in the anion structure makes strong interactions with water and disables the possibility to interact with lignin in aqueous solutions. When these PILs are weakly hydrated, they are able to establish interactions with lignin and its solubility increases.[18]

The results also demonstrated that HEAM presented poor ability to dissolve lignin when compared to HEASu at the same water content. The presence of an extra hydroxyl group on malate molecule may make the anionic part too polar, inducing the formation of hydrogen bond networks between water–PILs which impair the interactions between the anion and the lignin, reducing its ability to dissolve lignin. [38,41] Similar results were also observed by Xu et al. (2017) [42] applying choline carboxylate ILs aqueous solutions (derived from mono, di, and tricarboxylic acids as hydrogen bond donor – HBD, and choline chloride as hydrogen bond acceptor – HBA) to dissolve lignin, and according to the results obtained, the authors concluded that the presence of extra –OH groups enhances the hydrophilicity of these ILs, which strengthens the interactions between water–ILs, decreasing the lignin solubility. The negative impact of the presence of extra hydroxyl groups was also observed using deep eutectic solvents (derived from carboxylic acids, urea, alcohols, and sugars as HBD, and choline chloride, L(–)-proline,

betaine, and urea as hydrogen bond acceptor – HBA) to dissolve syringic acid (lignin monomeric model) by Soares et al. (2017) [40]

3.2 Kraft lignin solubility and cation structure effect

To investigate the influence of the PIL cationic part in the Kraft lignin solubility lactate was chosen, since it was the best anion between the tested in this study. The results of Kraft lignin solubility in BHEAL and THEAL at 323.15 K are presented in Figure 3. The Kraft lignin solubility values, and the respective standard deviations, are presented in Table S3 in ESI.

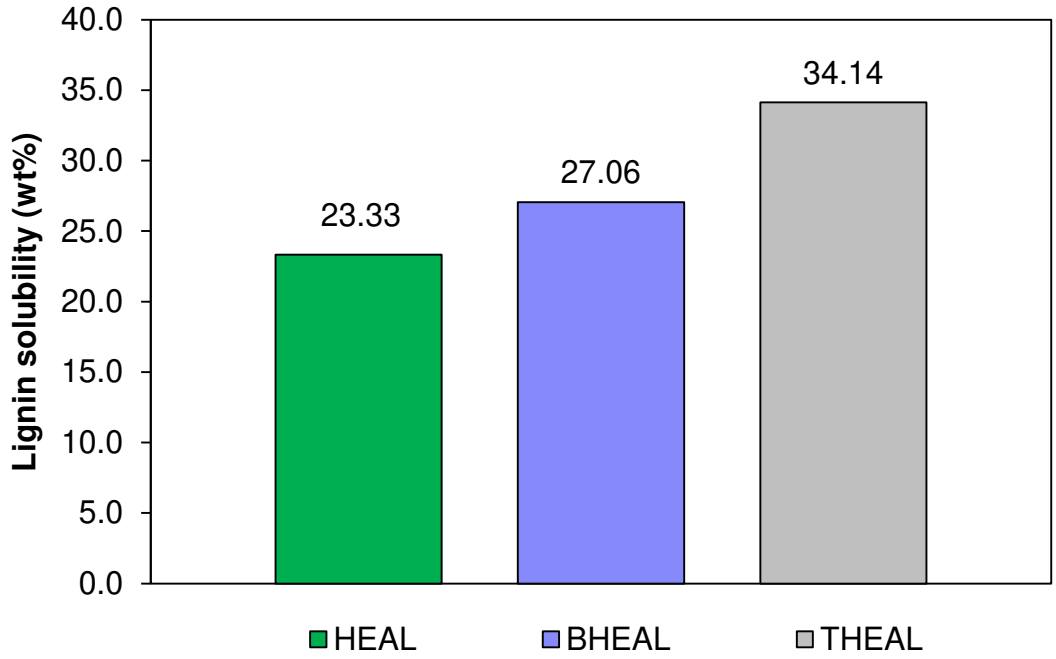

Figure 3 - Kraft lignin solubility in neat HEAL, BHEAL, and THEAL (5 wt% of water) at 323.15 K.

The results presented in Figure 3 shows a clear trend on the PILs capacity to dissolve Kraft lignin demonstrating that solubility is affected by the cationic part of the PIL, as well. The Kraft lignin solubility increases in the following sequence: THEAL > BHEAL > HEAL; indicating that larger cations of alkanolammonium based PILs using lactate as the anion are capable of dissolving more lignin. In our previous article we

have demonstrated that decreasing the cationic part of alkanolammonium-based PILs using propionic acid as precursor resulted in an increasing on the Kraft lignin solubility values, and that tris(2-hydroxyethyl)amine) propionate (THEAP) presented lower ability to dissolve lignin than 2-hydroxyethylamine propionate (HEAP). Interestingly, an opposite conclusion is reported here using lactate as the anion what lead us to further investigation about this behavior.

It is known that PILs are in equilibrium with neutral species, [20] therefore, the lignin solubility may be related mainly with the PILs interactions and in minor proportions with their neutral species (acid and base precursors) since in the final solution these neutral compounds are present in small fractions. Some studies demonstrated that the extension of proton transfer may be associated with the pKa values of the neutral species (acid and base), and that a large ΔpKa (pKa(base)–pKa(acid)) is usually suggestive of good proton transfer. [43,44] As reported in Table 1 comparing the bases used, the 2-hydroxyethylamine presented the highest pKa (9.5), while tris(2-hydroxyethyl)amine presented the lowest value (7.76). Based on this fact, it is expected that the reaction of PIL synthesis would be more driven to produce PILs in 2-hydroxyethylamine than in tris(2-hydroxyethyl)amine)-based PILs. This supposition is supported by Stoimenovski et al. (2010) that investigated the extent of proton transfer during the synthesis of primary and ternary amine-based PILs using acetic acid as precursor. The authors concluded that primary amines resulted in full proton transfer, while ternary amines presented poor proton transfer. These conclusions were qualitatively supported by Walden plot and by the deprotonation of an indicator acid by the authors. [45] Therefore, comparing the lactate and propionate-based PILs, it would be expected that more fractions of ions is present in HEAL and HEAP, while more neutral species would be present in THEAL and THEAP.

To exploit the role of neutral and ionic species on solubility, the ability of pure solvents (propionic and lactic acids, and 2-hydroxyethylamine, bis(2-hydroxyethyl)amine, and tris(2-hydroxyethyl)amine bases) to dissolve lignin was evaluated and the lignin solubility in these solvents are reported in Table S4 in ESI. The results revealed that propionic acid presented poor ability to dissolve lignin (14.76 wt%), however, the lactic acid was capable of dissolving more than 33.0 wt% of lignin at 323.15 K. The difference

between lactic and propionic acids ability to dissolve lignin is related with the presence of an extra hydroxyl group in the chemical structure of lactic acid. This extra hydroxyl group in absence of water may favor the dissolution of lignin due to the ability of these groups to establish hydrogen bond networks with lignin. [46,47] Based on these observations, we concluded that the increase of lignin solubility when small cation and lower number of hydroxyalkyl chains using propionate-based PILs and the opposite behavior of lignin solubility using acid lactic as precursor of PILs is due to the incomplete proton transfer during the synthesis of PILs. The neutral species will be more available to establish interactions with lignin when ternary amines are used to produce PILs, and because pure lactic acid presented high ability to dissolve lignin, the following sequence is observed and expected: THEAL > BHEAL > HEAL. On the other hand, pure propionic acid was poorly capable of dissolving lignin, and therefore, the ability of dissolving lignin is as follow: HEAP > BHEAP > THEAP.

Concerning the water effect on lignin solubility (Figure 4 and Table S3), once more the anti-solvent role of water and its negative influence on lignin solubility is reported. Besides, no significant differences between the PILs aqueous solutions ability to dissolve lignin was observed to water content higher than 40 wt%, what lead us to conclude that the cationic part of PIL affect mainly the solubility when it is presented in high amounts (≥ 75 wt%). [32] Based on that, the cationic part plays a secondary role, while the anionic part (Section 3.1) has a major role in the lignin dissolution process, as previously reported. [32,39,48,49]

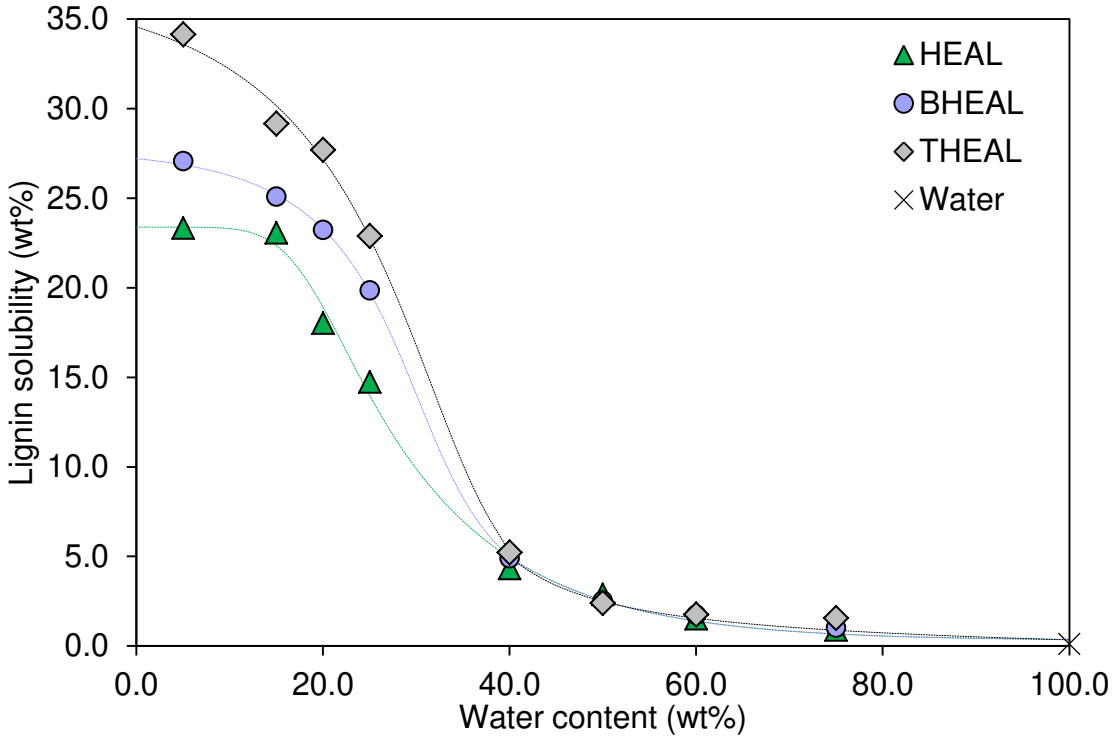

Figure 4 – Kraft lignin solubility in HEAL, BHEAL and THEAL aqueous solutions and pure water at 323.15 K.

Since THEAL presented the best ability to dissolve Kraft lignin, it was chosen to investigate the temperature effect in lignin solubility.

3.3 Kraft lignin solubility and temperature effect

The lignin solubility in pure water, in THEAL and its aqueous solutions at 313.15, 323.15, 333.15 and 353.15 K are shown in Figure 5. The Kraft lignin solubility values, and the respective standard deviations, are presented in Table S5 in ESI.

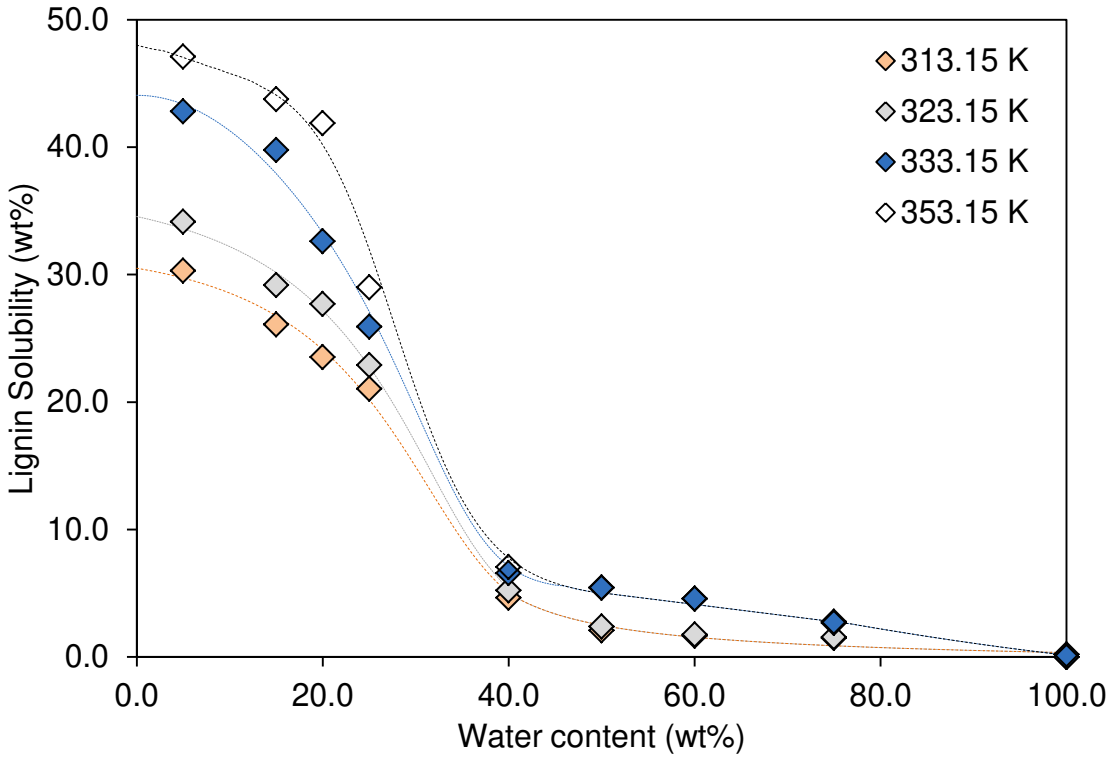

Figure 5 – Kraft lignin solubility in THEAL aqueous solutions and pure water at 313.15, 323.15, 333.15 and 353.15 K

As depicted in Figure 5, all solubility lignin curves presented the same trend: the temperature increase enhanced the dissolution process for higher PIL content, especially at contents superior to 75 wt%. On the other hand, the lignin solubility is slightly sensitive to the increasing of temperature to solutions containing high content of water (> 40 wt%) to all temperature tested. As expected, the temperature increase favored the dissolution process to all range of composition, since the addition of energy promotes the break of bonds in the solid phase, inducing the dissolution (endothermic process). [15,16]

The trends observed in solubility curves may be due the fact that water poorly dissolves lignin, and plays as anti-solvent role solvating the PILs molecules, what would hindrance the interactions between PIL-lignin. Therefore, to cases containing high water content in the solution, the temperature would not impact significantly on lignin solubility. On the other hand, when low contents of water are present in the solution, the PIL molecules, which presented high ability to dissolve lignin as previously demonstrated

(Sections 3.1 and 3.2), would be able to establish connections with the lignin, leading to a sharp increase in the solubility to this range of PIL content.

The HTEAL as media solvent was able to dissolve over than 30 wt% of lignin at 313.15 K after 24h, which is a noteworthy mark. Moreover, the best solubility result obtained in this study was (> 47 wt%) at 353.15 K using HTEAL, which was achieved using lower temperature in comparison to similar studies [16,35,50–53] and proves this PIL ability of dissolving considerable amounts of Kraft lignin.

3.4 Time-dependence of Kraft lignin dissolution in PILs

Time is a key factor to achieve economical success in industrial-scale processes, which the goal is achieve a maximum yield in the shortest time. To investigate the factor time, we have evaluated its influence on lignin dissolution in the neat PILs tested in this study.

The influence of the time on lignin dissolution is presented in Figure 6. The assays were performed with PILs aqueous solutions containing 5 wt% of water at 323.15 K, because this was the condition that present the maximum lignin solubility to all PILs used except HEASu, which is solid at these conditions. To HEASu, the water content was equal to 20 wt%. The Kraft lignin solubility, and the respective standard deviations, is presented in Table S6 in ESI.

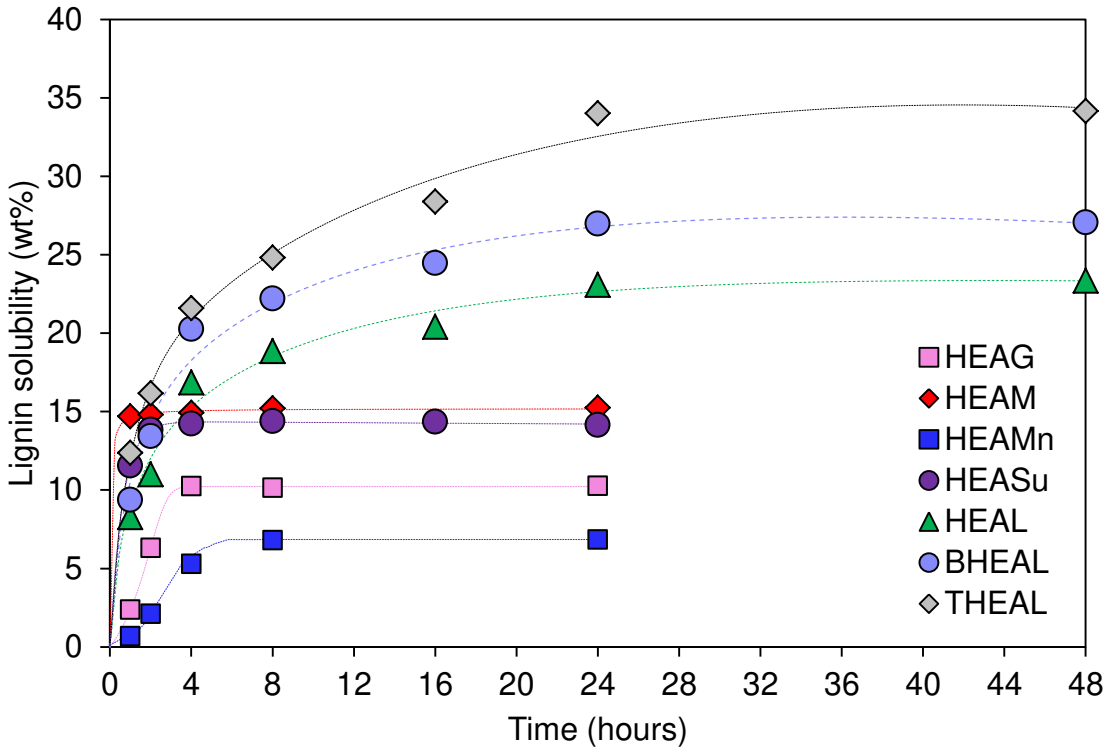

Figure 6 – Time-dependent solubility of lignin in PILs (95 wt%) at 323.15 K and different periods of time

Two different dissolution behaviors can be observed in Figure 6: the HEAG, HEAM, HEAMn and HEASu PILs reached the maximum solubility after 8 hours of assay, while the lactate-based PILs took longer time (24 hours) to achieve the saturation state. The lignin dissolution in HEASu presented a quick dissolution rate in which more than 81% of maximum solubility was reached within only 1 hour, and achieving the saturation after 4 hours, despite the fact that this PIL presented a significant solubility (14.15 wt%) when compared to 2-hydroxyethylammonium based PILs. The HEAM also exhibited this behavior, presenting an initial fast dissolution, achieving more than 96% of maximum solubility within 1 hour of assay, and a progressive but slower dissolution rate within 1 to 8 hours, reaching 15.20 wt% after this time.

A slow dissolution rate was observed to HEAG and more pronounced to HEAMn, and this behavior may be attributed to the poor ability of these PILs to dissolve lignin, and also, to their viscosity (Table S7 - ESI). Since HEAMn presents higher viscosity than HEAG it is expected that the lignin dissolution process would take longer

time to achieve the dissolution plateau. The HEAM achieves the saturation state through a slow and progressive dissolution step, and this behavior may be attributed to the notorious viscosity of HEAM which has greater viscosity at 323.15 K (almost 3-fold) when compared to any other PIL used in this study. This elevated viscosity may impair the mass transfer process, and consequently decreases the lignin dissolution rate at this final step. [54–56]

To reach the dissolution plateau, the lactate-based PILs have taken longer time when compared to the other PILs studied. Indeed, PILs formed by lactic acid as precursor (HEAL, BHEAL and THEAL) were able to dissolve more than 23 wt% of lignin, as demonstrated in Section 3.1, and due to this fact, a longer time was required to finalize the dissolution process (24 hours). The ability of lactate-PILs to dissolve lignin can be ordered as following: THEAL > BHEAL > HEAL; and the same trend in lignin dissolution curves is observed. Besides, the viscosity of these PILs (ESI - Table S7) can be ordered in the same sequence, therefore, the trend observed is explained by the viscosity and also by their ability to dissolve lignin.

As presented, some assays took long time (over than 24 hours) to dissolve completely the lignin in neat PILs using magnetic bar agitation (MBA), and this long period could be associated to a not efficient agitation provided by the MBA. Therefore, to investigate the possibility of decreasing the time required to fully dissolve lignin, some assays were performed using an ultrasound water bath (UWB) at 323.15 K to achieve the saturation state quicker.

To perform this study, some neat PILs which presented a slow dissolution rate, as demonstrated in Figure 7, were chosen: HEAMn, HEAG and THEAL. The PILs were dopped with 5 wt% of water since they presented maximum solubility at this composition, between the water proportions verified previously in this study. The lignin dissolution values are presented in Table S8 in ESI along with the respective standard deviations. The results of this study are presented in Figure 7.

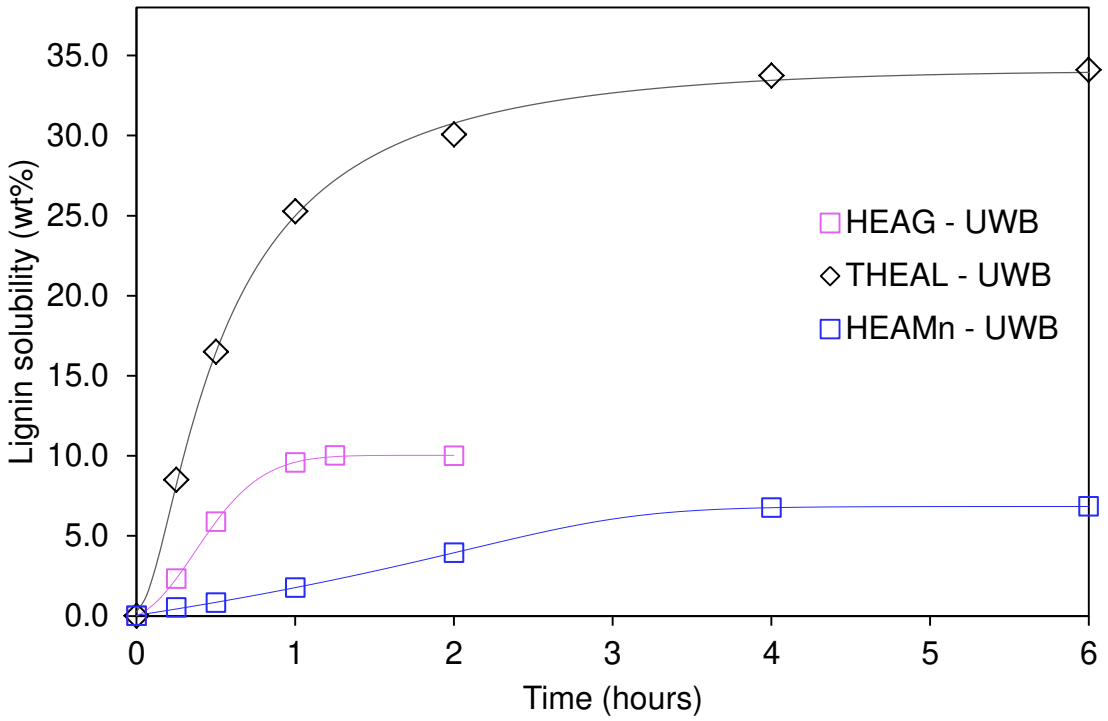

Figure 7 – Time-dependent solubility of lignin in PILs (95 wt%) at 323.15 K and different periods of time: using an Ultrasound Water Bath (UWB)

As described before, the HEAG and HEAMn reached the saturation value after 8h of constant agitation (200 rpm) provided by a MBA, while THEAL took 24h to attain saturation limit. In contrast, the saturation state was achieved within 1.25 hours to HEAG, and 4 hours to HEAMn and THEAL systems using the UWB. Besides, assays that took longer than 4 hours of sonication did not indicated signals of supersaturation since the lignin solubility reached a plateu state, as observed to THEAL and HEAMn systems.

As depicted in Figure 7, the UWB even in the absence of significant physical bulk movement of particles, enhanced the dissolution rate, when compared to the MBA. [57,58] Some authors have reported that ultrasound has the effect of fragmenting the solid particles by microjets that are created by the acoustic field, thus, the improvement in lignin dissolution observed in this study may be related to the fragmentation phenomenon. These solid particles fragmentation enhances the mass transfer rates due

to the increase of interfacial area available for the transport process promoted by the ultrasound. [59,60] In other words, when an ultrasonic wave is applied in a liquid phase, cavitation bubbles are formed. These bubbles collapse and produce shock waves, resulting in a microscopic turbulence around the solid particles reducing the boundary layer, which favors the mass transfer. [57,58]

An improvement in dissolution time was demonstrated and, as a result, the saturation (mass transfer process) was accelerated. The saturation was reached within 4 hours using the UWB apparatus, while it took 24 hours using the MBA, both with THEAL as media solvent at 323.15 K. Therefore, the use of PILs in combination with ultrasound technique is a quick and efficient method to dissolve Kraft lignin at low temperature (323.15 K).

3.5 Recycling of PIL

The recycling of PILs is a crucial step to achieve an economical and sustainable process. Some authors have reported the recovering of PILs after lignin extraction or dissolution through vacuum distillation.[14,15,61,62] The HEAM and THEAL were chosen to demonstrate the possibility of reusing PILs after lignin dissolution since this neat PIL has great ability to dissolve lignin and negligible capacity when water content is up to 50 wt%. This behavior favors the recyclability because additions of water precipitates almost all the lignin dissolved, and this amount of water can be easily distillated.

The recycling step was performed as described in Section 2.6. It was recovered up to 93 wt% of HEAM and 96 wt% of THEAL of the initial IL mass after the distillation process, which represents the recyclability potential of these PILs. The recovered PIL was applied for three cycles of lignin solubility. The assays presented an efficiency of 99.81, 99.69 and 99.56% for cycles 1, 2, and 3, respectively, when compared to the fresh HEAM initially used, and an efficiency of 99.83, 98.28, and 97.35% for cycles 1, 2, and 3, respectively, when compared to the fresh THEAL initially used (Figure 8). Therefore, we demonstrated, as proof of concept, a negligible loss in dissolution efficiencies. Besides, a residual lignin content of 0.29, 0.32, and 2.44 wt% presented in

HEAM was found in cycles 1, 2, and 3, respectively, and 2.96, 5.58, and 7.04 wt% presented in THEAL in cycles 1, 2, and 3, respectively, which is an indication that low molecular weight lignin fractions remained dissolved in HEAM and THEAL solution after the addition of water, as reported in our previous study.[32]

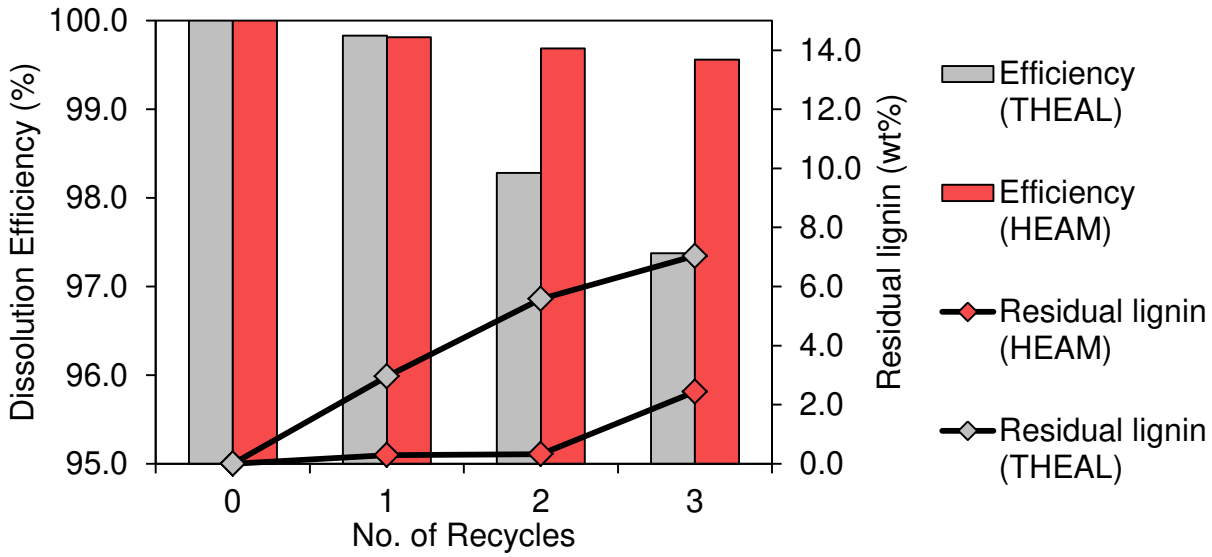

Figure 8 – Dissolution efficiency of lignin in fresh HEAM (95 wt%), fresh THEAL (95 wt%), recycled HEAM (95 wt%), recycled THEAL (95 wt%), and residual lignin

The recyclability was well performed and no significant loss in dissolution ability of HEAM and THEAL was observed, which demonstrated that these PILs are suitable candidates to realize this process.

4. CONCLUSIONS

A comprehensive study about the ability of alkanolammonium PILs and their aqueous solutions to dissolve Kraft lignin at low temperatures was performed. The results showed that PILs were solvated by water that impaired the interactions between PILs and lignin, and consequently its dissolution. The anionic part of PILs affected more significantly the lignin dissolution process, while the cationic part played a secondary role in this phenomenon. The THEAL was the best PIL tested in this work to dissolve Kraft lignin, achieving more than 47 wt% of lignin solubility at 353.15 K. The effect of the temperature was also demonstrated using THEAL and their aqueous solutions, and as

expected, the temperature favored the lignin dissolution. The kinetics of dissolution was investigated and the saturation state was achieved within 8 hours to all PILs tested in study, except to lactate-based PILs, which needed 24 hours to finalize the dissolution process. Also, an UWB was used to realize the dissolution of lignin, and presented faster lignin dissolution, when compared to the MBA. The UWB was capable of finalizing the dissolution process within 4 hours, while MBA achieved the same saturation state within, at least, 8 hours. Lastly, the recycle and reuse of HEAM and THEAL was successfully demonstrated, at least for 3 cycles, without losing its efficiency.

References

1 A. R. C. Morais, A. M. Da Costa Lopes and R. Bogel-Łukasik, *Chem. Rev.*, 2015, **115**, 3–27.

2 M. H. L. Silveira, A. R. C. Morais, A. M. Da Costa Lopes, D. N. Olekszyszen, R. Bogel-Łukasik, J. Andreaus and L. Pereira Ramos, *ChemSusChem*, 2015, **8**, 3366–3390.

3 C. H. Zhou, X. Xia, C. X. Lin, D. S. Tong and J. Beltramini, *Chem. Soc. Rev.*, 2011, **40**, 5588–5617.

4 D. R. Dodds and R. A. Gross, *Science*, 2007, **318**, 1250–1251.

5 J. R. Rostrup-Nielsen, *Science (80-.).*, 2005, **308**, 1421–1422.

6 J. W. Agger, T. Isaksen, A. Varnai, S. Vidal-Melgosa, W. G. T. Willats, R. Ludwig, S. J. Horn, V. G. H. Eijsink and B. Westereng, *Proc. Natl. Acad. Sci.*, 2014, **111**, 6287–6292.

7 P. Langan, L. Petridis, H. M. O'Neill, S. V. Pingali, M. Foston, Y. Nishiyama, R. Schulz, B. Lindner, B. Leif Hanson, S. Harton, W. T. Heller, V. Urban, B. R. Evans, S. Gnanakaran, A. J. Ragauskas, J. C. Smith and B. H. Davison, *Green Chem.*, 2014, **16**, 63–68.

8 E. M. Rubin, *Nature*, 2008, **454**, 841–5.

9 F. H. Isikgor and C. R. Becer, *Polym. Chem.*, 2015, **6**, 4497–4559.

10 J. Zakzeski, P. C. A. Bruijnincx, A. L. Jongerius and B. M. Weckhuysen, *Chem.*

Rev., 2010, **110**, 3552–3599.

11 C. Wang, A. Thygesen, Y. Liu, Q. Li, M. Yang, D. Dang, Z. Wang, Y. Wan, W. Lin and J. Xing, *Biotechnol. Biofuels*, 2013, **6**, 1–10.

12 R. J. A. Gosselink, E. De Jong, B. Guran and A. Abächerli, *Ind. Crops Prod.*, 2004, **20**, 121–129.

13 A. Brandt, J. Gräsvik, J. P. Hallett and T. Welton, *Green Chem.*, 2013, **15**, 550–583.

14 A. Brandt-Talbot, F. J. V. Gschwend, P. S. Fennell, T. M. Lammens, B. Tan, J. Weale and J. P. Hallett, *Green Chem.*, 2017, **19**, 3078–3102.

15 T. Rashid, C. F. Kait, I. Regupathi and T. Murugesan, *Ind. Crops Prod.*, 2016, **84**, 284–293.

16 Y. Pu, N. Jiang and A. J. Ragauskas, *J. Wood Chem. Technol.*, 2007, **27**, 23–33.

17 O. Merino, G. Fundora-Galano, R. Luque and R. Martínez-Palou, *ACS Sustain. Chem. Eng.*, 2018, **6**, 4122–4129.

18 A. Xu, X. Guo, Y. Zhang, Z. Li and J. Wang, *Green Chem.*, 2017, **19**, 4067–4073.

19 P. Alvira, E. Tomás-Pejó, M. Ballesteros and M. J. Negro, *Bioresour. Technol.*, 2010, **101**, 4851–4861.

20 A. Mirjafari, L. N. Pham, J. R. McCabe, N. Mobarrez, E. A. Salter, A. Wierzbicki, K. N. West, R. E. Sykora and J. H. Davis, *RSC Adv.*, 2013, **3**, 337–340.

21 D. R. MacFarlane and K. R. Seddon, *Aust. J. Chem.*, 2007, **60**, 3–5.

22 K. S. Egorova, E. G. Gordeev and V. P. Ananikov, *Chem. Rev.*, 2017, **117**, 7132–7189.

23 A. D. Sawant, D. G. Raut, N. B. Darvatkar and M. M. Salunkhe, *Green Chem. Lett. Rev.*, 2011, **4**, 41–54.

24 T. L. Greaves and C. J. Drummond, *Chem. Rev.*, 2008, **108**, 206–237.

25 A. Abate, D. J. Hollman, J. Teuscher, S. Pathak, R. Avolio, G. D'Errico, G. Vitiello, S. Fantacci and H. J. Snaith, *J. Am. Chem. Soc.*, 2013, **135**, 13538–13548.

26 Z. Duan, Y. Gu, J. Zhang, L. Zhu and Y. Deng, *J. Mol. Catal. A Chem.*, 2006, **250**, 163–168.

27 T. Rashid, N. Gnanasundaram, A. Appusamy, C. F. Kait and M. Thanabalan, *Ind. Crops Prod.*, 2018, **116**, 122–136.

28 B. Gorska, J. Pernak and F. Béguin, *Electrochim. Acta*, 2017, **246**, 971–980.

29 T. L. Greaves and C. J. Drummond, *Chem. Rev.*, 2015, **115**, 11379–11448.

30 O. Merino, G. Fundora-Galano, R. Luque and R. Martínez-Palou, *ACS Sustain. Chem. Eng.*, 2018, **6**, 4122–4129.

31 T. Rashid, C. F. Kait, I. Regupathi and T. Murugesan, *Ind. Crops Prod.*, 2016, **84**, 284–293.

32 R. M. Dias, A. M. da Costa Lopes, A. J. D. Silvestre, M. C. Costa and J. A. P. Coutinho, *Ind. Crops Prod,* **143**, 111866, 2020.

33 PubChem, National Institute of Health.

34 Y. Pu, N. Jiang and A. J. Ragauskas, *J. Wood Chem. Technol.*, 2007, **27**, 23–33.

35 H. Lateef, S. Grimes, P. Kewcharoenwong and B. Feinberg, *J. Chem. Technol. Biotechnol.*, 2009, **84**, 1818–1827.

36 T. Akiba, A. Tsurumaki and H. Ohno, *Green Chem.*, 2017, **19**, 2260–2265.

37 X. D. Hou, J. Xu, N. Li and M. H. Zong, *Biotechnol. Bioeng.*, 2015, **112**, 65–73.

38 B. Soares, D. J. P. Tavares, J. L. Amaral, A. J. D. Silvestre, C. S. R. Freire and J. A. P. Coutinho, *ACS Sustain. Chem. Eng.*, 2017, **5**, 4056–4065.

39 W. Ji, Z. Ding, J. Liu, Q. Song, X. Xia, H. Gao, H. Wang and W. Gu, *Energy and Fuels*, 2012, **26**, 6393–6403.

40 B. Soares, D. J. P. Tavares, J. L. Amaral, A. J. D. Silvestre, C. S. R. Freire and J. A. P. Coutinho, *ACS Sustain. Chem. Eng.*, 2017, **5**, 4056–4065.

41 Y. Wang, Y. Hou, W. Wu, D. Liu, Y. Ji and S. Ren, *Green Chem.*, 2016, **18**, 3089–3097.

42 A. Xu, L. Chen, X. Xu, Z. Xiao, R. Liu, R. Gao, M. Yuan and L. Zhang, *Polymers (Basel).*, 2018, **10**, 1–10.

43 C. A. Angell, N. Byrne and J. P. Belieres, *Acc. Chem. Res.*, 2007, **40**, 1228–1236.

44 M. Yoshizawa, W. Xu and C. A. Angell, *J. Am. Chem. Soc.*, 2003, **125**, 15411–15419.

45 J. Stoimenovski, E. I. Izgorodina and D. R. MacFarlane, *Phys. Chem. Chem. Phys.*, 2010, **12**, 10341–10347.

46 J. Sun, T. Dutta, R. Parthasarathi, K. H. Kim, N. Tolic, R. K. Chu, N. G. Isern, J. R. Cort, B. A. Simmons and S. Singh, *Green Chem.*, 2016, **18**, 6012–6020.

47 J. Sameni, S. Krigstin and M. Sain, *BioResources*, 2017, **12**, 1548–1565.

48 Y. Zhang, H. He, K. Dong, M. Fan and S. Zhang, *RSC Adv.*, 2017, **7**, 12670–12681.

49 J. M. Andanson, E. Bordes, J. Devémy, F. Leroux, A. A. H. Pádua and M. F. C. Gomes, *Green Chem.*, 2014, **16**, 2528–2538.

50 D. Glas, C. Van Doorslaer, D. Depuydt, F. Liebner, T. Rosenau, K. Binnemans and D. E. De Vos, *J. Chem. Technol. Biotechnol.*, 2015, **90**, 1821–1826.

51 A. Casas, M. Oliet, M. V. Alonso and F. Rodríguez, *Sep. Purif. Technol.*, 2012, **97**, 115–122.

52 M. M. Hossain and L. Aldous, *Aust. J. Chem.*, 2012, **65**, 1465.

53 A. Diop, A. H. Bouazza, C. Daneault and D. Montplaisir, *BioResources*, 2013, **8**, 4270–4282.

54 A. Radwan, G. L. Amidon and P. Langguth, 2012, **33**, 403–416.

55 H. Liu, P. Wang, X. Zhang, F. Shen and C. G. Gogos, *Int. J. Pharm.*, 2010, **383**, 161–169.

56 T. V. Duncan and K. Pillai, *ACS Appl. Mater. Interfaces*, 2015, **7**, 2–19.

57 L. H. Thompson and L. K. Doraiswamy, *Ultrason. Sonochem.*, 1999, **38**, 1215–1249.

58 D. Krishna Sandilya and A. Kannan, *Ultrason. Sonochem.*, 2010, **17**, 427–434.

59 H. Malaeke, M. R. Housaindokht, H. Monhemi and M. Izadyar, *J. Mol. Liq.*, 2018, **263**, 193–199.

60 S. Rezania, Z. Ye and R. E. Berson, *Appl. Biochem. Biotechnol.*, 2009, **153**, 103–115.

61 E. C. Achinivu, R. M. Howard, G. Li, H. Gracz and W. A. Henderson, *Green Chem.*, 2014, **16**, 1114–1119.

62 C. L. B. Reis, L. M. A. e. Silva, T. H. S. Rodrigues, A. K. N. Félix, R. S. de Santiago-Aguiar, K. M. Canuto and M. V. P. Rocha, *Bioresour. Technol.*, 2017, **224**, 694–701.

Acknowledgements

This study was financed in part by the Coordenação de Aperfeiçoamento de Pessoal de Nível Superior - Brasil (CAPES) - Finance Code 001. The authors also would like to thank CNPq [169743/2018-7], FAPESP [2014/21252-0] and FAEPEX/UNICAMP for financial support. This study was partially developed within the scope of the project CICECO-Aveiro Institute of Materials, POCI-01-0145-FEDER-007679 (FCT Ref. UID /CTM /50011/2013), financed by national funds through the FCT/MEC and when appropriate co-financed by FEDER under the PT2020 Partnership Agreement. DeepBiorefinery (PTDC/AGR-TEC/1191/2014) and Multibiorefinery: (POCI-01-0145-FEDER-016403) projects are also acknowledged.

Supplementary Information

An investigation of Kraft lignin solubility in protic ionic liquids and their aqueous solutions

Rafael M. Dias[1], Lívia C. G. Petrin[1], Filipe H. B, Sosa[1,2], André M. da Costa Lopes[2], João A. P. Coutinho[2], Mariana C. da Costa[1,].*

[1]Department of Process and Product Design (DDPP) - School of Chemical Engineering (FEQ), University of Campinas (UNICAMP), 13083-852, Campinas, São Paulo, Brazil.

[2]CICECO, Aveiro Institute of Materials, Department of Chemistry, University of Aveiro, 3810-193 Aveiro, Portugal.

*Corresponding author. E-mail address: mcosta@feq.unicamp.br

Table of contents

PILs characterization

FT-IR

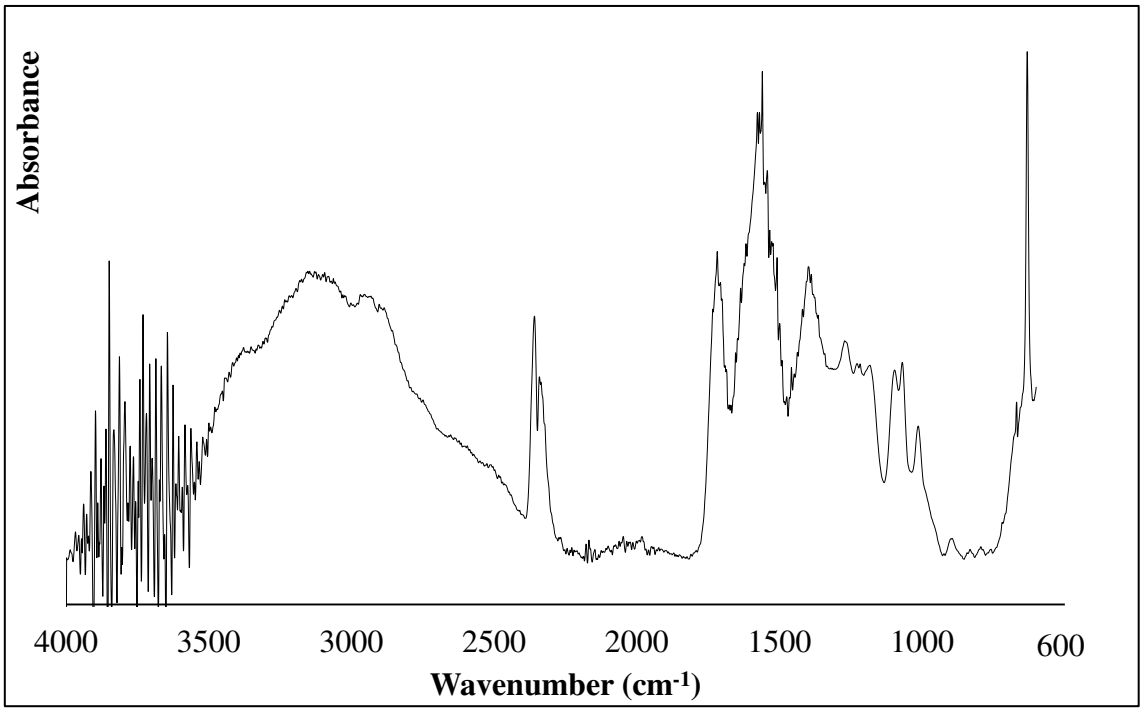

Figure S1 – FT-IR (HEAM)

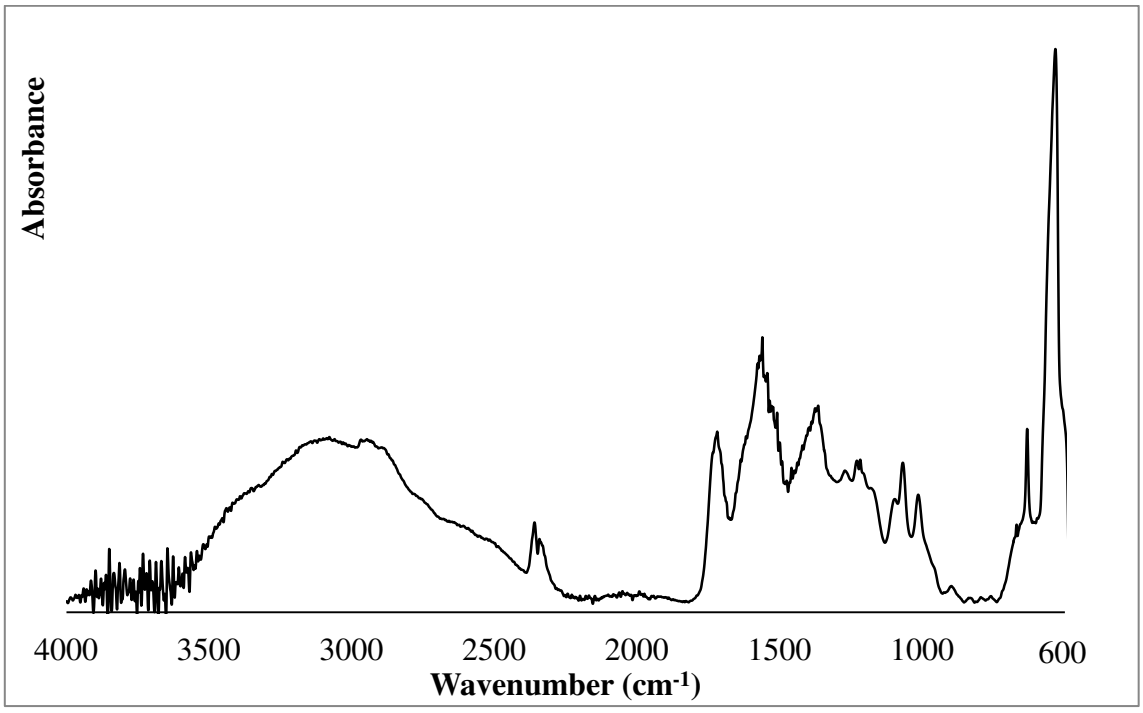

Figure S2 – FT-IR (HEAMn)

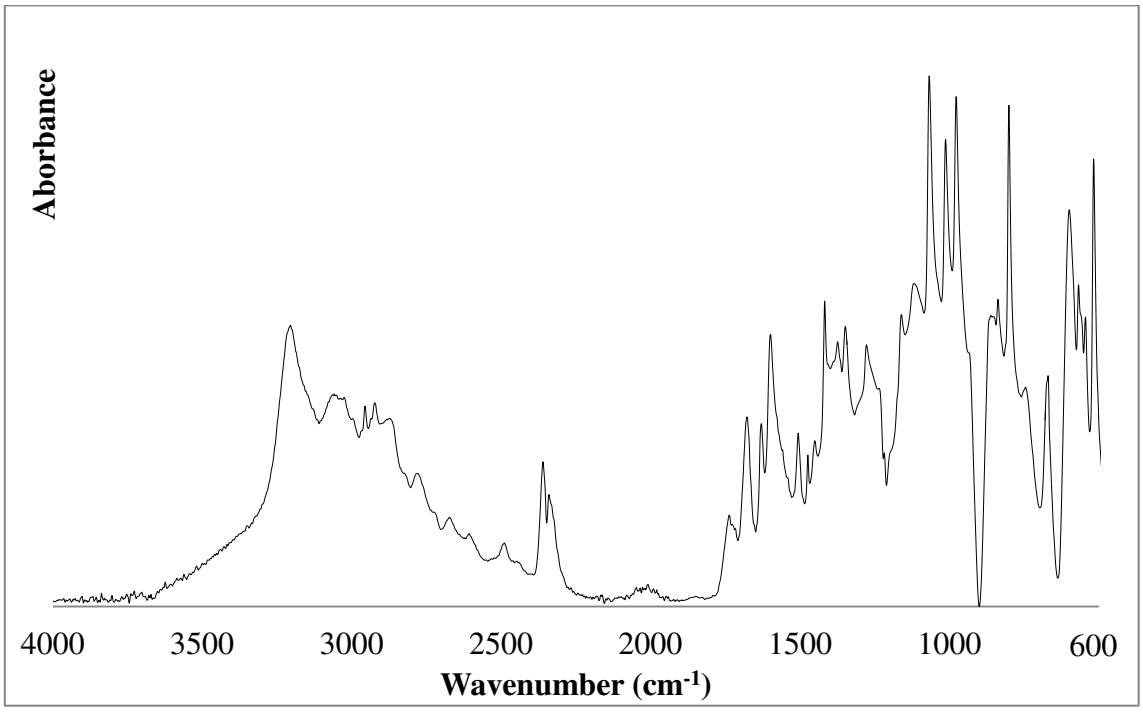

Figure S3 – FT-IR (HEASu)

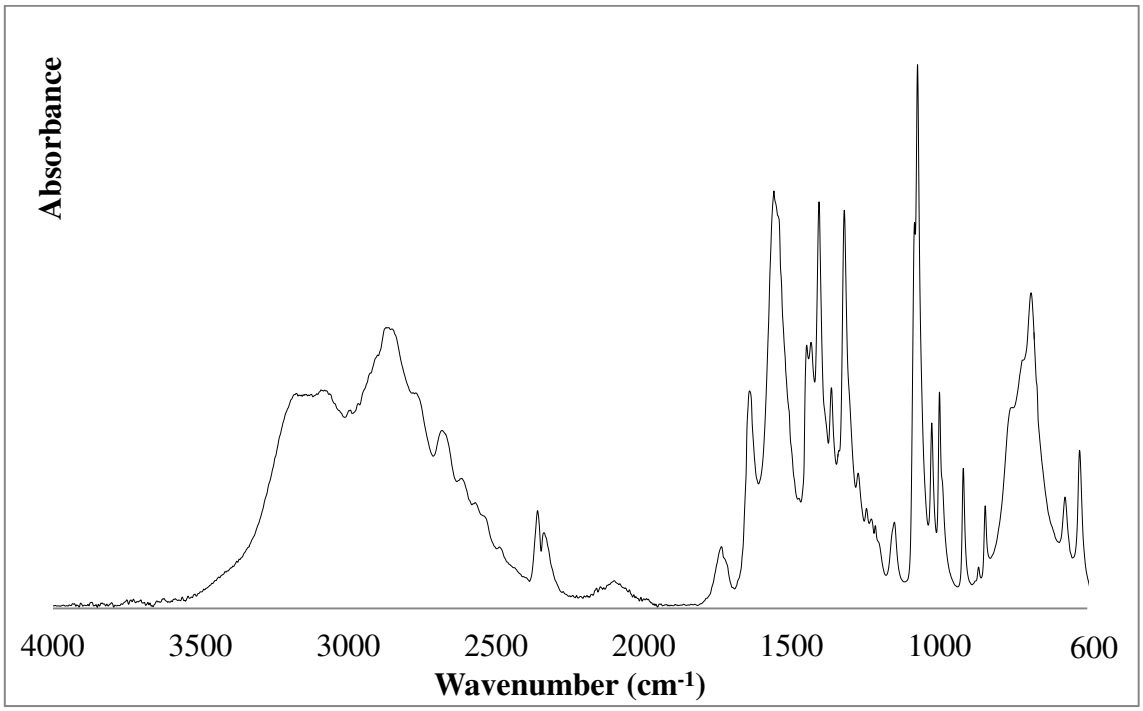

Figure S4 – FT-IR (HEAG)

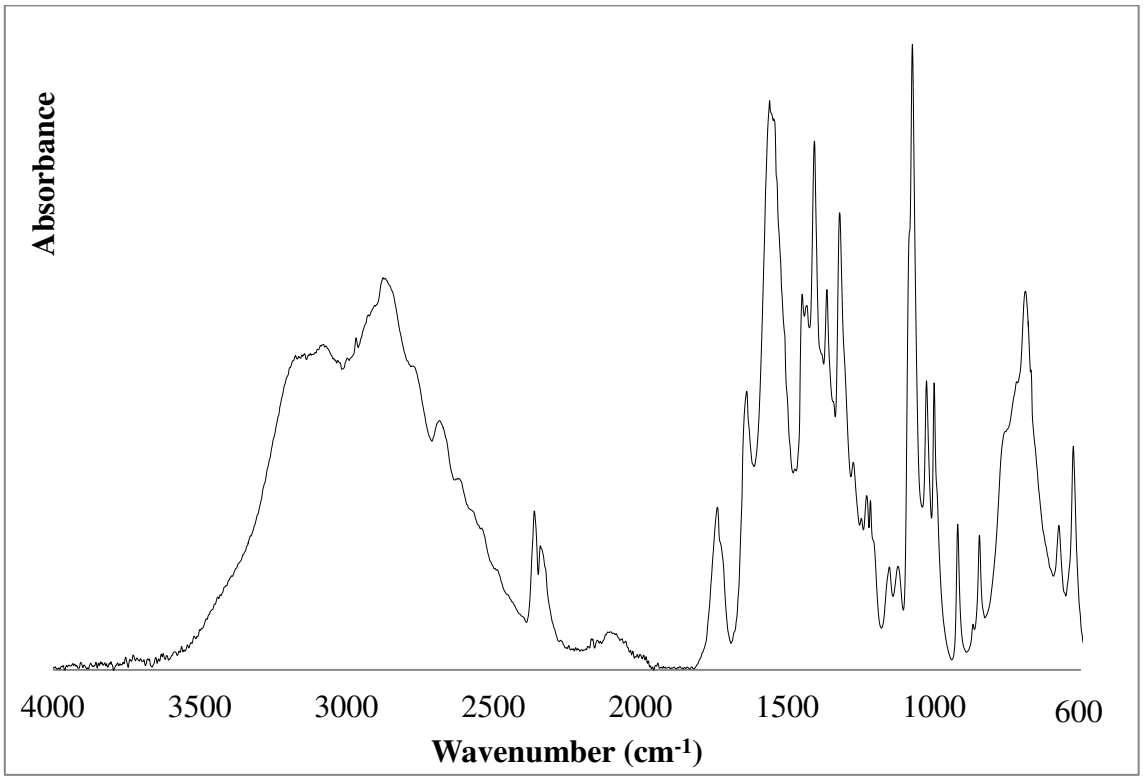

Figure S5 – FT-IR (HEAL)

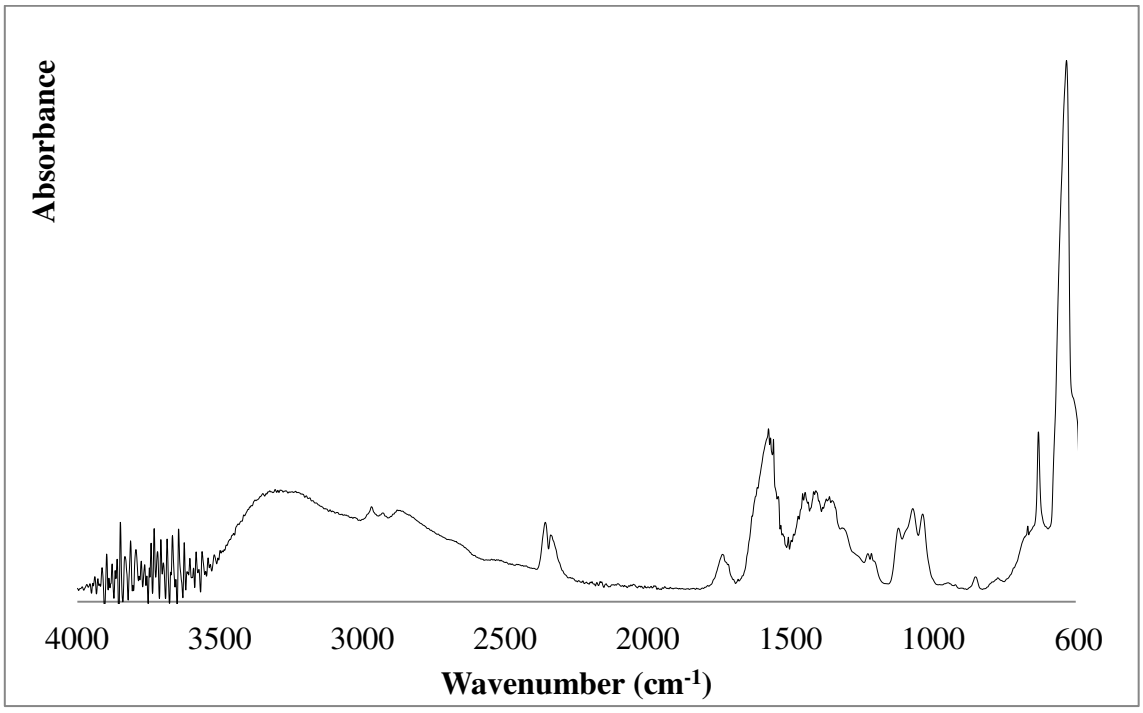

Figure S6 – FT-IR (BHEAL)

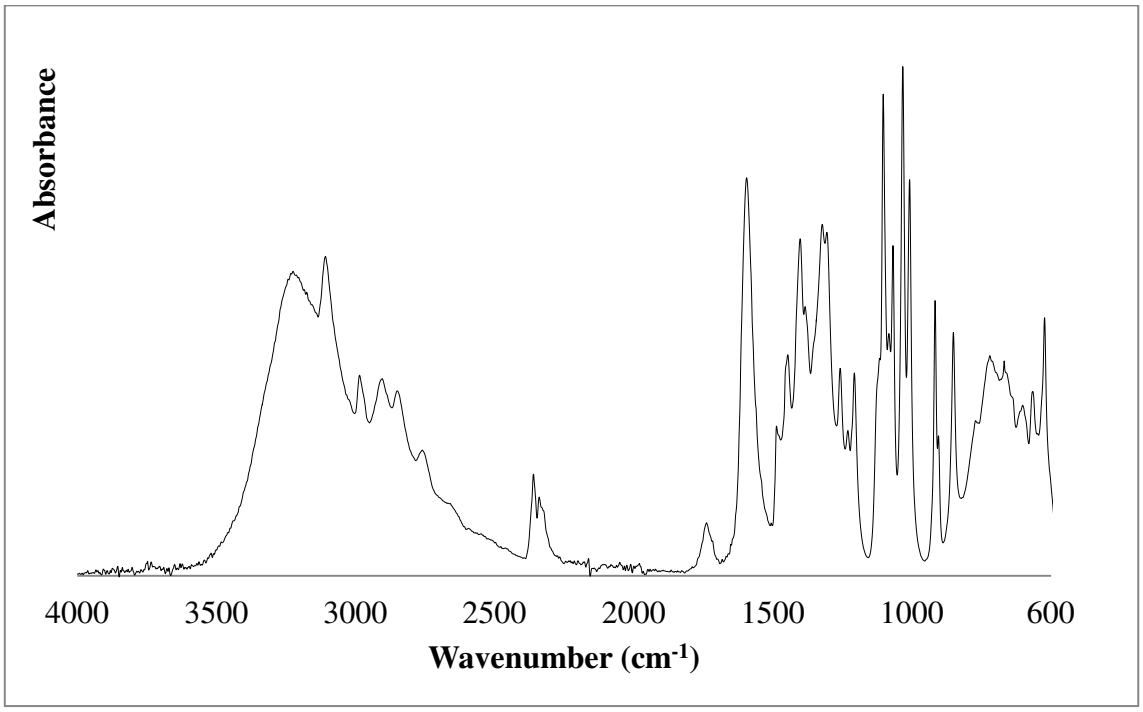

Figure S7 – FT-IR (THEAL)

^{1}H-NMR and ^{13}C NMR

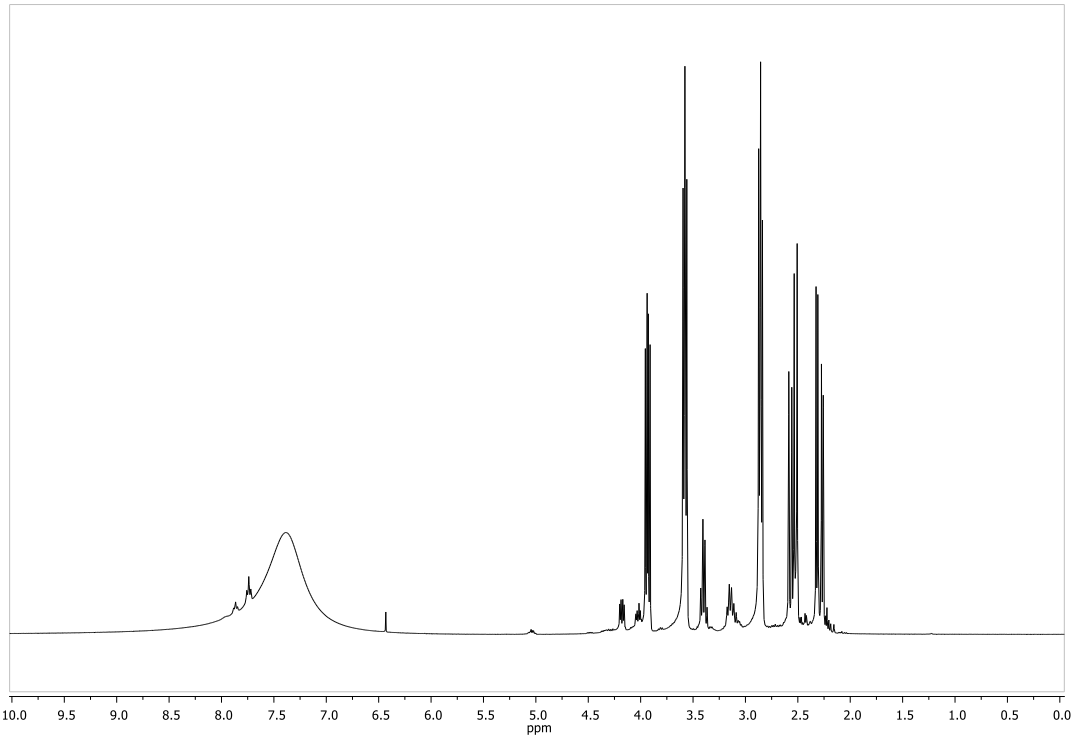

Figure S8 – ^{1}H-NMR (HEAM)

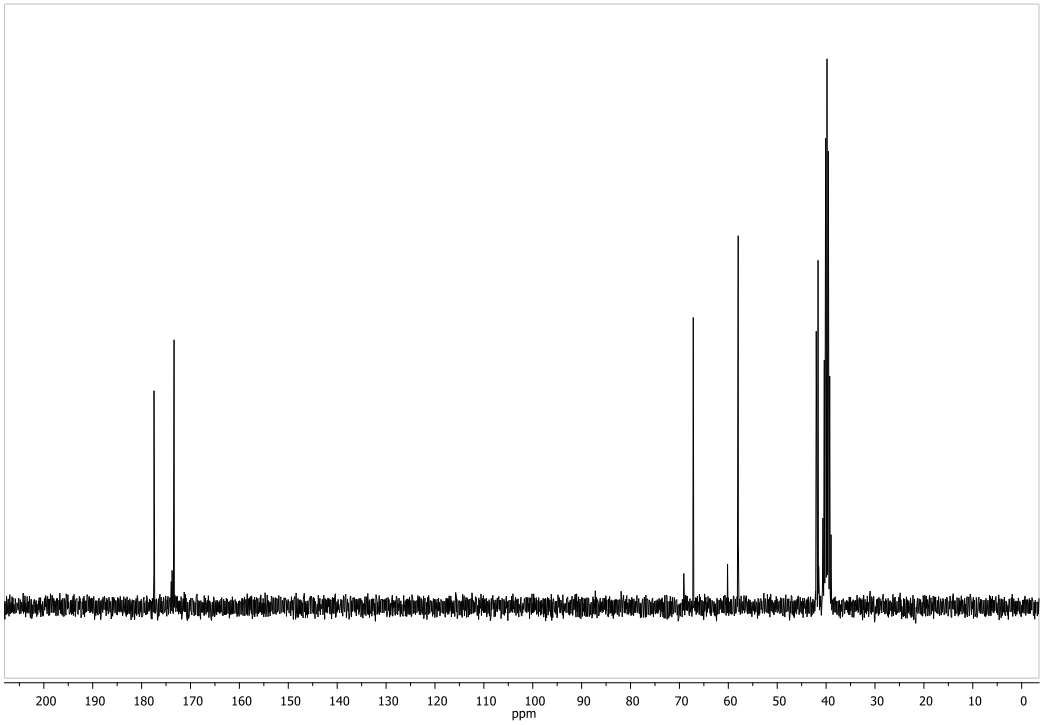

Figure S9 – ^{13}C-NMR (HEAM)

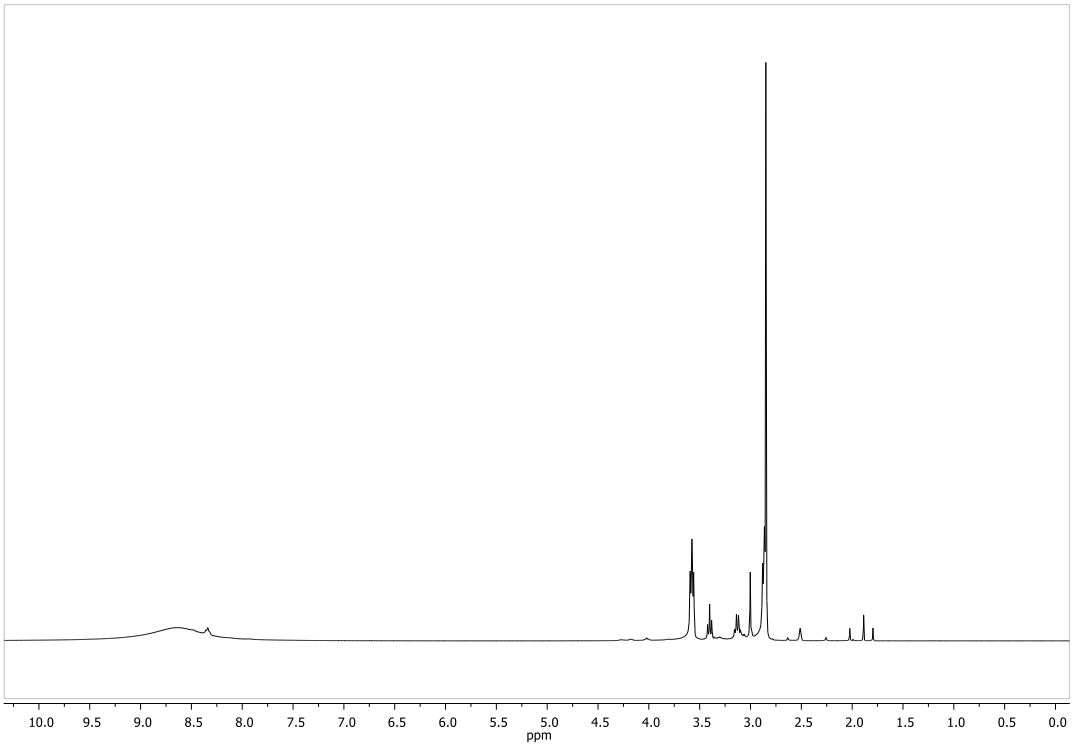

Figure S10 – ^{1}H-NMR (HEAMn)

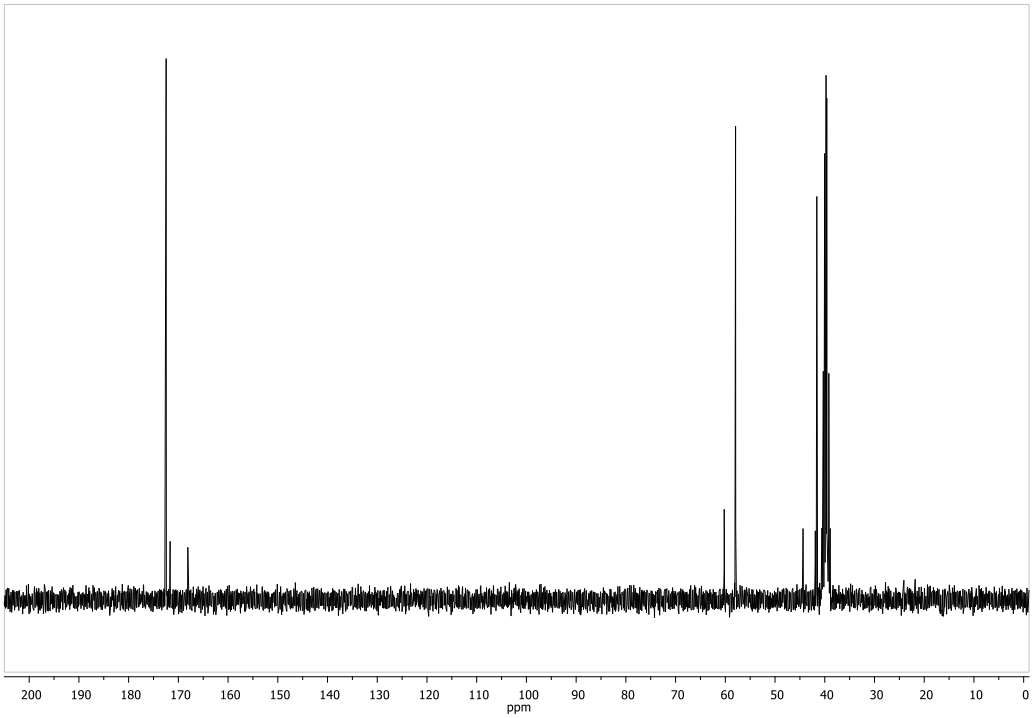

Figure S11 – ^{13}C-NMR (HEAMn)

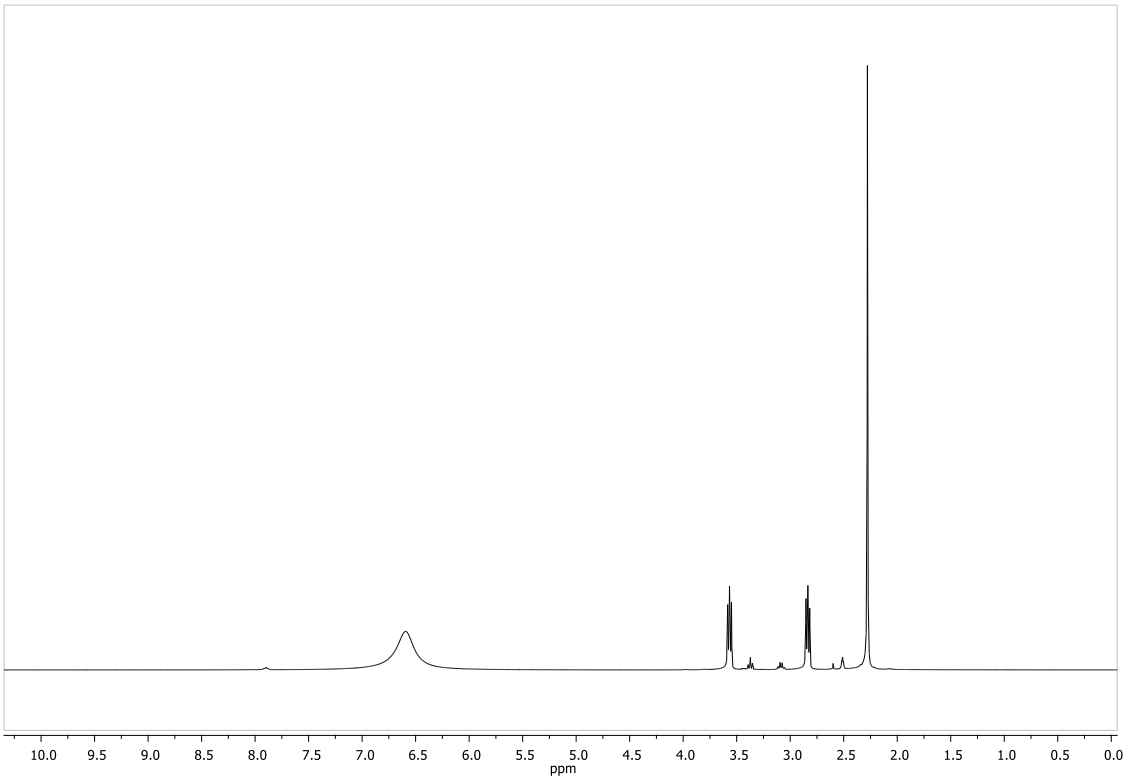

Figure S12 – ^{1}H-NMR (HEASu)

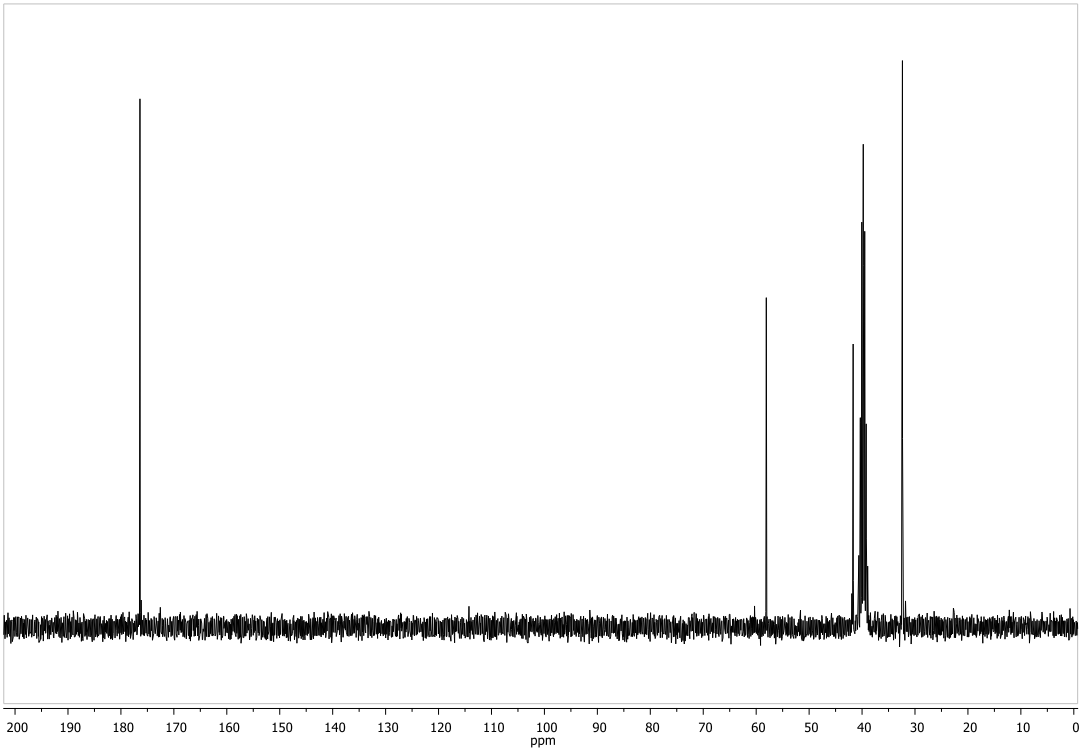

Figure S13 – ^{13}C-NMR (HEASu)

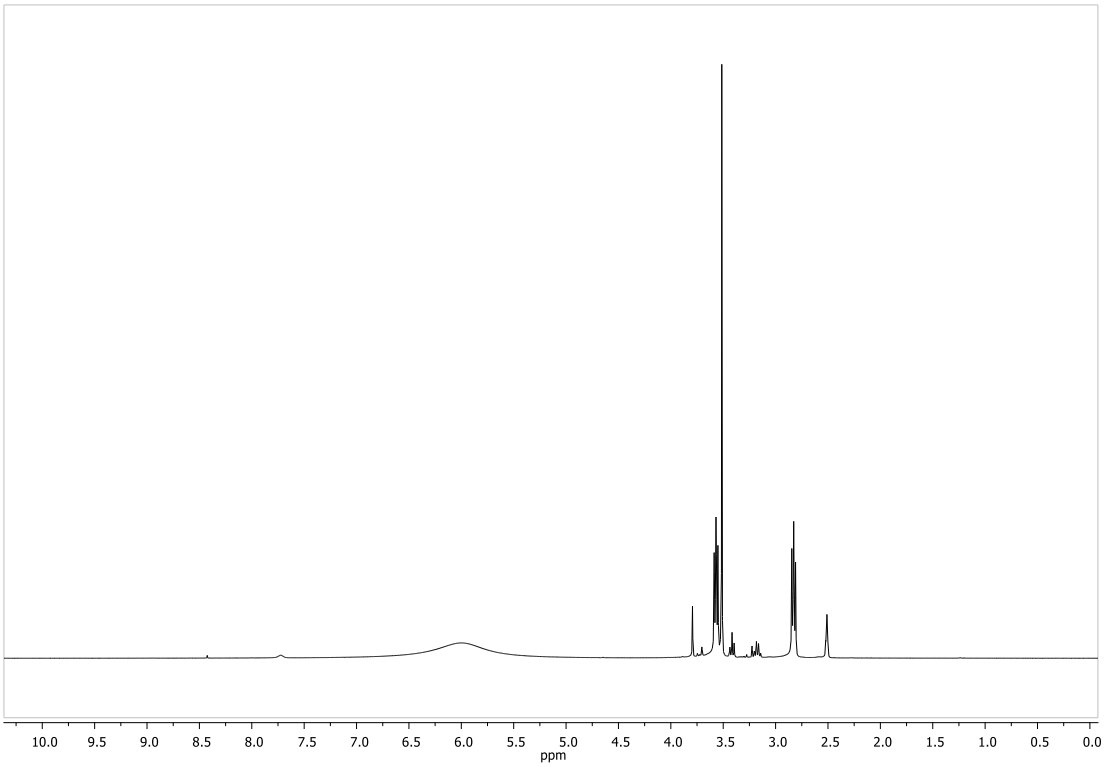

Figure S14 – ^{1}H-NMR (HEAG)

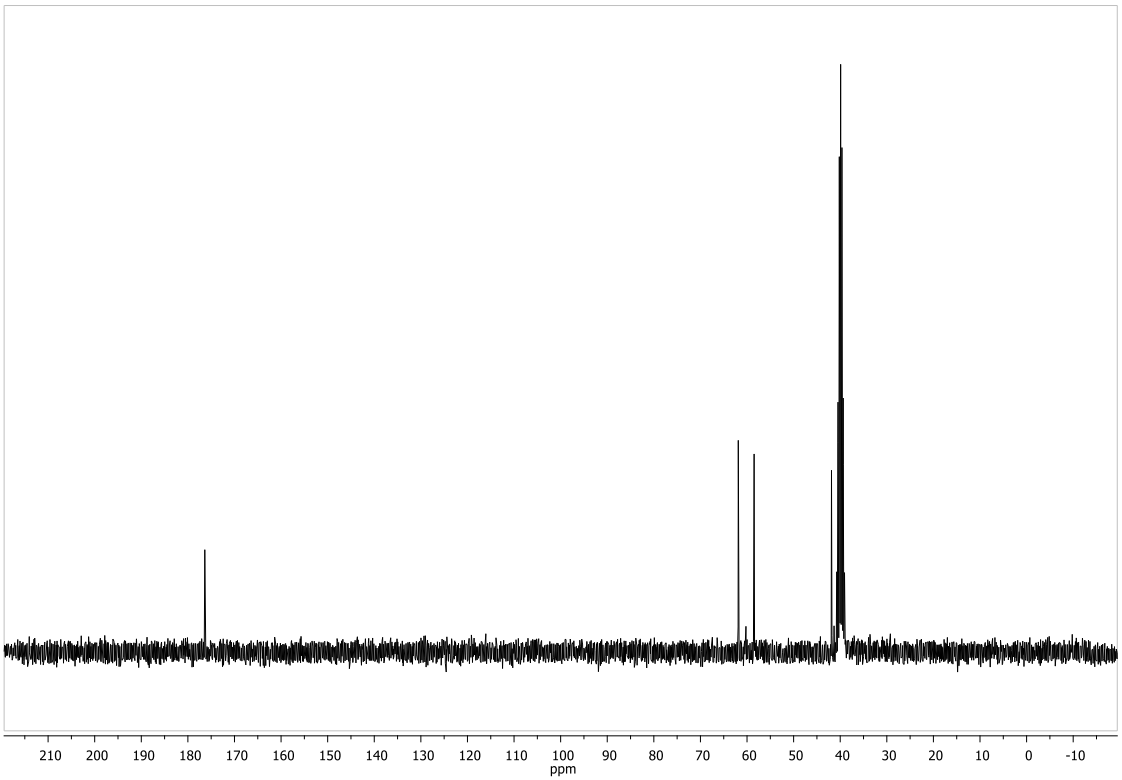

Figure S15 – ^{13}C-NMR (HEAG)

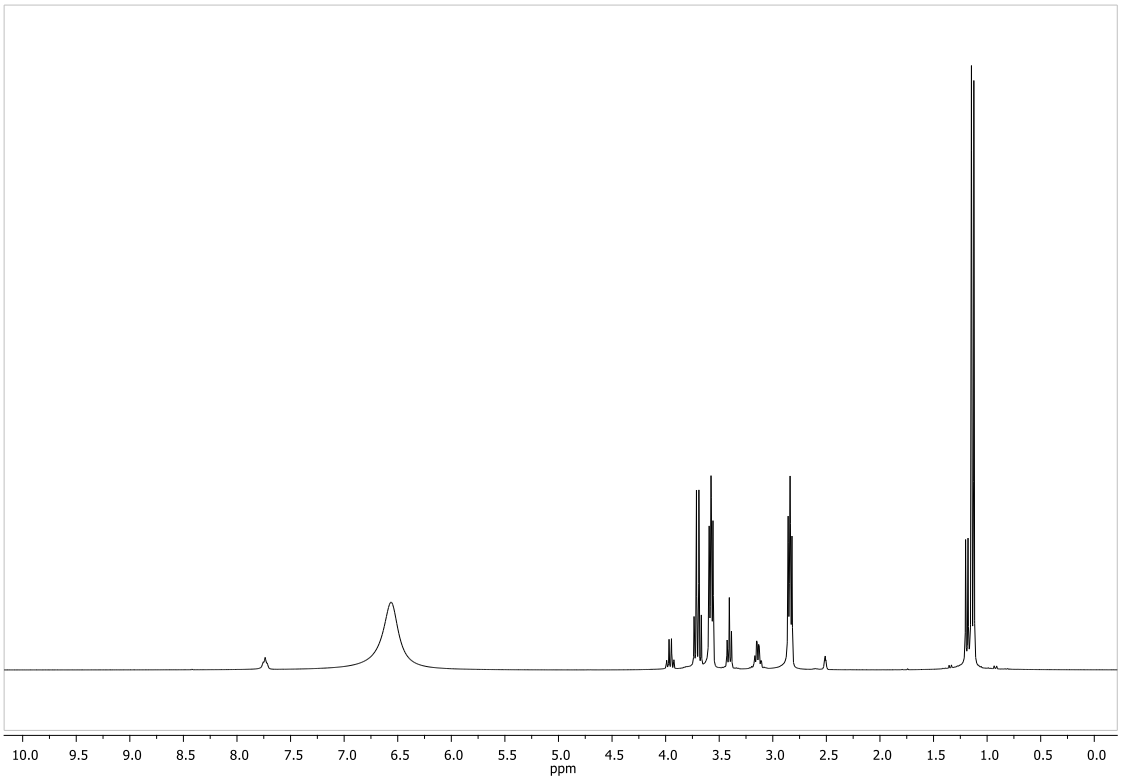

Figure S16 – ^{1}H-NMR (HEAL)

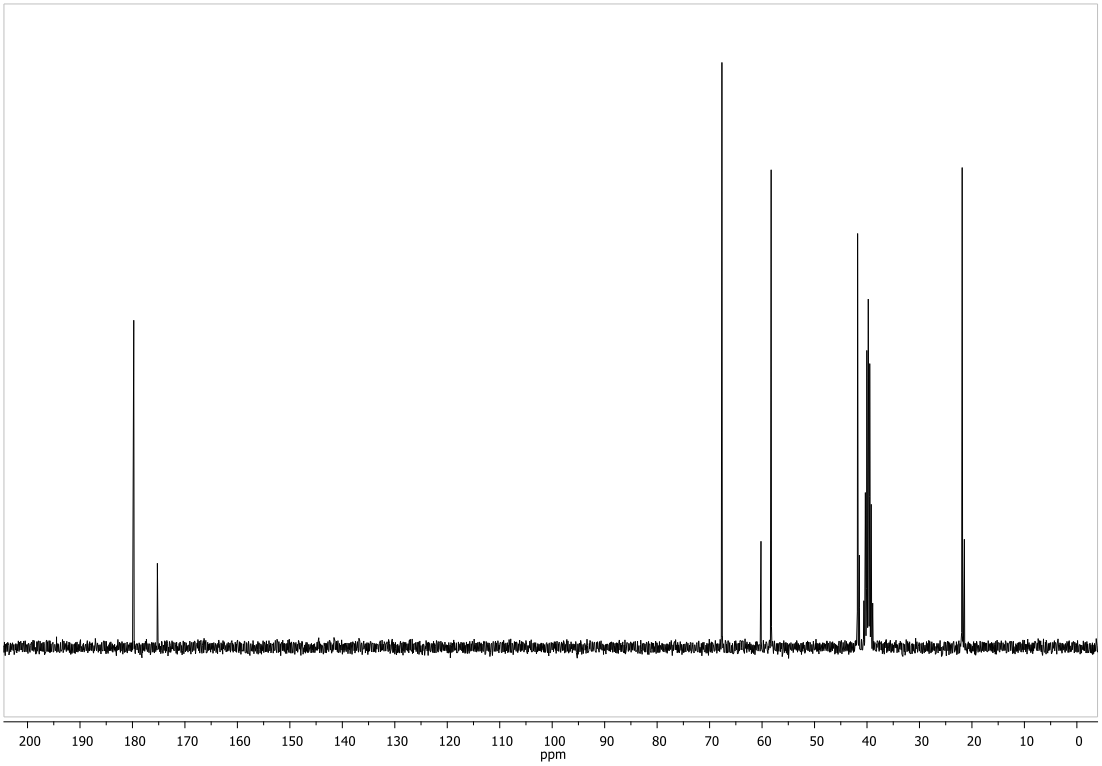

Figure S17 – ^{13}C-NMR (HEAL)

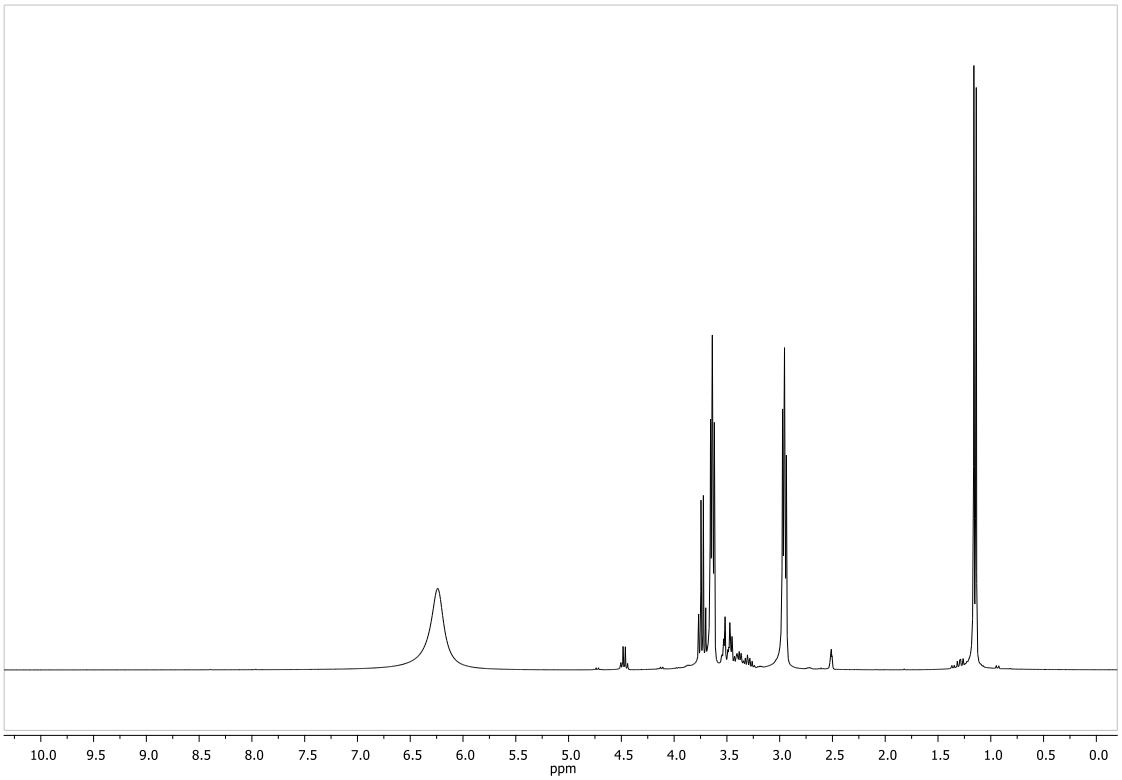

Figure S18 – ^{1}H-NMR (BHEAL)

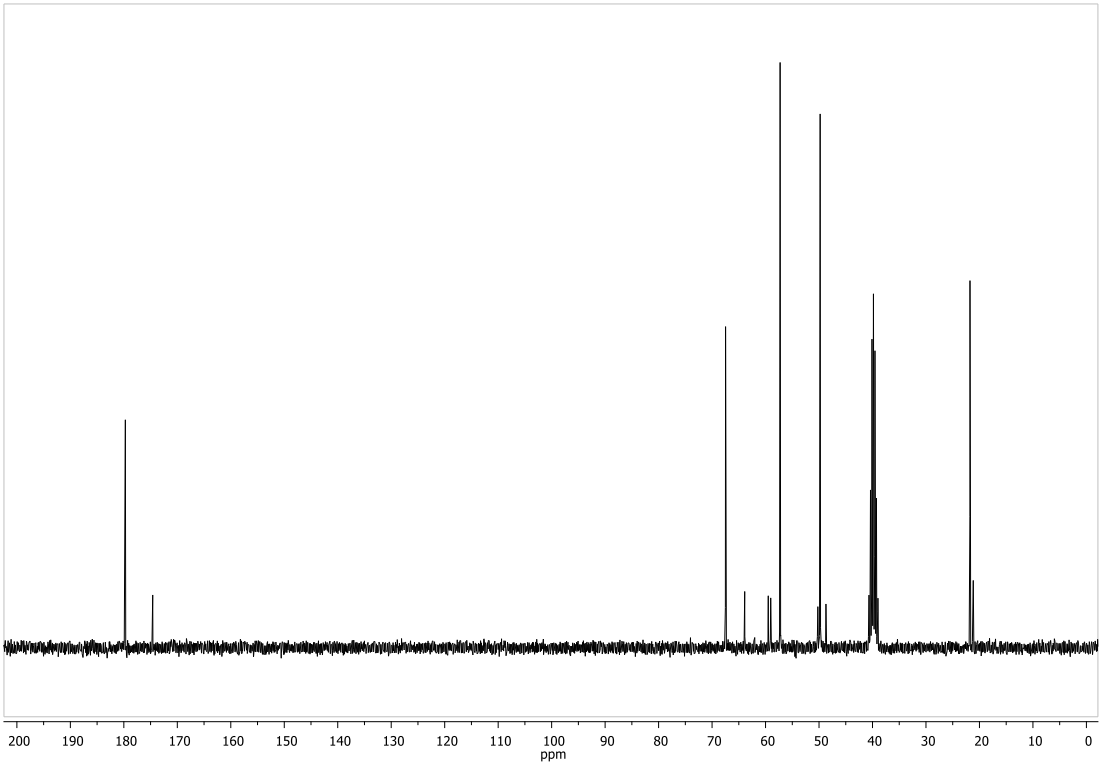

Figure S19 – ^{13}C-NMR (BHEAL)

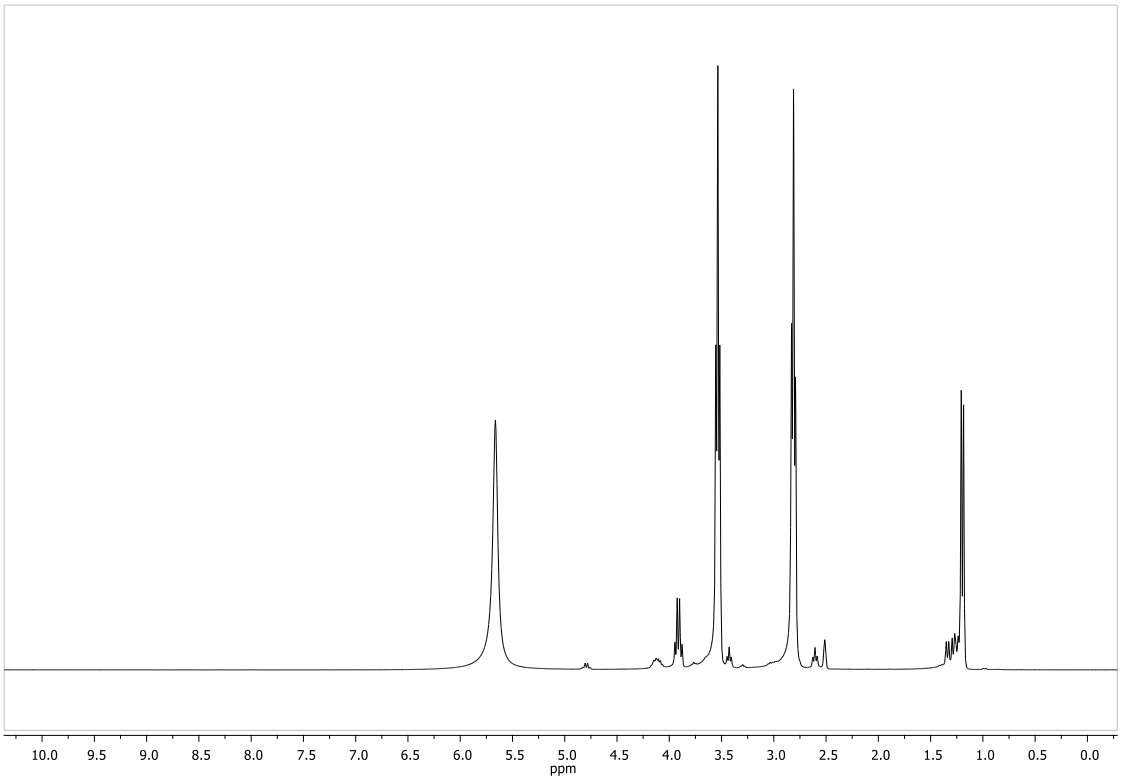

Figure S20 – ^{1}H-NMR (THEAL)

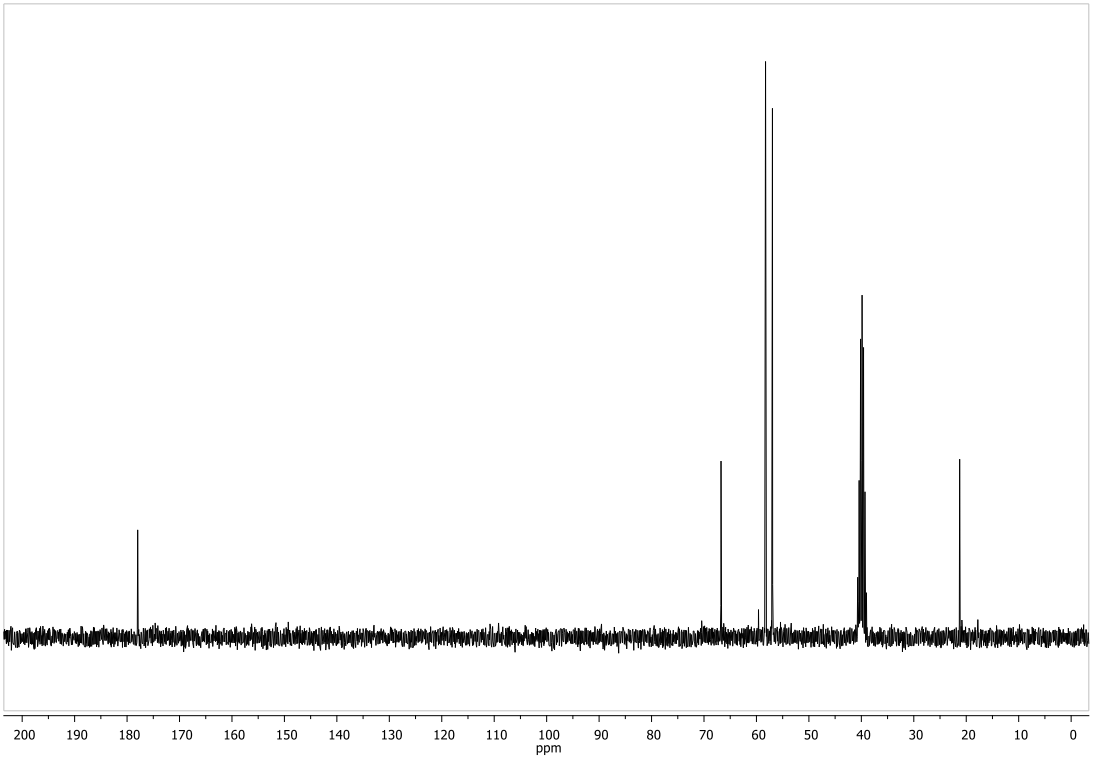

Figure S21 – ^{13}C-NMR (THEAL)

Calibration Curves – Kraft lignin

PIL	a†*	b†	R^2
HEAG	25409	0.0782	0.9977
HEAM	22078	0.1462	0.9934
HEAMn	24314	0.0216	0.9964
HEASu	24148	0.0762	0.9943
HEAL	23428	0.0050	0.9946
BHEAL	22948	0.1132	0.9925
THEAL	23681	0.0049	0.9978

Table S1 – Kraft lignin calibration curves in HEAG, HEAM, HEAMn, HEASu, HEAL, BHEAL and THEAL. († ABS = a*xlignin (mass) + b)

Kraft lignin solubility in PILs aqueous solutions and organic solvents at 323.15 K

Water (wt%)	HEAG	HEAL	HEAM	HEAMn	HEASu
100			0.10 ± 0.003		
95	1.16 ± 0.01	-	-	-	-
85	1.51 ± 0.01	-	-	-	-
75	1.94 ± 0.03	0.88 ± 0.06	0.12 ± 0.01	0.20 ± 0.07	0.35 ± 0.02
60	2.24 ± 0.02	1.52 ± 0.08	0.17 ± 0.01	0.53 ± 0.17	0.63 ± 0.02
50	2.68 ± 0.14	2.87 ± 0.28	0.17 ± 0.02	0.95 ± 0.20	1.16 ± 0.02
40	4.13 ± 0.04	4.31 ± 0.20	0.19 ± 0.02	1.04 ± 0.01	2.16 ± 0.06
25	8.04 ± 0.10	14.74 ± 0.55	0.21 ± 0.01	1.32 ± 0.56	4.73 ± 0.10
20	8.66 ± 0.04	18.02 ± 0.72	0.24 ± 0.01	2.19 ± 0.15	14.15 ± 0.36
15	9.59 ± 0.04	23.07 ± 1.25	1.54 ± 0.10	2.47 ± 0.10	-
12.5	-	-	7.92 ± 0.2	-	-
10	-	-	-	3.45 ± 0.01	
7.5	-	-	11.14 ± 0.14	-	-
5	10.26 ± 0.17	23.33 ± 1.32	15.25 ± 0.33	6.83 ± 0.08	-

Table S2 – Kraft lignin solubility (wt%) in HEAG, HEAL, HEAM, HEAMn and HEASu aqueous solutions at 323.15 K

Water (wt%)	HEAL	BHEAL	THEAL
100		0.10 ± 0.003	
75	0.88 ± 0.06	1.00 ± 0.02	1.56 ± 0.01
60	1.52 ± 0.08	1.73 ± 0.01	1.74 ± 0.01
50	2.87 ± 0.28	2.51 ± 0.01	2.38 ± 0.01
40	4.31 ± 0.20	4.89 ± 0.01	5.21 ± 0.08
25	14.74 ± 0.55	19.85 ± 0.17	22.88 ± 0.08
20	18.02 ± 0.72	23.23 ± 0.49	27.68 ± 0.50
15	23.07 ± 1.25	25.07 ± 0.37	29.16 ± 0.35
5	23.33 ± 1.32	27.06 ± 0.30	34.14 ± 0.56

Table S3 – Kraft lignin solubility (wt%) in HEAL, BHEAL and THEAL aqueous solutions at 323.15 K

Solvents	**Lignin solubility (wt %)**
Propionic acid	14.76 ± 0.29
Lactic acid†	33.00 ± 0.43
2-hydroxyethylamine	31.04 ± 0.50
bis(2-hydroxyethyl)amine	28.56 ± 0.06
tris(2-hydroxyethyl)amine	28.32 ± 0.55

Table S4 –Kraft lignin solubility (wt%) in pure solvents at 323.15 K. †Dopped with 2 wt% of water.

Kraft lignin solubility in THEAL aqueous solutions at 313.15, 323.15, 333.15 and 353.15 K

Water (wt%)	313.15 K	323.15 K	333.15 K	353.15 K
100	0.09 ± 0.01	0.10 ± 0.01	0.13 ± 0.01	0.20 ± 0.02
75	1.47 ± 0.01	1.56 ± 0.01	2.76 ± 0.06	2.65 ± 0.17
60	1.66 ± 0.02	1.74 ± 0.01	4.56 ± 0.01	4.56 ± 0.01
50	2.06 ± 0.03	2.38 ± 0.01	5.43 ± 0.03	5.42 ± 0.01
40	4.63 ± 0.08	5.21 ± 0.08	6.58 ± 0.03	7.05 ± 0.04
25	21.02 ± 0.01	22.88 ± 0.08	25.90 ± 0.01	29.00 ± 0.05
20	23.51 ± 0.17	27.68 ± 0.50	32.61 ± 0.07	41.87 ± 0.10
15	26.08 ± 0.07	29.16 ± 0.35	39.76 ± 0.16	43.76 ± 0.44
5	30.30 ± 0.38	34.14 ± 0.56	42.80 ± 0.23	47.09 ± 0.43

Table S5 – Kraft lignin solubility in THEAL aqueous solutions at 313.15, 323.15, 333.15 and 353.15 K

hours	HEAG	HEAM	HEAMn	HEASu	HEAL	BHEAL	THEAL
1	2.37 ± 0.14	14.70 ± 0.08	0.68 ± 0.09	11.55 ± 0.26	8.27 ± 0.06	9.37 ± 0.23	12.36 ± 0.08
2	6.31 ± 0.09	14.79 ± 0.12	2.10 ± 0.13	13.84 ± 0.32	10.99 ± 0.66	13.43 ± 0.49	16.16 ± 0.29
4	10.25 ± 0.13	14.92 ± 0.13	5.29 ± 0.06	14.23 ± 0.22	16.86 ± 0.51	20.25 ± 0.32	21.58 ± 0.03
8	10.15 ± 0.14	15.20 ± 0.06	6.80 ± 0.08	14.39 ± 0.23	18.86 ± 0.57	22.19 ± 0.15	24.81 ± 0.62
16	-	-	-	14.34 ± 0.14	20.40 ± 0.31	24.47 ± 0.27	28.37 ± 0.45
24	10.26 ± 0.17	15.25 ± 0.33	6.83 ± 0.08	14.15 ± 0.36	23.08 ± 0.66	26.97 ± 0.15	34.01 ± 0.58
48	-	-	-	-	23.33 ± 1.32	27.06 ± 0.30	34.14 ± 0.56

Table S6 – Kinetics of lignin dissolution at time using a magnetic bar agitation at 323.15 K

Viscosity of PILs at different temperatures

T (°C)	HEAM	HEAMn	HEASu	HEAG	HEAL	BHEAL	THEAL
30	-	1894.0715 ± 4.1705	192.8507 ± 0.0445	1028.3958 ± 5.9493	1639.3034 ± 3.9246	1949.2310 ± 4.0732	1999.8115 ± 5.2763
40	-	865.7696 ± 1.5461	112.0667 ± 0.3510	481.7131 ± 0.7612	703.6399 ± 2.7835	990.6089 ± 1.9889	1039.7802 ± 4.2480
50	1254.0151 ± 7.9540	442.0733 ± 0.9056	69.8481 ± 0.0996	249.8034 ± 0.4907	340.4312 ± 0.7467	473.7678 ± 0.2476	499.02426 ± 1.1719
60	593.9915 ± 13.1270	248.8409 ± 0.8006	46.3664 ± 0.0779	143.1802 ± 0.2876	183.2720 ± 0.1143	249.8837 ± 0.1468	267.6305 ± 0.8635

Table S7 – Viscosity of PILs at 303.15, 313.15, 323.15 and 333.15 K (mPa.s)

Kinetics of lignin dissolution using ultrasound water bath

hours	HEAG	HEAMn	THEAL
0.25	2.32 ± 0.22	0.52 ± 0.10	8.49 ± 0.43
0.50	5.88 ± 0.19	0.82 ± 0.11	16.49 ± 0.57
1.00	9.57 ± 0.25	1.76 ± 0.15	25.26 ± 0.51
1.25	10.01 ± 0.22	-	-
2.00	10.00 ± 0.30	3.95 ± 0.14	30.06 ± 0.46
4.00	-	6.76 ± 0.23	33.73 ± 0.60
6.00	-	6.84 ± 0.12	34.10 ± 0.58

Table S8 – Kinetics of lignin dissolution at time using an ultrasound water bath at 323.15 K

Considerações do Capítulo 6 e Objetivos Capítulo 7

Neste capítulo foi demonstrado que o ânion tem papel primordial na solubilidade da lignina, enquanto o cátion apresenta papel secundário. Além disso, o efeito anti-solvente da água na lignina foi demonstrado através de sucessivos experimentos para os LIPs usados. Métodos diferentes de agitação mecânica, ultrassom e agitação por barra magnética, foram utilizados e os resultados mostram que a primeira apresentou vantagens em relação ao tempo quando comparada com a agitação por barra magnética. Finalmente, foi demostrado que é possível reciclar os LIPs pela realização de sucessivos ensaios de dissolução de lignina, precipitação da macromolécula por adição de água, e evaporação da água excedente obtendo um LIP com baixo teor de umidade que foi usado novamente reiniciando-se o todo o processo.

Depois de demonstrada a capacidade das soluções aquosas de LIPs em dissolver quantidades consideráveis de lignina a baixas e moderadas temperaturas, e de se avaliar de qual forma parâmetros como estrutura do LIP (cátion e ânion), a quantidade de água (naturalmente presente na biomassa lignocelulósica e nos LIPs por serem higroscópicos) e a temperatura, por exemplo, influenciam na solubilidade, esta Tese teve como objetivo seguinte avaliar a estrutura da lignina recuperada depois de ser dissolvida nos LIPs, além de aprofundar o estudo a cerca da influencia do cátion e do ânion na solubilidade dessa macromolécula. As análises e conclusões dos resultados estão descritas no Capítulo 7.

7. **Uncovering the potentialities of protic ionic liquids based on alkanolammonium and carboxylate ions and their aqueous solutions as non-derivatizing solvents of Kraft lignin**

Industrial Crops & Products 143 (2020) 111866

Contents lists available at ScienceDirect

Industrial Crops & Products

journal homepage: www.elsevier.com/locate/indcrop

Uncovering the potentialities of protic ionic liquids based on alkanolammonium and carboxylate ions and their aqueous solutions as non-derivatizing solvents of Kraft lignin

Rafael M. Dias[a,b], André M. da Costa Lopes[b,*], Armando J.D. Silvestre[b], João A.P. Coutinho[b], Mariana C. da Costa[a]

[a] Department of Process and Product Design (DDPP) - School of Chemical Engineering (FEQ), University of Campinas (UNICAMP), Av. Albert Einstein, 500, Campinas, São Paulo, 13083-852, Brazil
[b] CICECO, Aveiro Institute of Materials, Department of Chemistry, University of Aveiro, 3810-193, Aveiro, Portugal

ARTICLE INFO

Keywords:
Protic ionic liquids
Kraft lignin solubility
Hydrotropic effect
Ionic liquid recycling
Non-derivatizing solvents

ABSTRACT

The present study scrutinized in depth the ability of alkanolammonium-based Protic Ionic Liquids (PILs) with carboxylate anions to dissolve Kraft lignin at 323.15 K. A focus was put on understanding the role of both PIL ions and water on the dissolution process. The results demonstrated that the anion plays a more important role in lignin dissolution than the cation. Furthermore, lignin dissolution was favored by increasing the alkyl chain of the carboxylate anion, while a smaller cation with lower number of hydroxyalkyl groups performed better. Among the studied solvents, the 2-hydroxyethylammonium hexanoate (HEAH) displayed the highest lignin solubility (37 wt%). In general, the addition of water had a negative influence on lignin solubility with the tested PILs. A sharp decrease in lignin solubility curves of 2-hydroxyethylammonium formate (HEAF) and acetate (HEAA) was observed, while a more softly effect was observed for 2-hydroxyethylammonium propionate (HEAP) and HEAH with the addition of water. However, a distinct behavior was observed for 2-hydroxyethylammonium octanoate (HEAO) that acted as hydrotrope enhancing lignin solubility in aqueous solutions to a maximum value at 40 wt% water content. Furthermore, by increasing the temperature, the lignin solubility was favored due to endothermic behavior of lignin dissolution process.

The dissolution of Kraft lignin was also performed at 393.15 K to unravel any lignin modification unleashed by PILs. GPC, FTIR-ATR and 2D NMR were employed for lignin characterization and the changes observed between native lignin and recovered lignin samples were negligible demonstrating the non-derivatizing character of the PILs. Moreover, the recycle of 2-hydroxyethylammonium propionate (HEAP) was successfully demonstrated for at least 3 cycles. In this way, PILs are herein revealed as promising solvents to apply in lignin valorization towards more efficient and eco-friendly processes.

1. Introduction

The current concerns about the environmental impact associated to fossil fuel consumption, the high energy demand and the growing need for commodities have been pushing the interest to use renewable resources, such as biomass, to provide biobased and sustainable products (Chang et al., 2017). In this context, the implementation of the biorefinery concept that relies on the use of biomass as feedstock to produce a wide range of biofuels, biobased chemicals and materials, has been attracting attention as a sustainable solution (Silveira et al., 2015).

Lignocellulosic biomass is a renewable and abundant resource comprising wood, agricultural and forestry residues, energy crops, cellulosic waste, among other streams. The worldwide production of these raw materials is estimated at 200 billion tons annually, making them suitable feedstocks for further processing and valorization (Dahmen et al., 2019). This type of biomass is composed of three major macromolecular components, namely cellulose (30–50 %) hemicelluloses (20–35 %) and lignin (15–30 %). The first two components make the polysaccharide fraction of biomass and assume a structural role in plant biomass, whereas lignin gives rigidity and protection against microbial attack. All these components are tightly bounded and organized in a rigid and complex structure hindering an efficient fractionation. Therefore, the chief challenge in biomass valorization lies on surpassing its recalcitrance and separating the macromolecular

* Corresponding author.
E-mail address: andremcl@ua.pt (A.M. da Costa Lopes).

https://doi.org/10.1016/j.indcrop.2019.111866
Received 2 June 2019; Received in revised form 27 September 2019; Accepted 14 October 2019
Available online 18 November 2019

fractions for further conversion by efficient and sustainable methods (Da Costa Lopes and Bogel-Lukasik, 2015). In particular, the selective biomass delignification and lignin dissolution steps are key examples that must be improved towards an efficient lignin valorization. The aromatic nature of this macromolecule is of extreme importance for a forecasted replacement of aromatic chemicals and products coming from fossil-based resources (Hu et al., 2018).

Amongst biomass components, lignin is the less susceptible to chemical and biological treatments hindering its fractionation and conversion. Several technologies, including Kraft, soda, organosolv, microwave or ultrasound, have been applied in delignification and lignin dissolution processes. However, these technologies present low efficiency, high expenditures and some of them are not considered environmentally friendly, hampering their implementation to large-scale processes. The application of selective and benign solvents could be a more sustainable approach and ionic liquids (ILs) stand as promising green solvents for biomass delignification and lignin dissolution (Zhu et al., 2018).

ILs are organic salts with melting point below 373.15 K and are composed by cations and anions. They present remarkable features, such as non-flammability, negligible vapor pressure, high chemical and thermal stabilities, among others (Welton, 2018). Furthermore, physicochemical properties like density, viscosity and solvation power can be tailored by changing the anion or cation. For this reason, ILs are considered designer solvents to apply in a myriad of tasks (Welton, 2018). ILs can be roughly divided in aprotic ionic liquids (AILs) or protic ionic liquids (PILs) and can be distinguished by the permanency of the positive cation charge after synthesis. For AILs, the positive charge of the cation is kept, and it is not in equilibrium with the corresponding neutral species. The contrary is observed for PILs, in which charged and neutral species are present at equilibrium. PILs have the advantage of being easier to prepare, since a simple neutralization between a base and an organic acid is required.

The study of PILs as sustainable solvents for lignin dissolution and biomass delignification has been addressed by several authors. Merino et al. (2018) evaluated the ability of eighteen protic multiaromatic ILs for Kraft lignin dissolution. According to authors, 1,2,4,5-tetraphenyl-1H-imidazolium methanesulfonate ([TPIM][$MeSO_3$]) was able to dissolve 42 wt% lignin under microwave irradiation at 363.15 K (Merino et al., 2018). Rashid et al. (2016) examined the dissolution of Kraft lignin in three pyridinium PILs, namely pyridinium formate ([Py][For]), pyridinium acetate ([Py][Ac]) and pyridinium propionate ([Py][Pro]). The highest lignin solubility was obtained with [Py][For] at 348.15 K reaching a value of 70 wt% (Rashid et al., 2016). The good performance of this PIL was confirmed with the successful lignin extraction from palm oil plant biomass (Rashid et al., 2018). In another work, Achinivu et al. (2014) demonstrated the extraction of > 70 wt% of the initial lignin content from corn stover using pyrrolidinium acetate ([Pyrr][Ac]) without significant impact on cellulose fibers (Achinivu et al., 2014). More recently, Miranda et al. (2019) investigated 12 ammonium-based PILs to perform pineapple crown delignification. In particular, bis(2-hydroxyethyl)ammonium propionate [BHEAP] showed > 90 wt% lignin extraction, which clearly demonstrates the outstanding capacity of ammonium-based ILs for this purpose (Miranda et al., 2019).

The presence of water seems to have impact on delignification process using PILs. A high delignification yield (85 wt%) was achieved in the treatment of *Miscanthus giganteus* at 393.15 K with aqueous triethylammonium hydrogen sulphate ([TEA][HSO_4]) solution (20 wt% water content) (Brandt-Talbot et al., 2017). Similar results were achieved in sugarcane bagasse delignification using the same PIL aqueous solution (Chambon et al., 2018). Less effective delignification was attained with an aqueous solution of 1-butylimidazolium hydrogen sulphate [HBIM][HSO_4], which removed 35 wt% of the initial lignin content from cotton stalks (Semerci and Güler, 2018).

The state-of-the-art shows good results in the application of neat PILs or their aqueous solutions to dissolve lignin and to achieve efficient and sustainable biomass delignification. However, there is still lack of detailed knowledge regarding the mechanisms and interactions between lignin and PILs that take place during the dissolution process. The influence of both PIL cation and anion on lignin dissolution is a key factor that must be scrutinized as well as the impact of water on this process that is far from being understood. Furthermore, limited information regarding the structural modifications of the recovered lignin has been provided in literature. In this sense, the present work contributes to suppress all these gaps by giving a comprehensive understanding of the solubility of Kraft lignin (as a model macromolecule) in PILs aqueous solutions composed of alkanolammonium cations and carboxylate anions with different aliphatic chain lengths. Moreover, lignin was dissolved in PILs at high temperature to simulate conditions often applied in biomass delignification and recovered lignin was characterized in detail to unveil structural modifications triggered by those solvents. The recovery and reuse of PIL was also addressed in this work.

2. Experimental

2.1. Chemicals

All acid and base precursors employed for the synthesis of PILs examined in this work are represented in Fig. 1. The compounds 2-hydroxyethylamine (≥98 %), bis(2-hydroxyethyl)amine (≥98 %) and tris(2-hydroxyethyl)amine (≥98 %) were purchased from Sigma-Aldrich. Formic (≥98 %) and acetic acids (> 99 %) were purchased from Merck. Propionic acid (≥99 %) was purchased from Acros Organics, while hexanoic (≥98 %) and octanoic acid (≥98 %) were supplied by Sigma Aldrich. All reagents were used as purchased.

Kraft lignin from *E. globulus* was directly supplied by Suzano Papel & Celulose (Brazil) after employing carbon dioxide (CO_2) to the industrial black liquor.

2.2. PILs synthesis and characterization

The following PILs were synthesized: 2-hydroxyethylammonium formate (HEAF), 2-hydroxyethylammonium acetate (HEAA), 2-hydroxyethylammonium propionate (HEAP), 2-hydroxyethylammonium hexanoate (HEAH), 2-hydroxyethylammonium octanoate (HEAO), bis(2-hydroxyethyl)ammonium propionate (BHEAP) and tris(2-hydroxyethyl)ammonium propionate (THEAP).

PILs were prepared according to the methodology described by

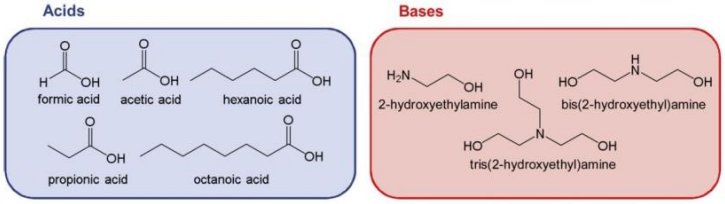

Fig. 1. Acid and base precursors used in this work to perform PILs synthesis.

Álvarez et al. (2010) and Iglesias et al. (2010). The amine was placed inside a three-necked flask equipped with a reflux condenser, a PT-100 temperature sensor for monitoring the temperature and a dropping funnel. Since the reaction is exothermic, a thermostatic bath (283.15 K) covering the three-necked flask was needed to avoid temperature increase during the reaction. The organic acid (formic, acetic, propionic, hexanoic or octanoic) was added dropwise to the flask and the solution was continuously stirred with a magnetic bar up to 24 h at room temperature. No solid precipitate or crystals in the mixture were observed during PILs' synthesis. PILs were then submitted to vacuum (70.0 Pa absolute pressure) with slight heating (333.15 K) and agitation to remove water and excess of reagents. The water content was measured after this step using a Metrohm 831 Karl Fischer coulometer and determined values were considered in the preparation of PILs aqueous solutions.

The success of PILs synthesis was confirmed by FTIR-ATR analysis and by both ^{1}H NMR and ^{13}C NMR techniques (Figs S1–S21 in electronic supporting information - ESI).

2.3. Lignin solubility assays

Kraft lignin in excess amount was added to 1.0 ± 0.05 g of each PIL aqueous solution (10, 25, 40, 50, 60, 75, 80, 85 and 97 wt%) or pure water in glass vials. The vials were sealed and placed on a specific aluminum disk support, which was transferred to a stirring plate with heat control Pt1000 (H03D Series from LBX Instruments). The solubility assays were performed at 323.15 K under constant agitation of 200 rpm. After saturation was reached, the samples were filtered using PTFE filters (0.45 µm pore size) allowing separation of the undissolved lignin from the liquid phase. Afterwards, the liquid phase was diluted with dimethylsulfoxide (DMSO) and the amount of dissolved lignin was quantified by UV-spectroscopy (SHIMADZU UV-1700, Pharma-Spec spectrometer) at a wavelength of 280 nm. Quantitative determination was assisted by appropriate calibration curves (Table S1 in ESI). All experiments were performed at least in duplicate and results were expressed as means (less than 5% variation).

2.4. Lignin recovery and PIL recycling

Deionized water was added to lignin/PIL solution and stirred for lignin precipitation. The solution was then introduced in an ice bath (278.15 K) to increase the efficiency of precipitation. The recovered lignin was separated by vacuum filtration and washed with deionized water to ensure that all PIL has been washed out. Precipitated lignin was dried under vacuum at 303.15 K for 24 h and the amount of lignin was determined gravimetrically. The resulting PIL aqueous solution from washing step was collected for recycle/reuse purposes. The solution was submitted to a simple distillation process at ambient pressure to remove major water fraction. Afterwards, the resulting solution was submitted to a vacuum evaporation process (333.15 K and 10 kPa) until approximately 15 wt% water content was achieved. The remaining PIL aqueous solution was reused in lignin solubility assays as described in Section 2.3.

2.5. Gel permeation chromatography (GPC)

Gel Permeation Chromatography was carried out with a PL-GPC 110 chromatograph (Polymer Laboratories, UK) equipped with two columns PL gel MIXED-D 5 µm (300 x 7.5 mm) protected by a PL aqua gel-OH Guard 5 µm pre-column. The columns, injector system and the detector (RI) were maintained at 343.15 K during the analysis. A solution of LiCl in dimethylformamide (0.1 mol L^{-1}) was prepared and used as eluent. Lignin samples were dissolved in the eluent solution to a concentration of about 1 wt% (10 mg mL^{-1}). The injection volume of samples was 100 µL and the eluent was pumped at a flow rate of 0.9 mL min^{-1}. The analytical columns were calibrated with lignin model compounds (monomer, dimmer and tetramer) with known molecular weight in the range of 1–4 kDa. The following equation was determined as the calibration curve: LogM = 6.283 – 0.2149 * T.

2.6. Fourier transform infrared analysis (FTIR-ATR)

FTIR spectra of PILs and lignin samples were acquired by a Perkin Elmer spectrometer (Spectrum BX) equipped with a single horizontal Golden Gate ATR cell (attenuated total reflectance) and a diamond crystal. The data was recorded with 32 scans at a resolution of 4 cm^{-1} and a wavenumber range between 4000 cm^{-1} and 600 cm^{-1}.

2.7. Nuclear magnetic resonance (NMR) spectroscopy

2.7.1. ^{1}H and ^{13}C NMR

The ^{1}H and ^{13}C NMR spectra of ILs were recorded by a Bruker AVANCE 300 MHz NMR at 300.13 MHz and 75.47 MHz, respectively, using deuterated dimethylsulfoxide (DMSO-d6) as solvent and tetramethylsilane (TMS) as the internal reference.

2.7.2. 2D HSQC NMR

In sample preparation, 50 mg of lignin was dissolved in 500 µL of DMSO-d6 with TMS as the internal reference and transferred to NMR tubes. 2D HSQC NMR spectra were acquired by a Bruker AVANCE 500 MHz NMR spectrometer equipped with an inverse gradient 5 mm TXI ^{1}H/^{13}C/^{15}N cryoprobe. ^{1}H–^{13}C correlation spectra were measured with the following Bruker standard pulse program: "hsqcetgpsi" sequence with 2D H-1/X correlation via double inept transfer (trim pulses), Echo/Antiecho-TPPI gradient selection for phase sensitivity improvement, and decoupling during acquisition. The chemical shifts were referenced to the central DMSO solvent peak (δC 39.5 ppm, δH 2.49 ppm). All the experiments were carried out at 298.15 K with the following parameters: spectral width of 11 ppm in the F2 (^{1}H) dimension and 165 ppm in the F1 (^{13}C) with 1024 data points, 194 scans and recycle delay of 1.5 s.

For semi-quantitative analysis, phase and baseline correction were performed to all HSQC spectra. The relative abundance of main interunit linkages and lignin substructures was determined as the percentage of total side chains from integration of ^{13}C-^{1}H cross signals in the HSQC spectra.

3. Results and discussion

3.1. The influence of water and PIL cation on lignin solubility

The presence of water in IL decreases its viscosity, reduces the amount of IL required for a dissolution process and saves costs in IL production (and recycling), since an energy-intensive drying step would be avoided. Therefore, the influence of water on the ability of PILs to dissolve lignin should be comprehensively scrutinized.

The importance of water and PIL cation in the solubility of Kraft lignin was first evaluated. Neat and aqueous solutions of HEAP, BHEAP and THEAP that share propionate anion were examined for Kraft lignin dissolution. The solubility values as function of PIL water content at 323.15 K are presented in Fig. 2 and Table S2 (ESI).

At first glance, the results showed a negative impact of water on the performance of PILs to dissolve Kraft lignin, *i.e.*, the higher water content, the lower is the solubility of lignin in the solvent. Adding water to PILs between 15.0 wt% and 75.0 wt% sharply decreases lignin solubility in all cases and when water content becomes higher than 75.0 wt%, lignin solubility is < 2.0 wt%. This trend was also observed in the Kraft lignin solubility with pyridinium-based PILs reported by Rashid et al. (2016). It is an expected behavior since water is usually employed as lignin anti-solvent in biomass fractionation processes with ILs (Brandt et al., 2015; Prado et al., 2013).

Regarding the PILs performance, HEAP depicted higher ability to

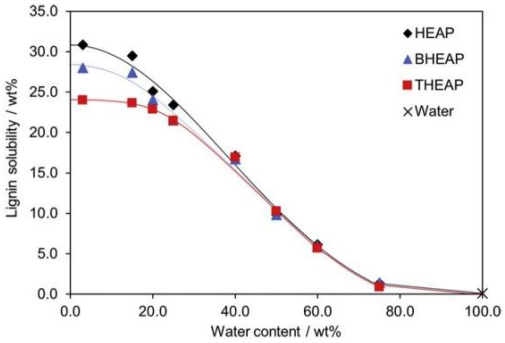

Fig. 2. Kraft lignin solubility (wt%) in HEAP, BHEAP, THEAP and their aqueous solutions at 323.15 K. Lines are guide for the eye.

dissolve Kraft lignin than BHEAP and THEAP for water contents ≤25 wt%. This can be attributed to the number of hydroxyalkyl chains in cation structure and the cation size as well. These factors seem to influence the lignin solubility for neat PIL and PIL aqueous solutions at low water content, in which lignin solubility is favored by a smaller cation size and a lower number of hydroxyalkyl groups provided by HEAP. The steric hindrance provided by higher number of carbon chains and cation size might occur and the lignin-cation interaction could be reduced, which may explain the decrease in lignin solubility (Hart et al., 2015).

However, no relevant differences were observed between the PILs for water content higher than 40 wt%. This means that adding water to these PILs at a certain point masks the influence of IL cation mentioned above, and thus, it can be concluded that the PIL cation plays a minor role in lignin solubility. This is also corroborated by results of several previous works that showed a major influence of IL anionic part on lignin solubility (Achinivu, 2018; Ji et al., 2012; Merino et al., 2018; Pu et al., 2007; Zhang et al., 2017).

3.2. The influence of PIL anion on lignin solubility

The impact of PIL anion on lignin solubility was also studied and 2-hydroxyethylammonium cation was chosen as reference to the detriment of other cations that presented lower performance. The solubility of Kraft lignin was tested in five PILs (neat and aqueous solutions) composed of anions with different alkyl chain length, namely formate (HEAF), acetate (HEAA), propionate (HEAP), hexanoate (HEAH) and octanoate (HEAO) at 323.15 K. The solubility results are depicted in Fig. 3 and Table S3 (ESI).

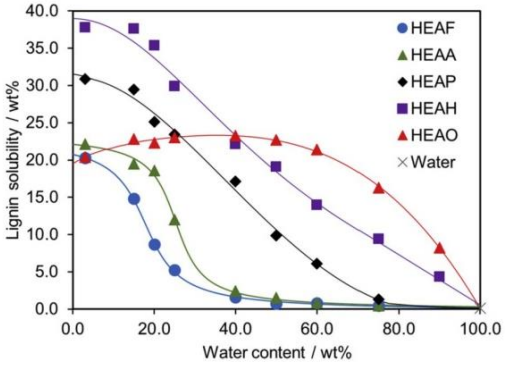

Fig. 3. Kraft lignin solubility (wt%) in HEAF, HEAA, HEAP, HEAH and HEAO their aqueous solutions at 323.15 K. Lines are guide for the eye.

The ability of neat PILs to dissolve lignin can be ordered as the following: HEAH > HEAP > HEAA > HEAF ≈ HEAO. Among examined PILs, HEAH stand as the best lignin solvent achieving a solubility value of 37.77 wt% at 323.15 K, which is similar to Kraft lignin solubility in other solvents at similar or even higher temperatures (Achinivu, 2018; Hart et al., 2015; Merino et al., 2018; Pu et al., 2007; Soares et al., 2019). Imidazolium-based ILs were tested by Pu et al. (2007) and Hart et al. (2015), and the best ILs were found to dissolve 344 g/L of Kraft lignin at 323.15 K, and 55 wt% of Kraft lignin at 298.15 K, respectively. Merino et al. (2018) evaluated several multi-aromatic PILs for kraft lignin dissolution task, achieving 42 wt% of solubility at 363.15 K, while Soares et al. (2019) demonstrated that aqueous solutions of DES formed by propionic acid:urea (2:1) reached more than 27 wt% of kraft lignin solubility at 353.15 K. The results obtained in this study evidence the strong capacity of these PILs to dissolve lignin at mild conditions (323.15 K), and are fairly comparable with AILs (Hart et al., 2015; Pu et al., 2007), other PILs (Achinivu, 2018; Merino et al., 2018), and also DES aqueous solutions (Soares et al., 2019).

When water is added to PILs different trends in lignin solubility were observed. For PILs with short alkyl chain anions (formate and acetate), the negative influence of water on lignin solubility is even higher than that observed for HEAP and HEAH. A sharp decrease of lignin solubility is achieved to water contents between 15.0 wt% and 40.0 wt% for HEAF and HEAA, while it softly decreases for both HEAP and HEAH at the same range of water content. Some authors have also reported the negative effect of water on lignin dissolution using ILs (Akiba et al., 2017; Rashid et al., 2016; Xu et al., 2017). According to Xu et al. (2017), the water crowd the hydrogen bond accepting sites of IL anions and impairs the interactions between lignin and ILs, resulting in the reduction of PILs dissolution ability (Xu et al., 2017). Theorical calculations were performed by Ji et al. (2012) to investigate the interactions between lignin-water-ILs. The authors have concluded that the active sites and the interaction energy of ILs-lignin are impaired by the presence of water making the bonds weaker or disrupted (Ji et al., 2012). However, there are some cases in which water does not significantly decrease the lignin solubility, as can be seen for HEAH, up to 15 wt% water content. This behavior was not observed for any other PIL studied. It is also surprising that 4.35 wt% lignin solubility was reached at highly diluted HEAH solutions (90 wt% water). Therefore, a higher alkyl chain length of the carboxylate anion allows a better affinity for lignin dissolution and the anti-solvent role of water is reduced, at least up to a six-carbon chain length. This is in agreement with lignin solubility results achieved with cholinium-based ILs containing different chain length alkanoate anions as reported by Hou et al. (2015). However, an opposite conclusion was disclosed by Rashid et al. (2016) when performing lignin solubility trials with pyridinium-based ILs. The researchers showed pyridinium formate as the best performing IL for lignin dissolution in comparison with the acetate and propionate counterparts (Rashid et al., 2016). Nevertheless, it is important to highlight that the same study also shows that molecular pyridine can reach a lignin solubility more than twice as that observed for formic acid (Rashid et al., 2016). Therefore, pyridinium cation may play a major role in lignin solubility in these type of ILs, which is explained by the π–π interactions established between IL cation and lignin aromatic rings. All these results lead us to conclude that the combination of IL cation and anion interferes with the individual role of each IL component in lignin dissolution.

On the other hand, a remarkably different behavior was observed for octanoate-based PIL (HEAO). As can be seen in Fig. 3, lignin solubility in neat HEAO is almost half of that observed for neat HEAH. In aqueous solutions, it can be noted that HEAO dissolves more lignin than other PILs for water contents > 40 wt%, reaching 23.27 wt% maximum lignin solubility. But suddenly, lignin solubility reduces in solutions containing higher water content. Indeed, the shape of the lignin solubility curve of HEAO is characterized by a maximum between pure

water and neat HEAO, suggesting that the solubility of lignin in this case is driven by a hydrotropic mechanism. Basically, the HEAO ions self-arrange in water and act as hydrotrope enhancing lignin solubility in aqueous solutions. This phenomenon was previously reported in the dissolution of phenolic compounds in IL aqueous solutions by Cláudio et al. (2015) and in the dissolution of lignin monomeric model compounds in deep eutectic solvent aqueous solutions by Soares et al. (2017).

Hence, it was demonstrated that increasing alkyl chain length of the anion in ethanolammonium-based ILs enhances lignin solubility, while water acts as lignin anti-solvent. This means that the hydrophobicity of the anion could play a positive role in lignin dissolution and, at certain point, the dissolution mechanism changes as consequence of the self-arrangement of amphiphilic IL anions (e.g. octanoate) around lignin macromolecules increasing its solubility in aqueous solutions.

Although water decreases lignin solubility, the use of PIL aqueous solutions at low water content (e.g. 15 wt%) may be beneficial for certain purposes, as for example, in biomass delignification processes. As shown elsewhere (Brandt-Talbot et al., 2017), 20 wt% water content improved the efficiency of [TEA][HSO_4] to extract lignin from *Miscanthus giganteus* reaching > 85 wt% delignification yield at 393.15 K. The low amount of water reduces the PIL viscosity, improving lignin extraction yields. Water is thus important to improve mass transfer during lignin extraction, but a low water content is desirable to not significantly affect lignin solubility.

3.3. The effect of temperature on lignin solubility

The HEAP was chosen, as proof of concept, to evaluate the influence of temperature in lignin solubility. The dissolution of lignin in HEAP aqueous solutions was evaluated at 313.15, 323.15, 333.15, and 353.15 K (Fig. 4 and Table S4).

In general, the same trend was observed to all solubility lignin curves: the lignin solubility softly decreases with the addition of water, as mentioned before. The increase of temperature favored the lignin dissolution as a result of the kinetic energy increase, allowing PIL molecules to break apart easily the lignin molecules enhancing the solubility. This behavior is in agreement with the general solubility rule (endothermic processes) (Fathi-Azarjbayjani et al., 2016; Kim et al., 2018; Long et al., 2017). A maximum lignin solubility of 38.15 wt% was observed in neat HEAP at 353.15 K.

Some authors have reported ILs ability to dissolve Kraft lignin at different temperatures. Glas et al. (2015) screened a series of ammonium-, phosphonium-, and pyrrolidinium-based ILs and achieved 460 g/L lignin solubility at 363.15 K using tributylmethylphosphonium methylsulfate ([P4441][$MeSO_4$]) as solvent medium. Mu et al. (2015) synthesized and tested several ILs formed by *N*-methyl-2-pyrrolidone and carboxylic acids and reported that this kind of ILs can reach 35–60 wt% of lignin solubility at 363.15 K. Regarding the ability of PILs to dissolve Kraft lignin, Rashid et al. (2016) achieved more than 70 wt% of lignin solubility using pyridinium formate ([Py][For]) at 348.15 K. Therefore, HEAP presents good capacity to dissolve Kraft lignin when compared with literature data (Glas et al., 2015; Mu et al., 2015; Rashid et al., 2016; Soares et al., 2019).

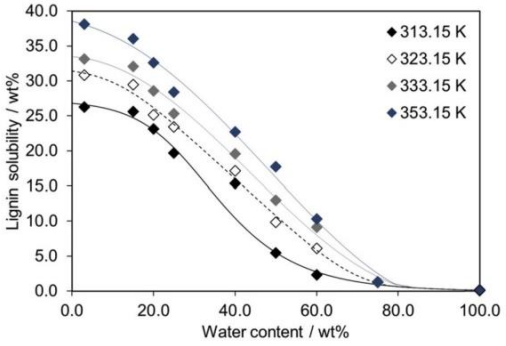

Fig. 4. Kraft lignin solubility (wt%) in HEAP aqueous solutions and in pure water at 313.15, 323.15, 333.15 and 353.15 K. Lines are guide for the eye.

3.4. Structural characterization of lignin submitted at high temperature in PILs

After careful evaluation of the potentialities of examined PILs to dissolve lignin at 323.15 K, a comprehensive lignin characterization was performed. At this stage, lignin was dissolved in neat PILs at 393.15 K for 6 h followed by its precipitation with water. These conditions were intended to simulate those usually applied in biomass delignification processes and to unveil any structural modification in lignin induced by PILs. A series of techniques, including GPC, FTIR-ATR and 2D-NMR were performed for the analysis of native Kraft lignin and recovered lignins. Given the limited technical resources and time consuming of analyses, recovered lignins from HEAF, HEAP and THEAP media were selected as representative samples to screen the influence of the PIL ions on lignin modification.

The impact of selected PILs on lignin molecular weight was first evaluated. The weight average molecular weight (Mw), the number average molecular weight (Mn) and the polydispersity index (PDI) of native Kraft lignin and recovered lignins from HEAF, HEAP and THEAP are presented in Table 1. The corresponding molecular weight distributions of all lignin samples are presented in Fig. S23 (in ESI).

The GPC data revealed a native Kraft lignin characterized by low molecular weight and narrow molecular weight distribution (low polydispersity). The process of Kraft pulping is in general a severe process, thus a drastic reduction of lignin molecular weight is expected (Hu et al., 2018). Contrasting to literature, the obtained values are consistent with those reported for *E. globulus* Kraft lignins (Tolbert et al., 2014). On the other hand, the thermal treatment of this lignin in PILs demonstrated a slight increase of Mw, Mn and PDI values in all cases. Hence, low chemical modification in lignin occurred or simply low molecular weight lignin fractions (oligomers) remained solvated after dissolution/precipitation steps. In order to better sort out these effects and to address any chemical modifications in recovered lignins, FTIR-ATR and 2D-NMR analyses were performed.

The acquired FTIR spectra of native Kraft lignin and recovered lignins after dissolution in HEAF, HEAP or HTEAP are presented in Fig. 5. The samples were analyzed according to lignin infrared characterization reported in literature (Cachet et al., 2014; Cademartori et al., 2013; García et al., 2012; Gordobil et al., 2015; Nevrez et al., 2011; Pandey and Pitman, 2003; Sun et al., 2012). Typical Kraft lignin absorption bands were observed in the region of 1800–750 cm^{-1} with remarkable high intensities at 838, 1109, 1212, 1327, 1456, 1514, 1600 and 2937 cm^{-1}. The characteristic lignin assignments are presented in detail in Table S5 (ESI).

The spectra of the native Kraft lignin and recovered lignins are comparable and only minor differences are noticeable. No extra vibrational bands were observed in spectra of HEAF and HEAP lignins,

Table 1
Calculated molecular weight numbers of native Kraft lignin and recovered lignin samples achieved by GPC analysis.

Lignin Sample	Mw (g mol^{-1})	Mn (g mol^{-1})	PDI
Native Kraft	1520	1345	1.13
HEAF	1725	1465	1.18
HEAP	1600	1395	1.15
THEAP	1650	1440	1.15

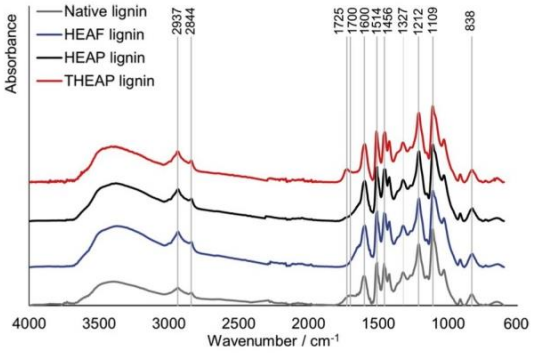

Fig. 5. FTIR-ATR spectra of native Kraft lignin and recovered lignins from HEAF, HEAP and THEAP. Recovered lignins were obtained after dissolution in PILs at 393.15 K and further precipitation with water.

but a band at 1700 cm^{-1} seems to disappear in these samples. This band can be attributed to C=O stretching in conjugated carbonyl groups present in lignin structure (Cachet et al., 2014), but also to moisture (water bending vibration) and protein impurities (Popescu et al., 2006) that could be removed after PIL treatment. On the other hand, the appearance of vibrational band at 1725 cm^{-1} is highlighted only in THEAP lignin spectrum that could be associated to C=O stretching in ester groups. Overall FTIR analysis showed small modifications in lignin chemical linkages and functional groups, but this technique alone gives limited and inconclusive information. Therefore, a more in-depth structural analysis was performed with 2D HQSC NMR technique.

Each lignin HSQC spectrum can be divided in three distinct regions, namely aliphatic side chain (δ_C/δ_H 5.0–35/0.5–2.5), oxygenated aliphatic side chain (δ_C/δ_H 50–95/2.5–5.0) and aromatic (δ_C/δ_H 100–135/6.0–8.5) regions (Fernández-Costas et al., 2014; Ralph and Landucci, 2010). The nonoxygenated aliphatic side chain region presents signals of lipids, degraded products of lignin and other organic contaminants that hinders a suitable analysis (Ibarra et al., 2007; Liitiä et al., 2003). Therefore, a higher focus was given to oxygenated aliphatic and aromatic regions. For example, these spectra regions of native Kraft lignin and HEAP lignin are depicted in Fig. 6.

The ^{1}H-^{13}C cross signals presented in the HSQC spectra were assigned by contrasting it with literature data (Ibarra et al., 2007; Wen et al., 2015, 2012; Yuan et al., 2011; Zhang et al., 2010). All assignments are depicted in Table S6 and cross signals from the different lignin subunits, including alkyl-aryl ether structures (β-*O*-4), resinols (β-β), phenylcoumaran (β-1), spirodienone (β-5) among others, are shown in Fig. 6. The identification of some of these subunits was also confirmed by 2D HMBC NMR technique (data not shown).

At first glance, both HSQC regions from native Kraft lignin and HEAP lignin (Fig. 6) as well as HEAF and THEAP lignins (Figure S22 in ESI) presented the same cross signals. This is indicative of null or low chemical modification of main inter-unit linkages present in lignin structure, confirming FTIR results. Nevertheless, a semi-quantitative analysis was attempted to stress out the effect of each PIL on the relative abundance of identified lignin subunits after its dissolution/precipitation steps. The obtained data is depicted in Table 2.

The HSQC semi-quantitative characterization of the side chains of native Kraft lignin structure demonstrated a high abundance in β-*O*-4 alkyl-aryl ether (48.6 %) and β-β resinol subunits (35.8 %). On the other hand, phenylcoumaran (2.6 %) and spirodienone (8.6 %) substructures represent a lower fraction of lignin. The remaining content (4.4 %) refers to *p*-hydroxycinnamyl derived subunits. These results are in agreement with literature data shown by NMR analysis of other Kraft lignins from *E. globulus* wood (Martinez et al., 2010). The relative analysis between each sample demonstrated that treating native Kraft lignin with PILs at 393.15 K followed by its precipitation have only a minor impact on its composition. In all cases, β-*O*-4 alkyl-ether substructures content in recovered lignins increased (between 13.1 and 34.4 % increase), while the opposite was observed for other lignin subunits, especially for β-β resinol type (between 10.6 % and 33.4 % reduction).

A major difference observed in β-*O*-4 and β-β contents can be contrasted with literature data and correlated with GPC results. Ragauskas et al. have shown in a recent study based on lignin fractionation by organic solvents (Wang et al., 2018) that high molecular weight lignin molecules tend to possess more β-*O*-4 linkages, while the subunits of oligomeric lignin molecules are preferably linked through C–C bonds (as consequence of intense α-*O*-4 and β-*O*-4 ether cleavage). As aforementioned, the treatment with PILs allowed the removal of low molecular weight lignin molecules, leading to a slight increase of Mw, Mn and PDI of the recovered lignin samples. Therefore, the reduction of β-β resinol subunits in lignin structure could be explained by this behavior. Although HSQC semi-quantitative analysis demonstrated differences in lignin structure between native Kraft lignin and PILs samples, this should be looked as little modification in agreement with GPC and FTIR results. It can be stated that lignin dissolution mechanism in examined PILs is mostly governed by the disruption of the intramolecular bonding of lignin macromolecules and the establishment of intermolecular non-covalent bonds with PILs, specially with the anionic part.

Regarding the PIL contamination in recovered lignin samples, NMR spectra showed very low intensity of characteristic chemical shifts from HEAF (δ_C/δ_H 40/3.20) and HEAP (δ_C/δ_H 42/3.15). On the contrary, the contamination of THEAP in recovered lignin was higher and it was identified as multiple derived compounds from esterification between the three hydroxyl groups in tris(2-hydroxyethyl)amine and propionic acid. This is in agreement with FTIR spectrum obtained for THEAP lignin showing the appearance of a vibrational band at 1725 cm^{-1} associated to C=O stretching in ester groups.

3.5. Recycling of PIL

The recycling of ILs are fundamental to obtain a sustainable and economical process. To achieve this goal, an easy way to extract lignin from lignocellulosic biomass is needed and afterwards an efficient separation of lignin from the IL medium is of utmost importance. In this work, we demonstrated the recovery of HEAP using distillation and evaporation under reduced pressure. Particularly, the recovery of HEAP is beneficial as it presents high and similar lignin solubility for neat PIL and for PIL at 15 wt% water content, while negligible lignin solubility is noticed for water content higher than 75 wt% (Fig. 3). This means that PIL with low water content can be used, avoiding a prior PIL drying step, and practically all lignin dissolved in the PIL can be precipitated with the addition of water. The key step comes with an efficient water evaporation. The recovered solvent was first submitted to a distillation process at ambient pressure achieving approximately 41 wt% water content, where no vapor was observed after this point. Afterwards, the solution was submitted to a vacuum evaporation process (333.15 K and 10 kPa for 1 h) to remove the remaining water and to reach 15 wt% water content. This method allowed successful HEAP recovery up to 95 % of the initial IL mass.

Lignin solubility in recovered HEAP (15 wt% water content) was then examined up to three cycles of PIL recovery/reuse. The solubility efficiencies contrasting to neat PIL were 99.6, 99.1 and 98.7 % for recycling cycles 1, 2 and 3, respectively (Fig. 7). Only a very minor decrease in the dissolution efficiency was observed in these recycle assays, showing that HEAP can be reused without significantly losing its performance.

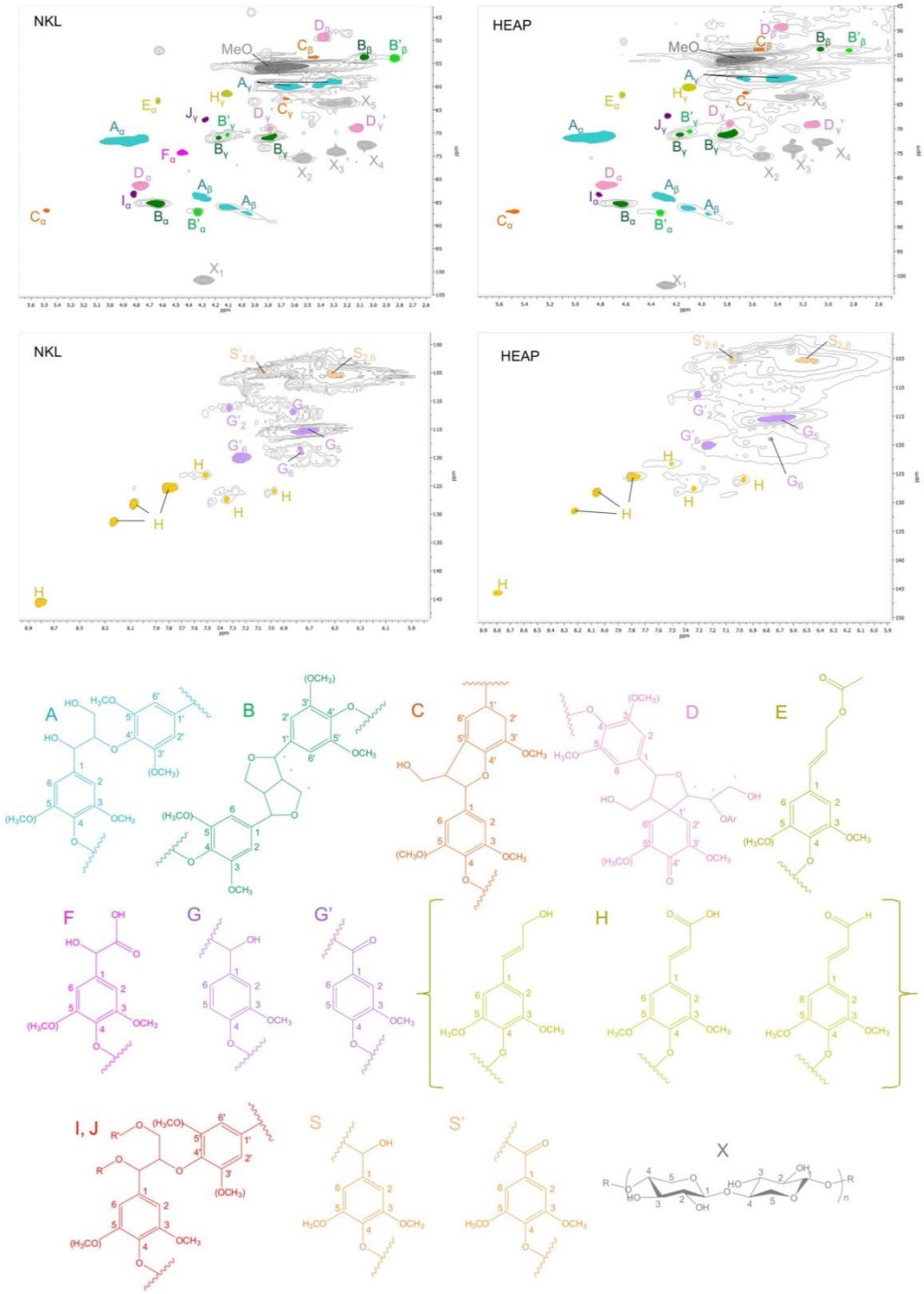

Fig. 6. 2D HSQC NMR of native Kraft lignin (NKL) and recovered lignin from HEAP (393.15 K) with corresponding ^{13}C-^{1}H cross signal assignments to main lignin subunits. The lignin substructures are the following: (A) β-*O*-4' linkages; (B) Resinol (β-β'); (C) Phenylcoumaran (β-5'); (D) Spirodienone (β-1'); (E) cinnamyl acetate end-groups; (F) Ar-CHOH-COOH unit (C_α-H_α); (G) Guaiacyl unit; (G') oxidized Guaiacyl unit with a C_α ketone or carboxyl group; (H) p-hydroxycynnamyl alcohol, aldehyde or carboxylic (aromatic and end groups); (I) β-*O*-4' substructure C_α etherified to carbohydrate (R, polysaccharide; R', H); (J) β-*O*-4' substructure C_γ etherified to carbohydrate (R, H; R', polysaccharide); ($S_{2,6}$) Syringyl unit; ($S'_{2,6}$) oxidized syringyl unit with a C_α ketone (phenolic); (X) Xylan.

Table 2
Relative abundance of main inter-unit linkages and lignin substructures as a percentage of total side chains from integration of ^{13}C-^{1}H cross signals in the HSQC spectra of native Kraft lignin and recovered lignins from PILs.

Linkage (Substructure) Type	Relative abundance % ([a])			
	Native Kraft lignin	HEAF lignin	HEAP lignin	THEAP lignin
β-O-4 (A)	48.6 (0.0)	62.7 (+22.5)	65.3 (+34.4)	55.0 (+13.1)
β-β (B)	35.8 (0.0)	25.5 (−28.8)	23.8 (−33.4)	32.0 (−10.6)
β-5 (C)	2.6 (0.0)	2.5 (−5.4)	2.2 (−15.3)	1.3 (-50.0)
β-1 (D)	8.6 (0.0)	5.6 (−34.8)	5.6 (−35.3)	7.8 (−9.4)
Others	4.4 (0.0)	3.7 (−15.3)	3.1 (−30.7)	3.9 (−10.9)

[a] Relative percentage deviation contrasting to the initial native Kraft lignin content.

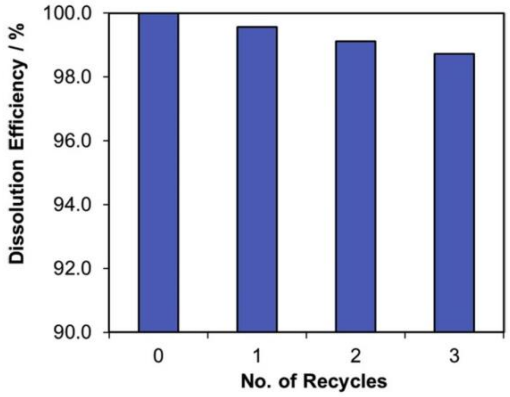

Fig. 7. Dissolution efficiency of lignin in HEAP (85 wt%) and recycled HEAP (85 wt%).

4. Conclusions

This work demonstrates the outstanding ability of alkylammonium PILs and their aqueous solutions to dissolve Kraft lignin at low temperature. The anion showed to play a major role in lignin dissolution than the cationic counterpart. The smaller cation with lower number of hydroxyalkyl groups favored the lignin dissolution process. On the other hand, the larger the alkyl carbon chain of the anion, the higher is the solubility of lignin in PIL. The results show that the presence of water is an important factor affecting the capacity of the PIL to dissolve this macromolecule. In general, the addition of water has a negative influence on the solubility process. Amongst examined solvents, hexanoate-based PIL (HEAH) presented the best performance for Kraft lignin dissolution allowing 37.7 wt% solubility at 323.15 K. On the other hand, HEAO stands as an exception, where the octanoate anion acts as hydrotropic agent promoting the lignin dissolution in water with a maximum solubility value at 40 wt% water content. A sharp decrease was observed using HEAF and HEAA as solvent media, while HEAP and HEAH present a softer reduction on lignin solubility with the addition of water. Regarding the temperature effect, the lignin dissolution was favored by temperature increase revealing the endothermic nature of the lignin dissolution process.

A comprehensive characterization of recovered lignin samples was performed after submitting lignin at 393.15 K for 6 h in selected PILs. As major conclusion, the molecular weight and relative abundance of lignin subunits slightly changed between native Kraft lignin and recovered lignin samples and seems to be connected. However, the modification is minimal, making PILs excellent non-derivatizing solvents of lignin. Moreover, consecutive steps of simple distillation and evaporation under reduced pressure allowed up to 95 % PIL recovery and the reuse of the solvent was accomplished for at least 3 cycles without losing its performance.

The disclosed results demonstrate a massive potential of PILs for application in biomass delignification and lignin dissolution processes and are in the way to accomplish higher sustainability in lignin valorization than traditional technologies.

Declaration of Competing Interest

None.

Acknowledgements

This work was developed within the scope of the project CICECO-Aveiro Institute of Materials, FCT Ref. UID/CTM/50011/2019, financed by national funds through the FCT/MCTES. The work was also funded by Fundação para a Ciência e Tecnologia (FCT) through the projects DeepBiorefinery [PTDC/AGR-TEC/1191/2014] and MultiBiorefinery [POCI-01-0145-FEDER-016403]. Authors acknowledge ISPT for funding A. M. da Costa Lopes postdoctoral grant. This study was financed in part by the Coordenação de Aperfeiçoamento de Pessoal de Nível Superior - Brasil (CAPES) - Finance Code 001. The authors would like also to thank national funding agencies the Banco Santander S. A., FAPESP [2014/21252-0, 2016/08566-1], CNPq [169743/2018-7, 310272/2017-3] and FAEPEX/UNICAMP for financial support. The Suzano Papel & Celulose was gratefully acknowledged for isolated Kraft lignin. The authors also thank Professor Dmitry Evtyugin for his kindly support in the analysis of lignin samples in GPC equipment.

Appendix A. Supplementary data

Supplementary material related to this article can be found, in the online version, at doi:https://doi.org/10.1016/j.indcrop.2019.111866.

References

Achinivu, E.C., 2018. Protic ionic liquids for lignin extraction—a lignin characterization study. Int. J. Mol. Sci. 19, 428. https://doi.org/10.3390/ijms19020428.

Achinivu, E.C., Howard, R.M., Li, G., Gracz, H., Henderson, W.A., 2014. Lignin extraction from biomass with protic ionic liquids. Green Chem. 16, 1114–1119. https://doi.org/10.1039/c3gc42306a.

Akiba, T., Tsurumaki, A., Ohno, H., 2017. Induction of lignin solubility for a series of polar ionic liquids by the addition of a small amount of water. Green Chem. 19, 2260–2265. https://doi.org/10.1039/c7gc00626h.

Álvarez, V.H., Dosil, N., Gonzalez-Cabaleiro, R., Mattedi, S., Martin-Pastor, M., Iglesias, M., Navaza, J.M., 2010. Brønsted ionic liquids for sustainable processes: synthesis and physical properties. J. Chem. Eng. Data 55, 625–632. https://doi.org/10.1021/je900550v.

Brandt, A., Chen, L., Van Dongen, B.E., Welton, T., Hallett, J.P., 2015. Structural changes in lignins isolated using an acidic ionic liquid water mixture. Green Chem. 17, 5019–5034. https://doi.org/10.1039/c5gc01314c.

Brandt-Talbot, A., Gschwend, F.J.V., Fennell, P.S., Lammens, T.M., Tan, B., Weale, J., Hallett, J.P., 2017. An economically viable ionic liquid for the fractionation of lignocellulosic biomass. Green Chem. 19, 3078–3102. https://doi.org/10.1039/c7gc00705a.

Cachet, N., Camy, S., Benjelloun-Mlayah, B., Condoret, J.S., Delmas, M., 2014. Esterification of organosolv lignin under supercritical conditions. Ind. Crops Prod. 58, 287–297. https://doi.org/10.1016/j.indcrop.2014.03.039.

Cademartori, P.H.G., dos Santos, P.S.B., Serrano, L., Labidi, J., Gatto, D.A., 2013. Effect of thermal treatment on physicochemical properties of Gympie messmate wood. Ind.

Crops Prod. 45, 360–366. https://doi.org/10.1016/j.indcrop.2012.12.048.
Chambon, C.L., Mkhize, T.Y., Reddy, P., Brandt-Talbot, A., Deenadayalu, N., Fennell, P.S., Hallett, J.P., 2018. Pretreatment of South African sugarcane bagasse using a low-cost protic ionic liquid: a comparison of whole, depithed, fibrous and pith bagasse fractions. Biotechnol. Biofuels 11, 247. https://doi.org/10.1186/s13068-018-1247-0.
Chang, W.R., Hwang, J.J., Wu, W., 2017. Environmental impact and sustainability study on biofuels for transportation applications. Renew. Sustain. Energy Rev. 67, 277–288. https://doi.org/10.1016/j.rser.2016.09.020.
Cláudio, A.F.M., Neves, M.C., Shimizu, K., Canongia Lopes, J.N., Freire, M.G., Coutinho, J.A.P., 2015. The magic of aqueous solutions of ionic liquids: ionic liquids as a powerful class of catanionic hydrotropes. Green Chem. 17, 3948–3963. https://doi.org/10.1039/c5gc00712g.
Da Costa Lopes, A.M., Bogel-Lukasik, R., 2015. Acidic ionic liquids as sustainable approach of cellulose and lignocellulosic biomass conversion without additional catalysts. ChemSusChem 8, 947–965. https://doi.org/10.1002/cssc.201402950.
Dahmen, N., Lewandowski, I., Zibek, S., Weidtmann, A., 2019. Integrated lignocellulosic value chains in a growing bioeconomy: status quo and perspectives. GCB Bioenergy 11, 107–117. https://doi.org/10.1111/gcbb.12586.
Fathi-Azarjbayjani, A., Mabhoot, A., Martínez, F., Jouyban, A., 2016. Modeling, solubility, and thermodynamic aspects of sodium phenytoin in propylene glycol-water mixtures. J. Mol. Liq. 219, 68–73. https://doi.org/10.1016/j.molliq.2016.02.089.
Fernández-Costas, C., Gouveia, S., Sanromán, M.A., Moldes, D., 2014. Structural characterization of Kraft lignins from different spent cooking liquors by 1D and 2D Nuclear Magnetic Resonance spectroscopy. Biomass Bioenergy 63, 156–166. https://doi.org/10.1016/j.biombioe.2014.02.020.
García, A., Erdocia, X., González Alriols, M., Labidi, J., 2012. Effect of ultrasound treatment on the physicochemical properties of alkaline lignin. Chem. Eng. Process. Process Intensif. 62, 150–158. https://doi.org/10.1016/j.cep.2012.07.011.
Glas, D., Van Doorslaer, C., Depuydt, D., Liebner, F., Rosenau, T., Binnemans, K., De Vos, D.E., 2015. Lignin solubility in non-imidazolium ionic liquids. J. Chem. Technol. Biotechnol. 90, 1821–1826. https://doi.org/10.1002/jctb.4492.
Gordobil, O., Delucis, R., Egüés, I., Labidi, J., 2015. Kraft lignin as filler in PLA to improve ductility and thermal properties. Ind. Crops Prod. 72, 46–53. https://doi.org/10.1016/j.indcrop.2015.01.055.
Hart, W.E.S., Harper, J.B., Aldous, L., 2015. The effect of changing the components of an ionic liquid upon the solubility of lignin. Green Chem. 17, 214–218. https://doi.org/10.1039/c4gc01888e.
Hou, X.D., Xu, J., Li, N., Zong, M.H., 2015. Effect of anion structures on cholinium ionic liquids pretreatment of rice straw and the subsequent enzymatic hydrolysis. Biotechnol. Bioeng. 112, 65–73. https://doi.org/10.1002/bit.25335.
Hu, J., Zhang, Q., Lee, D.J., 2018. Kraft lignin biorefinery: a perspective. Bioresour. Technol. 247, 1181–1183. https://doi.org/10.1016/j.biortech.2017.08.169.
Ibarra, D., Chávez, M.I., Rencoret, J., Del Río, J.C., Gutiérrez, A., Romero, J., Camarero, S., Martínez, M.J., Jiménez-Barbero, J., Martínez, A.T., 2007. Lignin modification during Eucalyptus globulus kraft pulping followed by totally chlorine-free bleaching: a two-dimensional nuclear magnetic resonance, Fourier transform infrared, and pyrolysis-gas chromatography/mass spectrometry study. J. Agric. Food Chem. 55, 3477–3490. https://doi.org/10.1021/jf063728t.
Iglesias, M., Gonzalez-Olmos, R., Cota, I., Medina, F., 2010. Brønsted ionic liquids: study of physico-chemical properties and catalytic activity in aldol condensations. Chem. Eng. J. 162, 802–808. https://doi.org/10.1016/j.cej.2010.06.008.
Ji, W., Ding, Z., Liu, J., Song, Q., Xia, X., Gao, H., Wang, H., Gu, W., 2012. Mechanism of lignin dissolution and regeneration in ionic liquid. Energy Fuel 26, 6393–6403. https://doi.org/10.1021/ef301231a.
Kim, K.H., Oh, H.K., Heo, B., Kim, N.A., Lim, D.G., Jeong, S.H., 2018. Solubility evaluation and thermodynamic modeling of β-lapachone in water and ten organic solvents at different temperatures. Fluid Phase Equilib. 472, 1–8. https://doi.org/10.1016/j.fluid.2018.05.005.
Liitiä, T.M., Maunu, S.L., Hortling, B., Toikka, M., Kilpeläinen, I., 2003. Analysis of technical lignins by two- and three-dimensional NMR spectroscopy. J. Agric. Food Chem. 51, 2136–2143. https://doi.org/10.1021/jf0204349.
Long, B., Xia, Y., Deng, Z., Ding, Y., 2017. Understanding the enhanced solubility of 1,3-benzenedicarboxylic acid in polar binary solvents of (acetone + water) at various temperatures. J. Chem. Thermodyn. 105, 105–111. https://doi.org/10.1016/j.jct.2016.10.011.
Martinez, A.T., Nieto, L., Kim, H., Gutierrez, A., Rencoret, J., Jimenez-Barbero, J., Faulds, C.B., Ralph, J., del Rio, J.C., 2010. Lignin composition and structure in young versus adult Eucalyptus globulus plants. Plant Physiol. 155, 667–682. https://doi.org/10.1104/pp.110.167254.
Merino, O., Fundora-Galano, G., Luque, R., Martínez-Palou, R., 2018. Understanding microwave-assisted lignin solubilization in protic ionic liquids with multiaromatic imidazolium cations. ACS Sustain. Chem. Eng. 6, 4122–4129. https://doi.org/10.1021/acssuschemeng.7b04535.
Miranda, R., Neta, J.V., Romanholo Ferreira, L.F., Gomes, W.A., do Nascimento, C.S., de B. Gomes, E., Mattedi, S., Soares, C.M.F., Lima, Á.S., 2019. Pineapple crown delignification using low-cost ionic liquid based on ethanolamine and organic acids. Carbohydr. Polym. 206, 302–308. https://doi.org/10.1016/j.carbpol.2018.10.112.
Mu, L., Shi, Y., Chen, L., Ji, T., Yuan, R., Wang, H., Zhu, J., 2015. [*N*-Methyl-2-pyrrolidone][C1-C4 carboxylic acid]: a novel solvent system with exceptional lignin solubility. Chem. Commun. 51, 13554–13557. https://doi.org/10.1039/c5cc04191k.
Nevrez, L.A.M., Casarrubias, L.B., Celzard, A., Fierro, V., Mũoz, V.T., Davila, A.C., Lubian, J.R.T., Snchez, G.G., 2011. Biopolymer-based nanocomposites: effect of lignin acetylation in cellulose triacetate films. Sci. Technol. Adv. Mater. 12, 045006. https://doi.org/10.1088/1468-6996/12/4/045006.
Pandey, K.K., Pitman, A.J., 2003. FTIR studies of the changes in wood chemistry following decay by brown-rot and white-rot fungi. Int. Biodeterior. Biodegrad. 52, 151–160. https://doi.org/10.1016/S0964-8305(03)00052-0.
Popescu, C.-M., Vasile, C., Popescu, M.-C., Singurel, G., Munteanu, B.S., Popa, V.I., 2006. Analytical methods for lignin characterisation. II) Spectroscopical studies. Cell. Chem. Technol. 40, 597–622.
Prado, R., Erdocia, X., Labidi, J., 2013. Lignin extraction and purification with ionic liquids. J. Chem. Technol. Biotechnol. 88, 1248–1257. https://doi.org/10.1002/jctb.3965.
Pu, Y., Jiang, N., Ragauskas, A.J., 2007. Ionic liquid as a green solvent for lignin. J. Wood Chem. Technol. 27, 23–33. https://doi.org/10.1080/02773810701282330.
Ralph, J., Landucci, L., 2010. NMR of lignins. Lignin and Lignans. https://doi.org/10.1201/ebk1574444865-c5.
Rashid, T., Kait, C.F., Regupathi, I., Murugesan, T., 2016. Dissolution of kraft lignin using protic ionic liquids and characterization. Ind. Crops Prod. 84, 284–293. https://doi.org/10.1016/j.indcrop.2016.02.017.
Rashid, T., Gnanasundaram, N., Appusamy, A., Kait, C.F., Thanabalan, M., 2018. Enhanced lignin extraction from different species of oil palm biomass: kinetics and optimization of extraction conditions. Ind. Crops Prod. 116, 122–136. https://doi.org/10.1016/j.indcrop.2018.02.056.
Semerci, I., Güler, F., 2018. Protic ionic liquids as effective agents for pretreatment of cotton stalks at high biomass loading. Ind. Crops Prod. 125, 588–595. https://doi.org/10.1016/j.indcrop.2018.09.046.
Silveira, M.H.L., Morais, A.R.C., Da Costa Lopes, A.M., Olekszyszen, D.N., Bogel-Łukasik, R., Andreaus, J., Pereira Ramos, L., 2015. Current pretreatment technologies for the development of cellulosic ethanol and biorefineries. ChemSusChem 8 (20), 3366–3390. https://doi.org/10.1002/cssc.201500282.
Soares, B., Tavares, D.J.P., Amaral, J.L., Silvestre, A.J.D., Freire, C.S.R., Coutinho, J.A.P., 2017. Enhanced solubility of lignin monomeric model compounds and technical lignins in aqueous solutions of deep eutectic solvents. ACS Sustain. Chem. Eng. 5, 4056–4065. https://doi.org/10.1021/acssuschemeng.7b00053.
Soares, B., Silvestre, A.J.D., Rodrigues Pinto, P.C., Freire, C.S.R., Coutinho, J.A.P., 2019. Hydrotropy and cosolvency in lignin solubilization with deep eutectic solvents. ACS Sustain. Chem. Eng. 7, 12485–12493. https://doi.org/10.1021/acssuschemeng.9b02109.
Sun, S.N., Li, M.F., Yuan, T.Q., Xu, F., Sun, R.C., 2012. Sequential extractions and structural characterization of lignin with ethanol and alkali from bamboo (Neosinocalamus affinis). Ind. Crops Prod. 37, 51–60. https://doi.org/10.1016/j.indcrop.2011.11.033.
Tolbert, Allison, Akinosho, Hannah, Khunsupat, Ratayakorn, Naskar, Amit K., Ragauskas, Arthur J., 2014. Characterization and analysis of the molecular weight of lignin. Biofuels Bioprod. Biorefining 8, 836–856. https://doi.org/10.1002/bbb.1500.
Wang, Y.Y., Li, M., Wyman, C.E., Cai, C.M., Ragauskas, A.J., 2018. Fast fractionation of technical lignins by organic cosolvents. ACS Sustain. Chem. Eng. 6, 6064–6072. https://doi.org/10.1021/acssuschemeng.7b04546.
Welton, T., 2018. Ionic liquids: a brief history. Biophys. Rev. 10, 691–706. https://doi.org/10.1007/s12551-018-0419-2.
Wen, J.L., Xue, B.L., Xu, F., Sun, R.C., 2012. Unveiling the structural heterogeneity of bamboo lignin by in situ HSQC NMR technique. Bioenergy Res. 5, 886–903. https://doi.org/10.1007/s12155-012-9203-5.
Wen, J.L., Sun, S.L., Yuan, T.Q., Sun, R.C., 2015. Structural elucidation of whole lignin from Eucalyptus based on preswelling and enzymatic hydrolysis. Green Chem. 17, 1589–1596. https://doi.org/10.1039/c4gc01889c.
Xu, A., Guo, X., Zhang, Y., Li, Z., Wang, J., 2017. Efficient and sustainable solvents for lignin dissolution: aqueous choline carboxylate solutions. Green Chem. 19, 4067–4073. https://doi.org/10.1039/c7gc01886j.
Yuan, T.Q., Sun, S.N., Xu, F., Sun, R.C., 2011. Characterization of lignin structures and lignin-carbohydrate complex (LCC) linkages by quantitative13C and 2D HSQC NMR spectroscopy. J. Agric. Food Chem. 59, 10604–10614. https://doi.org/10.1021/jf2031549.
Zhang, A., Lu, F., Sun, R.C., Ralph, J., 2010. Isolation of cellulolytic enzyme lignin from wood preswollen/dissolved in dimethyl sulfoxide/N-methylimidazole. J. Agric. Food Chem. 58, 3446–3450. https://doi.org/10.1021/jf903998d.
Zhang, Y., He, H., Dong, K., Fan, M., Zhang, S., 2017. A DFT study on lignin dissolution in imidazolium-based ionic liquids. RSC Adv. 7, 12670–12681. https://doi.org/10.1039/c6ra27059j.
Zhu, X., Peng, C., Chen, H., Chen, Q., Zhao, Z.K., Zheng, Q., Xie, H., 2018. Opportunities of ionic liquids for lignin utilization from biorefinery. ChemistrySelect 3, 7945–7962. https://doi.org/10.1002/slct.201801393.

Supplementary Information

Uncovering the potentialities of protic ionic liquids based on alkanolammonium and carboxylate ions and their aqueous solutions as non-derivatizing solvents of Kraft lignin

Rafael M. Dias[a,b], André M. da Costa Lopes[b,*], Armando J. D. Silvestre[b], João A. P. Coutinho[b] and Mariana C. da Costa[a].

[a]*Department of Process and Product Design (DDPP) - School of Chemical Engineering (FEQ), University of Campinas (UNICAMP), Av. Albert Einstein, 500, Campinas, São Paulo, 13083-852, Brazil.*

[b]*CICECO, Aveiro Institute of Materials, Department of Chemistry, University of Aveiro, 3810-193 Aveiro, Portugal.*

*corresponding author: andremcl@ua.pt

Table of contents

PILs characterization

FTIR-ATR

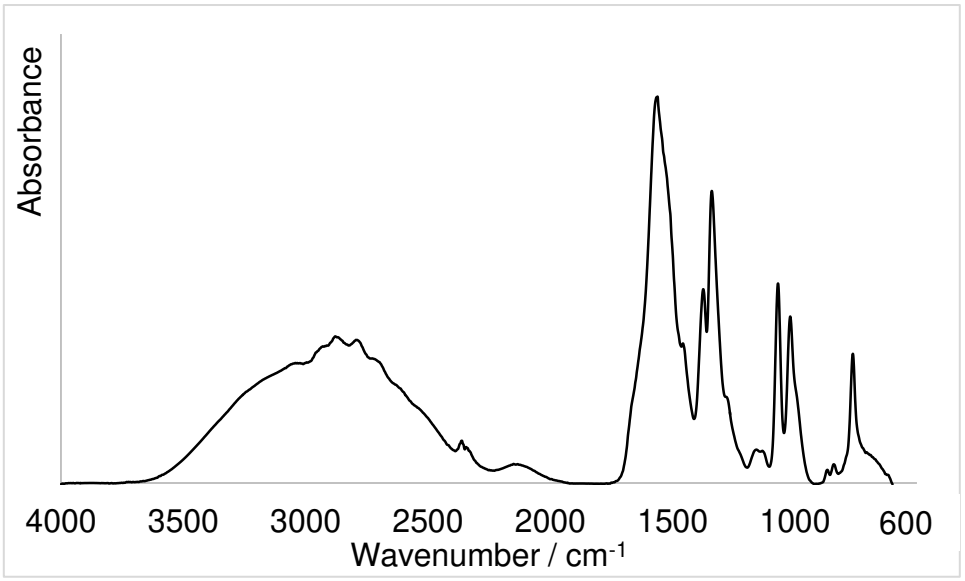

Figure S1. FTIR spectrum of HEAF

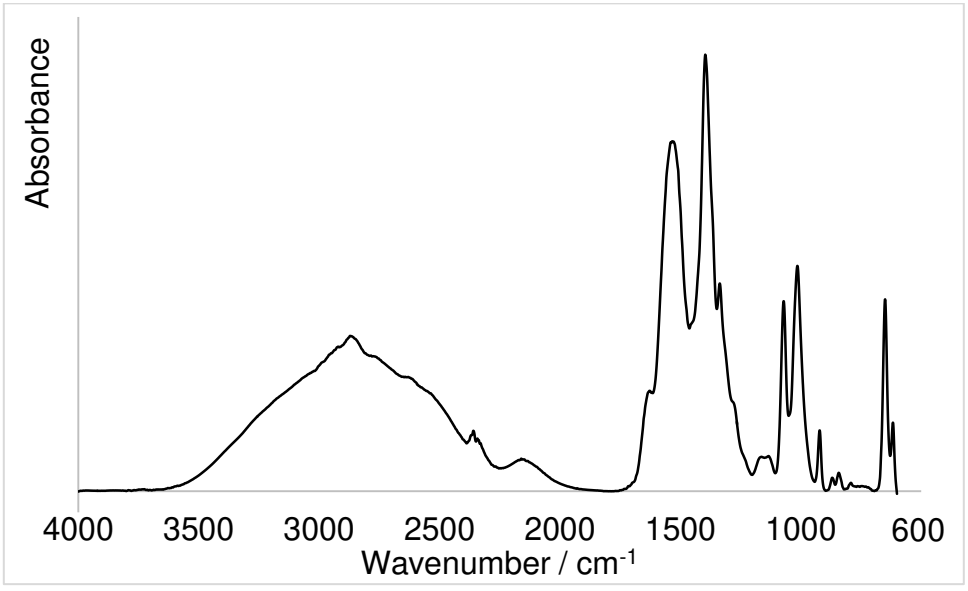

Figure S2. FTIR spectrum of HEAA

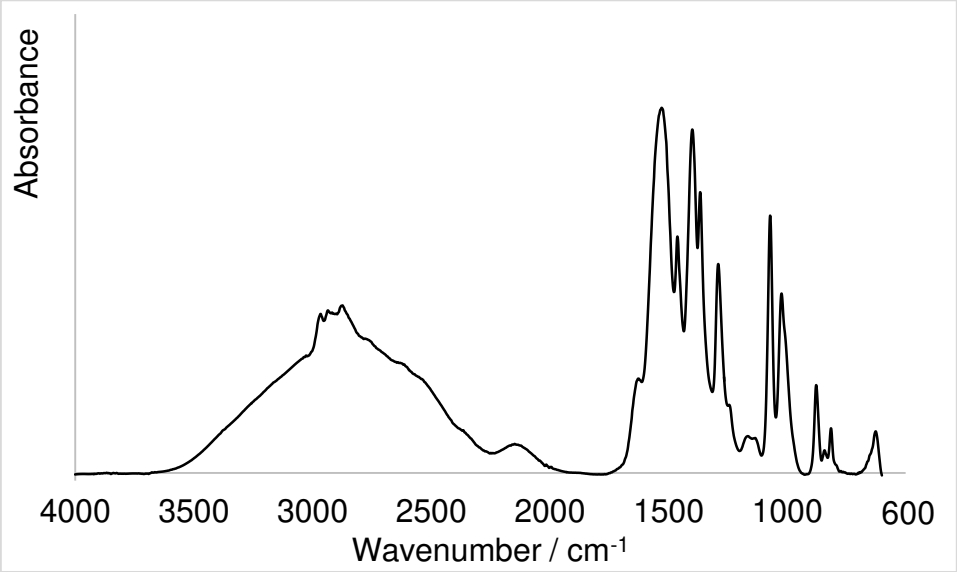

Figure S3. FTIR spectrum of HEAP

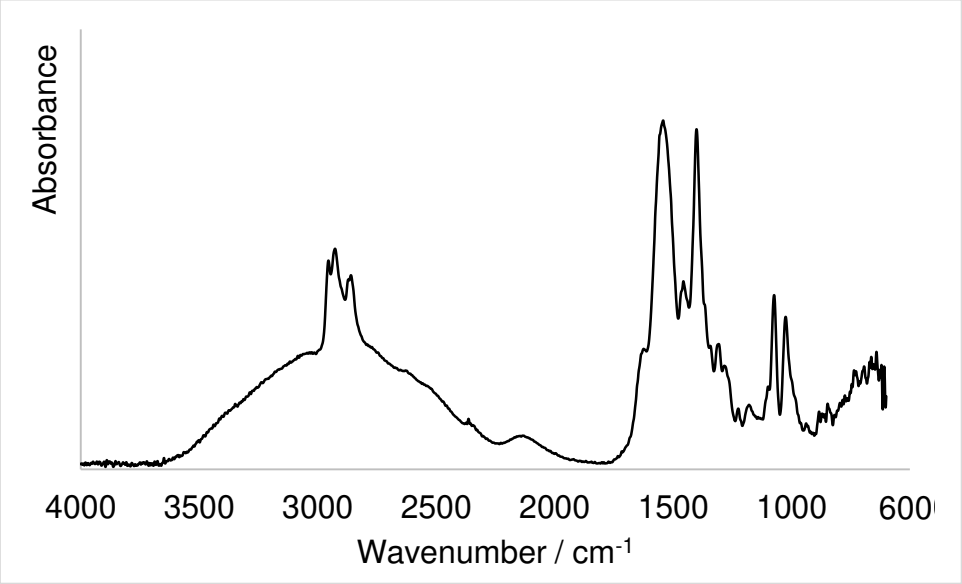

Figure S4. FTIR spectrum of HEAH

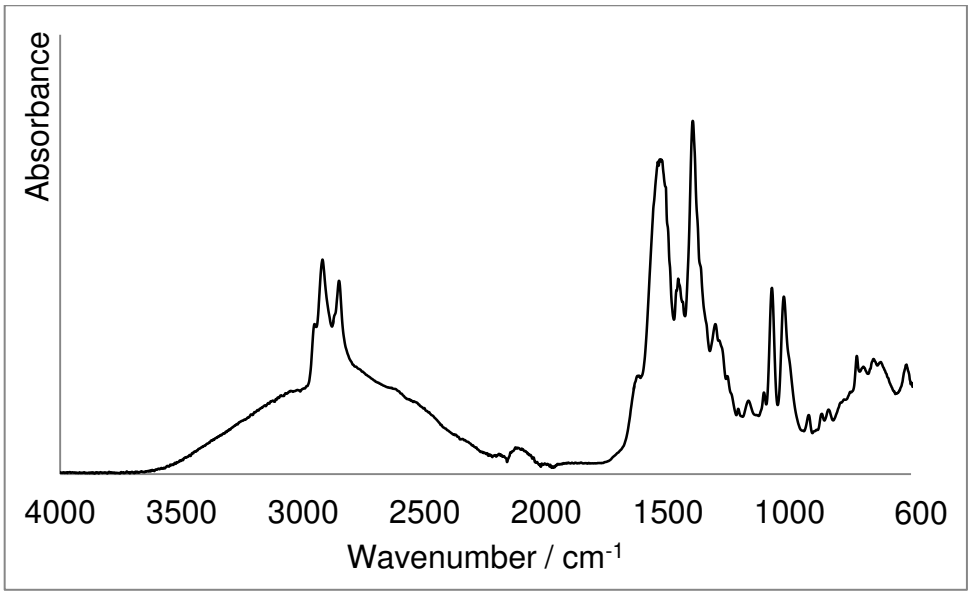

Figure S5. FTIR spectrum of HEAO

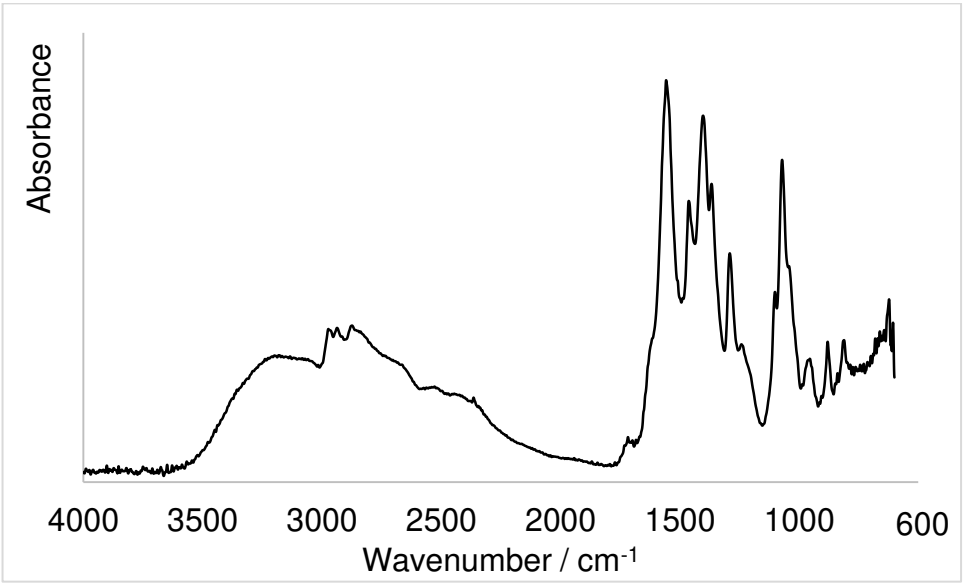

Figure S6. FTIR spectrum of BHEAP

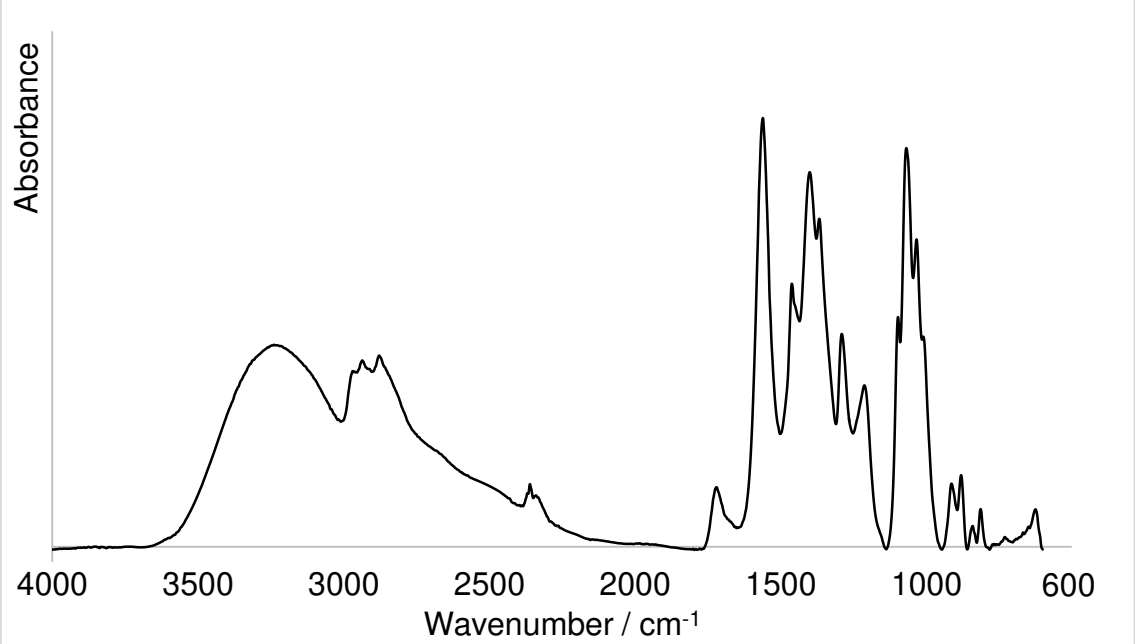

Figure S7. FTIR spectrum of THEAP

^{1}H and ^{13}C NMR

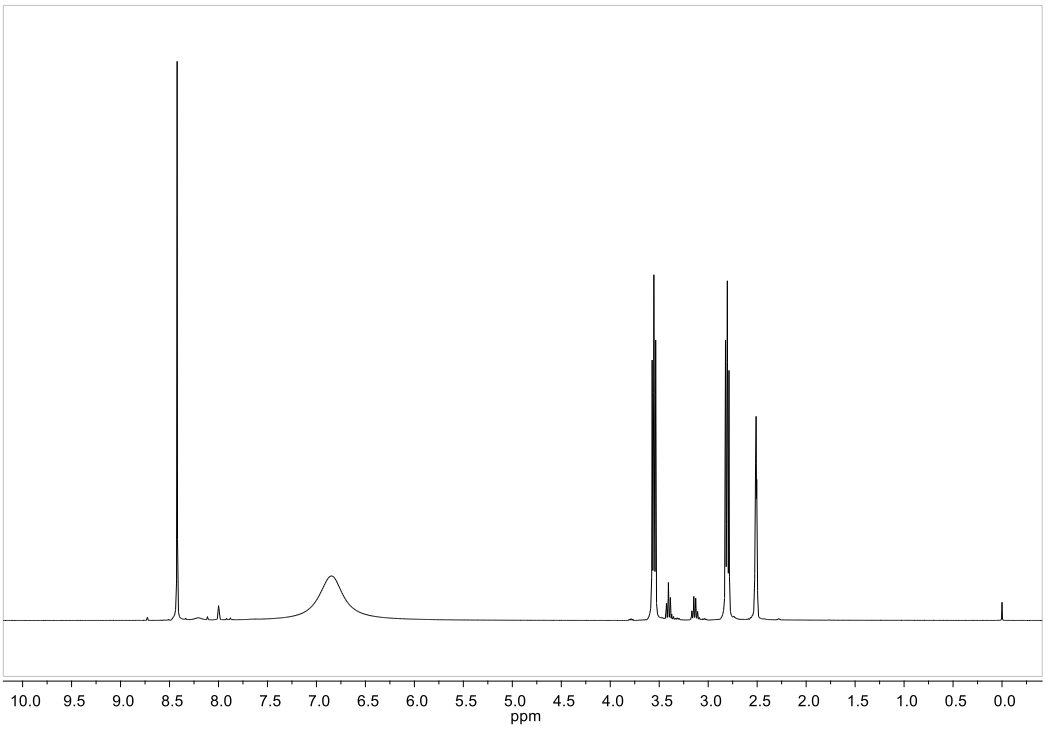

Figure S8. ^{1}H NMR spectrum of HEAF

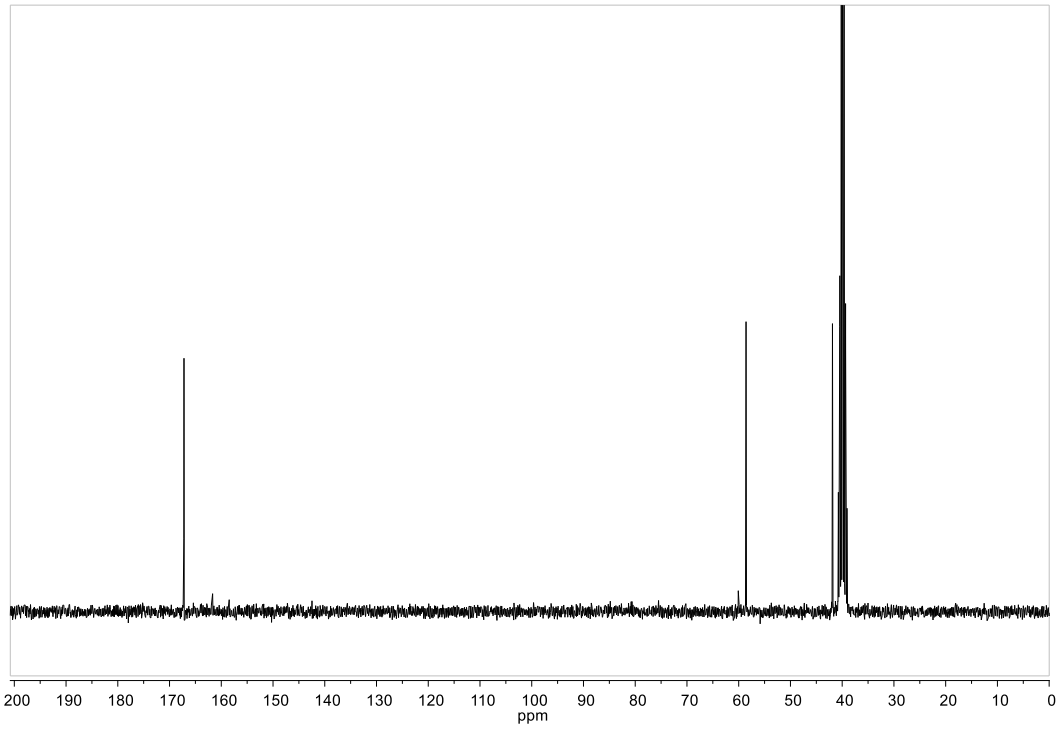

Figure S9. ^{13}C NMR spectrum of HEAF

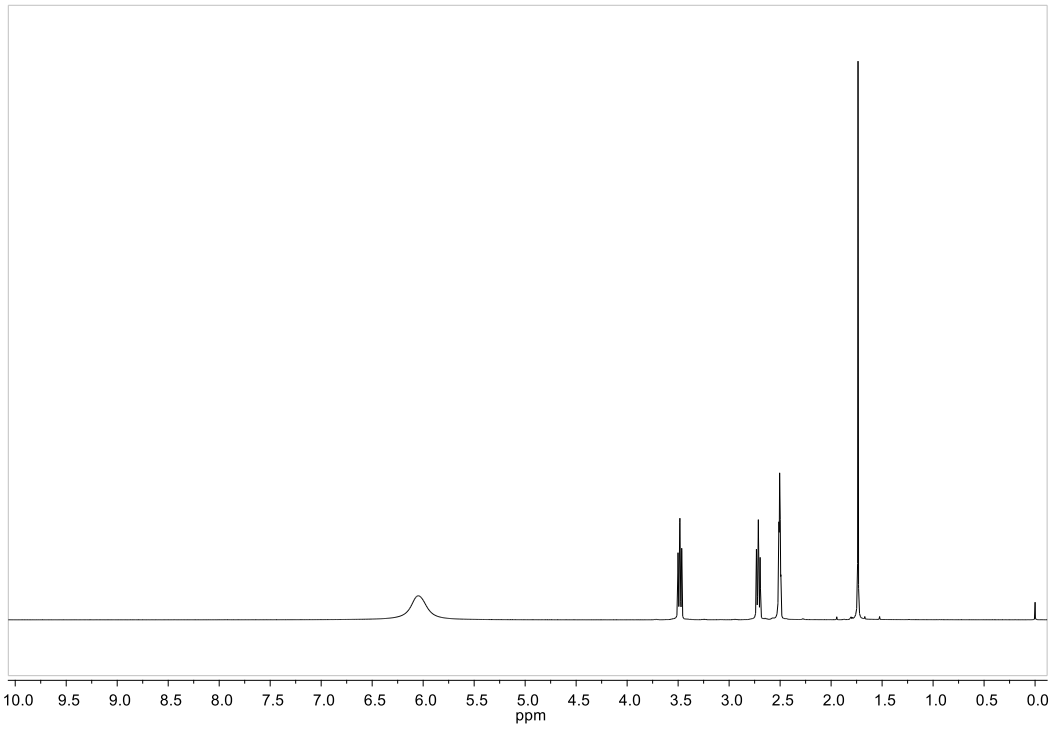

Figure S10. ^{1}H NMR spectrum of HEAA

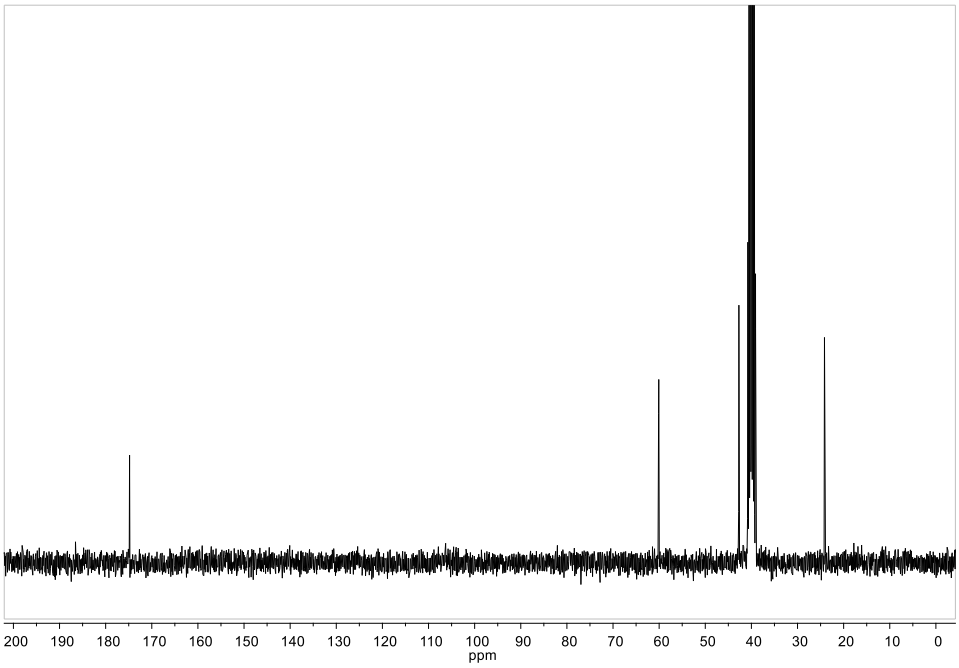

Figure S11. ^{13}C NMR spectrum of HEAA

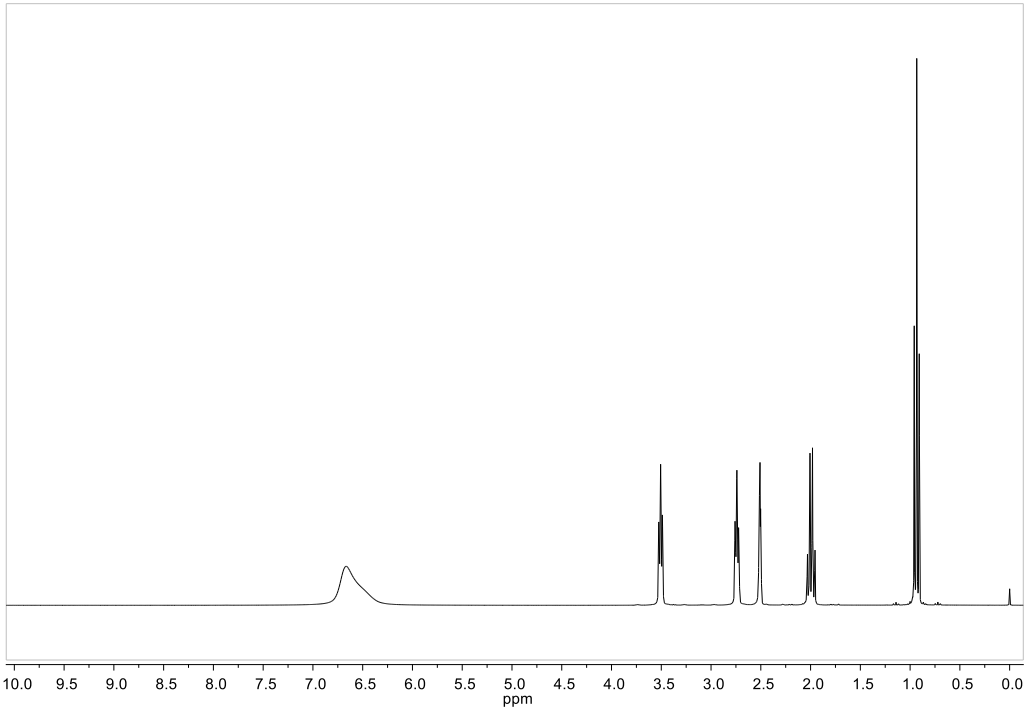

Figure S12. ^{1}H NMR spectrum of HEAP

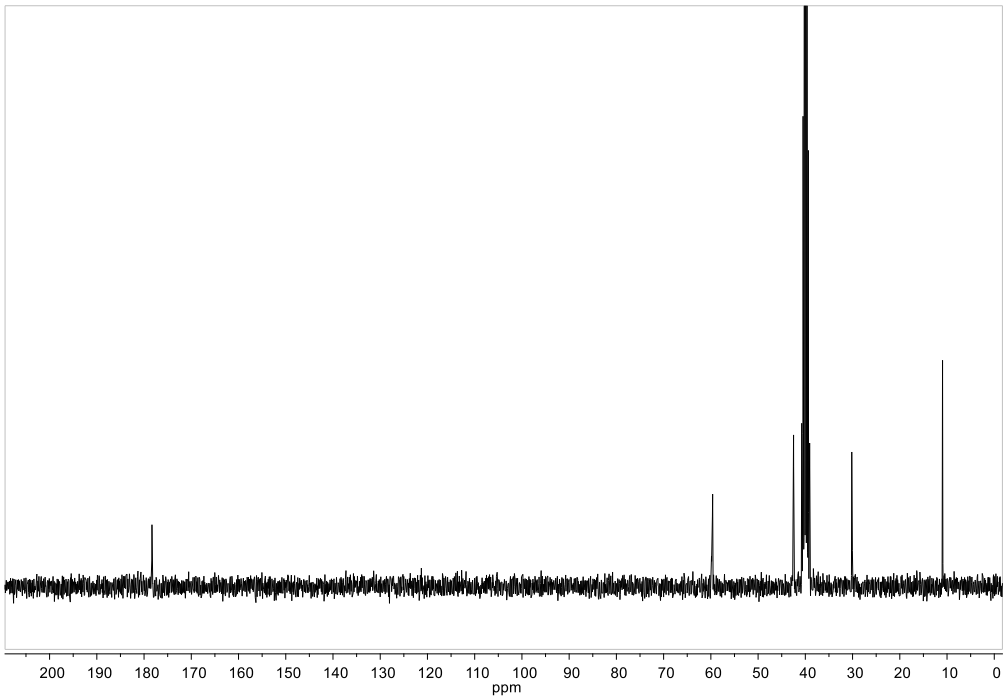

Figure S13. ^{13}C NMR spectrum of HEAP

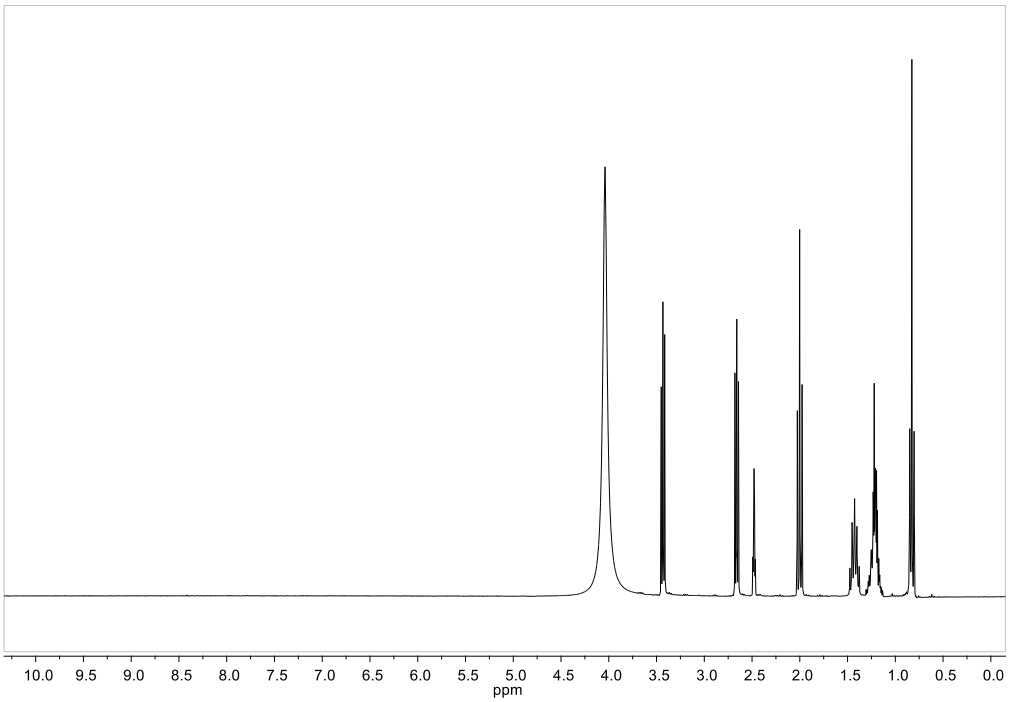

Figure S14. ^{1}H NMR spectrum of HEAH

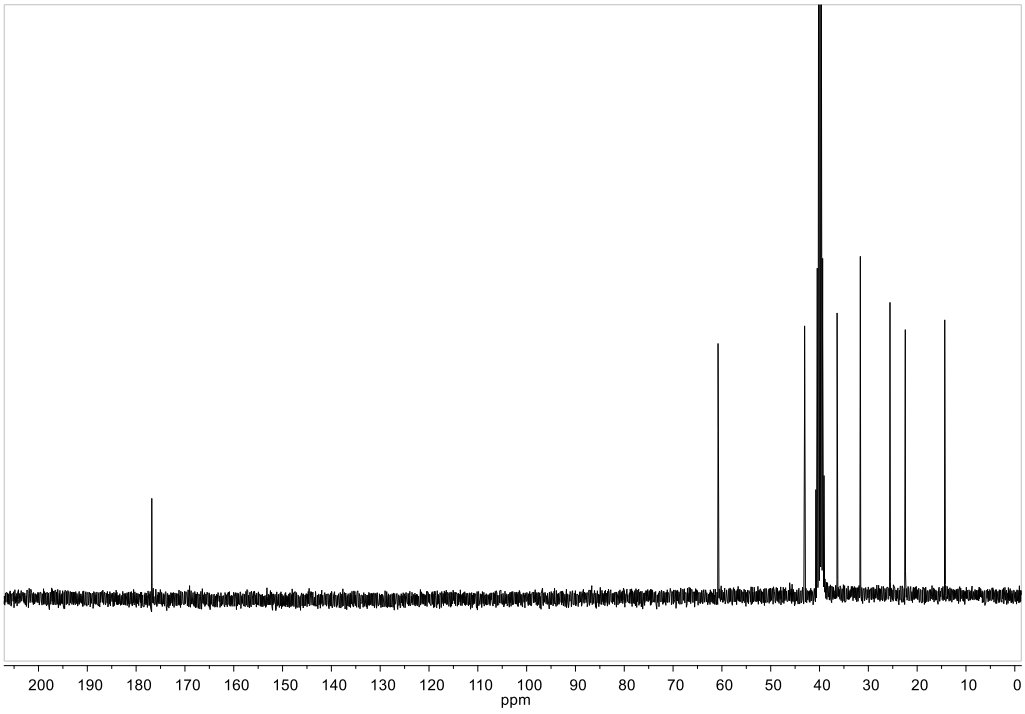

Figure S15. ^{13}C NMR spectrum of HEAH

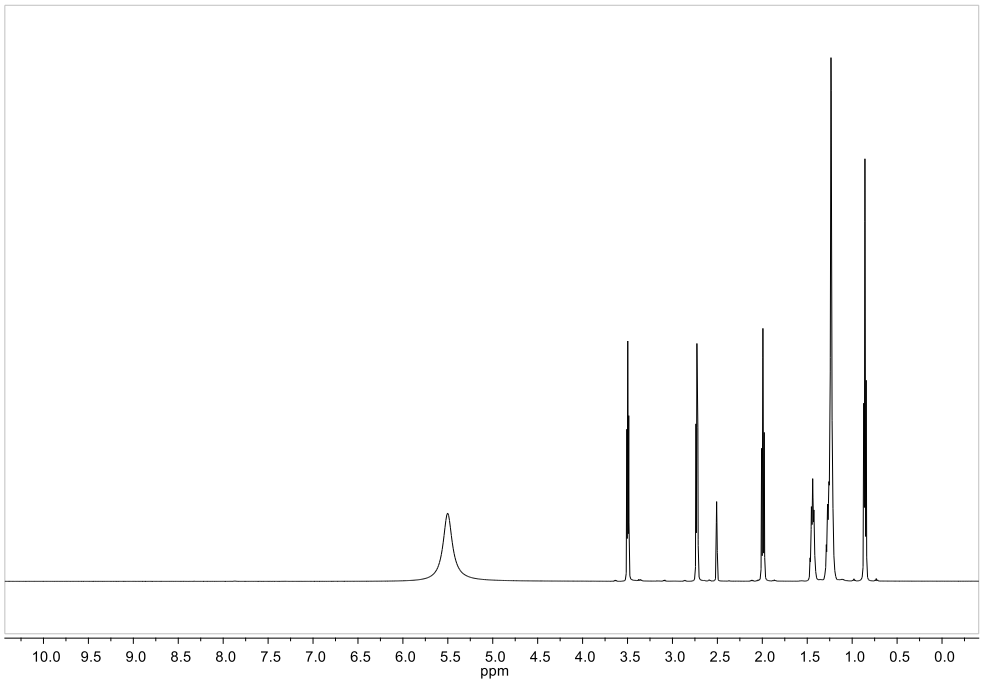

Figure S16. ^{1}H-NMR spectrum of HEAO

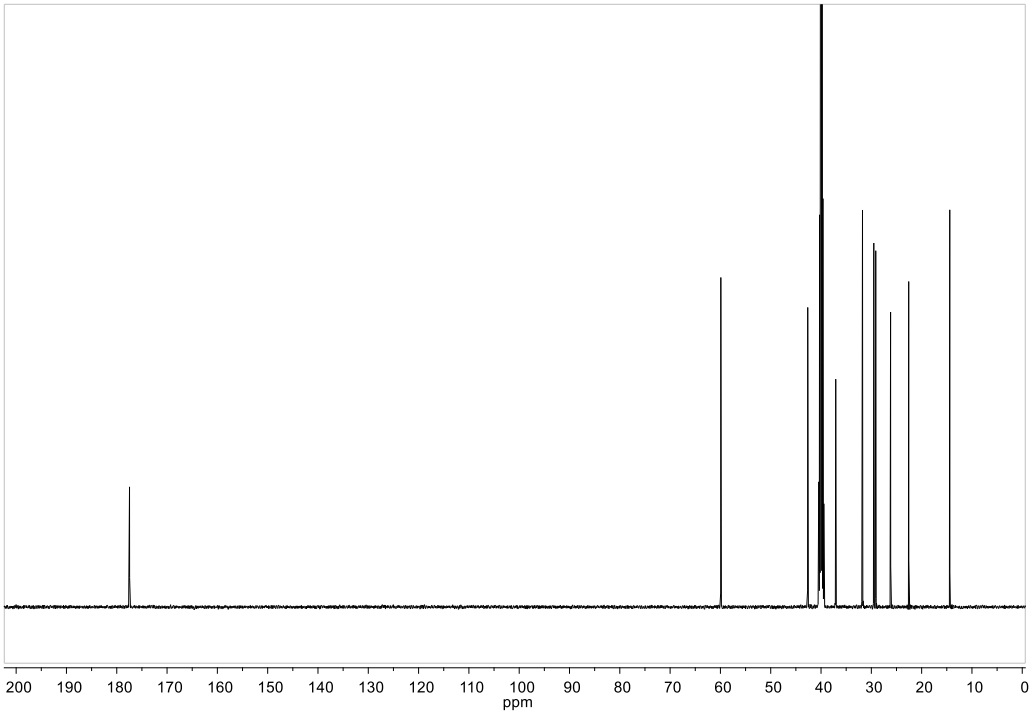

Figure S17. ^{13}C-NMR spectrum of HEAO

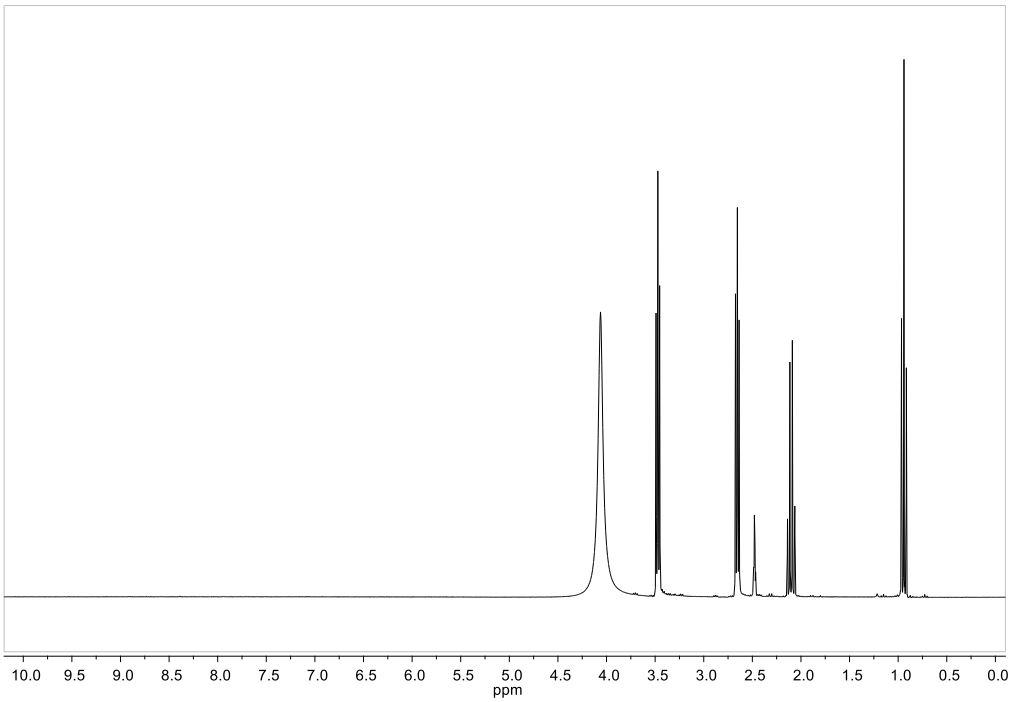

Figure S18. ^{1}H-NMR spectrum of BHEAP

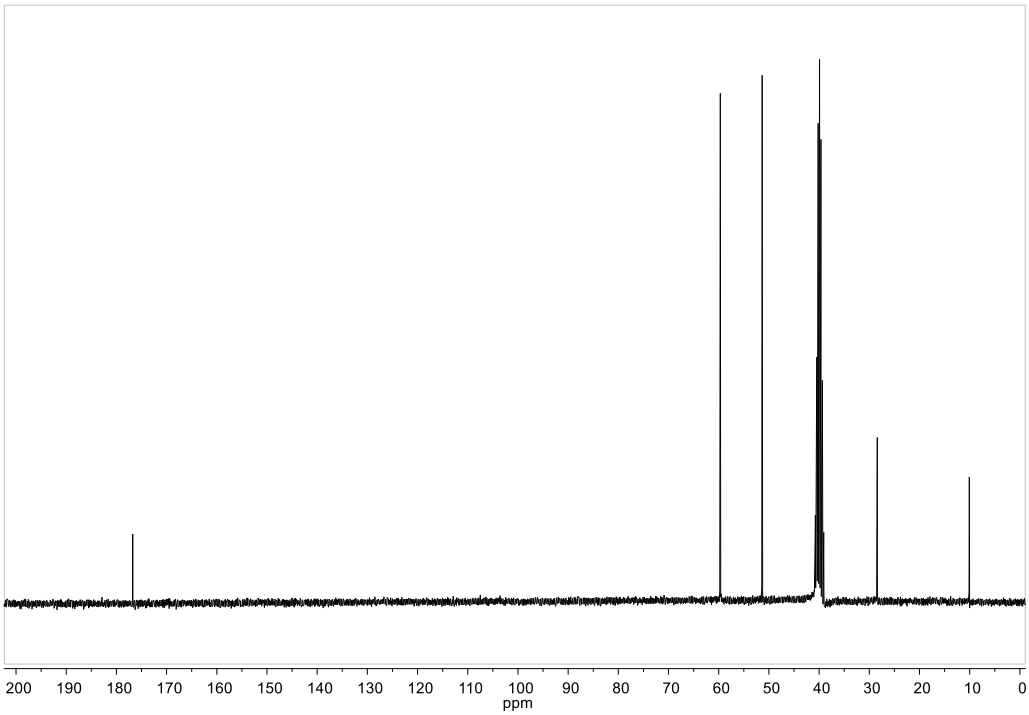

Figure S19. ^{13}C NMR spectrum of BHEAP

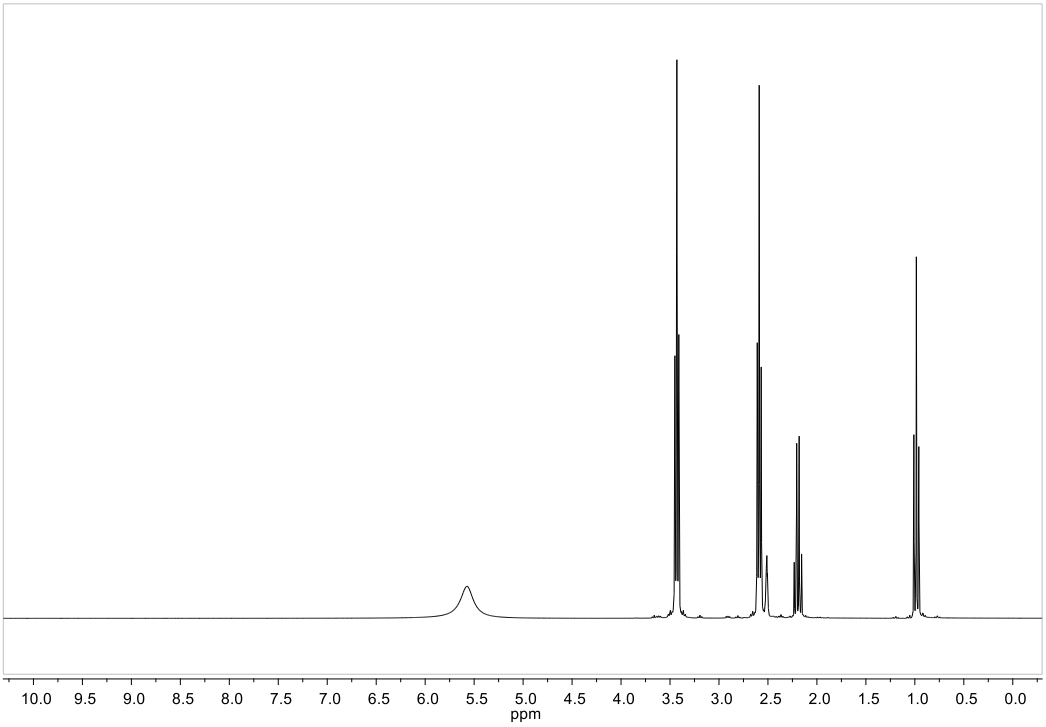

Figure S20. ^{1}H-NMR spectrum of THEAP

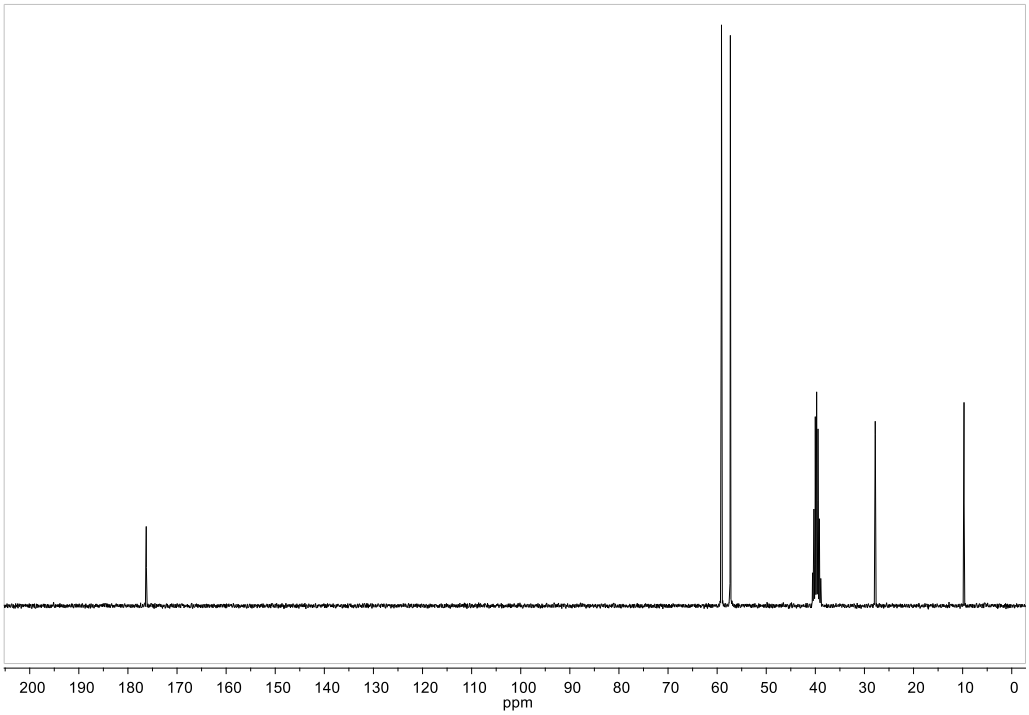

Figure S21. ^{13}C-NMR spectrum of THEAP

Lignin Calibration Curves

Table S1. Kraft lignin calibration curves in HEAF, HEAA, HEAP, BHEAP, THEAP, HEAH and HEAO (1M and 4M solutions). $y = mx + b$, where y corresponds to lignin absorbance and x to lignin mass (g).

Solution	***m***	***b***	**R^2**
HEAF (1M)	12867	0.1821	0.9992
HEAF (4M)	12788	0.1820	0.9976
HEAA (1M)	13149	0.1693	0.9991
HEAA (4M)	13106	0.1780	0.9976
HEAP (1M)	12960	0.2293	0.9956
HEAP (4M)	13186	0.2295	0.9963
HDEAP (1M)	13740	0.0641	0.9952
HDEAP (4M)	13100	0.1272	0.9990
HTEAP (1M)	12866	0.2977	0.9963
HTEAP (4M)	13056	0.2947	0.9929
HEAH (1M)	13825	0.1735	0.9975
HEAH (4M)	13326	0.0979	0.9960
HEAO (1M)	13645	0.1317	0.9967
HEAO (4M)	13454	0.0956	0.9974

Kraft lignin solubility values in PILs aqueous solutions

Table S2. Kraft lignin solubility values in HEAP, BHEAP and THEAP aqueous solutions at 323.15 K. The values are expressed as means.

Water (wt%)	HEAP	BHEAP	THEAP
100.0		0.10± 0.01	
75.0	1.32 ± 0.12	1.43 ± 0.12	0.87 ± 0.02
60.0	6.12 ± 0.04	5.98 ± 0.02	5.67 ± 0.09
50.0	9.85 ± 0.20	9.82 ± 0.68	10.27 ± 1.16
40.0	17.13 ± 0.08	16.72 ± 0.17	16.95 ± 0.38
25.0	23.43 ± 0.34	21.51 ± 0.57	21.45 ± 0.39
20.0	25.11 ± 0.12	24.04 ± 0.42	22.88 ± 0.66
15.0	29.49 ± 0.30	27.41 ± 0.11	23.65 ± 0.16
3.0	30.86 ± 0.76	28.01 ± 0.33	24.02 ± 0.40

Table S3. Kraft lignin solubility values in HEAF, HEAA, HEAP, HEAH and HEAO aqueous solutions at 323.15 K. The values are expressed as means.

Water (wt%)	HEAF	HEAA	HEAP	HEAH	HEAO
100.0			0.10± 0.01		
90.0	-	-	-	4.35 ± 0.49	8.25 ± 0.62
75.0	0.46 ± 0.02	0.47 ± 0.03	1.32 ± 0.12	9.44 ± 0.52	16.27 ± 0.20
60.0	0.78 ± 0.01	0.84 ± 0.03	6.12 ± 0.04	13.97 ± 0.71	21.42 ± 1.04
50.0	0.77 ± 0.01	1.53 ± 0.18	9.85 ± 0.20	19.08 ± 0.39	22.68 ± 0.94
40.0	1.60 ± 0.08	2.45 ± 0.15	17.13 ± 0.08	22.12 ± 0.24	23.27 ± 0.17
25.0	5.23 ± 0.32	11.98 ± 0.27	23.43 ± 0.34	29.90 ± 0.32	23.04 ± 1.21
20.0	8.68 ± 0.32	18.57 ± 0.21	25.11 ± 0.12	35.36 ± 0.26	22.33 ± 0.18
15.0	14.80 ± 0.20	19.50 ± 0.49	29.49 ± 0.30	37.65 ± 0.51	22.82 ± 0.31
3.0	20.27 ± 1.07	22.12 ± 0.37	30.86 ± 0.76	37.77 ± 0.20	20.40 ± 0.47

Table S4. Kraft lignin solubility values in HEAP aqueous solutions at 313.15, 323.15, 333.15, and 353.15 K. The values are expressed as means.

Water (wt%)	313.15 K	323.15 K	333.15 K	353.15 K
100.0	0.09 ± 0.01	0.10 ± 0.01	0.13 ± 0.01	0.20 ± 0.02
75.0	1.27 ± 0.08	1.32 ± 0.12	1.28 ± 0.04	1.28 ± 0.02
60.0	2.29 ± 0.36	6.12 ± 0.04	9.11 ± 0.41	10.34 ± 0.06
50.0	5.44 ± 0.15	9.85 ± 0.20	12.97 ± 0.12	17.71 ± 0.29
40.0	15.35 ± 0.05	17.13 ± 0.08	19.57 ± 0.35	22.72 ± 0.48
25.0	19.68 ± 0.38	23.43 ± 0.34	25.33 ± 0.17	28.38 ± 0.22
20.0	23.11 ± 0.14	25.11 ± 0.12	28.57 ± 0.32	32.63 ± 0.46
15.0	25.59 ± 0.32	29.49 ± 0.30	32.07 ± 0.03	36.05 ± 0.72
3.0	26.24 ± 0.98	30.86 ± 0.76	33.17 ± 0.97	38.15 ± 0.34

Lignin characterization

FTIR-ATR

Table S5. FTIR vibrational bands/regions and corresponding assignments for Kraft lignin.

Vibrational band/region (cm^{-1})	Assignments
3200-3500	O-H vibrations. (NEVREZ et al., 2011)
2844-2980	Aliphatic C–H and CH_2 stretching vibrations. (NEVREZ et al., 2011)
1700	Unconjugated C=O (ketone, carboxyl or ester stretching). (CACHET et al., 2014;CADEMARTORI et al., 2013;PANDEY; PITMAN, 2003)
1600	Aromatic skeletal vibration. (GARCÍA et al., 2012;SUN, S. N. et al., 2012)
1514	Aromatic skeletal vibration. (GARCÍA et al., 2012;SUN, S. N. et al., 2012)
1456	Aromatic skeletal vibration and C-H deformations. (GARCÍA et al., 2012;SUN, S. N. et al., 2012)
1425	Aromatic skeletal vibrations combined with C-H in-plane deformation. (GARCÍA et al., 2012;SUN, S. N. et al., 2012)
1327	Syringyl unit breathing with C=O stretching and condensed Guaiacyl rings. (GARCÍA et al., 2012;SUN, S. N. et al., 2012)
1212	C-C plus C-O plus C=O stretch; Guaiacyl condensed > Guaiacyl etherified. (GARCÍA et al., 2012;SUN, S. N. et al., 2012)
1109	Contribution of C-H in a plane deformation, C=O stretching of syringyl units and secondary alcohols. (GARCÍA et al., 2012;SUN, S. N. et al., 2012)
1040	Aromatic C H in-plane deformation (Guaiacyl > Syringyl) plus C-O deformation in primary alcohols plus C=O stretch (unconjugated). (GARCÍA et al., 2012;SUN, S. N. et al., 2012)
925	Aromatic C-H out-of-plane. (SUN, S. N. et al., 2012)
838	Aromatic C-H out-of-plane deformation in Guaiacyl and Syringyl units. (GORDOBIL et al., 2015)

2D HSQC NMR

Table S6. Assignments of main native Kraft lignin ^{1}H-^{13}C correlation signals found in the HSQC spectra.

Labels	Assignments	Chemical Shift (ppm)	
		^{13}C	^{1}H
MeO	CH in methoxyl groups	56.06	3.75
A_γ	$C_\gamma H_\gamma$ in β-O-4' substructures (A)	59.00	3.20
A_γ	$C_\gamma H_\gamma$ in β-O-4' substructures (A)	59.87	3.71
A_α	$C_\alpha H_\alpha$ in β-O-4' substructures (A)	71.62	4.91
A_β (G)	$C_\beta H_\beta$ in β-O-4' linked to G units	83.96	4.31
A_β (S)	$C_\beta H_\beta$ in β-O-4' linked to S units	87.23	3.96
B_γ	$C_\gamma H_\gamma$ in resinol substructures (B)	71.07	3.79
B_γ	$C_\gamma H_\gamma$ in resinol substructures (B)	71.14	4.20
B_α	$C_\alpha H_\alpha$ in resinol substructures (B)	85.30	4.67
B_β	$C_\beta H_\beta$ in resinol substructures (B)	53.50	3.07
B'_β	$C_\beta H_\beta$ in epiresinol substructures (B)	54.20	2.82
B'_β	$C_\beta H_\beta$ in epiresinol substructures (B)	70.56	4.09
B'_α	$C_\alpha H_\alpha$ in epiresinol substructures (B)	81.36	4.78
B'_α	$C_\alpha H_\alpha$ in epiresinol substructures (B)	87.22	4.33
C_β	$C_\beta H_\beta$ in β-5 phenylcoumaran	53.71	3.46
C_α	$C_\alpha H_\alpha$ in β-5 phenylcoumaran	82.92	5.51
C_γ	$C_\gamma H_\gamma$ in β-5 phenylcoumaran	63.26	3.89
D_β	$C_\beta H_\beta$ in β-1' spirodienone substructures (D)	49.61	3.39
D_β'	$C_\beta H_\beta$ in β-1' spirodienone substructures (D)	86.89	4.44
D_γ'	$C_\gamma H_\gamma$ in β-1' spirodienone substructures (D)	68.89	3.79
D_γ'	$C_\gamma H_\gamma$ in β-1' spirodienone substructures (D)	68.92	3.13
E_α	$C_\alpha H_\alpha$ in p-hydroxycinnamyl alcohol	63.16	4.64
F_α	C_α-H_α in Ar-CHOH-COOH unit	74.18	4.43
H_γ	$C_\gamma H_\gamma$ in p-hydroxycynnamyl alcohol	61.59	4.11
I_α	C_α-H_α in β-O-4' C_α- etherified with carbohydrate	83.41	4.83
J_γ	$C_\gamma H_\gamma$ in β-O-4' C_α- etherified with carbohydrate	66.88	4.28
X_1	$C_1 H_1$ in xylan	101.80	4.29
X_2	$C_2 H_2$ in xylan	75.84	3.53
X_3	$C_3 H_3$ in xylan	74.28	3.28
X_4	$C_4 H_4$ in xylan	72.85	3.06
X_5	$C_5 H_5$ in xylan	63.63	3.28
$S_{2,6}$	$C_{2,6} H_{2,6}$ in Siringyl units (S)	105.22	6.47

$S'_{2,6}$	$C_{2,6}H_{2,6}$ in oxidized Syringyl units (S')	104.88	7.07
G_2	C_2H_2 in Guaiacyl units (G)	111.00	6.95
G_2'	C_2H_2 in oxidized Guaiacyl units (G)	111.04	7.33
G_5	C_5H_5 in Guaiacyl units (G)	115.00	6.75
G_6	C_6H_6 in Guaiacyl units (G)	119.00	6.75
G_6'	C_6H_6 in oxidized Guaiacyl units (G)	120.14	7.24
H	Cynnamyl alcohols, aldehydes or acids (aromatic and end groups)	122.98	7.56
H	Cynnamyl alcohols, aldehydes or acids (aromatic and end groups)	125.53	7.79
H	Cynnamyl alcohols, aldehydes or acids (aromatic and end groups)	126.16	4.00
H	Cynnamyl alcohols, aldehydes or acids (aromatic and end groups)	127.01	7.35
H	Cynnamyl alcohols, aldehydes or acids (aromatic and end groups)	128.42	8.09
H	Cynnamyl alcohols, aldehydes or acids (aromatic and end groups)	131.29	8.23
H	Cynnamyl alcohols, aldehydes or acids (aromatic and end groups)	145.73	8.80

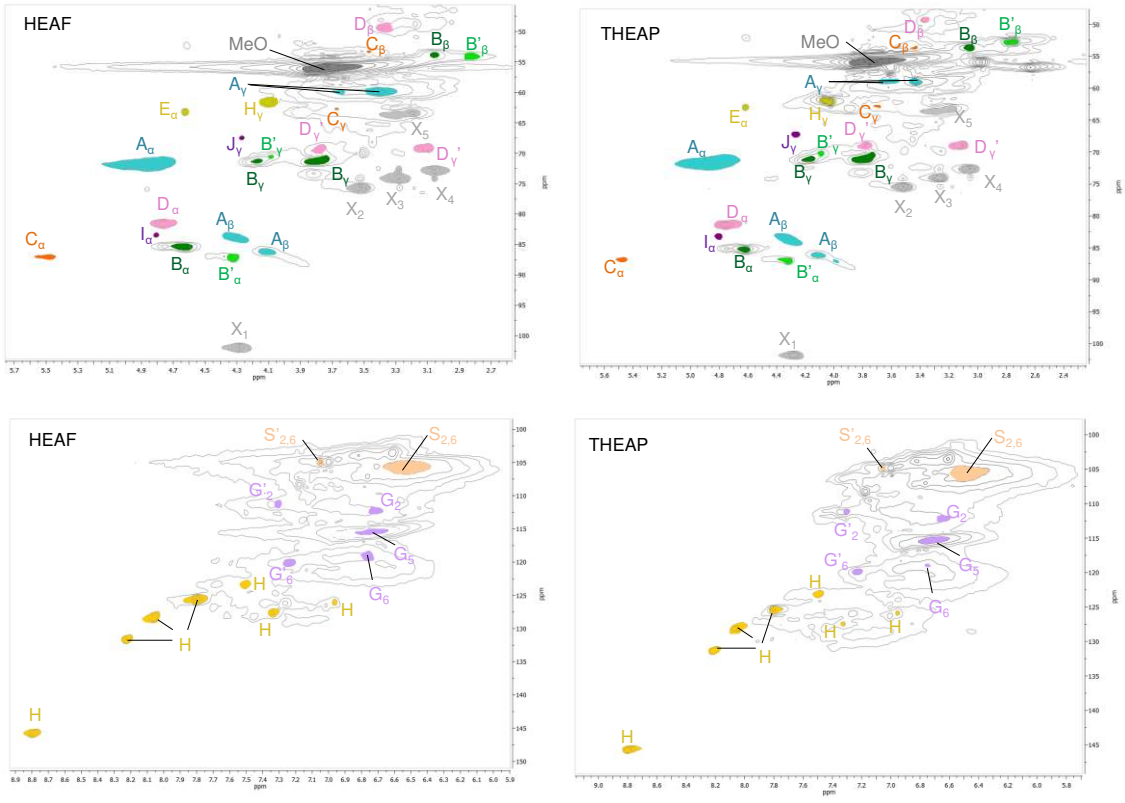

Figure S22. 2D HSQC NMR spectra of recovered lignins from HEAF and THEAP after thermal treatment at 393.15 K for 6h. Aliphatic oxygenated region at the top and aromatic region at the bottom.

GPC

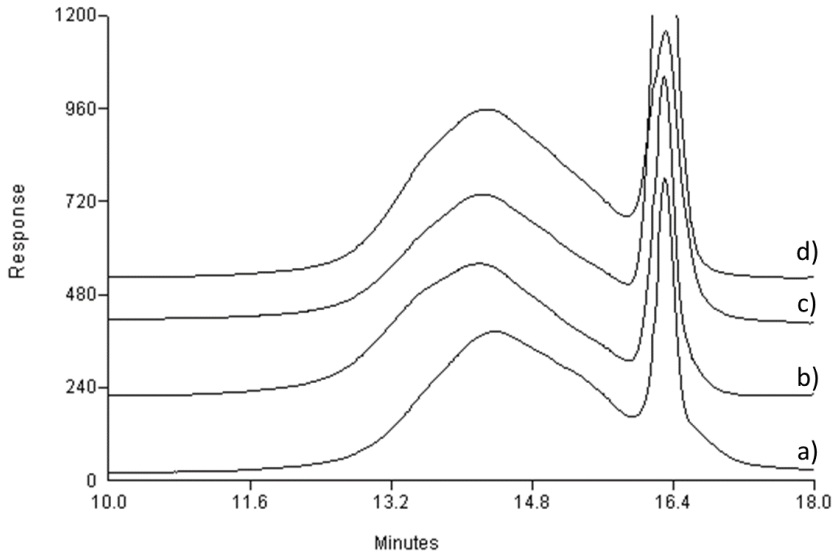

Figure S23. GPC chromatograms of native Kraft lignin (a); and recovered lignins from HEAF (b) HEAP (c) and THEAP (d) after thermal treatment at 393.15 K for 6 h.

References

Cachet, N., Camy, S., Benjelloun-Mlayah, B., Condoret, J.S., Delmas, M., 2014. Esterification of organosolv lignin under supercritical conditions. Ind. Crops Prod. 58, 287–297. https://doi.org/10.1016/j.indcrop.2014.03.039

Cademartori, P.H.G., dos Santos, P.S.B., Serrano, L., Labidi, J., Gatto, D.A., 2013. Effect of thermal treatment on physicochemical properties of Gympie messmate wood. Ind. Crops Prod. 45, 360–366. https://doi.org/10.1016/j.indcrop.2012.12.048

García, A., Erdocia, X., González Alriols, M., Labidi, J., 2012. Effect of ultrasound treatment on the physicochemical properties of alkaline lignin. Chem. Eng. Process. Process Intensif. 62, 150–158. https://doi.org/10.1016/j.cep.2012.07.011

Gordobil, O., Delucis, R., Egüés, I., Labidi, J., 2015. Kraft lignin as filler in PLA to improve ductility and thermal properties. Ind. Crops Prod. 72, 46–53. https://doi.org/10.1016/j.indcrop.2015.01.055

Nevrez, L.A.M., Casarrubias, L.B., Celzard, A., Fierro, V., Mũoz, V.T., Davila, A.C., Lubian, J.R.T., Snchez, G.G., 2011. Biopolymer-based nanocomposites: Effect of lignin acetylation in cellulose triacetate films. Sci. Technol. Adv. Mater. 12, 045006. https://doi.org/10.1088/1468-6996/12/4/045006

Pandey, K.K., Pitman, A.J., 2003. FTIR studies of the changes in wood chemistry following decay by brown-rot and white-rot fungi. Int. Biodeterior. Biodegrad. 52, 151–160. https://doi.org/10.1016/S0964-8305(03)00052-0

Sun, S.N., Li, M.F., Yuan, T.Q., Xu, F., Sun, R.C., 2012. Sequential extractions and structural characterization of lignin with ethanol and alkali from bamboo (Neosinocalamus affinis). Ind. Crops Prod. 37, 51–60. https://doi.org/10.1016/j.indcrop.2011.11.033

Elsevier License Terms and Conditions

"This article was published in **Industrial Crops and Products, Vol 143**, Dias, R. M.; da Costa Lopes, A. M.; Silvestre, A. J. D.; Coutinho, J. A. P.; Costa, M. C., Uncovering the potentialities of protic ionic liquids based on alkanolammonium and carboxylate ions and their aqueous solutions as non-derivatizing solvents of Kraft lignin, **Page 111866, Copyright Elsevier (2020).**"

Considerações – Capítulo 7

Novamente, foi demonstrada a capacidade de dissolver uma quantidade considerável de lignina nas soluções aquosas de LIPs, e que o aumento da cadeia carbônica da parte aniônica dos LIPs favorece a dissolução da lignina nesses solventes. Além disso, foi verificado uma mudança no mecanismo de dissolução da lignina com o aumento dessa cadeia (efeito hidrotrópico), em que altas concentrações de lignina foram dissolvidas na presença de grande quantidade de água no LIP octanoato de 2-hidroxietilamônio. A lignina recuperada demonstrou pequena modificação estrutural, e em geral, baixas frações moleculares da lignina permaneceram dissolvidas. Finalmente, o reciclo do HEAP foi demonstrado por 3 ciclos sem que perdas significativas na eficiência de dissolução fossem observadas.

CAPÍTULO 8 – DISCUSSÃO GERAL

8. Discussão Geral

No atual cenário mundial, sabe-se que a busca por alternativas mais sustentáveis no âmbito de materiais renováveis e também combustíveis se faz necessária. Neste contexto, surge a biorrefinaria, sendo a aplicação de biomassa uma solução promissora. Sabe-se que biomassa lignocelulósica é formada por celulose, hemicelulose e lignina, e que cada fração desta biomassa pode ser potencialmente convertida em produtos de alto-valor agregado, bem como combustíveis renováveis. Entretanto, alguns gargalos necessitam ser resolvidos para que a transformação da biomassa se torne cada vez mais eficiente, notadamente encontrar solventes capazes de dissolver significativamente e seletivamente os componentes da biomassa, o que acarretaria no desenvolvimento de novas tecnologias. Em destaque se encontra a lignina, que, dentre os componentes da biomassa, é a que menos tem aplicação desenvolvida, além de ser a menos suscetível a tratamentos químicos/biológicos, o que dificulta um processo eficiente de fracionamento e posterior conversão dos componentes. Em vista disso, nesta Tese foi avaliada a possibilidade de se usar os LIPs, considerados solventes de fácil síntese, para dissolver os principais componentes da biomassa.

Em um estudo preliminar (Capítulo 5), três LIPs (HEAF, HEAA, e HEAP) foram sintetizados e caracterizados, e sua capacidade de dissolver a biomassa foi testada em compostos modelo (α-celulose, D-(+)-xilose, e Lignina Álcali), usando a técnica de microscopia óptica de luz polarizada (MOP). Neste estudo preliminar, foram constatadas as capacidades destes LIPs em dissolver seletivamente os componentes testados (Figura 8).

Figura 8 – Dissolução de compostos modelo da biomassa lignocelulósica em LIPs utilizando a técnica de MOP com diferentes taxas de aquecimento

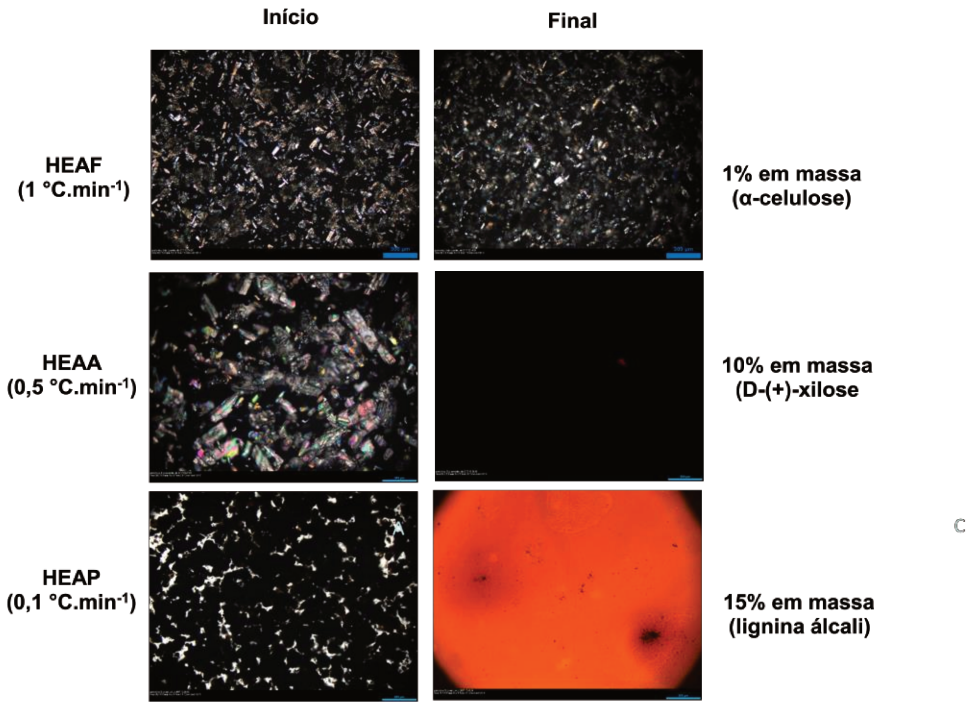

(Acervo Pessoal)

Como observado, os LIPs não são capazes de dissolver celulose, mas são capazes de dissolver xilose (monômero de hemicelulose) e lignina, o que pode indicar uma potencial aplicação destes solventes para produção de etanol de 2ª geração (2G). De fato, alguns estudos na literatura apontam para esta aplicação (Pin et al., 2019; Reis et al., 2017; Rocha et al., 2009).

Para investigar o potencial dos LIPs em dissolver xilose e lignina álcali, diferentes taxas de aquecimento foram aplicadas e constatou-se que taxas de aquecimento mais altas eram capazes de dissolver estes compostos mais rapidamente, entretanto, fez-se necessária uma temperatura final mais alta também para que os componentes fossem dissolvidos completamente. Tal fator é importante de ser analisado, visto que, embora seja mais rápido dissolver com taxas mais elevadas, uma temperatura maior é necessária, o que acarreta elevação nos custos energéticos, porém, o processo apresenta a vantagem de ser um processo mais rápido. Assim, uma análise de custo por tempo poderia ser interessante em estudos futuros.

Na tentativa de entender como a estrutura dos LIPs influencia na velocidade de dissolução dos compostos analisados, as propriedades dos LIPs, tais como densidade, viscosidade, e condutividade, foram relacionadas com a velocidade de dissolução destes componentes através do diagrama de *Walden*. Este diagrama permite uma análise qualitativa da "ionicidade" dos LIPs, uma medida que avalia a fração de íons disponíveis para participar do processo de condução. Assim, conclui-se que quanto maior a ionicidade do LIP, mais rapidamente ele era capaz de dissolver os componentes da biomassa, embora todos os LIPs testados fossem considerados "maus líquidos iônicos" (do inglês, *Poor Ionic Liquids*), assim como a maioria dos LIPs (YOSHIZAWA; XU; ANGELL, 2003).

Uma vez detectada a capacidade dos LIPs de dissolver seletivamente xilose e lignina, a próxima etapa consistiu em avaliar a possibilidade de se utilizar os LIPs na dissolução da lignina, visando desenvolver um processo industrial baseado em utilizar LIPs como meio solvente da lignina, uma vez que tal macromolécula é pouco explorada industrial e comercialmente.

Dessa forma, a continuidade da Tese teve como objetivo avaliar de que forma as estruturas dos LIPs (ânion e cátion) afetam a capacidade de dissolução de lignina Kraft, gentilmente fornecida pela empresa Suzano Papel & Celulose, a fim de se obter altos valores de solubilidade de uma lignina produzida industrialmente. Além da estrutura do LIP, fatores como temperatura, tempo e também teor de água presente na solução foram analisados. Para isso, quatorze LIPs foram sintetizados e caracterizados, e suas soluções aquosas testadas quanto à capacidade de dissolver a lignina Kraft. Tais LIPs foram selecionados visando analisar uma ampla gama de variáveis presentes nas estruturas dos solventes. No total, 3 bases (monoetanolamina, dietanolamina, e trietanolamina) e 10 ácidos orgânicos (glicólico, lático, málico, malônico, sucínico, fórmico, acético, propiônico, hexanóico, e octanóico) foram utilizados para sintetizar os LIPs aplicados nesse estudo.

De forma geral, o aumento da cadeia carbônica do ânion favorece a dissolução de lignina (PU; JIANG; RAGAUSKAS, 2007; Xu et al., 2017). De acordo com Xu et al. (2017), as interações entre os grupos carboxílicos e a lignina são

interrompidas devido à presença da água, e por isso, as interações entre a lignina e os LIPs são realizadas principalmente pela cadeia carbônica alquílica presente no ânion. Sendo assim, a cadeia alquílica tem papel principal na dissolução da lignina, enquanto os grupos carboxílicos têm pouca participação neste processo. Tal fato foi observado também nos estudos desenvolvidos nesta Tese, e se espera que quanto maior a cadeia alquílica do ânion, maior será a solubilidade de lignina neste solvente, uma vez que mais interações entre o LIP e a lignina serão realizadas. Apesar de um aumento da cadeia carbônica acarretar o aumento da solubilidade da lignina, alguns estudos já reportaram o efeito hidrotrópico da solubilidade de compostos fenólicos em LIAs e na dissolução de compostos modelo da lignina em soluções aquosas de *deep eutetic solvents*. Nos estudos desenvolvidos nesta Tese, foi demonstrado que, de fato, o aumento da cadeia alquílica induz o aumento da solubilidade da lignina, entretanto, o mecanismo de dissolução se altera em consequência de um "auto-arranjo" da parte anfifílica do ânion em torno das macromoléculas de lignina, que fica evidente quando se observam as tendências das curvas de solubilidade determinadas nos LIPs HEAH e HEAO. Assim, desde que não haja efeito hidrotrópico, haverá aumento da solubilidade com o aumento da cadeia carbônica da parte aniônica, entretanto, haverá maior probabilidade de ocorrer efeito hidrotrópico com o aumento desta cadeia, o que resulta em queda significativa da solubilidade da lignina.

Na literatura existem estudos reportando o papel principal da parte aniônica do LI na dissolução de lignina (Lateef et al., 2009; PU; JIANG; RAGAUSKAS, 2007). Nesta Tese, o mesmo se comprova, sendo atribuído ao cátion um papel secundário na dissolução da lignina, por isso, foi destinada uma menor ênfase no papel do cátion.

A água, na ausência do efeito hidrotrópico, sempre prejudica a formação de interações entre a lignina e o LIPs, entretanto, é importante avaliar o seu efeito, visto que ela está naturalmente presente na estrutura da biomassa lignocelulósica, e possivelmente em todos os processos envolvendo esta matéria-prima. Diferentes tendências nas curvas de solubilidade foram observadas, e, tais diferenças estão relacionadas ao poder de solvatação da água nos LIPs. Para os casos em que ocorre menor solvatação e também há presença de efeito hidrotrópico, altas solubilidades

foram obtidas com pouca quantidade de LIPs (notadamente em HEAP, HEAH, e HEAO). O contrário está bem definido nas tendências das curvas de solubilidade dos outros LIPs, em especial nos LIPs baseados em dicarboxílicos (HEAM, HEAMn, e HEASu), o que sugere maior solvatação destes LIPs pela água.

Quanto à temperatura, sabe-se que esse fator tem papel fundamental nos valores de solubilidade da lignina alcançados, e que quanto maior for seu valor, maiores serão os valores de solubilidade obtidos (PU; JIANG; RAGAUSKAS, 2007; Rashid et al., 2016). Nesta Tese, temperaturas baixas e brandas foram aplicadas nos ensaios, visto que, a princípio, desejou-se avaliar a capacidade dos LIPs em dissolver lignina a baixas temperaturas, o que acarreta em menor gasto energético. Entretanto, para efeitos demonstrativos, um estudo da influência da temperatura foi realizado com HEAP e THEAL, alguns dos melhores LIPs testados, a fim de demonstrar o potencial de aplicação dos LIPs na dissolução de altas quantidades de lignina. Como demonstrado, a 80 °C, o THEAL foi capaz de dissolver mais de 47%, e o HEAP dissolveu mais de 38%, em massa, de lignina Kraft, o que é uma notável realização, e comparável com valores de solubilidade de lignina Kraft obtidos em outros estudos utilizando LIAs (Glas et al., 2015) e LIPs (ACHINIVU, 2018; Merino et al., 2018) a temperaturas mais altas (90 °C). De todo modo, o efeito da temperatura já se encontra bem difundido e reportado na literatura (Casas et al., 2012; Glas et al., 2015; Lateef et al., 2009; Rashid et al., 2016), por isso, não foi dado grande enfoque quanto a esta questão nesta Tese.

Ademais, a influência do tempo na dissolução de lignina Kraft a temperatura constante (50 °C) também foi avaliada para alguns LIPs (HEAG, HEAMn, e THEAL) que apresentavam cinética de dissolução lenta através do comparativo de dois métodos: Banho Ultrassônico (BU), e Agitação por Barra Magnética (ABM). Quando comparados, o BU apresentou capacidade de dissolver a lignina mais rapidamente, e isso, de acordo com Krishna Sandilya; Kannan (2010), e Thompson; Doraiswamy (1999) se deve ao colapso das bolhas de cavitação que produzem ondas de choque que resultam em uma turbulência microscópica em volta das partículas sólidas de lignina reduzindo a camada limite. Tal turbulência auxilia no contato entre o LIP e a lignina, e provoca um aumento da velocidade de sua dissolução nos LIPs. No geral, 8 horas foram necessárias

utilizando a ABM para que toda a lignina fosse dissolvida, com exceção dos LIPs à base de ácido lático (24 horas), e isso se deve à sua elevada capacidade (significativamente maior que outros LIPs avaliados) de dissolver lignina Kraft, e também de sua viscosidade. Já nos casos aplicando BU, foram necessárias, no máximo, 4 horas para que a saturação do sistema fosse atingida, mesmo no caso em que se aplica LIPs à base de ácido lático. Tal fato demonstra a possibilidade de se aplicar BU na dissolução de lignina Kraft com uma velocidade significativamente maior que nos casos em que há agitação mecânica tradicional, o que aponta para um possível avanço tecnológico nesta tarefa.

Avaliar a possibilidade de reciclo dos LIPs após a sua aplicação na dissolução de lignina é um passo crucial na busca por um processo industrial sustentável ambiental e economicamente. Assim, foram feitos experimentos nos quais foi investigado o reciclo de três LIPs (THEAL, HEAM e HEAP). Esses LIPs foram escolhidos devido à sua elevada capacidade de dissolver lignina Kraft com pouca água no sistema, e devido sua pouca habilidade de dissolver lignina quando o sistema apresenta elevados teores de água. Tal fator facilita o processo de separação da lignina do restante da solução, visto que a sua recuperação foi feita através da adição de água ao sistema, o que induz a sua precipitação, uma vez que água atua como um antissolvente. Uma vez separada a lignina da solução, a água presente na mesma foi evaporada utilizando um rotaevaporador, a princípio à pressão ambiente, e posteriormente com vácuo, acarretando na recuperação dos LIPs testados. Aplicando tal procedimento, foi demonstrada a possibilidade de se recuperar estes LIPs por, pelo menos três ciclos (Tabela 5), sem perda significante da sua eficiência, o que viabiliza o potencial uso dos LIPs em processos industriais através do seu reciclo e reuso.

Tabela 5 – Eficiência na reutilização dos LIPs no processo de dissolução de lignina Kraft

LIP	% solubilidade (em massa)	1° Ciclo (%)	2° Ciclo (%)	3° Ciclo (%)
HEAM	15,25% (5% água)	99,8	99,7	99,6
HEAP	29,49% (15% água)	99,6	99,1	98,7
THEAL	34,14% (5% água)	99,8	98,3	97,4

(Acervo Pessoal)

Finalmente, a lignina recuperada após sua dissolução em LIPs foi caracterizada e comparada com a lignina sem qualquer tipo de tratamento (nativa). Inicialmente, a estrutura da lignina foi investigada através de GPC, que demonstrou um leve aumento na massa molar média, e no índice de polidispersividade. Tal observação indica que baixas modificações químicas podem ter ocorrido, ou que frações de baixa massa molar da lignina (oligômeros) podem ter permanecido dissolvidas nos LIPs. Assim, outras técnicas (FT-IR e RMN 2D HSQC) se fizeram necessárias para caracterizar completamente a lignina. De forma geral, a técnica de FT-IR demonstrou pequenas alterações na estrutura da lignina, ainda inconclusivas quanto à modificação que possa ter ocorrido. Por fim, uma caracterização semi-quantitativa dos principais grupos presentes na lignina foi feita utilizando os espectros obtidos através de RMN 2D HSQC. Foi observado um aumento relativo no número de subestruturas contendo β-O-4, enquanto que o contrário foi observado para as outras estruturas, notadamente para resinol β-β. Tal observação está associada à permanência de mais espécies de alta massa molar da lignina, que possuem mais ligações β-O-4, como corroborado pela análise de GPC (Wang et al., 2018). Assim, pequenas modificações na lignina foram observadas, em especial, espécies de baixa massa molar permaneceram dissolvidas no LIP.

Em suma, os resultados obtidos nesta Tese demonstram a capacidade dos LIPs em dissolver seletivamente os componentes da biomassa, notadamente lignina,

além de explorar o potencial destes LIPs em futuras aplicações em processos industriais como meio solvente da lignina sem que sua estrutura seja significativamente afetada.

PARTE 3

CONCLUSÕES GERAIS E DESAFIOS FUTUROS

CAPÍTULO 9 – CONCLUSÕES GERAIS E DESAFIOS FUTUROS

9. Conclusões

- Os LIPs testados nesta Tese, produzidos a partir de alcanolaminas e ácidos orgânicos como precursores, foram capazes de dissolver os principais componentes da biomassa, com exceção da celulose. Esse fator corrobora com alguns trabalhos na literatura que investigam suas aplicações no pré-tratamento da biomassa, seguida de hidrólise enzimática, para a produção de etanol 2G;
- A estrutura dos LIPs tem papel crucial na dissolução da lignina. Constatou-se que a parte aniônica tem papel majoritário, enquanto a parte catiônica tem participação secundária na dissolução da lignina, ou seja, nas interações realizadas entre os LIPs e a lignina;
- O aumento da cadeia aquílica da parte aniônica dos LIPs favorece a dissolução da lignina, entretanto, tal aumento pode acarretar alterações do mecanismo de interação entre água-lignina-LIP (efeito hidrotrópico) e reduzir as interações entre a lignina e os LIPs prejudicando a sua dissolução;
- A água atua como antissolvente na dissolução da lignina, reduzindo as interações entre os LIPs e a lignina (solvatação);
- Valores de solubilidade de lignina comparáveis com a literatura utilizando LIAs e outros LIPs foram obtidos nesta Tese, aplicando temperaturas mais baixas. O aumento da temperatura favorece o fenômeno de dissolução da lignina, embora isto acarrete maiores gastos energéticos em um possível processo industrial;
- A influência do tempo foi comparada através de dois métodos: Banho Ultrassônico (BU) e Agitação por Barra Magnética (ABM), sendo que o BU apresentou significativa diminuição no tempo necessário para atingir o estado de saturação do sistema (solubilidade da lignina);
- O reciclo de três LIPs foi demonstrado através de três ciclos, utilizando destilação à pressão ambiente e rotaevaporação a vácuo. Foi possível reutilizar os LIPs sem que houvesse significativa perda de eficiência no processo de dissolução da lignina;

- A lignina dissolvida nos LIPs e recuperada por precipitação com água apresentou pequenas modificações, o que foi constatado pelas técnicas de GPC, FT-IR e RMN 2D HSQC. As frações de maior massa molar foram recuperadas, enquanto as de mais baixa massa molar permaneceram dissolvidas nos LIPs;
- Os LIPs podem ser considerados potenciais solventes na dissolução da lignina, sem que isso acarrete profundas modificações estruturais da lignina.

Desafios futuros

Os desafios futuros são entender as alterações provocadas pelos LIPs na estrutura da lignina. Para isso, sugere-se a aplicação de técnicas como Difração de Raio-X, Análise Elementar (C,H,N), DSC, TGA, além de outros tipos de RMN, tal como HMBC.

Outro ponto interessante a ser estudado é a alteração do cátion (base), visto que, embora este fator tenha influência secundária nas interações com a lignina, a forma com que ele afeta estas interações foi pouco explorado nesta Tese.

Além disso, realizar simulação molecular, tal como a utilização de modelos e softwares capazes de predizer o comportamento da lignina em solventes como os LIPs, podem auxiliar na obtenção de solventes mais efetivos na tarefa de dissolver a lignina. Nesse sentido, a simulação molecular deve ser explorada para dar suporte a trabalhos futuros.

Finalmente, avaliar a possibilidade de aplicação de dissolução da lignina em soluções aquosas de LIPs em escala industrial, avaliando os parâmetros que influenciam no processo em grande escala, tal como agitação, temperatura, concentração de lignina. Assim como a viabilidade econômica do processo pela recuperação dos LIPs e seu posterior reuso.

10. Referências

Achinivu et al. **Lignin extraction from biomass with protic ionic liquids**. *Green Chemistry*, [s.l.], v. 16, nº 3, p. 1114–1119, 2014. ISSN: 14639262, DOI: 10.1039/c3gc42306a.

ACHINIVU, E. C. **Protic ionic liquids for lignin extraction—A lignin characterization study**. *International Journal of Molecular Sciences*, [s.l.], v. 19, nº 2, 2018. ISSN: 14220067, DOI: 10.3390/ijms19020428.

Álvarez et al. **Thermophysical properties of binary mixtures of {ionic liquid 2-hydroxy ethylammonium acetate+(water, methanol, or ethanol)}.** *J Chem Thermodyn* 43:997–1010, 2011. DOI: 10.1016/j.jct.2011.01.014

Alvira, P. et al. **Pretreatment technologies for an efficient bioethanol production process based on enzymatic hydrolysis: A review**. *Bioresource Technology*, [s.l.], v. 101, nº 13, p. 4851–4861, 2010. ISSN: 09608524, DOI: 10.1016/j.biortech.2009.11.093.

An et al. **Pretreatment of lignocellulosic biomass with renewable cholinium ionic liquids: Biomass fractionation, enzymatic digestion and ionic liquid reuse**. *Bioresource Technology*, [s.l.], v. 192, p. 165–171, 2015. ISSN: 18732976, DOI: 10.1016/j.biortech.2015.05.064.

Andanson et al. **Understanding the role of co-solvents in the dissolution of cellulose in ionic liquids**. *Green Chemistry*. v. 16, pp. 2528-2538, 2014.

Asakawa et al. **Comparison of choline acetate ionic liquid pretreatment with various pretreatments for enhancing the enzymatic saccharification of sugarcane bagasse**. *Industrial Crops and Products*, [s.l.], v. 71, p. 147–152, 2015. ISSN: 09266690, DOI: 10.1016/j.indcrop.2015.03.073.

BIANCHI, M. L. **Polpação de palha de milho utilizando diferentes processos organosolv.** - UNICAMP, 1995.

BIDLACK, J.; MALONE, M. **Molecular Structure and Component Integration of Secondary Cell Walls in Plants**. *Proceedings of the Oklahoma Academy of Science*, [s.l.], v. 72, p. 51–56, 1992.

BLEDZKI; A. K.; GASSAN, J. **Composities Reinforced with Cellulose Based Fibers**. *Progress in Polymer Science*, [s.l.], v. 24, nº 2, p. 221–274, 1996. ISSN: 0079-6700, DOI: 10.1016/S0079-6700(98)00018-5.

Brahim et al. **Delignification of rapeseed straw using innovative chemo-physical pretreatments**. *Biomass and Bioenergy*, [s.l.], v. 95, p. 92–98, 2016. ISSN: 18732909, DOI: 10.1016/j.biombioe.2016.09.019.

Brandt-Talbot et al. **An economically viable ionic liquid for the fractionation of lignocellulosic biomass**. *Green Chemistry*, [s.l.], v. 19, nº 13, p. 3078–3102, 2017. ISBN: 8621543400, ISSN: 14639270, DOI: 10.1039/c7gc00705a.

Brandt et al. **The effect of the ionic liquid anion in the pretreatment of pine wood chips**. *Green Chemistry*, [s.l.], v. 12, nº 4, p. 672–679, 2010. ISSN: 14639262, DOI: 10.1039/b918787a.

BRISTOW, A.; KOLSETH, P. **Paper structure and properties**. New York: M. Dekker, 1986.

BUSSEMAKER, M. J.; ZHANG, D. **Effect of ultrasound on lignocellulosic biomass as a pretreatment for biorefinery and biofuel applications**. *Industrial and Engineering Chemistry Research*, [s.l.], v. 52, nº 10, p. 3563–3580, 2013. ISBN: 08885885, ISSN: 08885885, DOI: 10.1021/ie3022785.

Casas et al. **Dissolution of Pinus radiata and Eucalyptus globulus woods in ionic liquids under microwave radiation: Lignin regeneration and characterization**. *Separation and Purification Technology*, [s.l.], v. 97, p. 115–122, 2012. ISSN: 13835866, DOI: 10.1016/j.seppur.2011.12.032.

Chambon et al. **Pretreatment of South African sugarcane bagasse using a low-cost protic ionic liquid: a comparison of whole, depithed, fibrous and pith bagasse fractions**. *Biotechnology for Biofuels*, [s.l.], v. 11, nº 1, p. 247–262, 2018. ISSN: 1754-6834, DOI: 10.1186/s13068-018-1247-0.

Chandel et al. **Bioconversion of Hemicellulose Into Ethanol and Value-Added Products**. *Advances in Sugarcane Biorefinery*. [s.l.]: Elsevier, 2018. p. 97–134. DOI: 10.1016/B978-0-12-804534-3.00005-7.

CHATEL, G.; ROGERS, R. D. **Review: Oxidation of lignin using ionic liquids-an innovative strategy to produce renewable chemicals**. *ACS Sustainable Chemistry and Engineering*, [s.l.], v. 2, nº 3, p. 322–339, 2014. ISSN: 21680485, DOI: 10.1021/sc4004086.

CHU, S.; MAJUMDAR, A. **Opportunities and challenges for a sustainable energy future**. *Nature*, [s.l.], v. 488, p. 294–303, 2012.

DAVIS, J. H. **Task-specific ionic liquids**. *Chemistry Letters*, [s.l.], v. 33, p. 1072–1077, 2004. ISSN: 14337851, DOI: doi.org/10.1246/cl.2004.1072.

DRUMMOND, A. R. F.; DRUMMOND, I. W. **Pyrolysis of Sugar Cane Bagasse in a Wire-Mesh Reactor**. *Industrial and Engineering Chemistry Research*, [s.l.], v. 35, nº 4, p. 1263–1268, 1996. ISSN: 08885885, DOI: 10.1021/ie9503914.

Dutta et al. **Survey of Lignin-Structure Changes and Depolymerization during Ionic Liquid Pretreatment**. *ACS Sustainable Chemistry and Engineering*, [s.l.], v. 5, nº 11, p.

10116–10127, 2017. ISSN: 21680485, DOI: 10.1021/acssuschemeng.7b02123.

EGOROVA, K. S.; GORDEEV, E. G.; ANANIKOV, V. P. **Biological Activity of Ionic Liquids and Their Application in Pharmaceutics and Medicine**. *Chemical Reviews*, [s.l.], v. 117, nº 10, p. 7132–7189, 2017. ISSN: 15206890, DOI: 10.1021/acs.chemrev.6b00562.

FATIH DEMIRBAS, M. **Biorefineries for biofuel upgrading: A critical review**. *Applied Energy*, [s.l.], v. 86, nº SUPPL. 1, p. S151–S161, 2009. ISSN: 03062619, DOI: 10.1016/j.apenergy.2009.04.043.

Ferrari et al. **Which Variables Matter for Process Design and Scale-Up? A Study of Sugar Cane Straw Pretreatment Using Low-Cost and Easily Synthesizable Ionic Liquids**. ACS Sustainable Chemical Engineering. v. 7, 12779-12788, 2019.

GANDLA, M. L.; MARTÍN, C.; JÖNSSON, L. J. **Analytical Enzymatic Saccharification of Lignocellulosic Biomass for Conversion to Biofuels and Bio-Based Chemicals**. *Energies*, [s.l.], v. 11, nº 11, p. 2936–2956, 2018. ISSN: 19961073, DOI: 10.3390/en11112936.

George et al. **The effect of ionic liquid cation and anion combinations on the macromolecular structure of lignins**. *Green Chemistry*, [s.l.], v. 13, p. 3375–3385, 2011. ISSN: 14639262, DOI: 10.1039/c1gc15543a.

George et al. **Design of low-cost ionic liquids for lignocellulosic biomass pretreatment**. *Green Chemistry*, [s.l.], v. 17, nº 3, p. 1728–1734, 2015. ISBN: 1463-9262, ISSN: 14639270, DOI: 10.1039/c4gc01208a.

Gillet et al. **Lignin transformations for high value applications: Towards targeted modifications using green chemistry**. *Green Chemistry*, [s.l.], v. 19, nº 18, p. 4200–4233, 2017. ISBN: 0902124459255, ISSN: 14639270, DOI: 10.1039/c7gc01479a.

Glas et al. **Lignin solubility in non-imidazolium ionic liquids**. *Journal of Chemical Technology and Biotechnology*, [s.l.], v. 90, n° 10, p. 1821–1826, 2015. ISBN: 02682575, ISSN: 10974660, DOI: 10.1002/jctb.4492.

Greaves et al. **Protic ionic liquids: Solvents with tunable phase behavior and physicochemical properties**. *Journal of Physical Chemistry B*, [s.l.], v. 110, n° 45, p. 22479–22487, 2006. ISBN: 1520-6106, ISSN: 15206106, DOI: 10.1021/jp0634048.

GREAVES, T. L.; DRUMMOND, C. J. **Protic ionic liquids: Properties and applications**. *Chemical Reviews*, [s.l.], v. 108, n° 1, p. 206–237, 2008. ISBN: 0009-2665, ISSN: 00092665, DOI: 10.1021/cr068040u.

GREAVES, T. L.; DRUMMOND, C. J. **Protic Ionic Liquids: Evolving Structure–Property Relationships and Expanding Applications**. *Chemical Reviews*, [s.l.], v. 115, p. 11379–11448, 2015. ISSN: 0009-2665, DOI: 10.1021/acs.chemrev.5b00158.

Grishkewich et al. Recent advances in the application of cellulose nanocrystals. Current opinion in colloids & interface science. v. 29, pp. 32-45, 2017.

HALLETT, J. P.; WELTON, T. **Room-Temperature Ionic Liquids. Solvents for Synthesis and Catalysis**. *Chemical Reviews*, [s.l.], v. 111, p. 3508–3576, 2011. ISSN: 0009-2665, DOI: 10.1021/cr980032t.

Iglesias et al. **Brønsted ionic liquids: Study of physico-chemical properties and catalytic activity in aldol condensations.** *Chemical Engineering Journal*. v. 162, pp. 802-808, 2010.

ISIKGOR, F. H.; BECER, C. R. **Lignocellulosic biomass: a sustainable platform for the production of bio-based chemicals and polymers**. *Polymer Chemistry*, [s.l.], v. 6, n° 25, p. 4497–4559, 2015. ISSN: 17599962, DOI: 10.1039/c5py00263j.

Jensen et al. **Fundamentals of Hydrofaction ™: Renewable crude oil from woody biomass**. *Biomass Conversion and Biorefinery*, [s.l.], v. 7, nº 4, p. 495–509, 2017. ISSN: 21906823, DOI: 10.1007/s13399-017-0248-8.

KIM, J. S.; LEE, Y. Y.; KIM, T. H. **A review on alkaline pretreatment technology for bioconversion of lignocellulosic biomass**. *Bioresource Technology*, [s.l.], v. 199, p. 42–48, 2016. ISSN: 18732976, DOI: 10.1016/j.biortech.2015.08.085.

Klemm et al. **Comprehensive Cellulose Chemistry: Functionalization of Cellulose**. In: KLEMM, D. et al. (Orgs.). 2 ed. Weinheim, FRG: Wiley-VCH Verlag GmbH & Co. KGaA, 1998. ISBN: 3527294139.

KRISHNA SANDILYA, D.; KANNAN, A. **Effect of ultrasound on the solubility limit of a sparingly soluble solid**. *Ultrasonics Sonochemistry*, [s.l.], v. 17, nº 2, p. 427–434, 2010. ISSN: 13504177, DOI: 10.1016/j.ultsonch.2009.10.005.

Kudakasseril Kurian et al. **Feedstocks, logistics and pre-treatment processes for sustainable lignocellulosic biorefineries: A comprehensive review**. *Renewable and Sustainable Energy Reviews*, [s.l.], v. 25, p. 205–219, 2013. ISSN: 13640321, DOI: 10.1016/j.rser.2013.04.019.

Langan et al. **Common processes drive the thermochemical pretreatment of lignocellulosic biomass**. *Green Chemistry*, [s.l.], v. 16, nº 1, p. 63–68, 2014. ISSN: 14639262, DOI: 10.1039/c3gc41962b.

Lateef et al. **Separation and recovery of cellulose and lignin using ionic liquids: A process for recovery from paper-based waste**. *Journal of Chemical Technology and Biotechnology*, [s.l.], v. 84, nº 12, p. 1818–1827, 2009. ISSN: 02682575, DOI: 10.1002/jctb.2251.

LIMAYEM, A.; RICKE, S. C.; lignocellulosic biomass for bioethanol production: current perspectives, potential issues and future prospects. **Prog. Energy Combust Sci**, v. 38, 449-467, 2012.

Luo et al. **The production of furfural directly from hemicellulose in lignocellulosic biomass: A review**. *Catalysis Today*, [s.l.], v. 319, nº December 2017, p. 14–24, 2019. ISSN: 09205861, DOI: 10.1016/j.cattod.2018.06.042.

Merino et al. **Screening of Ionic Liquids for Pretreatment of Taiwan Grass in Q-Tube Minireactors for Improving Bioethanol Production**. *Waste and Biomass Valorization*, [s.l.], v. 8, nº 3, p. 733–742, 2017. ISBN: 1264901696123, ISSN: 1877265X, DOI: 10.1007/s12649-016-9612-3.

Merino et al. **Understanding Microwave-Assisted Lignin Solubilization in Protic Ionic Liquids with Multiaromatic Imidazolium Cations**. *ACS Sustainable Chemistry and Engineering*, [s.l.], v. 6, nº 3, p. 4122–4129, 2018. ISSN: 21680485, DOI: 10.1021/acssuschemeng.7b04535.

Miranda et al. **Pineapple crown delignification using low-cost ionic liquid based on ethanolamine and organic acids**. *Carbohydrate Polymers*, [s.l.], v. 206, nº June 2018, p. 302–308, 2019. ISBN: 5579321821, ISSN: 01448617, DOI: 10.1016/j.carbpol.2018.10.112.

Mirjafari et al. **Building a bridge between aprotic and protic ionic liquids**. *RSC Advances*, [s.l.], v. 3, nº 2, p. 337–340, 2013. ISSN: 20462069, DOI: 10.1039/c2ra22752e.

Mora-Pale et al. **Room temperature ionic liquids as emerging solvents for the pretreatment of lignocellulosic biomass**. *Biotechnology and Bioengineering*, [s.l.], v. 108, nº 6, p. 1229–1245, 2011. ISSN: 00063592, DOI: 10.1002/bit.23108.

MORAIS, A. R. C.; COSTA LOPES, A. M. DA; BOGEL-ŁUKASIK, R. **Carbon dioxide in biomass processing: Contributions to the green biorefinery concept**. *Chemical Reviews*, [s.l.], v. 115, nº 1, p. 3–27, 2015. ISBN: 0009-2665, ISSN: 15206890, DOI: 10.1021/cr500330z.

Mosier et al. **Features of promising technologies for pretreatment of lignocellulosic biomass**. *Bioresource Technology*, [s.l.], v. 96, nº 6, p. 673–686, 2005. ISBN: 0960-8524 (Print)n0960-8524 (Linking), ISSN: 09608524, DOI: 10.1016/j.biortech.2004.06.025.

NANAYAKKARA, S.; PATTI, A. F.; SAITO, K. **Chemical depolymerization of lignin involving the redistribution mechanism with phenols and repolymerization of depolymerized products**. *Green Chemistry*, [s.l.], v. 16, nº 4, p. 1897–1903, 2014. ISBN: 1463-9262r1463-9270, ISSN: 14639270, DOI: 10.1039/c3gc41708e.

PASSOS, F.; CARRETERO, J.; FERRER, I. **Comparing pretreatment methods for improving microalgae anaerobic digestion: Thermal, hydrothermal, microwave and ultrasound**. *Chemical Engineering Journal*, [s.l.], v. 279, p. 667–672, 2015. ISBN: 1385-8947, ISSN: 13858947, DOI: 10.1016/j.cej.2015.05.065.

Pielhop et al. **Steam explosion pretreatment of softwood: The effect of the explosive decompression on enzymatic digestibility**. *Biotechnology for Biofuels*, [s.l.], v. 9, nº 1, p. 1–13, 2016. ISBN: 1306801605, ISSN: 17546834, DOI: 10.1186/s13068-016-0567-1.

Pin et al. **Screening of protic ionic liquids for sugarcane bagasse pretreatment**. *Fuel*, [s.l.], v. 235, nº March 2018, p. 1506–1514, 2019. ISSN: 00162361, DOI: 10.1016/j.fuel.2018.08.122.

Pinkert et al. **Ionic Liquids and Their Interaction with Cellulose**. *Chemical Reviews*, [s.l.], v. 109, nº 12, p. 6712–6728, 2009. ISSN: 0009-2665, DOI: 10.1021/cr9001947.

PINKERT, A.; MARSH, K. N.; PANG, S. **Reflections on the solubility of cellulose**. *Industrial and Engineering Chemistry Research*, [s.l.], v. 49, nº 22, p. 11121–11130, 2010. ISSN: 08885885, DOI: 10.1021/ie1006596.

PU, Y.; JIANG, N.; RAGAUSKAS, A. J. **Ionic liquid as a green solvent for lignin**. *Journal of Wood Chemistry and Technology*, [s.l.], v. 27, nº 1, p. 23–33, 2007a. ISSN: 02773813, DOI: 10.1080/02773810701282330.

Qing et al. **Mild alkaline presoaking and organosolv pretreatment of corn stover and their impacts on corn stover composition, structure, and digestibility**. *Bioresource Technology*, [s.l.], v. 233, p. 284–290, 2017. ISBN: 1873-2976 (Electronic)0960-8524 (Linking), ISSN: 18732976, DOI: 10.1016/j.biortech.2017.02.106.

RALPH, J.; LANDUCCI, L. **NMR of Lignins**. *Lignin and Lignans*. [s.l.]: [s.n.], 2010. DOI: 10.1201/ebk1574444865-c5.

Rashid et al. **Dissolution of kraft lignin using Protic Ionic Liquids and characterization**. *Industrial Crops and Products*, [s.l.], v. 84, p. 284–293, 2016a. ISBN: 09266690, ISSN: 09266690, DOI: 10.1016/j.indcrop.2016.02.017.

Rashid et al. **Enhanced lignin extraction from different species of oil palm biomass: Kinetics and optimization of extraction conditions**. *Industrial Crops and Products*, [s.l.], v. 116, nº January, p. 122–136, 2018. ISSN: 09266690, DOI: 10.1016/j.indcrop.2018.02.056.

RAVINDRAN, R.; JAISWAL, A. K.; A comprehensive review on pre-treatment strategy for lignocellulosic food industry waste: challenges and opportunities. **Bioresour Technol**, v. 199, 92-102, 2016.

Reis et al. **Pretreatment of cashew apple bagasse using protic ionic liquids:**

Enhanced enzymatic hydrolysis. Bioresource Technology, [s.l.], v. 224, p. 694– 701, 2017. ISSN: 18732976, DOI: 10.1016/j.biortech.2016.11.019.

Rocha et al. **Evaluation of the use of protic ionic liquids on biomass fractionation**. *Fuel*, [s.l.], v. 206, p. 145–154, 2017. ISSN: 00162361, DOI: 10.1016/j.fuel.2017.06.014.

Rocha et al. **Enzymatic hydrolysis and fermentation of pretreated cashew apple bagasse with alkali and diluted sulfuric acid for bioethanol production**. *Applied Biochemistry and Biotechnology*, [s.l.], v. 155, nº 1–3, p. 407–417, 2009. ISBN: 0273-2289, ISSN: 02732289, DOI: 10.1007/s12010-008-8432-8.

RUBIN, E. M. **Genomics of cellulosic biofuels.** *Nature*, [s.l.], v. 454, nº 7206, p. 841–5, 2008. ISSN: 1476-4687, DOI: 10.1038/nature07190.

Sawant et al. **Recent developments of task-specific ionic liquids in organic synthesis**. *Green Chemistry Letters and Reviews*, [s.l.], v. 4, nº 1, p. 41–54, 2011. ISSN: 17518253, DOI: 10.1080/17518253.2010.500622.

SAXENA, R. C.; ADHIKARI, D. K.; GOYAL, H. B. **Biomass-based energy fuel through biochemical routes: A review**. *Renewable and Sustainable Energy Reviews*, [s.l.], v. 13, nº 1, p. 167–178, 2009. ISSN: 13640321, DOI: 10.1016/j.rser.2007.07.011.

SEMERCI, I.; GÜLER, F. **Protic ionic liquids as effective agents for pretreatment of cotton stalks at high biomass loading**. *Industrial Crops and Products*, [s.l.], v. 125, nº April, p. 588–595, 2018. ISSN: 09266690, DOI: 10.1016/j.indcrop.2018.09.046.

Shao et al. **Selective production of arenes via direct lignin upgrading over a niobium-based catalyst**. Nature communications, v. 8, 16104, 2017. DOI: 10.1038/ncomms16104.

Sun et al. **Complete dissolution and partial delignification of wood in the ionic**

liquid 1-ethyl-3-methylimidazolium acetate. *Green Chemistry*, [s.l.], v. 11, nº 5, p. 646–655, 2009. ISSN: 14639262, DOI: 10.1039/b822702k.

Taha et al. **Commercial feasibility of lignocellulose biodegradation: Possibilities and challenges**. *Current Opinion in Biotechnology*, [s.l.], v. 38, p. 190–197, 2016. ISBN: 0958-1669, ISSN: 18790429, DOI: 10.1016/j.copbio.2016.02.012.

THOMPSON, L. H.; DORAISWAMY, L. K. **Sonochemistry: Science and Engineering**. *Ultrasonics Sonochemistry*, [s.l.], v. 38, p. 1215–1249, 1999. ISSN: 18732828, DOI: 10.1021/ie9804172.

Travaini et al. **Sugarcane bagasse ozonolysis pretreatment: Effect on enzymatic digestibility and inhibitory compound formation**. *Bioresource Technology*, [s.l.], v. 133, p. 332–339, 2013. ISSN: 18732976, DOI: 10.1016/j.biortech.2013.01.133.

VEKARIYA, R. L. **A review of ionic liquids: Applications towards catalytic organic transformations**. *Journal of Molecular Liquids*, [s.l.], v. 227, p. 44–60, 2017. ISSN: 01677322, DOI: 10.1016/j.molliq.2016.11.123.

Wang et al. **Bio-oil based biorefinery strategy for the production of succinic acid**. *Biotechnology for Biofuels*, [s.l.], v. 6, nº 1, p. 1–10, 2013. ISSN: 17546834, DOI: 10.1186/1754-6834-6-74.

WANG, H.; GURAU, G.; ROGERS, R. D. **Ionic liquid processing of cellulose**. *Chemical Society Reviews*, [s.l.], v. 41, nº 4, p. 1519–1537, 2012. ISSN: 03060012, DOI: 10.1039/c2cs15311d.

Wang et al. **Fast Fractionation of Technical Lignins by Organic Cosolvents**. *ACS Sustainable Chemistry and Engineering*, [s.l.], v. 6, nº 5, p. 6064–6072, 2018. ISSN: 21680485, DOI: 10.1021/acssuschemeng.7b04546.

WASSERCHEID, P.; WELTON, T. **Ionic liquids in synthesis**. [s.l.]: [s.n.], 2008.

WASSERSCHEID, P.; SCHRÖER, W. **Towards a better fundamental understanding of ionic liquids**. *Journal of Molecular Liquids*, [s.l.], v. 192, p. 1–2, 2014. ISSN: 01677322, DOI: 10.1016/j.molliq.2014.04.014.

WELTON, T. **Ionic liquids: a brief history**. *Biophysical Reviews*, [s.l.], v. 10, p. 691–706, 2018. ISSN: 18672469, DOI: 10.1007/s12551-018-0419-2.

Wen et al. **Understanding the chemical transformations of lignin during ionic liquid pretreatment**. *Green Chemistry*, [s.l.], v. 16, nº 1, p. 181–190, 2014. ISSN: 14639262, DOI: 10.1039/c3gc41752b.

WYMAN, C. E. **Ethanol Production from Lignocellulosic Biomass: Overview**. In: WYMAN, C. E. (Org.). *Handbook on Bioethanol Production and Utilization*. Washington: Taylor & Francis, 1996. p. 1–18.

Wyman et al. **Comparative sugar recovery data from laboratory scale application of leading pretreatment technologies to corn stover**. *Bioresource Technology*, [s.l.], v. 96, nº 18, p. 2026–2032, 2005. ISSN: 09608524, DOI: 10.1016/j.biortech.2005.01.018.

Xie et al. **Thorough Chemical Modification of Wood-Based Lignocellulosic Materials in Ionic Liquids**. *Biomacromolecules*, [s.l.], v. 8, nº 12, p. 3740–3748, 2007. ISSN: 1525-7797, DOI: 10.1021/bm700679s.

Xu et al. **Efficient and sustainable solvents for lignin dissolution: Aqueous choline carboxylate solutions**. *Green Chemistry*, [s.l.], v. 19, nº 17, p. 4067–4073, 2017. ISSN: 14639270, DOI: 10.1039/c7gc01886j.

XU, Y. P.; DUAN, P. G.; WANG, F. **Hydrothermal processing of macroalgae for producing crude bio-oil**. *Fuel Processing Technology*, [s.l.], v. 130, nº C, p. 268–274,

2015. ISBN: 0378-3820, ISSN: 03783820, DOI: 10.1016/j.fuproc.2014.10.028.

Yan et al. **Fractionation of lignin from eucalyptus bark using amine-sulfonate functionalized ionic liquids**. *Green Chemistry*, [s.l.], v. 17, nº 11, p. 4913–4920, 2015. ISSN: 14639270, DOI: 10.1039/c5gc01035g.

YOSHIZAWA, M.; XU, W.; ANGELL, C. A. **Ionic Liquids by Proton Transfer: Vapor Pressure, Conductivity, and the Relevance of ΔpKa from Aqueous Solutions**. *Journal of the American Chemical Society*, [s.l.], v. 125, nº 50, p. 15411–15419, 2003. ISBN: 0002-7863, ISSN: 00027863, DOI: 10.1021/ja035783d.

Zakzeski et al. **The Catalytic Valorization of Lignin for the Production of Renewable Chemicals**. *Chemical Reviews*, [s.l.], v. 110, nº 6, p. 3552–3599, 2010. ISSN: 0009-2665, DOI: 10.1021/cr900354u.

Zavrel et al. **High-throughput screening for ionic liquids dissolving (ligno-)cellulose**. *Bioresource Technology*, [s.l.], v. 100, nº 9, p. 2580–2587, 2009. ISSN: 09608524, DOI: 10.1016/j.biortech.2008.11.052.

ZHAO, X.; ZHANG, L.; LIU, D. **Biomass recalcitrance. Part I: the chemical compositions and physical structures affecting the enzymatic hydrolysis of lignocellulose**. *Biofuels, Bioproducts and Biorefining*, [s.l.], v. 6, nº 3, p. 465–482, 2012. ISSN: 1932104X, DOI: 10.1002/bbb.1331.

Zhu et al. **Sulfite pretreatment (SPORL) for robust enzymatic saccharification of spruce and red pine**. *Bioresource Technology*, [s.l.], v. 100, nº 8, p. 2411–2418, 2009. ISSN: 09608524, DOI: 10.1016/j.biortech.2008.10.057.